AN ABSTRACT OF THE THESIS OF

Li-Hwa Lin for the degree of Master of Ocean Engineering in Civil Engineering presented on December 16, 1983

Title: THE ANALYSIS OF DIRECTIONAL WAVE SPECTRA FROM CURRENT AND PRESSURE MEASUREMENTS



ABSTRACT APPROVED: Dr. Charles K. Sollitt

Directional wave spectra have been estimated in this study based upon simultaneous subsurface measurements of current and pressure. Two previously developed methods, the stochastic and deterministic approaches, have been reviewed and restudied. It is demonstrated by means of the Correlation Theorem that the stochastic and deterministic approaches are, under certain sonditions, identical. In order to improve directional spectrum results obtained from the combined stochastic/deterministic approach, a new method, the geometric approach, has been developed as part of this research effort. The geometric approach matches Fourier transformed wave properties to frequency dependent wavelet pairs in each frequency interval. The amplitude, direction and phase of each wavelet are uniquely specified by equating kinematic and dynamic properties for each frequency component. Wavelets evaluated in each frequency interval do not have an artificially imposed phase constraint in the geometric approach as they have in the stochastic/deterministic approach, providing a more realistic model to represent the directional properties of ocean random waves. This study shows that the geometric approach provides more reliable predictions of the water surface one-dimensional spectra as well as directional spectra. Finally, some semi-empirical equations are proposed and combined to represent the directional spectrum model. A least square error minimization analysis is used to quantify empirical equation parameters. The resulting directional spectra obtained from atlernative methods are compared based on either real ocean data or computer simulated data.

# THE ANALYSIS OF DIRECTIONAL WAVE SPECTRA FROM CURRENT AND PRESSURE MEASUREMENTS

by

Li-Hwa Lin

A THESIS
submitted to
Oregon State University

in partial fulfillment of
the requirements for the
degree of
Master of Ocean Engineering

Completed December 10, 1983
Commencement June 1984

APPROVED:

Redacted for Privacy

Professor of Civil Engineering in Charge of Major

Redacted for Privacy

Head of Department of Civil Engineering

Redacted for Privacy

Dean of Graduate School

Date thesis is presented December 16, 1983

Typed by Li-Chu Lee for Li-Hwa Lin

## ACKNOWLEDGEMENTS

The author wishes to express his sincere gratitude to Dr. Charles K. Sollitt for his guidance and encouragement throughout this research. The technical assistance provided by Mr. James Washburn and Mr. David Standley at the Wave Research Facility has been appreciated.

The author is also grateful to Dr. John H. Nath, Dr. Robert E. Wilson and Dr. Edward H. Piepmeier for their participation as Graduate Committee.

Financial support for this study was provided by the U.S. Army Corps of Engineers, Portland District, Contract No. DACW 57-79-C-0040, and is gratefully acknowledged.

TABLE OF CONTENTS

TABLE OF CONTENTS
(Continued)

LIST OF FIGURES

LIST OF FIGURES
(Continued)

LIST OF TABLES

LIST OF TABLES
(Continued)

# THE ANALYSIS OF DIRECTIONAL WAVE SPECTRA FROM CURRENT AND PRESSURE MEASUREMENTS

## 1. INTRODUCTION

### 1.1 Background

Spectral analysis has become a useful procedure for studying the stochastic properties of ocean waves. The induced wave spectrum implies the pattern of wave energy distribution with respect to several important variables. Common variables include: wave frequency, wave number, and direction of propagation. The wave number is often defined as the product of $2\pi$ with the reciprocal if wave length. Much of the knowledge concerning the generation, growth and decay of waves is based on the analysis of the one-dimensional spectrum, which is a function of wave number or frequency. The wave frequency spectrum quantifies the wave energy per unit water surface area per unit water weight per unit frequency as a function of wave frequency. However, to fully describe the behavior of ocean waves, one also needs to know how wave energy is distributed with respect to direction. The property of directional spreading of wave energy acknowledges that not all waves travel in the same direction. This leads to the concept of the directional spectrum, which is a topic of considerable interest in contemporary coastal engineering research. The directional spectrum of ocean waves is essentially a joint distribution of wave energy density per unit water surface area with respect to direction and either wave number or frequency.

A fundamental assumption in spectral analysis is that the irregular sea surface may be regarded as a linear superposition of many sinusoidal, small amplitude wavelets with respect to direction and wave number or frequency. From linear wave theory, the wave energy per unit water surface area per unit water weight of a sinusoidal, small amplitude wave is known to be identical to the mean square value of water surface elevation or half of the squared amplitude of that wave. Thus, the wave energy per unit water surface area per unit water weight for a parti-

cular directional interval and wave number or frequency range can be computed in accordance with linear wave theory; the resulting quantity divided by that direction interval and wave number or frequency range is defined as the directional spectrum of water surface waves. However , other spectral densities may be defined in terms of important wave properties such as velocity, pressure and acceleration, evaluated at some specified depth of interest. This is accomplished at that specified depth by transferring the water surface elevation of each sinusoidal, small amplitude wavelet to the wave properties of interest, utilizing linear wave theory.

An example graphical presentation of the directional spectrum of water surface waves as a function of wave frequency and direction of propagation appears in Fig. 1.1. The volume under the spectral surface for a specific interval of direction and frequency indicates the corresponding mean square value, or variance, of water surface elevation.

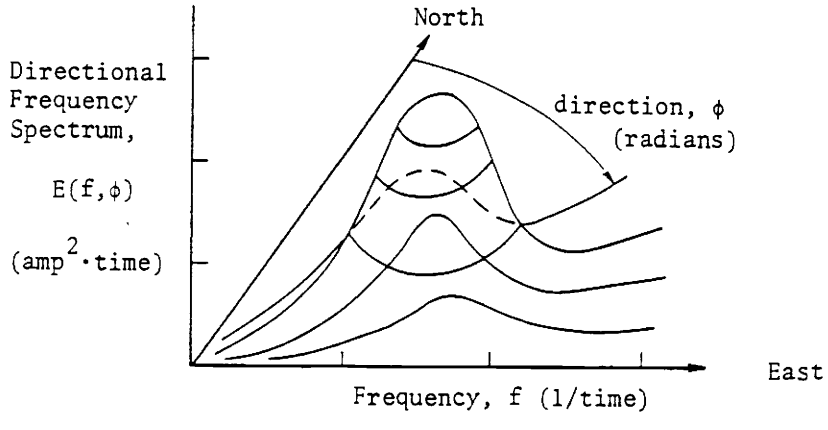


FIG. 1.1 Directional frequency spectrum of water surface waves

A cross section of the directional frequency spectrum in Fig. 1.1 for a given frequency shows the distribution of wave energy density with respect to direction. Such a profile is called a directional spectrum for that frequency; an example appears in Fig. 1.2. The integral of the directional spectrum over all directions presented as a function of frequency is simply the one-dimensional frequency spectrum, as shown in Fig. 1.3.

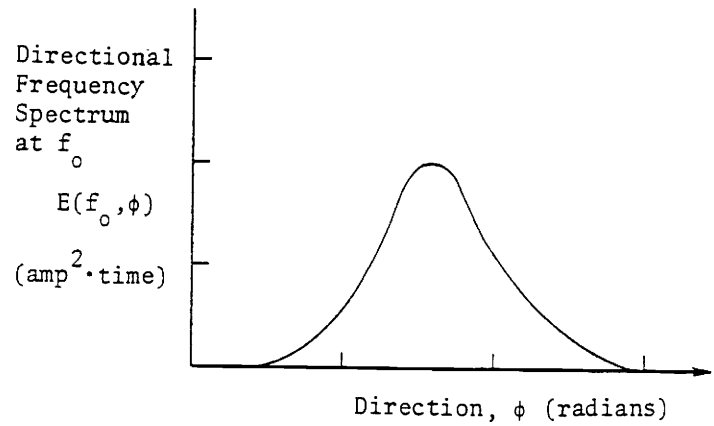


FIG. 1.2 Cross profile of directional frequency spectrum for a given frequency $f_o$

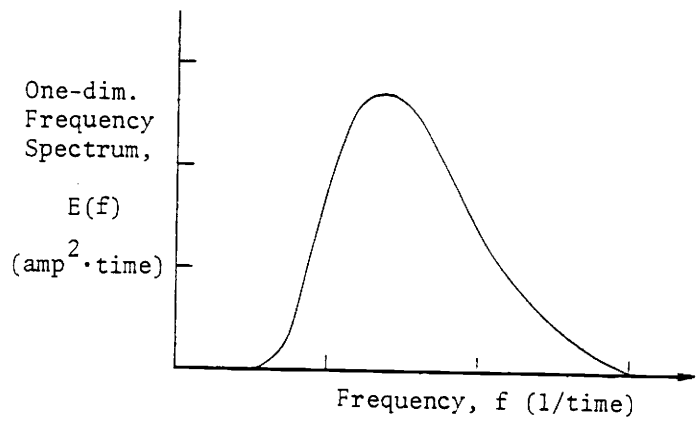


FIG. 1.3 One-dimensional frequency spectrum

The integral of the one-dimensional frequency spectrum over all frequencies gives the total mean square value of water surface elevation; the resulting quantity also indicates the total wave energy of ocean waves per unit water surface area per unit water weight. Therefore, the directional frequency spectrum which is presented in Fig. 1.1 can be interpreted as distribution of total mean square value of water surface elevation with respect to propagation direction and frequency.

The directional spectrum expressed as a function of wave number and direction is essentially a function of the vector wave number. That is, the directional spectrum allocated in a wave number plane is equivalent to the same surface allocated in a polar co-ordinates with direction and scalar wave number as radius. The wave number is a wave property which is related to wave frequency through a theoretically determined dispersion equation. Wave frequency is thought to be a more fundamental wave property than wave number. In particular, most records of wave properties are measured in time at a point and direct transformation of this record yields frequency dependence. Wave number dependence can only be obtained directly from spatial records, i.e., photographs, which do not have the required resolution for water surface elevation measurements. Consequently, the frequency spectrum is preferred by most researchers and is utilized exclusively in this study. However, the wave number spectrum can be obtained indirectly from the frequency spectrum via a transformation with the linear wave theory dispersion equation.

Another issue arising in spectral analysis is that both one-sided and two-sided spectra are used in various studies. The two-sided spectrum, which allows a symmetrical distribution about zero frequency, is preferred by some due to mathematical considerations of the Fast Fourier Transform technique. The one-sided spectrum concentrates the distribution of wave property variance along positive frequency axis, and hence provides an intuitive, more satisfying presentation of a physically measurable wave property. Therefore the one-sided spectrum concept is preferred for use in this study.

Two methods are presently utilized to resolve directional spectra based upon wave property measurements from a single point: the stochastic and deterministic methods. Both methods are based on Fourier transformation procedures and linear wave theory. The stochastic approach has been utilized in various applications of science and engineering since 1950. The algorithm used in the stochastic approach is based on evaluation of frequency dependent Fourier coefficients through cross spectral analysis of simultaneous wave property records. It is shown in

Chapter 2 that the directional spectrum can be estimated by its frequency dependent Fourier coefficients. The fact that the resulting Fourier coefficients can only provide a finite Fourier Series limits the results to an approximate representation of the directional spectrum. One attempt to improve the directional spectrum estimate utilizes the assumption that the spectral distribution is symmetric with respect to direction at all frequencies. The intuitive, symmetric distribution is represented analytically by a squared cosine function with a dependent power relationship which yields the definition for a spreading parameter. The symmetry center of individual angular distributions is located at a mean direction unique to each frequency. The overall distribution of these central angles with respect to frequency is referred as directional spreading of the central angle. Hence, the directional spectrum is characterized by those spreading parameters and central angles which are pre-calculated from the frequency dependent Fourier coefficients.

It should be noted, however, that in the real ocean, waves can be a superposition of many wave systems coming from various sources, each with its own directional spectrum. Althouth the individual spectra may be symmetric for each frequency with respect to direction, the superposed spectrum may not be symmetric for each frequency with respect to direction. Therefore the directional distribution of wave energy density for a given frequency may not be appropriately represented by a single square-cosine-power function. Neverthless, symmetric spectral shapes with respect to frequency can be reasonably assumed based on many real observations of the directional properties of ocean waves. Because of its simplicity and utility, the square-cosine-power function is utilized in estimating the directional properties in this study. The stochastic approach ignores phase information and therefore cannot be used to reproduce the irregular sea state which generated the measured random property records.

The deterministic approach was developed in 1978 as a phase resolving alternative to the stochastic approach. Its algorithm simply generates a group of infinitesimal amplitude wavelets directly from Fourier

coefficients of simultaneous wave property measurements. The relative frequency, direction and phase are determined for each mutually independent wavelet. The frequency dependent Fourier coefficients of the directional spectrum are obtained approximately by summing wavelet properties over small but finite frequency and direction intervals. The procedure used to obtain the directional properties in the deterministic approach then follows the method described in the stochastic approach, based on the square-cosine-power function. The deterministic approach was originally developed to provide a prediction of the sea surface as well as the subsurface kinematic field. In addition, it provides an estimate of the directional spectrum.

## 1.2 Scope of Work

The detailed research included in this study can be briefly discribed as follows:

(1) The stochastic and deterministic approaches are rederived, illustrating basic assumptions and fundamental principles.

(2) It is demonstrated by means of the Correlation Theorem that the stochastic and deterministic approaches are, under certain conditions, actually identical.

(3) A new method, called the geometric approach, is derived as a phase independent resolution alternative to the stochastic/deterministic approach.

(4) Computer algorithms for the stochastic/deterministic approach and the geometric approach are generated in order to input the simultaneous wave property measurements and output the one-dimensional frequency spectra and directional frequency spectra.

(5) Semi-empirical equations are proposed to represent one-dimensional frequency spectrum, spreading parameter and central angle, respectively, by utilizing a least square error minimization analysis.

(6) Results from the stochastic/deterministic approach and the geometric approach are compared.

(7) Correlation studies of the spreading parameter with other spectral parameters shows power function dependence between the spreading parameter and total wave energy density.

(8) A simulated sea surface and its subsurface kinematics are generated for testing the validity of various approaches of directional spectra.

A theoretical analysis of pre-existing methods has demonstrated that evaluation of the one-dimensional frequency spectrum is essential for estimating the directional frequency spectrum. Utilizing an inappropriate one-dimensional frequency spectrum can cause a considerable change in the resulting directional wave energy distribution properties. A Correlation theorem, which simply transforms correlation in the time domain to products in the frequency domain, is then used to analyze the one-dimensional frequency spectrum and improve the directional frequency spectrum estimate. This study shows that the stochastic and deterministic approaches can yield identical one-dimensional frequency spectra and directional frequency spectra. Thus, the two methods are theoretically equivalent. The stochastic approach is preferred by some due to its mathematical elegance while the deterministic approach is preferred in terms of its physical interpretation. A combined name, stochastic/deterministic approach, has been assigned to the method to identify that some improvements have been made in the frequency spectrum estimates. The stochastic/deterministic approach also provides a means for quantifying the time series of various other wave properties, not actually measured. A disadvantage of this method is that orthogonal components of the same frequency are by definition $90^{\circ}$ out of phase. This phase constraint is viewed as an arbitrary limitation by some investigators. Errors in the directional spectrum estimates caused by this constraint can not be corrected. It is concluded that a new uncontrained, phase resolving procedure would be desirable.

As part of this study effort, a geometric approach has been developed to satisfy this requirement. The algorithm of the geometric approach also utilizes the wavelet concept from the deterministic approach. However, a number of infinitesimal amplitude wavelets are generated with independent frequencies, directions and phases. Since these infinitesimal amplitude wavelets are solved from Fourier coefficients of simultaneous wave property measurements, they can be used to reproduce precisely the measured wave properties and to predict various other time series of wave properties not actually measured. The directional frequency spectrum is obtained utilizing a square-cosine-power spreading function.

One consequence of the wavelet concept is that the frequency dependent Fourier coefficients can be obtained by summing wavelet properties over small but finite frequency and direction intervals. Another consequence is that the induced directional frequency spectrum can be simply expressed by the product of the one-dimensional frequency spectrum and the normalized square-cosine-power function. Thus , the one-dimensional frequency spectrum, spreading parameter and directional spreading of central angle, all as functions of frequency, are combined to provide a quantitative description of the directional frequency spectrum.

The utility of a directional frequency spectrum representation can be enhanced immeasurably if the quantitative spectrum results can be summarized in equation form rather than on three dimensional graphs or in tabular matrix form. Equations allow one to quickly evaluate the spectral properties over any frequency and direction range of interest and to readily predict the behavior of related wave properties. Also, spectrum behavior at different times and locations can be quickly compared. To that end, the numerical representation of the directional spectrum has been discribed semi-empirically by defining some appropriate general models for the one-dimensional frequency spectrum, spreading parameter and central angle. A five parameter JONSWAP spectrum has been chosen as a general representation of the one-dimensional spec-

trum. The spreading parameter has been represented on each side of the spectral peak by unique, two parameter power functions of frequency. The central angle has been defined by a third-order polynomial function of frequency. The parameters of each semi-empirical equation are evaluated using a least square error analysis of a comparison between the proposed equation and actual, numerical results.

Bi-axial current meters with one pressure transducer were used in this study to measure simultaneous wave properties which include pressure and orthogonal components of horizontal water particle velocities. Comparisons between the proposed and smoothed directional frequency spectra are made, based on the analysis of real ocean data. The root mean square errors have been estimated for this purpose, and all errors are less than 2% of the smoothed directional spectral density. The resulting small errors indicate the validity of the proposed models. However, significant root mean square errors can be found between the measured one-dimensional frequency spectra and proposed JONSWAP spectra. It is noted that the JONSWAP spectrum model is suitable for describing a one-dimensional frequency spectrum with one spectral peak. However, for those measured one-dimensional frequency spectra which contain two or more spectral peaks, the JONSWAP spectrum is less applicable. Nevertheless, the JONSWAP spectrum is simple and useful, even if the accuracy is reduced for those frequency spectra with multiple peaks. The mean JONSWAP parameters obtained in this study indicate that spectra from offshore Coos Bay, Oregon, have sharper peaks than those measured in the JONSWAP project at North Sea.

The results obtained from the geometric and stochastic/deterministic approaches are compared based upon both ocean measured data and computer simulated data. The comparison shows that more stable results are obtained from the geometric approach than those obtained from the stochastic/deterministic approach. This study also shows that statistics of ocean waves estimated in the frequency domain would be more reliable than those estimated in the time domain.

# 2. THEORY

## 2.1 Introduction

Three methods have been employed in the present study for analyzing directional spectra based upon wave property measurements from a single point. These three methods are: (1) Stochastic Approach, (2) Deterministic Approach, and (3) Geometric Approach. The methods of the stochastic approach and deterministic approach were previously developed by other investigators. The geometric approach has been developed as a new method as part of this research effort. The material presented in this chapter includes the theoretical definitions of directional spectra as well as one-dimensional frequency spectra, and a presentation of the theoretical analysis of the three methods. It is shown that the stochastic approach and deterministic approach yield the same solution to the directional spectra. Hence, the numerical analysis of directional spectra in this study is actually limited to the geometric approach and combined stochastic/deterministic approach. The advantages and disadvantages of using these methods are discussed and summarized at the end of this chapter.

The mathematical analysis of the stochastic approach presented here is similar to that developed from buoy measurements, which was first suggested by Barber(1946) and was then used by Longuet-Higgins(1946,1955 ,1962) and by Cartwright and Smith(1964). The mathematical analysis of the deterministic approach presented here is similar to that described by Sand(1978). Finally, the derivation of the geometric approach is an extension of the deterministic approach with less restrictive assumptions regarding phase.

## 2.2 Spectrum Definitions

A directional wave spectrum is essentially a representation of the wave number spectrum of water surface waves that follow the linear wave theory dispersion relationship between wave number and wave frequency.

According to the superposition of linear waves, an irregular water surface can be approximated by taking the stochastic integral of linear waves over the wave number plane, s, which is identical to the still water surface plane. (Thomson, 1972).

$$\eta(\vec{s}_1,t)=\mathrm{Re}\left[\iint_S da(\vec{k})e^{i(\vec{k}\cdot\vec{s}_1-\sigma t)}\right]$$

$$=\iint_S \frac{1}{2}\left[da(\vec{k})e^{i(\vec{k}\cdot\vec{s}_1-\sigma t)}+da^*(\vec{k})e^{-i(\vec{k}\cdot\vec{s}_1-\sigma t)}\right] \qquad (2.1)$$

where $\eta$ is water surface elevation, t is time, $\vec{s}_1=(x_1,y_1)$ is the horizontal location of interest in rectangular co-ordinates (see Fig. 2.1), $\sigma$ is radian frequency, $\vec{k}=(k\cdot\cos\phi,k\cdot\sin\phi)$ is a vector wave number with magnitude $k=|\vec{k}|$ and direction $\phi$, $da(\vec{k})$ indicates an infinitesimal wave amplitude (complex number) which is the contribution of waves in a wave number interval $d\vec{k}$, an asterisk appearing in superscript indicates the complex conjugate, the operator Re[ ] indicates the real part of a complex number. Note that $da(\vec{k})$ can be denoted as $da(\sigma,\phi)$ since $\vec{k}$ can be expressed by a direction $\phi$ and a frequency $\sigma$. That is, to a first approximation, the wave frequency satisfies the well-known linear wave theory dispersion equation (Ippen, 1966).

$$\sigma^2=gk\cdot\tanh(kh), \qquad k=|\vec{k}| \qquad (2.2)$$

where g is gravitational constant and h is water depth (see Fig. 2.1). A small contribution of the water surface waves representing a specific vector wave number is

$$d\eta(\vec{s}_1,t)=\frac{1}{2}\left[da(\vec{k})e^{i(\vec{k}\cdot\vec{s}_1-\sigma t)}+da^*(\vec{k})e^{-i(\vec{k}\cdot\vec{s}_1-\sigma t)}\right] \qquad (2.3)$$

Thus, the mean square value of $d\eta$ can be evaluated, which has a form

$$\overline{[d\eta(\vec{s}_1,t)]^2}=\frac{1}{4}\lim_{T\to\infty}\frac{1}{T}\int_{-T/2}^{T/2}\{[da(\vec{k})]^2e^{i2(\vec{k}\cdot\vec{s}_1-\sigma t)}+2da(\vec{k})da^*(\vec{k})$$

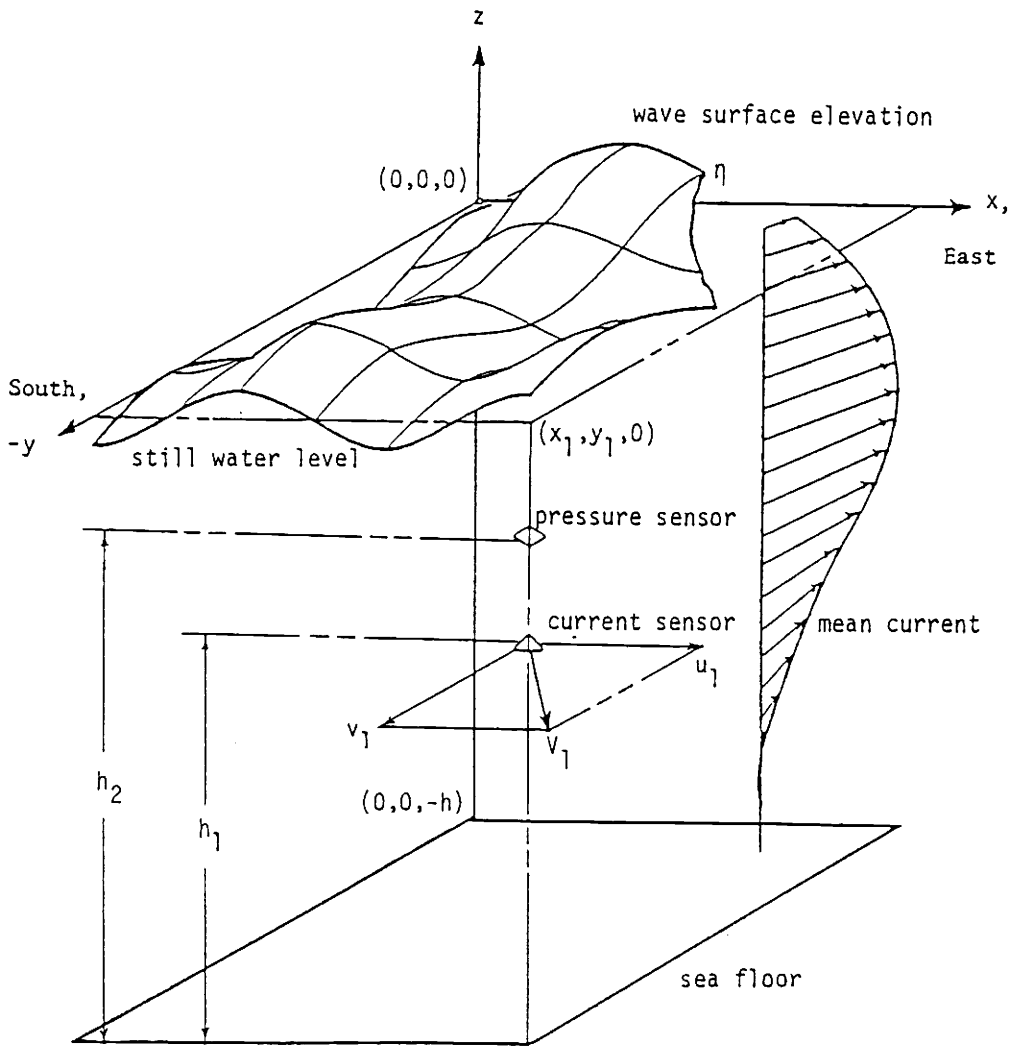


FIG. 2.1 Data collecting system at location $\vec{s}_1=(x_1,y_1)$

$$+[da^*(\vec{k})]^2 e^{-i2(\vec{k}\cdot\vec{s}_1-\sigma t)}\}dt = \frac{1}{2}da(\vec{k})da^*(\vec{k})$$

$$= \frac{1}{2}|da(\vec{k})|^2 = \frac{1}{2}|da(\sigma,\phi)|^2 = E(\sigma,\phi)d\sigma d\phi = dE(\sigma,\phi) \qquad (2.4)$$

where T is time duration of interest, an overhead bar indicates the operation of arithmatic mean; $E(\sigma,\phi)$ is the directional frequency spectrum which is defined as

$$E(\sigma,\phi) = \overline{[d\eta(\vec{s}_1,t)]^2}/d\sigma d\phi = \frac{1}{2}|da(\sigma,\phi)|^2/d\sigma d\phi \qquad (2.5)$$

According to linear wave theory, the wave energy per unit water surface area per unit water weight is equal to half the squared value of wave amplitude (Ippen, 1966). Therefore, Eq.(2.4) specifies a quantity proportional to wave energy associated with a particular frequency range, $d\sigma$, and directional interval, $d\phi$. However, Eq.(2.4) may be regarded as a contribution from an infinitesimal amplitude wave with amplitude $da(\sigma,\phi)$ at the mid $d\sigma$ and $d\phi$. Thus, $E(\sigma,\phi)$ is interpreted as the distribution of wave energy per unit water surface area per unit water weight per unit frequency per unit direction. The corresponding one-dimensional frequency spectrum $E(\sigma)$ is defined by integrating $E(\sigma,\phi)$ over all $\phi$.

$$E(\sigma) = \int_{-\pi}^{\pi} E(\sigma,\phi)d\phi \qquad (2.6)$$

The total wave energy per unit water surface area per unit water weight is defined by integrating $E(\sigma)$ over all $\sigma$, or integrating $E(\sigma,\phi)$ over all $\sigma$ and $\phi$.

$$E_{total} = \int_0^{\infty} E(\sigma)d\sigma = \int_{-\pi}^{\pi}\int_0^{\infty} E(\sigma,\phi)d\sigma d\phi \qquad (2.7)$$

Since the spectral density defined in Eq.(2.5) or Eq.(2.6) has dimensions of rate of change of wave energy density, the name 'power spectral density' is often used. However, an alternate name 'energy spectral density' is more commonly used in ocean engineering.

The spectral density may be defined in terms of wave properties other than water surface elevation. This is accomplished at a specified depth by transferring the frequency components of water surface elevation to the frequency components of wave properties of interest. Examples utilizing linear wave theory to transfer spectral density of water surface elevation to the subsurface spectral densities of wave-induced dynamic pressure and horizontal components of water particle velocity will be shown in Section 2.3.1.

## 2.3 Stochastic Approach

It is useful to think of an irregular sea as being made of the sum or superposition of many independent, small amplitude wavelets. The importance of this linear superposition is that spectral concepts can be established through Fourier analysis of various wave properties. Utilizing the linear superposition technique, the stochastic approach has been developed in order to obtain the directional spectra. The phase information is ignored in the method. A summary of steps used to derive the stochastic approach in this chapter is as follows.

(1) Based on linear wave theory, the water surface elevation is transferred to wave-induced dynamic pressure and horizontal components of water particle velocity by introducing transfer functions.

(2) The so called co-spectra are determined from the Fourier transforms of correlation functions among various wave properties and are utilized to evaluate the frequency dependent Fourier coefficients for an energy spectrum estimate.

(3) A directionally symmetric angular spreading function is introduced, which covers a broad range of spectral shapes with respect to direction at all frequencies. This angular spreading function is composed of a squared cosine function with a spreading parameter as its power and a central angle as its mean direction.

(4) The final expression of directional spectrum is as product of one-dimensional frequency spectrum with a normalized angular spreading function. Two methods are used in resolving the spreading parameter and central angle, as functions of frequency, with respect to the first-order and second-order frequency dependent Fourier coefficients. Hence, two separate directional spectra of a wave property can be obtained from the stochastic approach.

### 2.3.1 Linear Wave Superposition

A sinusoidal wave profile which is observed at a horizontal location $\vec{s}_1$ may be expressed as

$$\eta_1(\vec{s}_1,t)=a(\vec{k})\cos(\vec{k}\cdot\vec{s}_1-\sigma t+\theta) \tag{2.8-1}$$

where wave amplitude $a(\vec{k})$ is defined as a real number here, and $\theta$ is phase. The x, y, z co-ordinate system is defined as shown in Fig. 2.1. According to linear wave theory, the dynamic pressure due to this water surface wave at the same horizontal location but at a height $h_2$ above the bottom is (Ippen, 1966)

$$p_1(\vec{s}_1,t)=a(\vec{k})\gamma_0\frac{\cosh(kh_2)}{\cosh(kh)}\cos(\vec{k}\cdot\vec{s}_1-\sigma t+\theta) \tag{2.8-2}$$

where $\gamma_0$ is specific weight of sea water. The horizontal water particle velocity component at the same horizontal location but at a height $h_1$ above the bottom is (Ippen, 1966)

$$V_1(\vec{s}_1,t)=a(\vec{k})\sigma\frac{\cosh(kh_1)}{\sinh(kh)}\cos(\vec{k}\cdot\vec{s}_1-\sigma t+\theta) \tag{2.8-3}$$

Since the water surface elevation, the wave-induced dynamic pressure and horizontal velocity component are all in phase with one another, the phase $\theta$ is dropped from Eqs.(2.8-1,2,3). Note that the phase information is then ignored in the stochastic approach. Therefore, we have

$$\eta_1(\vec{s}_1,t)=a(\vec{k})\cos(\vec{k}\cdot\vec{s}_1-\sigma t) \tag{2.9-1}$$

$$p_1(\vec{s}_1,t)=a(\vec{k})K_p(\sigma)\cos(\vec{k}\cdot\vec{s}_1-\sigma t) \tag{2.9-2}$$

$$V_1(\vec{s}_1,t)=a(\vec{k})K(\sigma)\cos(\vec{k}\cdot\vec{s}_1-\sigma t) \tag{2.9-3}$$

where

$$K_p(\sigma)=\gamma_o[\cosh(kh_2)/\cosh(kh)] \tag{2.10}$$

$$K(\sigma)=\sigma[\cosh(kh_1)/\sinh(kh)] \tag{2.11}$$

are known as transfer functions. Now, the horizontal velocity $V_1$ is decomposed into x and y components, denoted as $u_1$ and $v_1$, respectively, according to a direction of propagation, $\phi_1$. The direction considered in mathematical derivations will be defined as follows: +x (East) is defined as the zero direction; positive rotation is in a counterclockwise direction. Directions utilized in example solutions are redefined as follows: +y (North) is defined as the zero direction; positive rotation is in a clockwise direction. Then,

$$u_1(\vec{s}_1,t)=V_1(\vec{s}_1,t)\cos\phi_1=a(\vec{k})K(\sigma)\cos(\vec{k}\cdot\vec{s}_1-\sigma t)\cos\phi_1 \tag{2.12-1}$$

and

$$v_1(\vec{s}_1,t)=V_1(\vec{s}_1,t)\sin\phi_1=a(\vec{k})K(\sigma)\cos(\vec{k}\cdot\vec{s}_1-\sigma t)\sin\phi_1 \tag{2.12-2}$$

Since all these wave properties are linearly proportional to the wave amplitude, a linear superposition of wavelets with various frequencies and directions at the water surface implies a similar superposition of these wave properties at a subsurface location. By assigning the horizontal location of interest to the origin of our co-ordinates, i.e., $\vec{s}_1=0$, superposing these wave properties can be expressed as integrations over all frequencies and directions. That is

$$p(t)=\int_{-\pi}^{\pi}\int_{o}^{\infty}\left[\frac{a(\sigma,\phi)}{d\sigma d\phi}\right]K_p(\sigma)\cos(\sigma t)\,d\sigma\,d\phi \tag{2.13-1}$$

and

$$u(t)=\int_{-\pi}^{\pi}\int_{0}^{\infty}[\frac{a(\sigma,\phi)}{d\sigma d\phi}]K(\sigma)\cos(\sigma t)\cos\phi d\sigma d\phi \qquad (2.13\text{-}2)$$

$$v(t)=\int_{-\pi}^{\pi}\int_{0}^{\infty}[\frac{a(\sigma,\phi)}{d\sigma d\phi}]K(\sigma)\cos(\sigma t)\sin\phi d\sigma d\phi \qquad (2.13\text{-}3)$$

where $a(\sigma,\phi)=a(\vec{k})$ represents a wavelet amplitude corresponding to the contribution in an interval $d\sigma d\phi$. That is, in each interval $d\sigma d\phi$ we assign a wavelet amplitude which is specified at the midpoint of that interval. Therefore, $a(\sigma,\phi)$ can be regarded as a discrete function. However, the bracketed terms in Eqs.(2.13-1,2,3) can be regarded as a continuous function.

Examples of spectral densities defined in terms of other wave properties and induced by a single sinusoidal, uni-direction wave are presented here. As an extension of spectral concepts from Eq.(2.4), the one-dimensional frequency spectrum of a particular wave property may be defined as half the squared amplitude of a wave property fluctuation in a frequency interval. Hence, the one-dimensional frequency spectrum of wave-induced dynamic pressure, defined in Eq.(2.9-2), is

$$E_{pp}(\sigma)=\frac{1}{2}[a(\sigma)K_{p}(\sigma)]^{2}/d\sigma=K_{p}^{2}(\sigma)E(\sigma) \qquad (2.14\text{-}1)$$

Note that $E_{pp}(\sigma)$ is simply the product of water surface frequency spectrum with the square of the transfer function. Similarly, the frequency spectra of x and y components of water particle velocities, defined in Eqs.(2.12-1,2), are

$$E_{uu}(\sigma)=\frac{1}{2}[a(\sigma)K(\sigma)\cos\phi_{1}]^{2}/d\sigma=K^{2}(\sigma)\cos^{2}\phi_{1}E(\sigma) \qquad (2.14\text{-}2)$$

$$E_{vv}(\sigma)=\frac{1}{2}[a(\sigma)K(\sigma)\sin\phi_{1}]^{2}/d\sigma=K^{2}(\sigma)\sin^{2}\phi_{1}E(\sigma) \qquad (2.14\text{-}3)$$

or the horizontal velocity frequency spectrum, denoted as $E_{VV}(\sigma)$, can be obtained by combining $E_{uu}(\sigma)$ and $E_{vv}(\sigma)$ as

$$E_{VV}(\sigma)= \frac{1}{2}[a(\sigma)K(\sigma)]^2/d\sigma= E_{uu}(\sigma)+E_{vv}(\sigma)=K^2(\sigma)E(\sigma) \qquad (2.14\text{-}4)$$

Note that the one-dimensional frequency spectrum of water surface wave can be obtained from $E_{pp}(\sigma)$ or $E_{VV}(\sigma)$. That is

$$E(\sigma)= E_{pp}(\sigma)/K_p^2(\sigma)= E_{VV}(\sigma)/K^2(\sigma) \qquad (2.15)$$

Therefore, a relationship between $E_{pp}(\sigma)$ and $E_{VV}(\sigma)$ is

$$E_{pp}(\sigma)= E_{VV}(\sigma)K_p^2(\sigma)/K^2(\sigma)=[E_{uu}(\sigma)+E_{vv}(\sigma)]K_p^2(\sigma)/K^2(\sigma) \qquad (2.16)$$

These expressions imply the usefulness of utilizing linear wave theory in spectral analysis since transformation among spectral densities of various wave properties makes random wave analysis both simple and direct.

### 2.3.2 Co-spectrum and Fourier Analysis

To obtain the one-dimensional spectrum, it is necessary to analyze only one wave property of interest in accordance with linear wave theory. However, to obtain the directional spectrum, it is necessary to analyze simultaneous wave property measurements relative to one another. The stochastic approach of directional spectrum calls for a cross spectral analysis (Cartwright, 1963) or a comparison of simultaneous wave properties. The cross spectrum is a useful product of spectral analysis; it quantities the frequency response of correlations between two simultaneous wave property measurements.

The definition of cross spectrum, denoted as $\zeta_{ij}(\sigma)$, is written as (Jenkins and Watts, 1968)

$$\zeta_{ij}(\sigma)=C_{ij}(\sigma)-iQ_{ij}(\sigma)=\lim_{T\to\infty} \frac{1}{2\pi}\int_{-T/2}^{T/2} \Pi_{ij}(\tau)e^{-i\sigma\tau}d\tau \qquad (2.17)$$

where subscript ij indicates the analysis between wave properties i and j, $C_{ij}(\sigma)$ is the real part of $\zeta_{ij}(\sigma)$ and is called the co-spectrum, $Q_{ij}(\sigma)$ is

the imaginary part of $\zeta_{ij}(\sigma)$ and is called the quadrature-spectrum; $\Pi_{ij}(\tau)$ is the covariance function defined as (Jenkins and Watts, 1968)

$$\Pi_{ij}(\tau)=\overline{\omega_i(t)\omega_j(t+\tau)}=\lim_{T\to\infty}\frac{1}{T}\int_{-T/2}^{T/2}\omega_i(t)\omega_j(t+\tau)dt \qquad (2.18)$$

where $\tau$ is a delay of time and is called lag, $\omega_i(t)$ and $\omega_j(t)$ are any two wave properties, and T is the total duration of interest. Note that cross spectrum is simply the Fourier transform of the covariance function. Two points should be mentioned concerning the cross spectrum. First, if i=j, the covariance function becomes the auto-covariance function and the induced cross spectrum is a real number and reduces to a one-dimensional frequency spectrum. This is because all auto-covariance functions are symmetric about a zero lag if a stationary process is presented. The imaginary part of the Fourier transform of the auto-covariance function (indicating an odd function transformation) will vanish since the symmetry of the auto-covariance function indicates an even function (Brighan, 1974). Second, the covariance functions of various wave properties shown here are actually correlations since all of these wave-induced properties have zero means. Therefore terms containing the means of relative wave properties vanish in Eq.(2.18) because of these zero means. This has been regarded as an important property for applying the Correlation Theorem in spectral analysis as discussed in Section 2.4.3.

An example of the covariance function and cross spectrum of velocity component u(t) is given as follows (Nagata, 1964). Combining Eqs.( 2.18) and (2.13-2) yields

$$\Pi_{uu}(\tau)=\overline{u(t)u(t+\tau)}=\lim_{T\to\infty}\frac{1}{T}\int_{-T/2}^{T/2}u(t)u(t+\tau)dt$$

$$=\lim_{T\to\infty}\frac{1}{T}\int_{-T/2}^{T/2}\{\int_{-\pi}^{\pi}\int_{0}^{\infty}[\frac{a(\sigma',\phi')}{d\sigma'd\phi'}]K(\sigma')\cos(\sigma' t)\cos\phi' d\sigma' d\phi'\cdot$$

$$\int_{-\pi}^{\pi}\int_{0}^{\infty}[\frac{a(\sigma,\phi)}{d\sigma d\phi}]K(\sigma)\cos(\sigma(t+\tau))\cos\phi d\sigma d\phi\}dt \qquad (2.19\text{-}1)$$

The equations are simplified by assuming that interactions among waves coming from various directions can be ignored. Hence, $\phi=\phi'$ and one integral of direction vanishes from Eq.(2.19-1).

$$\Pi_{uu}(\tau)=\lim_{T\to\infty}\frac{1}{T}\int_{-\pi}^{\pi}\int_{0}^{\infty}\int_{0}^{\infty}[\frac{a(\sigma',\phi)a(\sigma,\phi)}{d\sigma' d\sigma d\phi}]K(\sigma')K(\sigma)\cos^2\phi\cdot$$

$$\{\int_{-T/2}^{T/2}\cos(\sigma' t)\cos(\sigma(t+\tau))dt\}d\sigma' d\sigma d\phi$$

$$=\int_{-\pi}^{\pi}\int_{0}^{\infty}\int_{0}^{\infty}[\frac{a(\sigma',\phi)a(\sigma,\phi)}{d\sigma' d\sigma d\phi}]K(\sigma')K(\sigma)\cos^2\phi\cdot$$

$$\{\lim_{T\to\infty}\frac{1}{T}\cos(\sigma\tau)[\frac{\sin((\sigma'-\sigma)T/2)}{\sigma'-\sigma}+\frac{\sin((\sigma'+\sigma)T/2)}{\sigma'+\sigma}]\}d\sigma' d\sigma d\phi$$

(2.19-2)

Now, the function $\sin(qT/2)/(qT/2)$, where $q=\sigma'-\sigma$ or $q=\sigma'+\sigma$, behaves like an impulse function as $T\to\infty$ (Brighan, 1974).

$$\lim_{T\to\infty}\frac{\sin(qT/2)}{(qT/2)}=\delta(q) \qquad (2.20)$$

where $\delta(q)$ indicates a Dirac $\delta$ function which is a unit impulse. The Sifting property (Brighan, 1974) of the $\delta$ function is

$$\int_{-\infty}^{\infty}F(\sigma)\delta(\sigma'-\sigma)d\sigma=F(\sigma') \qquad (2.21)$$

where $F(\sigma)$ is an analytic function. The interpretation of Eq.(2.21) is

that if one lets $\sigma'$ continuously vary one can sift out each value of the function $F(\sigma)$.

Combining Eq.(2.19-2) and Eqs.(2.20,21) yields

$$\Pi_{uu}(\tau)=\int_{-\pi}^{\pi}\int_{0}^{\infty}\int_{0}^{\infty}\left[\frac{a(\sigma',\phi)\,a(\sigma,\phi)}{d\sigma' d\sigma d\phi}\right]K(\sigma')K(\sigma)\cos^2\phi\cdot$$

$$\frac{\cos(\sigma\tau)}{2}\left[\delta(\sigma'-\sigma)+\delta(\sigma'+\sigma)\right]d\sigma' d\sigma d\phi$$

$$=\int_{-\pi}^{\pi}\int_{0}^{\infty}\left[\frac{a^2(\sigma',\phi)}{2d\sigma' d\phi}\right]K^2(\sigma')\cos^2\phi\cos(\sigma'\tau)d\sigma' d\phi \qquad (2.22)$$

Since $\sigma'\geq 0$, $\sigma\geq 0$, $\delta(\sigma'+\sigma)$ gives no contribution to Eq.(2.22)

The corresponding cross spectrum, upon substitution of Eq.(2.22) into Eq.(2.17), becomes

$$\zeta_{uu}(\sigma)=\lim_{T\to\infty}\frac{1}{2\pi}\int_{-T/2}^{T/2}\left\{\int_{-\pi}^{\pi}\int_{0}^{\infty}\left[\frac{a^2(\sigma',\phi)}{2d\sigma' d\phi}\right]K^2(\sigma')\cos^2\phi\cos(\sigma'\tau)d\sigma' d\phi\right\}e^{-i\sigma\tau}d\tau$$

$$=\frac{1}{2\pi}\int_{-\pi}^{\pi}\int_{0}^{\infty}\left[\frac{a^2(\sigma',\phi)}{2d\sigma' d\phi}\right]K^2(\sigma')\cos^2\phi\cdot$$

$$\left\{\lim_{T\to\infty}\left[\frac{\sin((\sigma'-\sigma)T/2)}{\sigma'-\sigma}+\frac{\sin((\sigma'+\sigma)T/2)}{\sigma'+\sigma}\right]\right\}d\sigma' d\phi$$

$$=\frac{1}{2\pi}\int_{-\pi}^{\pi}\int_{0}^{\infty}\left[\frac{a^2(\sigma',\phi)}{2d\sigma' d\phi}\right]K^2(\sigma')\cos^2\phi\left\{\frac{T}{2}\left[\delta(\sigma'-\sigma)+\delta(\sigma'+\sigma)\right]\right\}d\sigma' d\phi$$

(2.23-1)

Note that the covariance function $\Pi_{uu}(\tau)$ is an even function and, thus, the cross spectrum $\zeta_{uu}(\sigma)$ is a real number, i.e., $\zeta_{uu}(\sigma)=C_{uu}(\sigma)$. The

imaginary part has vanished in Eq.(2.23-1). Also note that there is no limit to $\sigma$ in Eq.(2.23-1), i.e., $\sigma$ could be negative and this is allowed in the Fourier transformation as well. However, if $\sigma$ is regarded as a positive variable, based on the one-sided spectral concept, the term containing $\delta(\sigma'+\sigma)$ vanishes and a factor 2 must be inserted in Eq.(2.23-1). Furthermore, the fundamental frequency $d\sigma=2\pi/T$ considered in the Fourier transformation is also substituted into Eq.(2.23-1). Utilizing the Sifting property again in Eq.(2.23-1) yields

$$\zeta_{uu}(\sigma)=2\int_{-\pi}^{\pi}\int_{o}^{\infty}\left[\frac{a^2(\sigma',\phi)}{2d\sigma' d\phi}\right]K^2(\sigma')\cos^2\phi\left[\frac{1}{2d\sigma}\delta(\sigma'-\sigma)\right]d\sigma' d\phi$$

$$=\int_{-\pi}^{\pi}\left[\frac{a^2(\sigma,\phi)}{2d\sigma d\phi}\right]K^2(\sigma)\cos^2\phi d\phi$$

$$=\int_{-\pi}^{\pi}E(\sigma,\phi)K^2(\sigma)\cos^2\phi d\phi \qquad (2.23\text{-}2)$$

where $E(\sigma,\phi)$ is the directional spectrum as defined in Eq.(2.5).

Similarly, various other cross spectra among p(t), u(t), and v(t), may be derived. All are real numbers and, therefore, are co-spectra. Co-spectra result because the individual covariance functions are even. A list of these co-spectra are as follows:

$$C_{pp}(\sigma)=K_p^2(\sigma)\int_{-\pi}^{\pi}E(\sigma,\phi)d\phi \qquad (2.24\text{-}1)$$

$$C_{pu}(\sigma)=K(\sigma)K_p(\sigma)\int_{-\pi}^{\pi}E(\sigma,\phi)\cos\phi d\phi \qquad (2.24\text{-}2)$$

$$C_{pv}(\sigma)=K(\sigma)K_p(\sigma)\int_{-\pi}^{\pi}E(\sigma,\phi)\sin\phi d\phi \qquad (2.24\text{-}3)$$

$$C_{uv}(\sigma)=K^2(\sigma)\int_{-\pi}^{\pi}E(\sigma,\phi)\sin\phi\cos\phi d\phi \qquad (2.24\text{-}4)$$

$$C_{uu}(\sigma)=K^2(\sigma)\int_{-\pi}^{\pi}E(\sigma,\phi)\cos^2\phi d\phi \qquad (2.24\text{-}5)$$

$$C_{vv}(\sigma)=K^2(\sigma)\int_{-\pi}^{\pi}E(\sigma,\phi)\sin^2\phi d\phi \qquad (2.24\text{-}6)$$

The left side of Eqs.(2.24-1,2,3,4,5,6) can be evaluated numerically by a Fast Fourier Transform (FFT) technique. These co-spectra are presented here because they are so closely related to the directional spectrum that they provide an estimate to the directional spectrum properties.

The directional spectrum can be expanded in a Fourier Series with respect to direction at all frequencies. That is

$$E(\sigma,\phi)=\frac{1}{2}A_o(\sigma)+\sum_{n=1}^{\infty}[A_n(\sigma)\cos(n\phi)+B_n(\sigma)\sin(n\phi)] \qquad (2.25\text{-}1)$$

in which

$$A_n(\sigma)+iB_n(\sigma)=\frac{1}{\pi}\int_{-\pi}^{\pi}E(\sigma,\phi)e^{in\phi}d\phi, \qquad n=0,1,2,\cdots\cdots \qquad (2.25\text{-}2)$$

and $A_n(\sigma)$, $B_n(\sigma)$ are called frequency dependent Fourier coefficients. The relationships among the first five frequency dependent Fourier coefficients and the co-spectrum listed in Eqs.(2.24-1,2,3,4,5,6) are derived as follows:

$$A_o(\sigma)=\frac{1}{\pi}\int_{-\pi}^{\pi}E(\sigma,\phi)d\phi=\frac{E(\sigma)}{\pi}=\frac{C_{pp}(\sigma)}{\pi K_p^2(\sigma)} \qquad (2.26\text{-}1)$$

$$A_1(\sigma)+iB_1(\sigma)=\frac{1}{\pi}\int_{-\pi}^{\pi}E(\sigma,\phi)e^{i\phi}d\phi=\frac{C_{pu}(\sigma)+iC_{pv}(\sigma)}{\pi K(\sigma)K_p(\sigma)}$$

$$A_1(\sigma)=\frac{C_{pu}(\sigma)}{\pi K(\sigma)K_p(\sigma)} \qquad (2.26\text{-}2)$$

$$B_1(\sigma)=\frac{C_{pv}(\sigma)}{\pi K(\sigma)K_p(\sigma)} \qquad (2.26\text{-}3)$$

$$A_2(\sigma)+iB_2(\sigma)= \frac{1}{\pi}\int_{-\pi}^{\pi} E(\sigma,\phi)e^{i2\phi}d\phi$$

Then

$$A_2(\sigma)= \frac{1}{\pi}\int_{-\pi}^{\pi} E(\sigma,\phi)\cos(2\phi)d\phi$$

$$= \frac{1}{\pi}\int_{-\pi}^{\pi} E(\sigma,\phi)(\cos^2\phi-\sin^2\phi)d\phi= \frac{C_{uu}(\sigma)-C_{vv}(\sigma)}{\pi K^2(\sigma)} \qquad (2.26\text{-}4)$$

or

$$A_2(\sigma)= \frac{1}{\pi}\int_{-\pi}^{\pi} E(\sigma,\phi)(2\cos^2\phi-1)d\phi= \frac{2C_{uu}(\sigma)}{\pi K^2(\sigma)} - A_o(\sigma) \qquad (2.26\text{-}5)$$

or

$$A_2(\sigma)= \frac{1}{\pi}\int_{-\pi}^{\pi} E(\sigma,\phi)(1-2\sin^2\phi)d\phi= A_o(\sigma)- \frac{2C_{vv}(\sigma)}{\pi K^2(\sigma)} \qquad (2.26\text{-}6)$$

and

$$B_2(\sigma)= \frac{1}{\pi}\int_{-\pi}^{\pi} E(\sigma,\phi)\sin(2\phi)d\phi$$

$$= \frac{1}{\pi}\int_{-\pi}^{\pi} E(\sigma,\phi)(2\sin\phi\cos\phi)d\phi= \frac{2C_{uv}(\sigma)}{\pi K^2(\sigma)} \qquad (2.26\text{-}7)$$

Combining Eqs.(2.26-5,6) and (2.26-1) yields

$$C_{pp}(\sigma)= \frac{K_p^2(\sigma)}{K^2(\sigma)}\,[C_{uu}(\sigma)+C_{vv}(\sigma)] \qquad (2.27)$$

Since the auto-covariance function is always even, a Fourier transform of the auto-covariance function yields the frequency spectrum which is essentially the co-spectrum of the measured variable. Therefore, the co-spectra, $C_{pp}(\sigma)$, $C_{uu}(\sigma)$, and $C_{vv}(\sigma)$, are essentially the frequency

spectra, $E_{pp}(\sigma)$, $E_{uu}(\sigma)$, and $E_{vv}(\sigma)$, respectively. Hence, Eq.(2.27) is identical to Eq.(2.16), and the one-dimensional frequency spectrum of water surface waves can be estimated from Eq.(2.15).

Since the first five Fourier coefficients, $A_o(\sigma)$, $A_1(\sigma)$, $B_1(\sigma)$, $A_2(\sigma)$, and $B_2(\sigma)$, can be computed from Eqs.(2.26-1,2,3,4,7), the directional spectrum is then approximated by the first five terms of the Fourier Series in Eq.(2.25-1). That is

$$\hat{E}(\sigma,\phi)= \frac{1}{2}A_o(\sigma)+A_1(\sigma)\cos\phi+B_1(\sigma)\sin\phi$$
$$+A_2(\sigma)\cos 2\phi+B_2(\sigma)\sin 2\phi \qquad (2.28)$$

where $\hat{E}(\sigma,\phi)$ indicates an estimator of directional spectrum. It is impossible to obtain more higher-order frequency dependent Fourier coefficients if only p(t), u(t) and v(t) are measured. In order to obtain more higher-order frequency dependent Fourier coefficients, quantities such as components of velocity gradients $\partial u(x,y,z,t)/\partial x$, $\partial u(x,y,z,t)/\partial y$, $\partial v(x,y,z,t)/\partial y$, etc., are necessarily measured. The cross spectra among the wave-induced pressure, two components of horizontal orbital velocities and three components of horizontal orbital velocity gradients enable one to compute the Fourier coefficients up to the fourth-order in Eq.(2.25-1), i.e., nine coefficients (Mitsuyasu et al., 1975).

### 2.3.3 Directional Spreading Analysis

In order to see how the first five Fourier coefficients present an estimation to the directional spectrum, $A_o(\sigma)$, $A_1(\sigma)$, $B_1(\sigma)$, $A_2(\sigma)$, and $B_2(\sigma)$ specified in Eq.(2.25-2) are substituted in Eq.(2.28). The notation $\phi$ appearing in these five Fourier coefficients is changed to $\phi'$ to distinguish the angle $\phi$ in Eq.(2.28). Then,

$$\hat{E}(\sigma,\phi)= \frac{1}{\pi}\int_{-\pi}^{\pi} E(\sigma,\phi')\left[\frac{1}{2} + \cos\phi'\cos\phi+\sin\phi'\sin\phi\right.$$
$$\left. + \cos(2\phi')\cos(2\phi)+ \sin(2\phi')\sin(2\phi)\right]d\phi'$$

$$= \frac{1}{2\pi}\int_{-\pi}^{\pi} E(\sigma,\phi')[1+2\cos(\phi'-\phi)+2\cos(2\phi'-2\phi)]d\phi$$

$$= \frac{1}{2\pi}\int_{-\pi}^{\pi} E(\sigma,\phi')\frac{\sin[\frac{5}{2}(\phi'-\phi)]}{\sin[\frac{1}{2}(\phi'-\phi)]}d\phi$$

$$= \frac{1}{2\pi}\int_{-\pi}^{\pi} E(\sigma,\phi')W(\phi'-\phi)d\phi \qquad (2.29\text{-}1)$$

where

$$W(\phi'-\phi)=\sin[\frac{5}{2}(\phi'-\phi)]/\sin[\frac{1}{2}(\phi'-\phi)] \qquad (2.29\text{-}2)$$

behaves as a weighting function (Barber, 1946). It is apparent that this directional spectrum estimaton, Eq.(2.24), is a smoothed spectrum of the actual directional spectrum $E(\sigma,\phi')$ by the weighting function $W(\phi'-\phi)$. A sketch of this weighting function is shown in Fig. 2.2 and a dummy varible $\phi^*=\phi'-\phi$ is utilized.

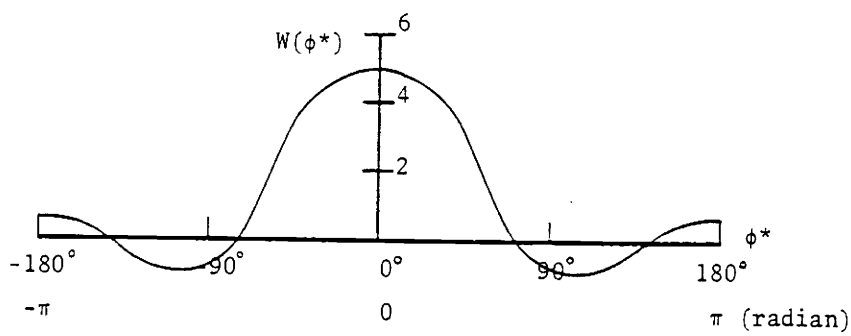


FIG. 2.2 Weighting function $W(\phi^*)=\sin[\frac{5}{2}\phi^*]/\sin[\frac{1}{2}\phi^*]$

Since $W(\phi^*)$ can be negative, it is possible that $\tilde{E}(\sigma,\phi)$ in Eq.(2.24) may become negative too, whereas the directional spectrum itself is positive in real physical systems. An alternate approximation to the weighting function to maintain a positive estimate to the energy spectrum is

presented as follows (Longuet-Higgins et al., 1963). Using the identities:

$$1+\cos\phi^*=2\cos^2(\phi^*/2), \qquad (1+\cos\phi^*)^s=2^s\cos^{2s}(\phi^*/2)$$

Let s=2, a modified weighting function is then defined as

$$\underline{W}(\phi^*)= 1+ \frac{4}{3}\cos(\phi^*)+ \frac{1}{3}\cos(2\phi^*)= \frac{8}{3}\cos^4(\phi^*/2) \tag{2.30}$$

where $\phi^*=\phi'-\phi$. Thus, the directional spectrum estimator due to $\underline{W}(\phi'-\phi)$ is

$$\tilde{E}(\sigma,\phi)= \frac{1}{2\pi}\int_{-\pi}^{\pi} E(\sigma,\phi')\underline{W}(\phi'-\phi)d\phi'$$

$$= \frac{1}{2\pi}\int_{-\pi}^{\pi} E(\sigma,\phi')[\ \frac{8}{3}\cos^4(\frac{\phi'-\phi}{2})]d\phi'$$

$$= \frac{1}{2\pi}\int_{-\pi}^{\pi} E(\sigma,\phi')[1+ \frac{4}{3}\cos(\phi'-\phi)+ \frac{1}{3}\cos(2\phi'-2\phi)]d\phi' \tag{2.31-1}$$

Using the addition formula for cosine functions in Eq.(2.31-1) yields

$$\tilde{E}(\sigma,\phi)= \frac{1}{2}A_o(\sigma)+ \frac{2}{3}[A_1(\sigma)\cos\phi+B_1(\sigma)\sin\phi]$$

$$+ \frac{1}{6}[A_2(\sigma)\cos 2\phi+B_2(\sigma)\sin 2\phi] \tag{2.31-2}$$

Since $\underline{W}(\phi^*)$ defined in Eq.(2.30) is always positive, the resulting $\tilde{E}(\sigma,\phi)$ in Eq.(2.31-1) is also positive. A sketch of $\underline{W}(\phi^*)$ appears in Fig. 2.3. The weighting function $\underline{W}(\phi^*)$ is not only non-negative but a decreasing function of $|\phi^*|$. This smoothed weighting function has the disadvantage of making the resolution of any distribution narrower than $\cos^4(\phi^*/2)$ impossible. Equation (2.31-2) provides different weights in front of each frequency dependent Fourier coefficient in contrast to those in Eq.(2.28).

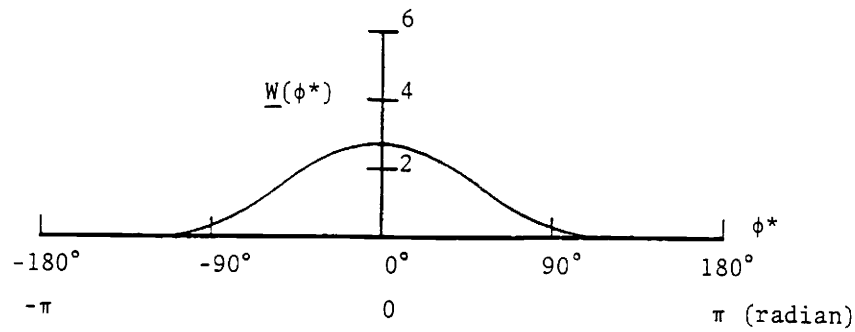


FIG. 2.3 Smoothed weighting function $\underline{W}(\phi^*)=\frac{8}{3}\cos^4[\frac{1}{2}\phi^*]$

Since both Eqs.(2.28) and (2.31-2) are based on finite Fourier Series, they are limited to an approximate representation of the directional spectrum. However, spectral analysis using Eqs.(2.28) and (2.31-2) quantifies many useful properties of directional spectra.

The analysis of directional properties of real ocean waves based on Eqs.(2.28) and (2.31-2) has revealed that directional distribution of wave energy density for any given frequency is approximately symmetric about a central direction. Accordingly, it is assumed that a fundamental property of directional distribution for any frequency is one that is summetric about a central direction. In order to make the assumed symmetric directional distribution have a more universal shape, the so called Angular Distribution function is defined as the ratio ( Cartwright, 1963)

$$H(\sigma,\phi)= \frac{E(\sigma,\phi)}{E(\sigma)} \tag{2.32}$$

Therefore, the directional spectrum becomes

$$E(\sigma,\phi)=E(\sigma)H(\sigma,\phi)= \pi A_o(\sigma)H(\sigma,\phi) \tag{2.33}$$

A number of functional forms of $H(\sigma,\phi)$ have been suggested (Sand, 1979) but all have similar shape, i.e., they are symmetric about a central direction. It is usually difficult to choose one in prefer-

ence to another in practical applications. A commonly used function, which is proportional to a power cosine function, is adopted here not only for its simplicity but its similarity to Eq.(2.30). This angular distribution function possesses the following properties (Sand, 1979).

$$(1) \quad H(\sigma,\phi) \geq 0 \tag{2.34-1}$$

$$(2) \quad \int_{-\pi}^{\pi} H(\sigma,\phi)d\phi = \int_{-\pi}^{\pi} E(\sigma,\phi)d\phi / E(\sigma) = 1 \tag{2.34-2}$$

$$(3) \quad H(\sigma,\phi) = G(s)\cos^{2s}\left(\frac{\phi-\phi_o}{2}\right), \quad s=s(\sigma), \quad \phi_o=\phi_o(\sigma) \tag{2.34-3}$$

where $s(\sigma)$ is called a spreading parameter, which is always positive and a function of frequency, $\phi_o(\sigma)$ is called a central angle, and $G(s)$ is a normalizing factor. It is apparent that $H(\sigma,\phi)$ is always positive and symmetric about a central angle $\phi_o(\sigma)$. Also $H(\sigma,\phi)$ is a function that tends to expand the one-dimensional frequency spectrum to a directional spectrum. Therefore, the procedure to determine the directional spectrum reduces to determining the corresponding one-dimensional frequency spectrum, the spreading parameter and the central angle.

The spreading parameter and central angle dependence on frequency is determined as follows. Substituting Eq.(2.34-3) into Eq.(2.34-2), $G(s)$ is solved as

$$G(s) = \frac{2^{2s-1}}{\pi} \frac{(s!)(s!)}{(2s)!} = \frac{2^{2s-1}}{\pi} \frac{\Gamma^2(s+1)}{\Gamma(2s+1)} \tag{2.35}$$

where $\Gamma(s)=\int_o^{\infty} r^{s-1}e^{-r}dr$, the Gamma function. Thus, $H(\sigma,\phi)$ has an explicit form as

$$H(\sigma,\phi) = \frac{2^{2s-1}}{\pi} \frac{\Gamma^2(s+1)}{\Gamma(2s+1)} \cos^{2s}\left(\frac{\phi-\phi_o}{2}\right) \tag{2.36}$$

Combining Eqs.(2.36) and (2.33) yields

$$E(\sigma,\phi)=E(\sigma)H(\sigma,\phi)=\pi A_o(\sigma)G(s)\cos^{2s}(\frac{\phi-\phi_o}{2})$$

$$=E(\sigma)\ \frac{2^{2s-1}}{\pi}\ \frac{\Gamma^2(s+1)}{\Gamma(2s+1)}\ \cos^{2s}(\frac{\phi-\phi_o}{2}) \qquad (2.37)$$

Equation (2.37) can be also expanded in a Fourier Series (Sand, 1979) which has the following form

$$E(\sigma,\phi)=\pi A_o(\sigma)H(\sigma,\phi)$$

$$=\frac{A_o(\sigma)}{2}+A_o(\sigma)\sum_{n=1}^{\infty}[C_n\cos(n\phi_o)\cos(n\phi)+C_n\sin(n\phi_o)\sin(n\phi)] \qquad (2.38\text{-}1)$$

in which

$$C_n=\frac{\Gamma^2(s+1)}{\Gamma(s+n+1)\Gamma(s-n+1)} \qquad (2.38\text{-}2)$$

Since only first five frequency dependence Fourier coefficients can be computed with simultaneous measurements of p(t), u(t) and v(t), the directional spectrum can be approximated by the first five terms in the Fourier Series. That is

$$E(\sigma,\phi)=\frac{1}{2}A_o+(C_1A_o\cos\phi_o)\cos\phi+(C_1A_o\sin\phi_o)\sin\phi$$

$$+(C_2A_o\cos2\phi_o)\cos2\phi+(C_2A_o\sin2\phi_o)\sin2\phi \qquad (2.38\text{-}3)$$

Comparing Eq.(2.38-3) with Eq.(2.28) allows one to evaluate two solutions to s as well as $\phi_o$ from the first-order and second-order coefficients, respectively.

Comparing the first-order coefficients from Eqs.(2.38-3) and (2.28), we have

$$A_1=C_1A_o\cos\phi_o, \qquad B_1=C_1A_o\sin\phi_o \qquad (2.39\text{-}1)$$

Then

$$\phi_{o1}=\phi_o= \tan^{-1}\left(\frac{B_1}{A_1}\right) \tag{2.39-2}$$

$$C_1=\sqrt{A_1^2+B_1^2}\ /A_o= \frac{s}{s+1} \tag{2.39-3}$$

$$s_1=s= \frac{C_1}{1-C_1} \tag{2.39-4}$$

To identify the solutions solved from Eqs.(2.39-1,2,3,4), the subscript 1 has been reserved for the resulting parameters. The directional properties obtained from this case will be referred to as the One Angle Mode solution in this study.

Comparing the second-order coefficients from Eqs.(2.38-3) and (2.28), we have

$$A_2=C_2A_o\cos 2\phi_o, \qquad B_2=C_2A_o\sin 2\phi_o \tag{2.40-1}$$

Then

$$\phi_{o2}=\phi_o= \frac{1}{2}\tan^{-1}\left(\frac{B_2}{A_2}\right) \tag{2.40-2}$$

$$C_2=\sqrt{A_2^2+B_2^2}\ /A_o= \frac{s(s-1)}{(s+1)(s+2)} \tag{2.40-3}$$

$$s_2=s= \frac{1+3C_2+\sqrt{(1+3C_2)^2+8C_2(1-C_2)}}{2(1-C_2)} \tag{2.40-4}$$

To identify the solutions solved from Eqs.(2.40-1,2,3,4), the subscript 2 has been reserved for the resulting parameters. The directional properties solved from this case will be referred to as the Double Angle Mode solution.

The wave property measurements, p(t), u(t), and v(t), are necessary

input for the one angle mode solution. However, u(t), v(t) are sufficient input for the double angle mode solution. This is because $A_o(\sigma)$ can be obtained from the velocity components in accordance with Eqs.(2.26-1) and (2.27). The latter has a problem in that the estimate of the central angle could be indeterminate by $180^o$, since the angle is estimated by half of the inverse tangent function as indicated in Eq.(2.40-2). This indeterminate angle is usually corrected by either estimating the gross main travel direction of waves, e.g., towards the coastline, or by referring to the central angle obtained from the one angle mode solution.

Substituting Eq.(2.39-4) into Eq.(2.40-3), the relationship between $C_1$ and $C_2$ is obtained under the condition $s_1=s_2$ (Cartwright, 1963).

$$C_2 = \frac{C_1(2C_1-1)}{2-C_1} \tag{2.41}$$

If the angular distribution function is valid to describe the real directional distribution of wave energy density at a particular frequency, the resulting $C_1$ and $C_2$ of that frequency should satisfy Eq.(2.41). A comparison of Eq.(2.41) to real ocean data obtained in this study is graphed in Fig. 2.4.

It has been observed by many investigators that the skewness of angular distribution of wave energy is negligible, and a symmetric shape of angular distribution function is deemed suitable. Hence, the function $H(\sigma,\phi)$ used in this analysis provides a reasonable approximation to real ocean data. Therefore, Eq.(2.37) has been chosen as a reasonable representation of the directional spectrum. To utilize this directional spectrum, it is necessary to evaluate the one-dimensional spectrum, the spreading parameter, and the central angle, all as functions of frequency.

The variation of angular distribution shape relative to a central angle is dependent on the spreading parameter. A normalized form of Eq.(2.37), used to represent this variation of angular distribution shape relative to a central angle, is (Mitsuyasu, 1975)

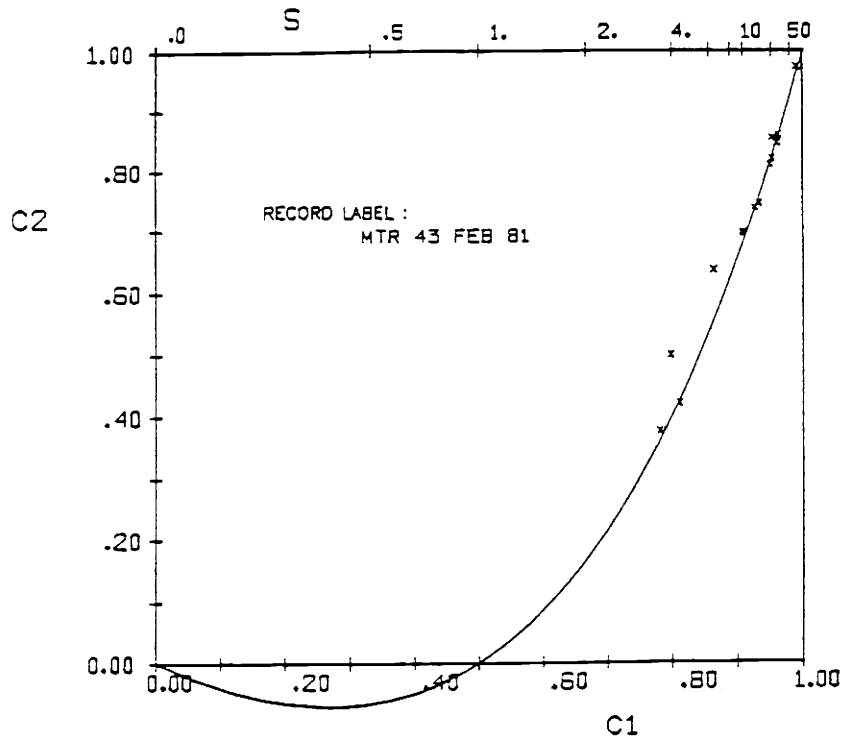


FIG. 2.4 Theoretical curve and sample values of $C_1$ and $C_2$

$$E^*(\sigma,\phi') = \frac{E(\sigma,\phi')}{A_o(\sigma)} = \pi G(s)\cos^{2s}\left(\frac{\phi'}{2}\right) \qquad (2.42)$$

where $\phi' = \phi - \phi_o$. A graphical presentation of Eq.(2.42) for different values of s is shown in Fig. 2.5. Note that large values of s provide narrow angular spreading of spectral energy while small values of s provide broad angular spreading of spectral energy. In practice s and $\phi_o$ are found to vary with frequency.

It has been observed that the variation of the central angle with respect to frequency is mainly dependent on the actual wind direction while the variation of the spreading parameter with respect to frequence is rather independent of wind, but very dependent on frequency. An example of the spreading parameter dependence on frequency, obtained

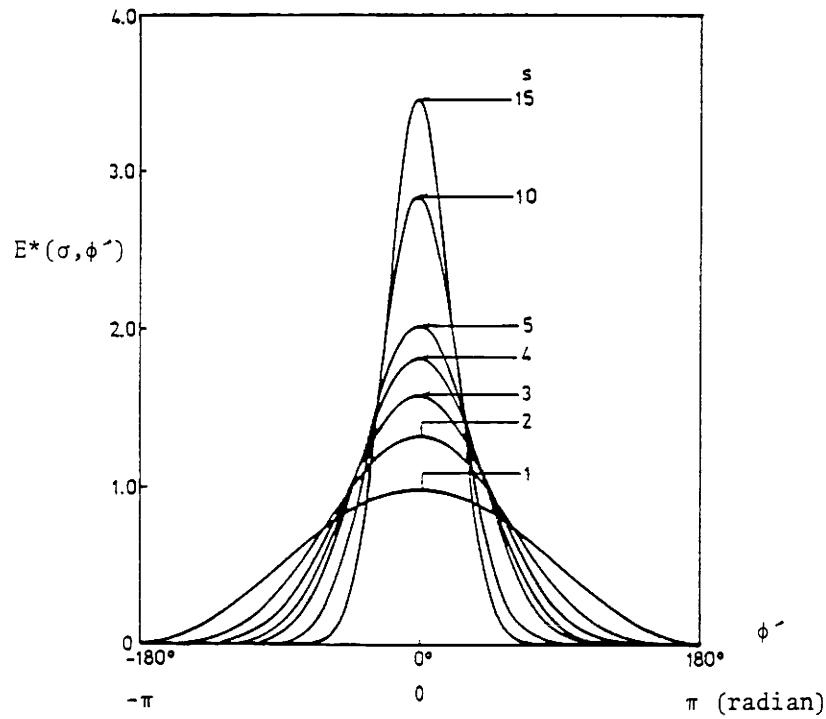


FIG. 2.5 Normalized angular distribution function $E^*(\sigma,\phi')$ (Sand, 1979)

by Longuet-Higgins, Cartwright and Smith(1963) using buoy measurements, is shown in Fig. 2.6. Another example showing the one-dimensional spectrum, as well as variations of s and $\phi_o$ appears in Fig. 2.7; this was obtained by Mitsuyasu et al.(1975) using a cloverleaf buoy in the Pacific Ocean in 1971. Also, directional properties obtained by Forristall et al.(1978) using measurements of $\eta(t)$, $u(t)$, and $v(t)$, (Gulf of Mexico, tropical hurricane Delia, 1973) are shown in Fig. 2.8. The proceduce used to analyze the directional properties in these examples is the stochastic approach. From these examples, one can deduce that the central angles of low frequency waves vary with long period swell from multiple storm sources, while the high frequency components follow the local wind direction. The great variation in $\phi_o$ for hurricane measurements as seen in Fig. 2.8 is due to the relatively rapid change in the storm track. The variation in the spreading parameter, however, shows a

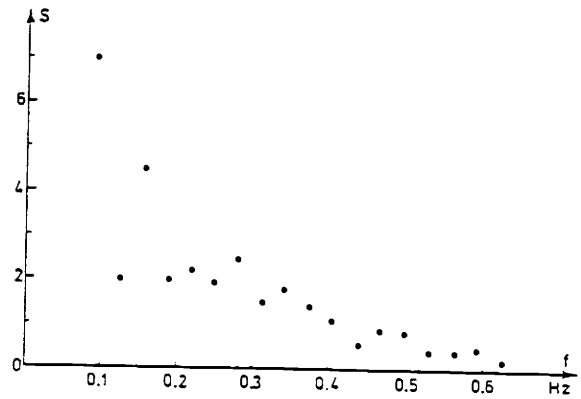


FIG. 2.6 Parameter s verses frequency $f=\sigma/2\pi$ (Longuet-Higgins et al., 1963)

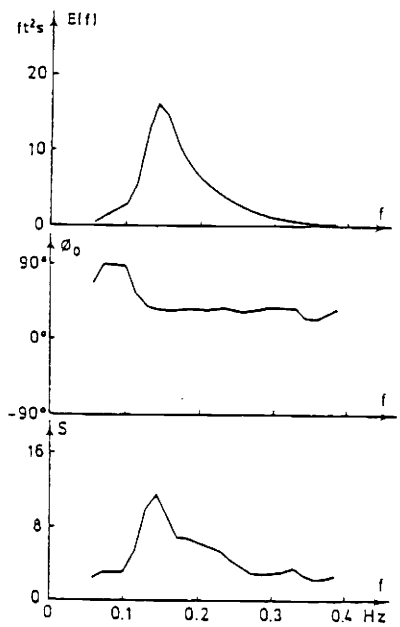


FIG. 2.7 Example frequency spectrum, central angle, spreading parameter behavior (Mitsuyasu et al., 1975)

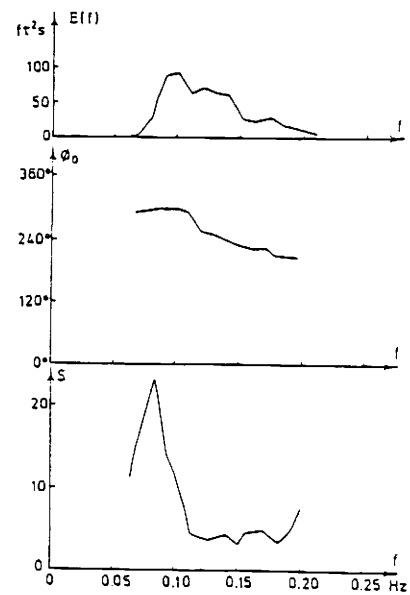


FIG. 2.8 Example frequency spectrum, central angle, spreading parameter behavior (Forristall et al., 1978)

maximum near the spectral peak, decreasing on both sides of the peak. These are features commonly observed by many researchers utilizing this method of analysis on real ocean data.

The decrease of the spreading parameter on the low frequency, left side, of the spectral peak is not always significant. It is believed that a high spreading parameter should be reasonable for low frequency components if the measured wave properties are generated by a single storm. The low frequency wave components generally decay very slow and resist angular dispersion due to cross wind and currents. Consequently, low frequency waves must have high spreading parameters which indicate narrow angular distributions of wave energy. In contrast, a broad angular distribution of wave energy, which occurs for low spreading parameters, will spread energy over a wide range of directions. This will appear as a rapid decay of wave amplitude with distance. An irregular water surface elevation may be composed of swell coming from various remote storms. This could appear, numerically, as a high degree of spreading at low frequency yielding low spreading parameter values.

The variation of the spreading parameter with respect to spectral shape has been studied by Sand(1979). Utilizing the least square method , an empirical formulation has been defined in his research as (Sand, 1979)

$$s(\sigma)= 5\cdot(\sigma^*_{1,-1})^{-2.7}= 5\cdot(\frac{\sigma}{\sigma_{1,-1}})^{-2.7} \qquad (2.43\text{-}1)$$

where

$$\sigma_{1,-1}= \sqrt{m_1/m_{-1}} \ , \qquad (2.43\text{-}2)$$

$\sigma^*_{1,-1}$ is a dimensionless parameter, $m_n$ is the n'th moment of the one-dimensional spectrum. The reason he chose the parameter $\sigma_{1,-1}$ is that the mean frequency $\sigma_{1,o}=m_1/m_o$ emphasizes the high frequency components, while $\sigma_{o,-1}=m_o/m_{-1}$ emphasizes the low frequency components. Therefore,

a reasonable parameter seems to be $\sigma_{1,-1}=\sqrt{m_1/m_{-1}}$. The variation of the spreading parameter with respect to $\sigma^*_{1,-1}$ for the Baltic Sea (Sand et al., 1979) is compared with similar functions obtained in the Gulf of Mexico (Forristall et al., 1978) and in the Atlantic Ocean (Longuet-Higgins et al., 1963), in Fig. 2.9. Although the data have been obtained in quite different conditions, the curves, appearing in Fig. 2.9, agree well with the empirical formula.

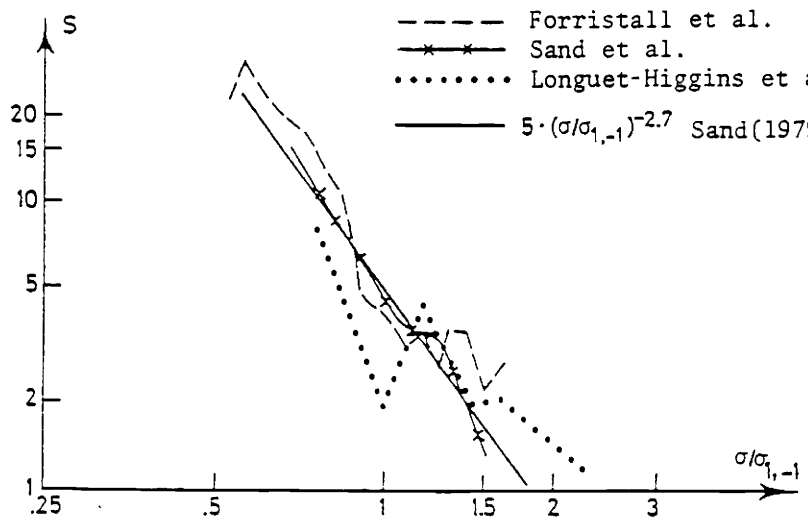


FIG. 2.9 Parameter s verses dimensionless frequency $\sigma^*_{1,-1}$ (Sand, 1979)

## 2.4 Deterministic Approach

It has been mentioned in the theoretical development of the stochastic approach that the phase information is ignored in the method. This limitation does not interfer with directional spectrum calculations, however, it does preclude computations required to predict the water surface profile or other wave properties. Thus, for applications wherein interest lies in the actual shapes of the higher waves, or wave grouping, etc., a description of the phase relationship among the decomposed

frequency components of various wave property measurements must be included in the spectral analysis. A procedure which analyzes directional wave properties utilizing phase information has been derived by Sand (1978). The method is called the Deterministic approach, and it is based on generating a group of small amplitude wavelets directly from a Fourier decomposition of simultaneous wave property measurements. The frequencies of the individual wavelets are uniformly spaced along the frequency axis in accordance with traditional Fourier analyses. The directions and phases are also determined for these wavelets at each frequency. Then, the one-dimensional frequency spectrum and its directional wave properties are evaluated from the relative wavelet properties at each frequency. Further interpretation of the wavelet properties leads to an estimate of the directional spectrum. The deterministic approach provides sufficient information to predict the sea surface profile as well as subsurface kinematic and dynamic wave properties. However, a disadvantage of the method is that orthogonal components of the same frequency are by definition $90^{\circ}$ out of phase. It will be demonstrated later that this phase constraint is an arbitrary limitation, and will cause inappropriate estimates to the directional wave properties.

A summary of the steps used to derive the deterministic directional spectrum in the following discussion is presented below.

(1) The linear decomposition of various wave property measurements is performed by Fourier transformation.

(2) Orthogonal components of various wave property measurements at the same frequency are used to determine a pair of wavelets at that frequency, each propagating with its own direction and phase. However, the phases of such a pair of wavelets have been specified to be $0^{\circ}$ and $90^{\circ}$, respectively, by representing one component as a cosine wave and the other as a sine wave.

(3) The wavelets can be obtained from either the pressure record

or the two velocity component records. The two solutions are combined via a redistribution procedure based upon a least square error analysis.

(4) Utilizing the wave energy density concept of linear wave theory, a progressive wavelet quantifies a parcel of wave energy in the direction of the wavelet. Thus, the frequency dependent Fourier coefficients, which have been introduced in Section 2.3.2, can be evaluated by the relative wavelet properties. The procedure used to quantify the central angle and spreading parameter then follows the method elaborated in section 2.3.3.

### 2.4.1 Deterministic Study of Ocean Waves

To start the analysis, a simple harmonic fluctuation at the water surface is assumed to be observed from a single point and is expressed by taking the real part of a complex number presentation of wave profile

$$\eta_n(\vec{s}_1,t)=Re[\alpha_\eta(\sigma_n)e^{i(\vec{k}\cdot\vec{s}_1-\sigma_n t)}] \qquad (2.44\text{-}1)$$

where $\alpha_\eta(\sigma_n)$ denotes a complex number amplitude at a frequency $\sigma_n$. Let $\alpha_\eta(\sigma_n)=a_\eta(\sigma_n)+ib_\eta(\sigma_n)$ and translate the origin of our co-ordinates to the point where the measurements are made, i.e., $\vec{s}_1=0$. Thus, Eq.(2.44-1) can be simplified as

$$\eta_n(t)=\eta_n(0,t)=Re[(a_\eta(\sigma_n)+ib_\eta(\sigma_n))e^{i(-\sigma_n t)}]$$

$$=a_\eta(\sigma_n)\cos\sigma_n t+b_\eta(\sigma_n)\sin\sigma_n t$$

$$=a_{\eta n}\cos\sigma_n t+b_{\eta n}\sin\sigma_n t \qquad (2.44\text{-}2)$$

where subscript n indicates the frequency $\sigma_n$. Equation (2.44-2) may be interpreted in two different ways. The traditional interpretation for one-dimensional waves is that orthogonal components can be combined to present one single harmonic wave propagating unidirectionally with a phase specified by the relative magnitudes of $a_{\eta n}$ and $b_{\eta n}$. However, for

directional wave analysis, each of the orthogonal components of the same frequency may be regarded as a simple harmonic wave propagating with its own unique direction and phase. The latter prescribes the existence of a cosine wave and a sine wave propagating on the water surface in different directions. However, the sine and cosine waves are by definition $90^{o}$ out of phase.

By a linear superposition, an irregular sea surface can be represented by summing together numerous frequency dependent harmonic wavelets, identified in Eq.(2.44-2). This representation of surface waves, subsurface wave-induced dynamic pressure and horizontal velocity components is summarized below.

$$\eta(t)=\sum_{n=1}^{\infty} Re[\alpha_{\eta n}e^{-i\sigma_n t}]=\sum_{n=1}^{\infty}[a_{\eta n}\cos\sigma_n t+b_{\eta n}\sin\sigma_n t] \tag{2.45-1}$$

$$u(t)=\sum_{n=1}^{\infty} Re[\alpha_{un}e^{-i\sigma_n t}]=\sum_{n=1}^{\infty}[a_{un}\cos\sigma_n t+b_{un}\sin\sigma_n t] \tag{2.45-2}$$

$$v(t)=\sum_{n=1}^{\infty} Re[\alpha_{vn}e^{-i\sigma_n t}]=\sum_{n=1}^{\infty}[a_{vn}\cos\sigma_n t+b_{vn}\sin\sigma_n t] \tag{2.45-3}$$

$$p(t)=\sum_{n=1}^{\infty} Re[\alpha_{pn}e^{-i\sigma_n t}]=\sum_{n=1}^{\infty}[a_{pn}\cos\sigma_n t+b_{pn}\sin\sigma_n t] \tag{2.45-4}$$

Note that Eqs.(2.45-1,2,3,4) anticipate the application of Fourier analysis, and the zero-order coefficients have been omitted due to zero-mean wave properties. Therefore, the relative Fourier coefficients are expressed as

$$a_{\eta n}+ib_{\eta n}=\alpha_{\eta n}=\frac{2}{T}\int_{-T/2}^{T/2}\eta(t)e^{i\sigma_n t}dt \tag{2.46-1}$$

$$a_{un}+ib_{un}=\alpha_{un}=\frac{2}{T}\int_{-T/2}^{T/2}u(t)e^{i\sigma_n t}dt \tag{2.46-2}$$

$$a_{vn}+ib_{vn}=\alpha_{vn}=\frac{2}{T}\int_{-T/2}^{T/2} v(t)e^{i\sigma_n t}dt \qquad (2.46\text{-}3)$$

$$a_{pn}+ib_{pn}=\alpha_{pn}=\frac{2}{T}\int_{-T/2}^{T/2} p(t)e^{i\sigma_n t}dt \qquad (2.46\text{-}4)$$

where T is the total record length, and n=1,2,3,$\cdots$. A factor, 2, appears in Eq.(2.46-1,2,3,4) because only the positive frequency has been considered in this analysis. According to the Fourier transformation, the fundamental frequency is inversely proportional to total record length T and is defined as

$$\Delta\sigma=\frac{2\pi}{T}$$

Then, frequencies are equally spaced on both positive and negative sides of frequency axis. If a total of N points is applied in the Fourier transformation, the positive frequencies which are considered here will be represented as

$$\sigma_n=n\Delta\sigma, \qquad n=1,2,\cdots,N/2$$

From linear wave theory, the water surface components, Eq.(2.46-1), can be transferred to subsurface wave property components, Eqs.(2.46-2,3,4), and such a procedure can be easily reversed. Utilizing transfer functions, defined in Eqs.(2.10) and (2.11), we have the following identities for an arbitrary frequency $\sigma_n$:

$$a_{un}+ib_{un}=K_n[a_{2\eta n}\cos\phi_{an}+ib_{2\eta n}\cos\phi_{bn}] \qquad (2.47\text{-}1)$$

$$a_{vn}+ib_{vn}=K_n[a_{2\eta n}\sin\phi_{an}+ib_{2\eta n}\sin\phi_{bn}] \qquad (2.47\text{-}2)$$

$$a_{pn}+ib_{pn}=K_{pn}[a_{0\eta n}+ib_{0\eta n}] \qquad (2.47\text{-}3)$$

where subscript 0 indicates the wavelet properties obtained from the

pressure record p(t), subscript 2 indicates the wavelet properties obtained from the velocity records u(t) and v(t), and $\phi_{an}$, $\phi_{bn}$ are the propagating directions of the frequency dependent cosine and sine wavelets, respectively. Therefore, the wavelets and their propagating directions can be solved simultaneously from Eqs.(2.47-1,2,3).

$$a_{0\eta n} = a_{pn}/K_{pn}, \qquad b_{0\eta n} = b_{pn}/K_{pn} \tag{2.48-1}$$

$$|a_{2\eta n}| = \sqrt{a_{un}^2 + a_{vn}^2}\ /K_n, \quad |b_{2\eta n}| = \sqrt{b_{un}^2 + b_{vn}^2}\ /K_n \tag{2.48-2}$$

$$\phi_{an} = \tan^{-1}\left(\frac{a_{vn}}{a_{un}}\right), \qquad \phi_{bn} = \tan^{-1}\left(\frac{b_{vn}}{b_{un}}\right) \tag{2.48-3}$$

The sign of $a_{2\eta n}$ and $b_{2\eta n}$ is determined from $a_{pn}$ and $b_{pn}$, respectively. Negative values are possible for $a_{0\eta n}$ and $b_{0\eta n}$, and this will change the wavelet direction by $180^\circ$ relative to positive amplitudes. Accordingly, the sign of the pressure amplitude is used to interpret the sign of the wavelet amplitude, and to remove the $180^\circ$ ambiguity from the wavelet direction. Thus,

$$a_{2\eta n} = |a_{2\eta n}|\ \frac{|a_{pn}|}{a_{pn}}, \qquad b_{2\eta n} = |b_{2\eta n}|\ \frac{|b_{pn}|}{b_{pn}} \tag{2.48-4}$$

$$\phi_{an} = \tan^{-1}\left[\frac{(a_{vn}|a_{pn}|/a_{pn})}{(a_{un}|a_{pn}|/a_{pn})}\right], \quad \phi_{bn} = \tan^{-1}\left[\frac{(b_{vn}|b_{pn}|/b_{pn})}{(b_{un}|b_{pn}|/b_{pn})}\right] \tag{2.48-5}$$

Fourier analysis of the pressure and velocity records provides six known pressure and velocity coefficients at each frequency to solve for two wavelet amplitudes and two wave directions. The deterministic approach prescribes the phase of the sine and cosine wavelets, thereby eliminating two more unknowns which could be solved from the six Fourier coefficients. As a result the solution is overprescribed, yielding one set of wavelet amplitudes from the pressure measurements, Eq.(2.48-1), and

one set of wavelet amplitudes from the velocity measurements corrected for sign with pressure in Eq.(2.48-4). Then a single set of wavelet amplitudes is determined by minimizing the difference between the two solutions in a least square error sense (Sand, 1979). In this procedure, wavelets of a frequency band comprising L successive frequencies are used to evaluate the final wavelet amplitudes, denoted as $a_{\eta n}$ and $b_{\eta n}$, according to:

$$\{\sum_{n=\ell-L/2}^{\ell+L/2}(a_{\eta n}-a_{0\eta n})\}^2+\{\sum_{n=\ell-L/2}^{\ell+L/2}(a_{\eta n}-a_{2\eta n})\}^2 = \text{minimum} \qquad (2.49\text{-}1)$$

$$\{\sum_{n=\ell-L/2}^{\ell+L/2}(b_{\eta n}-b_{0\eta n})\}^2+\{\sum_{n=\ell-L/2}^{\ell+L/2}(b_{\eta n}-b_{2\eta n})\}^2 = \text{minimum} \qquad (2.49\text{-}2)$$

where $\ell=1+L/2,\ 2+L/2,\cdots,(N-L)/2$. The solution from Eqs.(2.49-1,2) can be approximated by (Sand, 1979)

$$a_{\eta n}= a_{2\eta n}+ \frac{1}{2L}\sum_{\ell=n-L/2}^{n+L/2}[a_{0\eta\ell}-a_{2\eta\ell}] \qquad (2.50\text{-}1)$$

$$b_{\eta n}= b_{2\eta n}+ \frac{1}{2L}\sum_{\ell=n-L/2}^{n+L/2}[b_{0\eta\ell}-b_{2\eta\ell}] \qquad (2.50\text{-}2)$$

Finally, the directions can be corrected from the wavelets quantified in Eqs.(2.50-1,2) as

$$\phi_{an}= \tan^{-1}\left[\frac{(a_{vn}|a_{\eta n}|/a_{\eta n})}{(a_{un}|a_{\eta n}|/a_{\eta n})}\right],\quad \phi_{bn}= \tan^{-1}\left[\frac{(b_{vn}|b_{\eta n}|/b_{\eta n})}{(b_{un}|b_{\eta n}|/b_{\eta n})}\right] \qquad (2.50\text{-}3)$$

The choice of the number of frequencies in the frequency band, L, has been determined by trial and error. The appropriate choice for the band is said to be sufficiently small to provide detailed information on frequency dependence while allowing the error to be minimized over a finite number of adjacent frequency components.

One direct consequence of the deterministic approach is that the

water surface elevation at a site near the point where measurements were made can be predicted as

$$\eta(x,y,t)=\sum_{n=1}^{N/2}\{a_{\eta n}\cos[k_n\cos(\phi_{an})x+k_n\sin(\phi_{an})y-\sigma_n t]$$

$$+ b_{\eta n}\sin[k_n\cos(\phi_{bn})x+k_n\sin(\phi_{bn})y-\sigma_n t]\} \qquad (2.51\text{-}1)$$

where $k_n$ is the wave number. Also, a prediction of subsurface wave properties is available by transferring the water surface wavelets to the subsurface wavelet properties. For example, the wave-induced subsurface dynamic pressure and horizontal velocity components can be represented as follows:

$$p(x,y,t)=\sum_{n=1}^{N/2}K_{pn}\{a_{\eta n}\cos[k_n\cos(\phi_{an})x+k_n\sin(\phi_{an})y-\sigma_n t]$$

$$+ b_{\eta n}\sin[k_n\cos(\phi_{bn})x+k_n\sin(\phi_{bn})y-\sigma_n t]\} \qquad (2.51\text{-}2)$$

$$u(x,y,t)=\sum_{n=1}^{N/2}K_n\{a_{\eta n}\cos[k_n\cos(\phi_{an})x+k_n\sin(\phi_{an})y-\sigma_n t]\cos(\phi_{an})$$

$$+ b_{\eta n}\sin[k_n\cos(\phi_{bn})x+k_n\sin(\phi_{bn})y-\sigma_n t]\cos(\phi_{bn})\} \qquad (2.51\text{-}3)$$

$$v(x,y,t)=\sum_{n=1}^{N/2}K_n\, a_{\eta n}\cos[k_n\cos(\phi_{an})x+k_n\sin(\phi_{an})y-\sigma_n t]\sin(\phi_{an})$$

$$+ b_{\eta n}\sin[k_n\cos(\phi_{bn})x+k_n\sin(\phi_{bn})y-\sigma_n t]\sin(\phi_{bn})\} \qquad (2.51\text{-}4)$$

### 2.4.2 Estimating the Wave Spectrum

In the previous section, it has been shown that orthogonal wave property components of the same frequency are used to determine a pair of wavelets at that frequency. Since wavelet frequencies have been uniformly spaced on a frequency axis, a pair of wavelets of the same frequency actually represent the contribution of the irregular water

surface profile within a fundamental frequency interval centered at that frequency. Then, the one-dimensional frequency spectrum can be estimated as

$$E(\sigma_n)=E_n=\frac{1}{2}(a_{\eta n}^2+b_{\eta n}^2)/\Delta\sigma \tag{2.52}$$

where $\Delta\sigma$ is a fundamental radian frequency interval. The total wave energy per unit water surface area per unit water weight can be estimated by summing together all wave energy contributions with respect to frequency. The expression of this total energy density,

$$E_{total}=\sum_{n=1}^{N/2}\frac{1}{2}(a_{\eta n}^2+b_{\eta n}^2)=\sum_{n=1}^{N/2}E_n\Delta\sigma \tag{2.53}$$

is equivalent to Eq.(2.7), and Eq.(2.53) indicates the application of Parseval's theorem (Brighan, 1974). Parseval's theorem says that the energy density computed in the time domain is equal to the energy computed in the frequency domain.

To prove Parseval's theorem, it is necessary to first prove the Correlation theorem, which transforms correlation in the time domain to simple products in the frequency domain by utilizing the Fourier transformation (Brighan, 1974). Substituting Eq.(2.18) into Eq.(2.17) yields

$$\zeta_{ij}(\sigma)=\lim_{T\to\infty}\frac{1}{2\pi T}\int_{-T/2}^{T/2}\omega_i(t)\left[\int_{-T/2}^{T/2}\omega_j(t+\tau)e^{-i\sigma\tau}d\tau\right]dt \tag{2.54-1}$$

Let $t'=t+\tau$, then $\tau=t'-t$, $d\tau=dt'$, and

$$\zeta_{ij}(\sigma)=\lim_{T\to\infty}\frac{1}{4\pi}\int_{-T/2}^{T/2}\omega_i(t)\left[\frac{2}{T}\int_{-T/2}^{T/2}\omega_j(t')e^{-i\sigma t'}dt'\right]e^{i\sigma t}dt \tag{2.54-2}$$

The bracketed term is a complex conjugate of Eqs.(2.46-1,2,3,4),etc. Equation (2.54-2) can be further simplified as

$$\zeta_{ij}(\sigma)=\lim_{T\to\infty}\frac{T}{8\pi}\left[\frac{2}{T}\int_{-T/2}^{T/2}\omega_i(t)e^{i\sigma t}dt\right][a_j(\sigma)-ib_j(\sigma)]$$

$$=\lim_{T\to\infty}\frac{T}{8\pi}[a_i(\sigma)+ib_i(\sigma)][a_j(\sigma)+ib_j(\sigma)]^* \qquad (2.54\text{-}3)$$

As mentioned in Section 2.3.2, a factor of 2 must be inserted in Eq. (2.54-3) to convert from a two-sided spectrum to a one-sided spectrum. Also, the fundamental frequency interval, $\Delta\sigma=2\pi/T$, is substituted in Eq. (2.54-3). Thus, we have

$$\zeta_{ij}(\sigma)=\lim_{\Delta\sigma\to\infty}\frac{[a_i(\sigma)+ib_i(\sigma)][a_j(\sigma)+ib_j(\sigma)]^*}{2\Delta\sigma} \qquad (2.54\text{-}4)$$

Now, the wave properties considered here, i.e., p(t), u(t) and v(t), are all in phase; refer to Eqs.(2.13-1,2,3). Therefore, the correlation functions among them are even functions, e.g., Eq.(2.22), and the induced cross spectra are all real numbers, i.e., co-spectra $C_{ij}(\sigma)$. That is

$$C_{ij}(\sigma)=\mathrm{Re}[\zeta_{ij}(\sigma)]=\frac{1}{2}[\zeta_{ij}(\sigma)+\zeta^*_{ij}(\sigma)]=\frac{1}{2}[\zeta_{ij}(\sigma)+\zeta_{ji}(\sigma)]$$

$$=\lim_{\Delta\sigma\to\infty}\frac{[a_i(\sigma)a_j(\sigma)+b_i(\sigma)b_j(\sigma)]}{2\Delta\sigma} \qquad (2.54\text{-}5)$$

where $\zeta^*_{ij}(\sigma)=\zeta_{ji}(\sigma)$ from Eq.(2.54-2). Equation (2.54-4) presents a general expression of the Correlation theorem, while Eq.(2.54-5) provides a particular case of the Correlation theorem for p(t), u(t) and v(t), measured at the same horizontal location. However, for i=j, the auto-correlation function will always be even and the induced spectrum will be real; this is represented by Eq.(2.54-5). Thus,

$$C_{ii}(\sigma)=\lim_{\Delta\sigma\to\infty}\frac{1}{2}[a_i^2(\sigma)+b_i^2(\sigma)]/\Delta\sigma=E(\sigma) \qquad (2.55)$$

which is a definition of the one-dimensional spectrum. Also, the correlation function can be expressed as a inverse Fourier transform of the cross spectrum. An equivalent expression is

$$\Pi_{ij}(\tau)=\lim_{T\to\infty}\frac{1}{T}\int_{-T/2}^{T/2}\omega_i(t)\omega_j(t+\tau)dt=\int_0^{\infty}\zeta_{ij}(\sigma)e^{-i\sigma\tau}d\sigma$$

Let $\tau=0$ and $i=j$,

$$\overline{\omega_i^2(t)}=\int_0^{\infty}C_{ii}(\sigma)d\sigma=\int_0^{\infty}E_{ii}(\sigma)d\sigma$$

$$=\sum_{n=1}^{N/2}E_{ii}(\sigma_n)\Delta\sigma=\sum_{n=1}^{N/2}\frac{1}{2}[a_{in}^2+b_{in}^2]/\Delta\sigma \qquad (2.56)$$

The expression represented by Eq.(2.56) is Parseval's theorem. According to Parseval's theorem, the mean square value, or variance, of a wave property record $\omega_i(t)$ computed in the time domain can be obtained from a computation in the frequency domain. Note that the existence of Eq.(2.56) provides that $a_{in}$ and $b_{in}$ are directly computed from Fourier transform of the wave property record $\omega_i(t)$. Since the wavelet amplitudes $a_{\eta n}$ and $b_{\eta n}$ which appear in Eq.(2.53) are not the direct Fourier coefficients, Eq.(2.53) does not present a mean square value of the time series $\eta(t)$. However, the value computed in Eq.(2.53) may be interpreted in a mean square sense via the presentation of Eq.(2.4). That is, a total mean square value of waves is a summation of each mean square value of frequency component wavelets. Therefore, the value computed in Eq.(2.53) is interpreted as a mean square value of waves, and the value computed in Eq.(2.56) is interpreted as a mean square value of the time series of a wave property, either measured or predicted.

The analysis of directional wave properties in the deterministic approach is similar to the procedure described in the stochastic approach in Section 2.3.3. The directional spectrum has been expressed as a Fourier series with simple harmonic direction components and frequency dependent coefficients. The Fourier coefficients are defined by the integral in Eq.(2.25-2). The deterministic approach yields two unique wave components at specified directions in each of the equally spaced frequency intervals. Therefore, the continuous integral in Eq.(2.25-2) becomes a simple summation of weighted energy densities of the two di-

rectional components. The first five frequency dependent Fourier coefficients are evaluated from wavelet properties at that same frequency in accordance with:

$$A_{on} = \frac{1}{2}[a_{\eta n}^2 + b_{\eta n}^2]/\Delta\sigma \qquad (2.57\text{-}1)$$

$$A_{1n} = \frac{1}{2}[a_{\eta n}^2 \cos\phi_{an} + b_{\eta n}^2 \cos\phi_{bn}]/\Delta\sigma \qquad (2.57\text{-}2)$$

$$B_{1n} = \frac{1}{2}[a_{\eta n}^2 \sin\phi_{an} + b_{\eta n}^2 \sin\phi_{bn}]/\Delta\sigma \qquad (2.57\text{-}3)$$

$$A_{2n} = \frac{1}{2}[a_{\eta n}^2 \cos 2\phi_{an} + b_{\eta n}^2 \cos 2\phi_{bn}]/\Delta\sigma \qquad (2.57\text{-}4)$$

$$B_{2n} = \frac{1}{2}[a_{\eta n}^2 \sin 2\phi_{an} + b_{\eta n}^2 \sin 2\phi_{bn}]/\Delta\sigma \qquad (2.57\text{-}5)$$

With these five coefficients, the directional frequency spectrum can be estimated with respect to the one angle mode and the double angle mode solution techniques summarized in Section 2.3.3.

### 2.4.3 Similarities Between the Stochastic and Deterministic Approaches

Two uncertainties related to the minimum error principle mentioned in Eqs.(2.49-1,2) should not be ignored. First, the number of frequencies considered in each redistribution of wavelet amplitudes, $a_{\eta n}$ and $b_{\eta n}$, is apriori unknown. Second, numerical results have shown that the wavelet amplitudes estimated from Eqs.(2.48-1) and (2.48-4),separately, do not often relate to each other. Also, a redistribution of wavelet amplitudes will change the estimate of the one-dimensional frequency spectrum and the Fourier coefficients expressed in Eqs.(2.57-1,2,3,4,5). Although the directions, $\phi_{an}$ and $\phi_{bn}$, which are evaluated from measured velocity data will not be affected by the redistribution of wavelet amplitudes, the directional properties of energy distribution can be in error if the frequency component energy densities are not correct. Therefore, the determination of frequency component energy densities

will be restudied in this section by comparing the stochastic and deterministic solutions to the one angle mode and double angle mode directional distributions of wave energy dnesities. This study is based on the Correlation theorem and is summarized as follows.

According to the Correlation theorem, the co-spectrum among simultaneous wave property measurements, p(t), u(t) and v(t), can be expressed in terms of Fourier coefficients of these wave properties.

$$C_{ppn} = \frac{1}{2}[a_{pn}^2 + b_{pn}^2]/\Delta\sigma \qquad (2.58\text{-}1)$$

$$C_{pun} = \frac{1}{2}[a_{pn}a_{un} + b_{pn}b_{un}]/\Delta\sigma \qquad (2.58\text{-}2)$$

$$C_{pvn} = \frac{1}{2}[a_{pn}a_{vn} + b_{pn}b_{vn}]/\Delta\sigma \qquad (2.58\text{-}3)$$

$$C_{uvn} = \frac{1}{2}[a_{un}a_{vn} + b_{un}b_{vn}]/\Delta\sigma \qquad (2.58\text{-}4)$$

$$C_{uun} = \frac{1}{2}[a_{un}^2 + b_{un}^2]/\Delta\sigma \qquad (2.58\text{-}5)$$

$$C_{vvn} = \frac{1}{2}[a_{vn}^2 + b_{vn}^2]/\Delta\sigma \qquad (2.58\text{-}6)$$

Note that Eqs.(2.58-1,2,3,4,5,6) are estimated at equally spaced frequencies. Substituting Eqs.(2.58-1,2,3,4,5,6) into Eqs.(2.26-1,2,3,4,7), the first five frequency dependent Fourier coefficients in the stochastic approach yield

$$A_{on} = \frac{1}{2\pi K_{pn}^2}[a_{pn}^2 + b_{pn}^2]/\Delta\sigma \qquad (2.59\text{-}1)$$

$$A_{1n} = \frac{1}{2\pi K_n K_{pn}}[a_{pn}a_{un} + b_{pn}b_{un}]/\Delta\sigma \qquad (2.59\text{-}2)$$

$$B_{1n} = \frac{1}{2\pi K_n K_{pn}}[a_{pn}a_{vn} + b_{pn}b_{vn}]/\Delta\sigma \qquad (2.59\text{-}3)$$

$$A_{2n} = \frac{1}{2\pi K_n^2}[a_{un}^2 + b_{un}^2 - a_{vn}^2 - b_{vn}^2]/\Delta\sigma \qquad (2.59\text{-}4)$$

$$B_{2n} = \frac{1}{2\pi K_n^2}[a_{un}a_{vn} + b_{un}b_{vn}]/\Delta\sigma \qquad (2.59\text{-}5)$$

Also, $A_{on}$ can be expressed in terms of $C_{uun}$ and $C_{vvn}$ from Eqs.(2.26-1) and (2.27).

$$A_{on} = \frac{1}{2\pi K_n^2}[a_{un}^2 + b_{un}^2 + a_{vn}^2 + b_{vn}^2]/\Delta\sigma \qquad (2.59\text{-}6)$$

Obviously $A_{on}$, which is evaluated in Eq.(2.59-6), should be used in procedures utilizing the double angle mode solutions. This is because $A_{2n}$ will be unique from either Eq.(2.26-4) or Eq.(2.26-5) or Eq.(2.26-6). The coefficients $A_{1n}$ and $B_{1n}$ in the one angle mode solution procedure are expressed in terms of $C_{pun}$ and $C_{pvn}$ which are defined by the integral in Eq.(2.24-2,3). However, there is no evidence which $A_{on}$, i.e., that obtained from either Eq.(2.59-1) or Eq.(2.59-6), should be used in a procedure utilizing the one angle mode solutions.

In the deterministic approach, the first five Fourier coefficients are approximated by the summations of relative wavelet properties in Eqs.(2.57-1,2,3,4,5). Thus, all five coefficients, estimated from Eqs. (2.57-1,2,3,4,5) can be in error if a redistribution of wavelet amplitudes is not exact the induced spectra from these five Fourier coefficients will be in question relative to accuracy. Since $\phi_{an}$ and $\phi_{bn}$ solved in Eq.(2.48-5) in the deterministic approach are more dependent on the velocity component data, and less dependent on pressure data, they can be regarded to provide relatively accurate direction information. Thus, with the Fourier coefficients $A_{1n}$, $B_{1n}$, $A_{2n}$, $B_{2n}$, and the wavelet directions $\phi_{an}$, $\phi_{bn}$, one may obtain alternative solutions to $A_{on}$ depending on whether the one angle mode or the double angle mode solutions are utilized. Alternative solutions to $A_{on}$ are obtained as follows.

To express $\cos\phi_{an}$, $\sin\phi_{an}$, $\cos\phi_{bn}$, $\sin\phi_{bn}$ in terms of $a_{pn}$, $b_{pn}$, $a_{un}$, $b_{un}$, $a_{vn}$, $b_{vn}$, we have

$$\cos\phi_{an} = \frac{a_{un}}{(a_{un}^2 + a_{vn}^2)^{1/2}} \frac{|a_{pn}|}{a_{pn}}, \quad \sin\phi_{an} = \frac{a_{vn}}{(a_{un}^2 + a_{vn}^2)^{1/2}} \frac{|a_{pn}|}{a_{pn}} \qquad (2.60\text{-}1)$$

$$\cos\phi_{bn}=\frac{b_{un}}{(b_{un}^2+b_{vn}^2)^{1/2}}\frac{|b_{pn}|}{b_{pn}},\quad \sin\phi_{bn}=\frac{b_{vn}}{(b_{un}^2+b_{vn}^2)^{1/2}}\frac{|b_{pn}|}{b_{pn}} \qquad (2.60\text{-}2)$$

Then, $\cos2\phi_{an}$, $\sin2\phi_{an}$, $\cos2\phi_{bn}$, and $\sin2\phi_{bn}$ can be derived as

$$\cos2\phi_{an}=\frac{a_{un}^2-a_{vn}^2}{a_{un}^2+a_{vn}^2},\qquad \sin2\phi_{an}=\frac{2a_{un}a_{vn}}{a_{un}^2+a_{vn}^2} \qquad (2.60\text{-}3)$$

$$\cos2\phi_{bn}=\frac{b_{un}^2-b_{vn}^2}{b_{un}^2+b_{vn}^2},\qquad \sin2\phi_{bn}=\frac{2b_{un}b_{vn}}{b_{un}^2+b_{vn}^2} \qquad (2.60\text{-}4)$$

By substituting $\cos2\phi_{an}$, $\sin2\phi_{an}$, $\cos2\phi_{bn}$, $\sin2\phi_{bn}$, derived above, into right sides of Eqs.(2.57-4,5) and $A_{2n}$, $B_{2n}$, derived in Eqs.(2.59-4, 5), into left sides of Eqs.(2.57-4,5), a pair of wavelet amplitudes can be solved at each frequency, $\sigma_n$.

$$|a_{2\eta n}|=\frac{(a_{un}^2+a_{vn}^2)^{1/2}}{K_n},\qquad |b_{2\eta n}|=\frac{(b_{un}^2+b_{vn}^2)^{1/2}}{K_n} \qquad (2.61\text{-}1)$$

Similar to Eq.(2.48-4), the sign of wavelet amplitudes obtained in Eq.( 2.61-1) is determined from the pressure components. Thus,

$$a_{2\eta n}=|a_{2\eta n}|\cdot|a_{pn}|/a_{pn},\qquad b_{2\eta n}=|b_{2\eta n}|\cdot|b_{pn}|/b_{pn} \qquad (2.61\text{-}2)$$

Note that Eqs.(2.61-1,2) are identical to Eqs.(2.48-2,4), and therefore wavelet amplitudes solved from Eq.(2.61-2) or (2.48-4) are suitable in a procedure estimating directional spectrum from the double angle mode solution. The subscript 2 appearing in Eqs.(2.61-1,2) indicates that the wavelet amplitudes solved from Eqs.(2.61-1,2) are more related to velocity component data and are suitable for the double angle mode solution procedure in both stochastic and deterministic approaches.

Now, by substituting $\cos\phi_{an}$, $\sin\phi_{an}$, $\cos\phi_{bn}$, $\sin\phi_{bn}$, derived in Eq. (2.60-1,2), into the right sides of Eqs.(2.57-2,3) and $A_{1n}$, $B_{1n}$, derived

in Eqs.(2.59-2,3), into left sides of Eqs.(2.57-2,3), another pair of wavelet amplitudes can be solved at each frequency, $\sigma_n$.

$$|a_{1\eta n}|=\{\frac{\sqrt{a_{un}^2+a_{vn}^2}|a_{pn}|}{K_n K_{pn}}\}^{\frac{1}{2}}=\{|a_{2\eta n}|\cdot|a_{0\eta n}|\}^{\frac{1}{2}},$$

$$|b_{1\eta n}|=\{\frac{\sqrt{b_{un}^2+b_{vn}^2}|b_{pn}|}{K_n K_{pn}}\}^{\frac{1}{2}}=\{|b_{2\eta n}|\cdot|b_{0\eta n}|\}^{\frac{1}{2}} \qquad (2.62\text{-}1)$$

Note that $a_{0\eta n}$ and $b_{0\eta n}$ are the wavelet amplitudes estimated from pressure data, i.e., Eq.(2.48-1). The sigh of wavelet amplitudes obtained in Eq.(2.62-1) is determined from the pressure components. Thus,

$$a_{1\eta n}=|a_{1\eta n}|\cdot|a_{pn}|/a_{pn}, \qquad b_{1\eta n}=|b_{1\eta n}|\cdot|b_{pn}|/b_{pn} \qquad (2.62\text{-}2)$$

The wavelet amplitudes solved from Eqs.(2.62-1,2) are suitable for procedures estimating directional spectrum from the one angle mode solution. The subscript 1 appearing in Eqs.(2.62-1,2) indicates that the wavelet amplitudes solved from Eqs.(2.62-1,2) are suitable for the one angle mode solution procedure in both stochastic and deterministic approaches.

It is apparent that the magnitude of $a_{1\eta n}$ is equivalent to the geometric mean of the magnitudes of $a_{2\eta n}$ and $a_{0\eta n}$, and the magnitude of $b_{1\eta n}$ is equivalent to the geometric mean of the magnitudes of $b_{2\eta n}$ and $b_{0\eta n}$. Therefore, the wavelet energy density estimates of $a_{0\eta n}$, $b_{0\eta n}$, $a_{1\eta n}$, $b_{1\eta n}$, $a_{2\eta n}$ and $b_{2\eta n}$, have the following properties:

$$E_{1an}=\frac{1}{2}a_{1\eta n}^2/\Delta\sigma=\{E_{0an}\cdot E_{2an}\}^{\frac{1}{2}}, \quad E_{1bn}=\frac{1}{2}b_{1\eta n}^2/\Delta\sigma=\{E_{0bn}\cdot E_{2bn}\}^{\frac{1}{2}} \qquad (2.63)$$

where

$$E_{0an}=\frac{1}{2}a_{0\eta n}^2/\Delta\sigma, \qquad E_{0bn}=\frac{1}{2}b_{0\eta n}^2/\Delta\sigma \qquad (2.64)$$

$$E_{2an}=\frac{1}{2}a_{2\eta n}^2/\Delta\sigma, \qquad E_{2bn}=\frac{1}{2}b_{2\eta n}^2/\Delta\sigma \qquad (2.65)$$

Thus, the one-dimensional frequency spectra of water surface elevation may be estimated by either of the following three expressions:

$$E_{0n}=E_{0an}+E_{0bn}=\frac{1}{2}(a^2_{0\eta n}+b^2_{0\eta n})/\Delta\sigma \tag{2.66-1}$$

$$E_{1n}=E_{1an}+E_{1bn}=\frac{1}{2}(a^2_{1\eta n}+b^2_{1\eta n})/\Delta\sigma \tag{2.66-2}$$

$$E_{2n}=E_{2an}+E_{2bn}=\frac{1}{2}(a^2_{2\eta n}+b^2_{2\eta n})/\Delta\sigma \tag{2.66-3}$$

$E_{0n}$ is estimated from pressure data alone. $E_{1n}$ is estimated from both pressure and velocity data and is referred to as the one angle mode solution. $E_{2n}$ is estimated from velocity data alone and is referred to as the double angle mode solution.

Substituting the relative energy estimates from the one angle mode and double angle mode solutions for $A_{1n}$, $B_{1n}$, $A_{2n}$, $B_{2n}$ in Eqs.(2.57-2,3,4,5) and then combining these equations with the directional wave property estimators in Eqs.(2.39-1) and (2.40-1), we have the following identities:

$$A_{1n}=E_{1an}\cos\phi_{an}+E_{1bn}\cos\phi_{bn}=E_{1n}C_{1n}\cos\phi_{o1n} \tag{2.67-1}$$

$$B_{1n}=E_{1an}\sin\phi_{an}+E_{1bn}\sin\phi_{bn}=E_{1n}C_{1n}\sin\phi_{o1n} \tag{2.67-2}$$

$$A_{2n}=E_{2an}\cos2\phi_{an}+E_{2bn}\cos2\phi_{bn}=E_{2n}C_{2n}\cos2\phi_{o2n} \tag{2.67-3}$$

$$B_{2n}=E_{2bn}\sin2\phi_{an}+E_{2bn}\sin2\phi_{bn}=E_{2n}C_{2n}\sin2\phi_{o2n} \tag{2.67-4}$$

Therefore, $C_{1n}$, $\phi_{o1n}$, $C_{2n}$ and $\phi_{o2n}$ can be solved as

$$C_{1n}=\frac{\sqrt{E^2_{1an}+E^2_{1bn}+2E_{1an}E_{1bn}\cos(\phi_{an}-\phi_{bn})}}{E_{1n}} \tag{2.68-1}$$

$$\phi_{o1n}=\tan^{-1}\frac{E_{1an}\sin\phi_{an}+E_{1bn}\sin\phi_{bn}}{E_{1an}\cos\phi_{an}+E_{1bn}\cos\phi_{bn}} \tag{2.68-2}$$

$$C_{2n} = \frac{\sqrt{E_{2an}^2 + E_{2bn}^2 + 2E_{2an}E_{2bn}\cos 2(\phi_{an} - \phi_{bn})}}{E_{2n}} \qquad (2.68\text{-}3)$$

$$\phi_{o2n} = \frac{1}{2}\tan^{-1}\frac{E_{2an}\sin 2\phi_{an} + E_{2bn}\sin 2\phi_{bn}}{E_{2an}\cos 2\phi_{an} + E_{2bn}\cos 2\phi_{bn}} \qquad (2.68\text{-}4)$$

The ambiguity in direction $\phi_{o2n}$ by $180^{o}$ can be corrected by the methods mentioned in section 2.3.3.

The Correlation theorem has been used as a main tool in the similarity study between the stochastic and deterministic approaches in this section. Correlation theorem says that the Fourier transform of the correlation function is equal to products of the relative Fourier coefficients of individual time series at the same frequency. Evidently, the stochastic method estimates the directional distribution of wave energy from the Fourier transform of correlation function of simultaneous wave property measurements. The deterministic method estimates the directional distribution of wave energy from the direct Fourier transform of simultaneous wave property measurements. Hence, utilizing the interpretation of Correlation theorem, both stochastic and deterministic approaches should yield the same method. Since a redistribution of wavelet amplitudes based upon a minimum error principle in the deterministic approach may not improve the estimates of directional energy spreading, the indeterminate wavelet amplitudes make it different to evaluate the frequency dependent Fourier coefficients $A_{on}$, $A_{1n}$, $B_{1n}$, $A_{2n}$ and $B_{2n}$, which are necessary in directional frequency spectrum estimate. However, coefficients $A_{1n}$, $B_{1n}$, $A_{2n}$ and $B_{2n}$, can be obtained from the stochastic solutions. These four coefficients, $A_{1n}$, $B_{1n}$, $A_{2n}$, $B_{2n}$, and two wavelet directions, $\phi_{an}$, $\phi_{bn}$, obtained from the deterministic approach enable us to solve the wavelet amplitudes and determine the coefficient $A_{on}$. However, the similarity study between the stochastic and deterministic approaches described herein suggests alternative evaluations of the one-dimensional spectrum or the coefficient $A_{on}$ for the one and double angle mode solutions. A combined name, stochastic/deterministic approach, is assigned to the resulting combined method to identify that some improve-

ments have been made for directional spectrum estimates.

The combined stochastic/deterministic one angle mode solution to wave energy spreading is summarized in Eqs.(2.68-1,2). The spreading parameter, s, may be evaluated in terms of $C_1$ via Eq.(2.39-4). The one-dimensional spectrum is evaluated from Eq.(2.66-2).

The combined stochastic/deterministic double angle mode solution to wave energy spreading is summarized in Eqs.(2.68-3,4). The spreading parameter, s, may be evaluated in terms of $C_2$ via Eq.(2.40-4). The one-dimensional spectrum is evaluated from Eq.(2.66-3).

## 2.5 Geometric Approach

It has been demonstrated theoretically in the previous section that a combined stochastic/deterministic approach is superior to the traditional stochastic or deterministic approaches. One limitation of the method, however, is that the deterministic wavelet pairs at each frequency are arbitrarily defined to be $90^{\circ}$ out of phase. Also, a contradiction exists for one-dimensional frequency spectrum estimates between the one angle mode and double angle mode solutions.

To correct these limitations, a geometric approach is proposed which releases the phase constraint mentioned above and which employs both pressure and velocity data to quantify a single one angle mode solution. The geometric approach is an extension of the deterministic approach, utilizing a pair of wavelets in each frequency. A Fourier analysis of pressure and horizontal velocity records provides three known coefficient pairs to quantify two wave amplitudes, two wave directions and two wave phases at each specified frequency.

### 2.5.1 Kinematic Description

The geometric approach defines two simple harmonic wavelets at the water surface to reproduce the behavior of each frequency component of the Fourier analyzed pressure and velocity records. It will be shown

that the measurements of pressure and horizontal vector velocity are sufficient to specify the amplitude, phase and direction of two wavelets at each frequency. Additional measurements would be required to quantify additional wavelet components. The subsurface kinematics and dynamics due to each wavelet are transferred linearly from each wavelet to the subsurface. Furthermore, the gross subsurface kinematics and dynamics are expressed as a linear summation of the transformed wavelet properties (Nagata, 1964).

Now, let us define two wavelets at each frequency as cosine functions with unspecified phase. Let $a_{3\eta n}$, $b_{3\eta n}$ denote the wavelet amplitudes and $\phi_{3an}$, $\phi_{3bn}$, $\theta_{3an}$, $\theta_{3bn}$ denote their directions and phases, respectively, at the frequency $\sigma_n$. The subscript 3 on wavelet amplitude, direction and phase, identifies the results of the geometric method. Let $A(\sigma_n)$ and $B(\sigma_n)$ denote horizontal orbital velocity amplitudes of surface wavelets $a_{3\eta n}$ and $b_{3\eta n}$, respectively, at a height $h_1$ above bottom. Then, according to Eq.(2.9-3), we have

$$A(\sigma_n)= a_{3\eta n}K_n, \qquad B(\sigma_n)= b_{3\eta n}K_n \tag{2.69}$$

In Fig. 2.10, two vector velocities induced by two such surface wavelets are shown by solid lines and a resultant velocity is shown by a bold line. From the addition formula of cosine functions, the individual horizontal velocities can be expanded by the following identities:

$$A(\sigma_n)\cos(\sigma_n t-\theta_{3an})=A(\sigma_n)(\cos\sigma_n t\cos\theta_{3an}+\sin\sigma_n t\sin\theta_{3an})$$

$$=Ac_n\cos\sigma_n t+As_n\sin\sigma_n t \tag{2.70-1}$$

$$B(\sigma_n)\cos(\sigma_n t-\theta_{3bn})=B(\sigma_n)(\cos\sigma_n t\cos\theta_{3bn}+\sin\sigma_n t\sin\theta_{3bn})$$

$$=Bc_n\cos\sigma_n t+Bs_n\sin\sigma_n t \tag{2.70-2}$$

where

$$Ac_n=A(\sigma_n)\cos\theta_{3an}, \qquad As_n=A(\sigma_n)\sin\theta_{3an}, \tag{2.71-1}$$

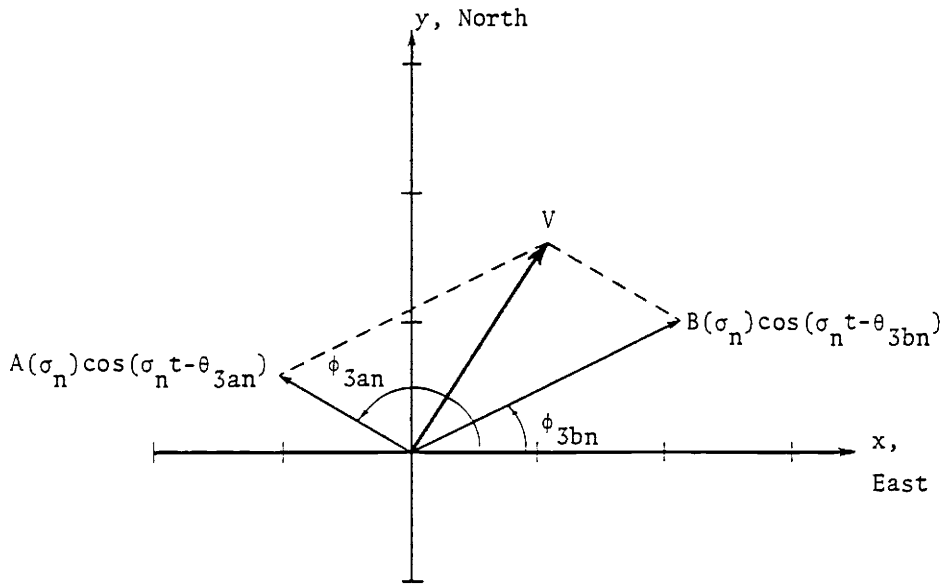


FIG. 2.10 Directional velocity components

$$Bc_n=B(\sigma_n)\cos\theta_{3bn}, \qquad Bs_n=B(\sigma_n)\sin\theta_{3bn}, \tag{2.71-2}$$

are unknown constants.

The Fourier transform of velocity components u(t) and v(t) yields coefficients $a_{un}$ and $a_{vn}$ corresponding to the $\cos(\sigma_n t)$ transform, while $b_{un}$ and $b_{vn}$ correspond to a $\sin(\sigma_n t)$ transform. Thus, Eqs.(2.70-1,2) can be decomposed into x-axis and y-axis components with respect to directions $\phi_{3an}$ and $\phi_{3bn}$, respectively, and equated to the coefficients $a_{un}$, $a_{vn}$, $b_{un}$, $b_{vn}$, of the corresponding $\cos(\sigma_n t)$ and $\sin(\sigma_n t)$ components. Four equations can be expressed as follows:

$\cos(\sigma_n t)$ component on x-axis:

$$a_{un}=Ac_n\cos\phi_{3an}+Bc_n\cos\phi_{3bn} \tag{2.72-1}$$

$\sin(\sigma_n t)$ component on x-axis:

$$b_{un}=As_n\cos\phi_{3an}+Bs_n\cos\phi_{3bn} \tag{2.72-2}$$

$\cos(\sigma_n t)$ component on y-axis:

$$a_{vn}=Ac_n\sin\phi_{3an}+Bc_n\sin\phi_{3bn} \tag{2.72-3}$$

$\sin(\sigma_n t)$ component on y-axis:

$$b_{vn}=As_n\sin\phi_{3an}+Bs_n\sin\phi_{3bn} \tag{2.72-4}$$

The Fourier transform of wave-induced dynamic pressure p(t) yields the coefficient $a_{pn}$ corresponding to a $\cos(\sigma_n t)$ transform, while $b_{pn}$ corresponds to a $\sin(\sigma_n t)$ transform. Since pressure is a scalar, the amplitudes $a_{pn}$ and $b_{pn}$ can be simply transferred to orthogonal components of velocity, denoted as $V_{an}$ and $V_{bn}$, at a height $h_1$ above bottom without considering wavelet direction. Thus, two more equations are obtained by equating the corresponding terms of velocity components expressed in Eqs.(2.70-1,2) to orthogonal velocity components obtained from pressure data, separated as coefficients of the $\cos(\sigma_n t)$ and $\sin(\sigma_n t)$ transformations.

$\cos(\sigma_n t)$ component:

$$V_{an}=a_{pn}K_n/K_{pn}=Ac_n+Bc_n, \tag{2.72-5}$$

$\sin(\sigma_n t)$ component:

$$V_{bn}=b_{pn}K_n/K_{pn}=As_n+Bs_n, \tag{2.72-6}$$

Therefore, at each frequency, we have six equations, Eqs.(2.72-1,2,3,4,5,6), with six unknown parameters, $Ac_n$, $Bc_n$, $As_n$, $Bs_n$, on the right hand side and known values on the left hand side. It is possible to solve the six equations simultaneously to obtain the amplitude, phase and direction of two wavelets at each frequency.

2.5.2 A Solution Procedure

With wave property measurements of p(t), u(t) and v(t), one can solve two wavelets at each frequency with independent directions and phases as given by governing equations, Eqs.(2.72-1,2,3,4,5,6). In the stochastic/deterministic approach, there are also two wavelets defined in each frequency with independent directions but with established phases. This phase constraint may be a severe restriction in directional spectrum estimates. Therefore, Eqs.(2.72-1,2,3,4,5,6) represent a new, geometrically significant, method which is likely to yield improved directional spectrum estimates.

Solving six simultaneous equations can be a tedious, time consuming procedure. Some algebraic operations are performed on the equations in this section to provide a numerically efficient solution technique.

As a first step, $\cos\phi_{3an}$ and $\cos\phi_{3bn}$ can be expressed as follows, from Eqs.(2.72-1,2).

$$\cos\phi_{3an} = \frac{Bs_n a_{un} - Bc_n b_{un}}{Bs_n Ac_n - Bc_n As_n}, \qquad \cos\phi_{3bn} = \frac{Ac_n b_{un} - As_n a_{un}}{Bs_n Ac_n - Bc_n As_n} \tag{2.73-1}$$

Similarly, $\sin\phi_{3an}$ and $\sin\phi_{3bn}$ can be derived as follows, from Eqs.(2.72-3,4)

$$\sin\phi_{3an} = \frac{Bs_n a_{vn} - Bc_n b_{vn}}{Bs_n Ac_n - Bc_n As_n}, \qquad \sin\phi_{3bn} = \frac{Ac_n b_{vn} - As_n a_{vn}}{Bs_n Ac_n - Bc_n As_n} \tag{2.73-2}$$

Combining Eqs.(2.73-1) and (2.73-2) yields

$$(Bs_n a_{un} - Bc_n b_{un})^2 + (Bs_n a_{vn} - Bc_n b_{vn})^2 = (Bs_n Ac_n - Bc_n As_n)^2 \tag{2.74}$$

Then, substracting the square of Eq.(2.72-5) from the sum of the squares of Eq.(2.72-1) and Eq.(2.72-3) yields

$$a_{un}^2 + a_{vn}^2 - V_{an}^2 = 2Ac_n Bc_n \cos(\phi_{3an} - \phi_{3bn}) \tag{2.75-1}$$

Similarly, the same procedure can be applied to Eqs.(2.72-2,4,6).

$$b_{un}^2+b_{vn}^2-V_{bn}^2=2As_n Bs_n \cos(\phi_{3an}-\phi_{3bn}) \tag{2.75-2}$$

Dividing Eq.(2.75-1) by Eq.(2.75-2) yields

$$\frac{a_{un}^2+a_{vn}^2-V_{an}^2}{b_{un}^2+b_{vn}^2-V_{bn}} = \frac{Ac_n Bc_n}{As_n Bs_n} \tag{2.75-3}$$

Now, two parameters, $X_{an}$ and $X_{bn}$, are defined by the following expressions, according to Eqs.(2.72-5,6).

$$Ac_n = \frac{1}{2}(V_{an}+X_{an}), \qquad Bc_n = \frac{1}{2}(V_{an}-X_{an}) \tag{2.76-1}$$

$$As_n = \frac{1}{2}(V_{bn}+X_{bn}), \qquad Bs_n = \frac{1}{2}(V_{bn}-X_{bn}) \tag{2.76-2}$$

Substituting Eqs.(2.76-1,2) into Eqs.(2.74) and (2.75-3), respectively, yields two equations with two unknowns, $X_{an}$ and $X_{bn}$.

$$[(V_{bn}-X_{bn})a_{un}-(V_{an}-X_{an})b_{un}]^2+[(V_{bn}-X_{bn})a_{vn}-(V_{an}-X_{an})b_{vn}]^2$$
$$=[V_{bn}X_{an}-V_{an}X_{bn}]^2 \tag{2.77-1}$$

$$\frac{a_{un}^2+a_{vn}^2-V_{an}^2}{b_{un}^2+b_{vn}^2-V_{bn}^2} = \frac{V_{an}^2-X_{an}^2}{V_{bn}^2-X_{bn}^2} \tag{2.77-2}$$

Then, the parameters $X_{an}$ and $X_{bn}$ are solved as

$$|X_{an}| = \sqrt{\frac{(a_{un}^2+a_{vn}^2)(P_n+Q_n)-V_{an}^2 R_n}{P_n+Q_n-R_n}} \tag{2.77-3}$$

$$|X_{bn}| = \sqrt{\frac{(b_{un}^2+b_{vn}^2)(P_n+Q_n)-V_{bn}^2 R_n}{P_n+Q_n-R_n}} \tag{2.77-4}$$

where

$$P_n=(a_{un}V_{bn}-b_{un}V_{an})^2,\quad Q_n=(a_{vn}V_{bn}-b_{vn}V_{an})^2,\quad R_n=(a_{un}b_{vn}-a_{vn}b_{un})^2 \tag{2.77-5}$$

The correct sign of $X_{an}$ and $X_{bn}$ is determined as follows. Two solutions may be obtained from

$$Ac_n=\frac{1}{2}(V_{an}+|X_{an}|),\qquad Bc_n=\frac{1}{2}(V_{an}-|X_{an}|) \tag{2.78-1}$$

$$As_n=\frac{1}{2}(V_{bn}\mp|X_{bn}|),\qquad Bs_n=\frac{1}{2}(V_{bn}\pm|X_{bn}|) \tag{2.78-2}$$

Two more solutions can be obtained by changing the sign simultaneously in Eq.(2.78-1). However, these are equivalent to the above two solutions since the two wavelets are apriori unknown. Now, only one exact solution is possible from Eqs.(2.78-1,2). Each solution from Eqs.(2.78-1,2) is used to compute sine and cosine angles in Eqs.(2.73-1,2) and, hence, regress $a_{un}$, $b_{un}$, $a_{vn}$, $b_{vn}$ in Eqs.(2.72-1,2,3,4). The correct solution should be able to return the original known values of $a_{un}$, $b_{un}$, $a_{vn}$, $b_{vn}$. The other does not.

Finally, the amplitudes, directions and phases of two independent wavelets of frequency $\sigma_n$ can be expressed as

$$a_{3\eta n}=\frac{A(\sigma_n)}{K_n}=\frac{1}{K_n}\sqrt{Ac_n^2+As_n^2}\ ,\ b_{3\eta n}=\frac{B(\sigma_n)}{K_n}=\frac{1}{K_n}\sqrt{Bc_n^2+Bs_n^2} \tag{2.79-1}$$

$$\theta_{3an}=\tan^{-1}(\frac{As_n}{Ac_n}),\qquad \theta_{3bn}=\tan^{-1}(\frac{Bs_n}{Bc_n}) \tag{2.79-2}$$

$$\phi_{3an}=\tan^{-1}\frac{[(Bs_n a_{vn}-Bc_n b_{vn})/U_n]}{[(Bs_n a_{un}-Bc_n b_{un})/U_n]} \tag{2.79-3}$$

$$\phi_{3bn}=\tan^{-1}\frac{[(Ac_n b_{vn}-As_n a_{vn})/U_n]}{[(Ac_n b_{un}-As_n a_{un})/U_n]} \tag{2.79-4}$$

where $U_n=Bs_nAc_n-Bc_nAs_n$; $U_n$ is used to maintain the correct direction

estimates in Eqs.(2.79-3,4). Note that Eqs.(2.79-3,4) are derived from Eqs.(2.73-1,2) and $U_n$ is the denominator in those equations presented in Eqs.(2.79-3,4).

The amplitudes obtained from Eq.(2.79-1) are always positive since $A(\sigma_n)$ and $B(\sigma_n)$ have been defined as positive values in Eq.(2.79-1). Negative signs in $Ac_n$, $Bc_n$, $As_n$, $Bs_n$, are included in phase values to maintain positive amplitudes. To check the values in the radicals of Eqs.(2.77-3,4), one may substitute Eqs.(2.72-1,2,3,4,5,6) into Eqs.(2.77-3,4), and obtain

$$|X_{an}| = \sqrt{\frac{S_n(Ac_n - Bc_n)^2}{S_n}} = |Ac_n - Bc_n| \tag{2.80-1}$$

$$|X_{bn}| = \sqrt{\frac{S_n(As_n - Bs_n)^2}{S_n}} = |As_n - Bs_n| \tag{2.80-2}$$

where

$$S_n = A^2(\sigma_n)B^2(\sigma_n)\sin^2(\theta_{3an} - \theta_{3bn})[1+\cos(\phi_{3an} - \phi_{3bn})]^2 \tag{2.80-3}$$

The frequency dependent Fourier coefficients, $A_{on}$, $A_{1n}$, $B_{1n}$, $A_{2n}$, $B_{2n}$, can be approximated by summing the appropriate wavelet properties in Eqs.(2.57-1,2,3,4,5), in accordance with the deterministic approach. Directional wave property analysis then proceeds as discussed in section 2.3.3. It should be noted that the one angle mode solution for the geometric approach is more appropriate than the double angle mode solution. Wavelets are obtained from the geometric approach utilizing both pressure and velocity data. It follows that the one angle mode solution, which also utilizes both pressure and velocity information, should provide an analytically consistent method of resolving the direction properties of the geometric wave energy distribution.

## 2.6 Discussion and Comparison of Alternative Methods

In the Section 2.5.2, the unconstrained wavelet phase relationship

has distinguished the geometric approach from the stochastic/deterministic approach. In this section, however, the differences among individual methods will be investigated from various other point of views including both theory and application. The central points included in this discussion are: (1) the one-dimensional frequency spectrum estimators, (2) the theoretical basis of the methods, and (3) the ability to predict the water surface elevation and its subsurface kinematics.

The one-dimensional frequency spectrum estimate in the geometric approach can be simply evaluated from the water surface wavelet amplitudes.

$$E_{3n}=E_{3an}+E_{3bn}=\frac{1}{2}(a_{3nn}^2+b_{3nn}^2)/\Delta\sigma=\frac{1}{2K_n^2}[A^2(\sigma_n)+B^2(\sigma_n)]/\Delta\sigma \qquad (2.81)$$

The geometric approach one-dimensional spectrum estimate, Eq.(2.81), is compared with various other frequency spectrum estimates as follows, by expressing the latter, summarized in Section 2.4.3, in terms of the geometric approach parameters $A(\sigma_n)$, $B(\sigma_n)$, $\phi_{3an}$, $\phi_{3bn}$, $\theta_{3an}$, and $\theta_{3bn}$. The pressure data frequency spectrum in Eq.(2.66-1) becomes

$$E_{0n}=\frac{1}{2K_{pn}^2\Delta\sigma}(a_{pn}^2+b_{pn}^2)=\frac{1}{2K_n^2\Delta\sigma}(V_{an}^2+V_{bn}^2)$$

$$=\frac{1}{2K_n^2\Delta\sigma}[A^2(\sigma_n)+B^2(\sigma_n)+2A(\sigma_n)B(\sigma_n)\cos(\theta_{3an}-\theta_{3bn})] \qquad (2.82\text{-}1)$$

The stochastic/deterministic approach one angle mode frequency spectrum in Eq.(2.66-2) becomes

$$E_{1n}=\frac{1}{2K_n^2\Delta\sigma}(|V_{an}|\sqrt{a_{un}^2+a_{vn}^2}+|V_{bn}|\sqrt{b_{un}^2+b_{vn}^2})$$

$$=\frac{1}{2K_n^2\Delta\sigma}\{[A_n^2\cos^2\theta_{3an}+2A_nB_n\cos\theta_{3an}\cos\theta_{3bn}+B_n^2\cos^2\theta_{3bn}]\cdot$$

$$[A_n^2\cos^2\theta_{3an}+B_n^2\cos^2\theta_{3bn}+2A_nB_n\cos\theta_{3an}\cos\theta_{3bn}\cos(\phi_{3an}-\phi_{3bn})]\}^{\frac{1}{2}}+$$

$$\frac{1}{2K_n^2\Delta\sigma}\{[A_n^2\sin^2\theta_{3an}+2A_nB_n\sin\theta_{3an}\sin\theta_{3bn}+B_n^2\sin^2\theta_{3bn}]\cdot$$

$$[A_n^2\sin^2\theta_{3an}+B_n^2\sin\theta_{3bn}+2A_nB_n\sin\theta_{3an}\sin\theta_{3bn}\cos(\phi_{3an}-\phi_{3bn})]\}^{\frac{1}{2}}$$

(2.82-2)

The frequency spectrum, $E_{1n}$, is an intermediate value between $E_{0n}$ and $E_{2n}$ as derived in Eqs.(2.66-1,3). The stochastic/deterministic approach double angle mode frequency spectrum in Eq.(2.66-3) becomes

$$E_{2n}=\frac{1}{2K_n^2\Delta\sigma}(a_{un}^2+a_{vn}^2+b_{un}^2+b_{vn}^2)$$

$$=\frac{1}{2K_n^2\Delta\sigma}[A^2(\sigma_n)+B^2(\sigma_n)+2A(\sigma_n)B(\sigma_n)\cos(\theta_{3an}-\theta_{3bn})\cos(\phi_{3an}-\phi_{3bn})]$$

(2.82-3)

In general, $E_{0n}$ is not equal to $E_{2n}$ or $E_{1n}$, which is indicated in Eqs.(2.82-1,2,3). However, this is in conflict with the concept that the one-dimensional frequency spectrum of water surface waves should be unique whether it is estimated from pressure or velocity data, or both wave property data. Also Eqs.(2.82-1,2,3) show that the phase differential, $\theta_{3an}-\theta_{3bn}$, has been included in the frequency spectrum estimates, $E_{0n}$, $E_{1n}$, $E_{2n}$, and the direction differential, $\phi_{3an}-\phi_{3bn}$, has been included in the frequency spectrum estimates, $E_{1n}$ and $E_{2n}$. But from a spectral point of view, neither wave phase nor wave direction should appear in the one-dimensional frequency spectrum estimates. A unique one-dimensional frequency spectrum estimate, $E_{3n}$, is obtained from the geometric method and is independent to wavelet direction and phase. To interpret this condition more explicitly, if only two waves of the same frequency are propagating on the water surface with different directions and phases, the correct frequency spectrum estimate will be provided by the geometric approach, not the stochastic/deterministic approach. Therefore, the procedure of estimating the frequency spectrum in the stochastic/deterministic

approach, based on a direct Fourier transform of the auto-covariance functions of wave properties is not totally satisfactory. Note however that if $\theta_{3an}-\theta_{3bn}=90^{o}$, as specified for the stochastic/deterministic approach, all frequency spectrum estimates in Eqs.(2.82-1,3) and (2.81) are identical. Since $\theta_{3an}$ and $\theta_{3bn}$ which are solved from the geometric method do not present this phase relation, $\theta_{3an}-\theta_{3bn}=90^{o}$, in general, the geometric approach would be desirable in estimating the frequency spectrum of water surface waves.

Also note that if all wavelets are propagating in the same direction, i.e., for the one-dimensional waves, we will have $a_{vn}=b_{vn}=0$ and $\phi_{3an}=\phi_{3bn}$ in the geometric method, $\phi_{an}=\phi_{bn}$ in the stochastic/deterministic method. Therefore, $V_{an}=a_{un}$ and $V_{bn}=b_{un}$ from Eqs.(2.72-1,2,3,4,5,6). Note that we assume $\phi_{3an}=\phi_{3bn}=\phi_{an}=\phi_{bn}=0^{o}$. Two results can be solved from the geometric method. One solution shows that $B(\sigma_n)=0$, $A^2(\sigma_n)=a_{un}^2+b_{un}^2$, and $\theta_{3an}=\tan^{-1}(b_{un}/a_{un})$. Another solution shows that $A(\sigma_n)=a_{un}$, $B(\sigma_n)=b_{un}$, $\theta_{3an}=\theta_{an}=0^{o}$ and $\theta_{3bn}=\theta_{bn}=90^{o}$, where $\theta_{an}$ and $\theta_{bn}$ denote the phases of two wavelets at a frequency $\sigma_n$ in the stochastic/deterministic approach. Essentially, the two results are theoretically equivalent and deduce that $E_{0n}=E_{1n}=E_{2n}=E_{3n}$ for one-dimensional waves.

The theoretical similarity between the geometric and deterministic approaches is that they are, in fact, satisfying the simultaneous equations of measured wave properties. In the deterministic approach, three, complex number, fundamental equations are equivalent to six, real number, equations. In the geometric approach, the theory also solves six, real number, simultaneous equations. These fundamental equations are somewhat similar when comparing methods. Actually, the Fourier transform of wave property records on the left hand side of these equations are identical. However, the relationships specified on the right hand side of these equations are not the same for both methods. The solution is over specified in the deterministic approach because only two unknown amplitudes and directions are sought. In the geometric approach, two wavelet amplitudes, two directions and two phases are the unknown parameters in six equations. Thus, the geometric approach seeks a unique solution.

A further advantage of the geometric approach is evident if one has additional measured wave properties. Then, one may solve for more than two wavelets with their respective directions and phases at each frequency and present a closer approximation to the actual directional wave energy distribution. In the stochastic/deterministic approach, one will always obtain additional versions of the frequency spectrum with additional wave property measurements. The redistribution of wavelet amplitudes, or frequency spectra, for the error minimizing procedure will not necessarily provide an improved representation of the directional wave properties. For example, if one has more wave property measurements such as velocity gradients $u_x(t)$, $u_y(t)$ and $v_x(t)$, two additional wavelets can be solved at each frequency in the geometric approach, while five alternative representations of the water surface spectra can be estimated in the stochastic/deterministic approach.

Both the stochastic/deterministic and geometric approaches are capable of predicting the original measured wave properties. Example predictions from the stochastic/deterministic approach were expressed in Eqs.(2.51-1,2,3,4), where the water surface wavelet amplitudes can either be solved from the pressure data or from the one angle mode or double angle mode methods. The water surface elevation due to waves at sites adjacent to the point of measurement can be expressed from the geometric approach as

$$\eta(x,y,t)=\sum_{n=1}^{N/2}\{a_{3\eta n}\cos[k_n\cos(\phi_{3an})x+k_n\sin(\phi_{3an})y+\sigma_n t-\theta_{3an}]$$

$$+\, b_{3\eta n}\sin[k_n\cos(\phi_{3bn})x+k_n\sin(\phi_{3bn})y+\sigma_n t-\theta_{3bn}]\} \qquad (2.83)$$

Predictions of subsurface kinematics and dynamics due to this predicted sea state can be obtained by simply transferring the surface wavelet information, i.e., the right hand side of Eq.(2.83), to subsurface wave properties. As a check, one may calculate the wave properties originally measured at the origin, x=0, y=0. The geometric approach has the ability to return the original measured, wave-induced data since the resolved water surface wavelets are exact solutions of simul-

taneous wave property measurements. However, the stochastic/deterministic approach has the ability to return only a portion of the original wave-induced data, depending on which wave property dominates the one-dimensional frequency spectrum estimate. For example, if the frequency spectrum is estimated from pressure data, the original measured pressure record can be exactly returned without error, but not the measured velocity components. If the frequency spectrum is estimated from velocity components, the original measured velocity components can be precisely returned, but not the pressure data. If the frequency spectrum is estimated from an average or a redistribution of the pressure and velocity data, neither the original measured pressure nor velocity component records can be precisely returned.

It is concluded that the geometric approach presents a good explanation of the theory and provides an appropriate one-dimensional frequency spectrum estimate. Moreover, the geometric approach can reproduce the original measured wave properties. Therefore, results from the geometric approach should provide reliable directional wave energy distribution information for directional spectrum estimates.

# 3. NUMERICAL MODELS

## 3.1 Introduction

Fourier analysis in spectral analysis presents a frequency response of a time series. The application of Fourier analysis implies a linear transformation. The validity of a spectral analysis utilizing Fourier analysis is dependent upon the existence of a linear system, which in time series terminology is said to be a stationary process. A property of a stationary process is that the covariance function of the time series is a function of lag only, not time. Therefore, the covariance functions of simultaneous wave properties derived in Section 2.3.2 have been theoretically defined as lag dependent functions.

A stochastic process may not be stationary. For the non-stationary process time series are characterized by random changes of frequencies, amplitudes and phases. Therefore, Fourier analysis which is based upon the assumption of fixed frequencies, amplitudes and phases is likely to break down when applied to non-stationary processes. Hence, when the spectrum estimate, namely the sample spectrum, is quantified for such a time series its behavior may be so erratic as to render it useless for estimation purposes. In order to overcome this non-stationary effect in spectral analysis, it is necessary to smooth the sample spectrum. This smoothing procedure produces the spectrum estimate, namely the smoothed spectrum, emphasizing the linear behavior of a time series from a statistical point of view. Hence, the smoothed spectrum provides a means of extracting the linear properties of a system, as if the time series were a stationary process (Jenkins and Watts, 1968).

In Chapter 2, theoretical analyses show that the spreading parameter and central angle are also functions of frequency. This implies that the spreading parameter and central angle are also affected by non-stationary processes. Therefore, a smoothing technique, different from that used to generate the sample spectrum, has been employed to evaluate the spreading parameter and central angle. The directional spectrum

obtained from the smoothed frequency spectrum and the smoothed spreading parameter and central angle is named the smoothed directional spectrum.

The utility of a smoothed directional spectrum representation can be enhanced measurably if the quantitative spectrum results can be briefly summarized in equation form. From the equation form, directional spectra can be simply reproduced and quickly applied to other research purposes. In this study, general models have been defined for the one-dimensional frequency spectrum, spreading parameter and central angle to represent the measured directional spectrum.

In the following sections of this chapter, both spectral smoothing and model building will be discussed for directional spectra. A pre-calculation of wave property time domain records will be described first. This will be followed by a summary of computer computational procedures.

## 3.2 Pre-calculations for Measured Wave Properties

Two methods are presented to analyze directional spectra; they are the stochastic/deterministic approach and the geometric approach. Computer algorithms of these two methods have been developed as part of this research effort, applying the theoretical results of Chapter 2. The algorithms used in both approaches are based upon a wavelet concept, i.e., Eqs.(2.68-1,2,3,4), (2.79-1,2,3,4) and (2.81). Therefore, the co-spectra are not evaluated in the stochastic/deterministic approach, although they can be efficiently computed by means of the Correlation theorem as demonstrated in Section 2.4.2.

Both algorithms require zero-mean input data of wave-induced dynamic pressure and horizontal orbital velocity components. However, the original recorded data are simultaneously measured, instaneous pressure and horizontal velocity components. The mean current and hydrostatic pressure have been included in the measurements. Thus, a pre-calculation is necessary to process the original recorded data. The tasks included in this pre-calculation are: (1) evaluating the magnitude and

direction of the current, (2) estimating the water depth from the mean pressure, (3) calculating the zero-mean wave properties, (4) collecting some statistical values from time domain calculations, and (5) computing Fourier coefficients of each measured wave property.

Let $p_r(t_n)$, $u_r(t_n)$, $v_r(t_n)$ denote the original recorded pressure and horizontal velocity components, where the subscript n is the index of discrete time $t_n$. The mean current of the measured record is defined as

$$\bar{u}=\sum_{n=1}^{N} u_r(t_n)/N, \qquad \bar{v}=\sum_{n=1}^{N} v_r(t_n)/N \tag{3.1}$$

$$V_c=\sqrt{(\bar{u})^2+(\bar{v})^2} \tag{3.2}$$

$$\phi_c=\frac{\pi}{2}-\tan^{-1}\left(\frac{\bar{v}}{\bar{u}}\right) \tag{3.3}$$

where $V_c$, $\phi_c$ denote the magnitude and direction, respectively, of the mean current. Note that the final expression of direction in this research corresponds to the poles of the compass, i.e., $0^o$ indicates north.

The water depth can be estimated from the mean pressure as

$$\bar{p}=\sum_{n=1}^{N} p_r(t_n)/N, \qquad h=h_2+\frac{\bar{p}}{\gamma_o} \tag{3.4}$$

where $h_2$ is the height of the pressure sensor above the sea floor, and $\gamma_o$ is the specific weight of sea water. This water depth is compared with the depth measured by a sensor installed on the bottom of the research vessel.

The zero-mean dynamic pressure and horizontal orbital velocity components can be then obtained by subtracting the relative mean values from the original measurements. That is,

$$u(t_n)=u_r(t_n)-\bar{u}, \quad v(t_n)=v_r(t_n)-\bar{v}, \quad p(t_n)=p_r(t_n)-\bar{p} \tag{3.5}$$

The statistics of interest calculated in the time domain are the variance of the zero-mean horizontal velocity and the gross propagating direction of waves. The variance, or sample mean square value, of zero-mean horizontal velocity can be simply calculated as

$$\overline{V_t^2} = \sum_{n=1}^{N} [u^2(t_n) + v^2(t_n)]/N \tag{3.6}$$

where the subscript t indicates the sample variance, $\overline{V_t^2}$, computed in the time domain. The root mean square value of zero-mean horizontal velocity evaluated in frequency domain may not equal this value according to the results of the geometric approach. However, the double angle mode solution of the stochastic/deterministic approach can return precisely the sample variance, $\overline{V_t^2}$, from a frequency domain evaluation, since the frequency components are directly computed from Fourier transform of the time domain data. The latter can be simply proved from Eq.(2.56) by specifying that i=V and $a_{Vn}^2 = a_{un}^2 + a_{vn}^2$, and $b_{Vn}^2 = b_{un}^2 + b_{vn}^2$.

The gross propagating direction of waves can be approximated as

$$\overline{\phi} = \frac{\pi}{2} - \frac{\sum_{n=1}^{N} V(t_n) \cdot \phi_n}{\sum_{n=1}^{N} V(t_n)} \tag{3.7-1}$$

where

$$V(t_n) = \sqrt{u^2(t_n) + v^2(t_n)}, \tag{3.7-2}$$

and

$$\phi_n = \begin{cases} \tan^{-1}\left[\dfrac{v(t_n)}{u(t_n)}\right] \\ \tan^{-1}\left[\dfrac{v(t_n)}{u(t_n)}\right] \pm \pi \end{cases} \tag{3.7-3}$$

The option in Eq.(3.7-3) is selected by estimating the gross main travel direction of waves e.g., towards the coastline.

The zero-mean time series in discrete form, Eq.(3.5), are satisfactory inputs for directional spectrum analysis utilizing either the stochastic/deterministic or geometric approach. Computer software included in this research is based on FORTRAN V. The Fast Fourier Transform technique employed here is based on the Cooley-Tukey procedure, requiring a number of data points equal to some power of two (Brighan, 1974); hence, $N=2^P$ (P is a positive integer). An elementary flow chart which presents the logical route of this pre-calculation software appears in Fig. 3.1.

## 3.3 Smoothing Procedures for Directional Spectrum Estimations

Random wave property measurements are not necessarily stationary processes, thus any linearly transformed frequency response of zero-mean wave properties needs to be smoothed. As a result, the one-dimensional frequency spectrum, spreading parameter and central angle require smoothing in directional spectrum analyses.

### 3.3.1 Smoothing Procedure for the One-dimensional Frequency Spectrum

A general class of smoothing techniques for one-dimensional frequency spectra has been developed by others (Jenkins and Watts, 1968). The idea of this smoothing procedure is to estimate the one-dimensional spectrum in sub-sections and to compute the total record spectrum from the mean of the spectra from the sub-sections. The total record length T is subdivided into J sections of length M and J spectra are averaged. However, an efficient and equivalent way to do this smoothing is to convolve the total sample spectrum with a function called the spectral window (Jenkins and Watts, 1968). A number of spectral windows are commonly used in spectral analysis but all have similar shape. The choice of a spectral window in the smoothing procedure is of secondary importance. A commonly used spectral window, the Bartlett window, is utilized and denoted as Y(f) in this study. Note that $f=\sigma/(2\pi)$ the wave frequency with units 1/time. The wave frequency f is simply the reciprocal of wave period for a simple harmonic wave. The wave fre-

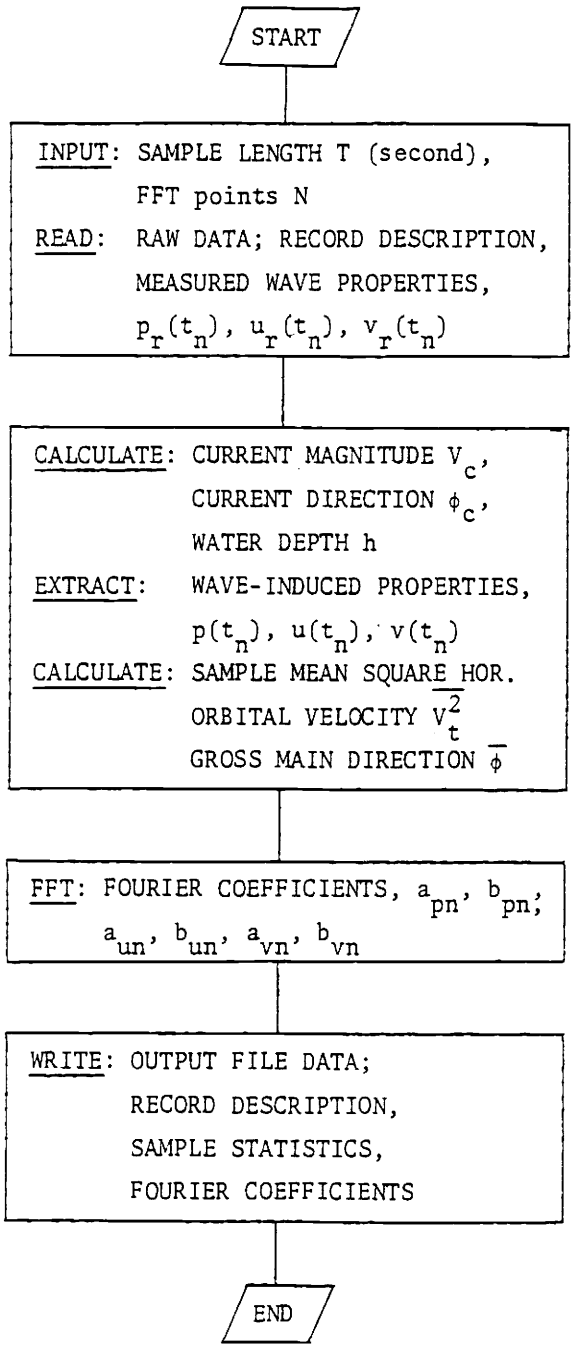


FIG. 3.1 Flow chart of pre-calculation system

quency used in the following discussion will be the frequency f instead of $\sigma$. Also, the wave frequency considered in results of spectrum estimates will be the frequency f instead of $\sigma$. This is because one can easily calculate the wave period for a specified wave frequency f in accordance with linear wave theory. Thus, we have

$$E(f_n)= \frac{1}{2}(a^2_n+b^2_n)/\Delta f= 2\pi\ (\frac{1}{2})(a^2_n+b^2_n)/\Delta\sigma= 2\pi E(\sigma_n) \tag{3.8-1}$$

where

$$\Delta f= \frac{1}{T} = \frac{2\pi}{T}(\frac{1}{2\pi})= \frac{\Delta\sigma}{2\pi} \tag{3.8-2}$$

The smoothing procedure for the one-dimensional frequency spectrum by means of Bartlett spectral window is

$$E(f)=\int_{-\infty}^{\infty}\hat{E}(f-f')Y(f')df' \tag{3.9}$$

where E(f) denotes the smoothed spectrum, $\hat{E}(f)$ denotes the sample spectrum, and

$$Y(f)= M[\frac{\sin(\pi fM)}{\pi fM}]^2 \tag{3.10}$$

is the Bartlett spectral window (Jenkins and Watts, 1968). Equation (3.9) shows that the one-dimensional frequency spectrum is smoothed from the convolution of the sample spectrum and spectral window.

The Bartlett spectral window is plotted in Fig. 3.2 and is seen to be symmetric about the origin. The area under the curve of the spectral sindow is one, or

$$\int_{-\infty}^{\infty} Y(f)df=1 \tag{3.11}$$

Therefore, the one-dimensional frequency spectrum is smoothed in an average sense. The total energy density of water surface waves will not change by this smoothing procedure.

The base width of the Bartlett window, that is, the distance between the first zeros on either side, is 2/M (Hz). By controlling the length M of the sub-sections, one can quantify the base width of the spectral window. There is no rigid rule for determining the number of sub-sections, J, or size M. Ideally, the larger the number of sub-sections and the larger the size M, the more accurate is the resulting spectrum estimate. Hence, T must be sufficiently large. Also, as M is large, the Bartlett spectral window behaves like an impulse function. However, the statistics of wave properties may change considerably during a long time period. Thus, one is compelled to chose an intermediate length T and size M. A general study of spectral smoothing suggests that the base width of the spectral window should be of the same order as the narrowest important detail in the spectrum. For example, in order to estimate the property of the spectral peak, the base width of the spectral window should be chosen to be of the same order as the width of the spectral peak (Jenkins and Watts, 1968).

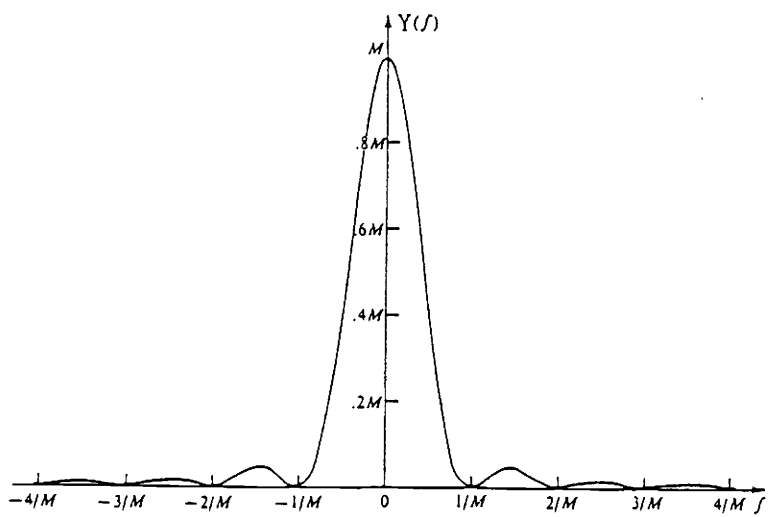


FIG. 3.2 Bartlett spectral window (Jenkins and Watts, 1968)

It will be shown later that a sample length of 512 seconds, digitized every second, satisfies the input requirement for spectral analy-

sis in this study. The base width of the spectral window has been chosen as .016 (Hz) for a sample length of 512 seconds and is assumed to present the narrowest detail required to cover the width of the spectral peak. Hence, the smoothing procedure is equivalent to subdividing the sample length of 512 seconds into four sub-sections of 128 seconds. Since the fundamental frequency interval is 1/T, we have (2/M)/(1/T)=2T/M=8 fundamental intervals in a base width of .016 (Hz). The discrete convolution in Eq.(3.9) is then performed by products of the sample spectrum with seven weighted coefficients, which are normalized constants of the spectral window in the discrete formula. These seven weighted coefficients are: 1/36, 4/36, 8/36, 10/36, 8/36, 4/36, 1/36.

### 3.3.2 Smoothing of the Spreading Parameter and Central Angle

The spreading parameter and central angle also require smoothing in order to remove irregularities due imperfect data sets and digital numerical procedures. Equations (2.39-4) and (2.40-4) reveal that the one angle and double angle mode spreading parameters are functions of $C_1$ and $C_2$, respectively. Thus, the spreading parameter is smoothed by smoothing the coefficients $C_1$ and $C_2$.

Instead of estimating $C_{1n}$, $C_{2n}$, $\phi_{o1n}$, $\phi_{o2n}$ at frequency $f_n$, as indicated in Eqs.(2.67-1,2,3,4) and (2.68-1,2,3,4), wavelets in the neighborhood of $f_n$ are included in this smoothing procedure. That is, a wider frequency band is considered to yield the directional wave property estimates at the central frequency, $f_n$, of that band. Parameters $C_{1n}$, $C_{2n}$, $\phi_{o1n}$, $\phi_{o2n}$, are computed in a smooth, or local average, sense. The number of frequencies, denoted as I, involved in this wider band should be of the same order as the width of the narrowest important detail of frequency dependent directional wave properties. Then, Eqs.(2.67-1,2,3,4) are rewritten as

$$\sum_{i=n-I/2}^{n+I/2}\{E_{1an}\cos\phi_{an}+E_{1bn}\cos\phi_{bn}\}_i=C_{1n}\cos\phi_{o1n}\sum_{i=n-I/2}^{n+I/2}\{E_{1n}\}_i \qquad (3.12\text{-}1)$$

$$\sum_{i=n-I/2}^{n+I/2}\{E_{1an}\sin\phi_{an}+E_{1bn}\sin\phi_{bn}\}_i=C_{1n}\sin\phi_{o1n}\sum_{i=n-I/2}^{n+I/2}\{E_{1n}\}_i \qquad (3.12\text{-}2)$$

$$\sum_{i=n-I/2}^{n+I/2}\{E_{2an}\cos2\phi_{an}+E_{2bn}\cos2\phi_{bn}\}_i=C_{2n}\cos2\phi_{o2n}\sum_{i=n-I/2}^{n+I/2}\{E_{2n}\}_i \qquad (3.12\text{-}3)$$

$$\sum_{i=n-I/2}^{n+I/2}\{E_{2an}\sin2\phi_{an}+E_{2bn}\sin2\phi_{bn}\}_i=C_{2n}\sin2\phi_{o2n}\sum_{i=n-I/2}^{n+I/2}\{E_{2n}\}_i \qquad (3.12\text{-}4)$$

where the subscript n indicates the frequency $f_n$. In the geometric approach, $E_{1an}$ and $E_{2an}$ will be replaced by $E_{3an}$, and $E_{1bn}$, $E_{2bn}$ will be replaced by $E_{3bn}$; $E_{1n}$ and $E_{2n}$ will be replaced by $E_{3n}$, and $\phi_{an}$, $\phi_{bn}$ will be replaced by $\phi_{3an}$, $\phi_{3bn}$, respectively. Note that the one-dimensional frequency spectra appearing on the right hand side of Eqs.(3.12-1,2,3,4) are the smoothed spectra. Thus, the wavelet energy densities appearing on the left hand side of Eqs.(3.12-1,2,3,4) are considered as smoothed energy densities, corrected by the ratio of the sample spectrum to the smoothed frequency spectrum at each frequency. In this research, I=5 has been chosen for a total sample length of 512 seconds. This is equivalent to smoothing the information from five adjacent wavelet pairs to obtain the smoothed spreading parameter and central angle for the central frequency in each band.

The smoothed directional wave spectrum is then evaluated in Eq.( 2.37) with respect to a smoothed one-dimensional frequency spectrum, a smoothed spreading parameter and central angle at each frequency. The smoothed directional spectrum of other wave properties can be evaluated by simply transferring the smoothed frequency spectrum of water surface wave elevation to any other wave property.

## 3.4 Proposed Models for Directional Wave Spectra

In this study, the one-dimensional frequency spectrum, spreading parameter and central angle have been identified as frequency dependent variables which control the behavior of the direction spectrum. Therefore, proposing a model for the directional spectrum is equivalent to proposing models for the one-dimensional frequency spectrum, spreading parameter and central angle. Some general semi-empirical equations will be defined in the following sections.

### 3.4.1 JONSWAP Spectrum

The JONSWAP spectrum is selected to describe the frequency dependence of the one-dimensional frequency spectrum. The JONSWAP spectrum is known to cover a large range of spectral shapes (Hasselmann et al., 1975). The expression

$$E_J(f_n)=\frac{\alpha g^2}{(2\pi)^4 f_n^5}\gamma^{\beta}\exp[-\frac{5}{4}(\frac{f_p}{f_n})^4] \tag{3.13}$$

gives the general form of the JONSWAP spectrum, where

$$\beta=\exp[-\frac{(f_n-f_p)^2}{2\sigma_{LR}^2 f_p^2}]$$

$$\sigma_{LR}=\begin{cases}\sigma_L, & \text{for } f_n\leq f_p\\ \sigma_R, & \text{for } f_n>f_p\end{cases} \qquad n=1,2,\cdots,n_p,\cdots,N/2$$

$n_p$= index of frequency at maximum $E(f_n)$

$f_p$= frequency at maximum $E(f_n)$

The parameters defined in the JONSWAP spectrum are: $\alpha$ the Phillips' constant, $\gamma$ the ratio of the maximum spectral density of $E_J(f)$ to that of the corresponding Pierson-Moskowitz spectrum, $\sigma_L$ and $\sigma_R$ are constants proportional to the widths of the left and right sides of the spectral

peak. These parameters are evaluated via a least square error analysis using the measured, smoothed frequency spectrum. The derivation of this least square error analysis is presented in Appendix A.1.

The error of the proposed JONSWAP spectrum compared to the smoothed spectrum, $E(f_n)$, has been defined in a root mean square sense in this study as

$$\varepsilon_{rms,1\text{-}D} = \frac{\sqrt{\sum_{n=1}^{N} [E_J(f_n)-E(f_n)]^2}}{\sum_{n=1}^{N} E(f_n)} \tag{3.14}$$

Since $\varepsilon_{rms,1\text{-}D}$ presents a ratio of total root square error to total energy density, a small value of $\varepsilon_{rms,1\text{-}D}$ implies that the proposed JONSWP spectrum is a good approximation to the measured, smoothed spectrum.

The statistical values collected from this proposed JONSWAP spectrum in the frequency domain are: total spectral density $E_{total}$, peak spectral density $E_p$, and dimensionless frequency $f_{1,-1}$ which is identical to $\sigma_{1,-1}$ defined in Eq.(2.43-2). This dimensionless frequency, $f_{1,-1}$, is relatively insensitive to slight changes in spectral shape. Since a slight change in spectral shape may cause a considerable change in the JONSWAP parameters, $f_{1,-1}$ may be viewed as an important indicator of spectral shapes.

### 3.4.2 Proposed Equations for the Spreading Parameter and Central Angle

In Section 2.3.3, a general description of the spreading parameter distribution identified a maximum value near the spectral peak frequency with decreasing values for larger or smaller frequencies. The frequency at which the maximum spreading parameter occurs is called the critical frequency in this study and denoted as $f_c$. The maximum spreading parameter is $s_c$. Usually $f_c$ is smaller than $f_p$. The observed slow decrease in the spreading parameter on the right side of $s_c$ occurs because high

frequency waves experience greater directional spreading due to cross currents and winds. The observed decreases in the spreading parameter on the left side of $s_c$ occur because low frequency energy may be composed of many persistent long waves arriving from independent storm sources and unique directions.

Accordingly, the spreading parameter is represented on each side of $s_c$ by unique, two parameter power functions of frequency as

$$s_e(f_n)=A_{LR}f_n^{B_{LR}} \tag{3.15}$$

where

$$(A_{LR},B_{LR})=\begin{cases}(A_L,B_L), & \text{for } f_n<f_c\\ (A_R,B_R), & \text{for } f_n\geq f_c\end{cases} \qquad n=1,2,\cdot\cdot,n_c,\cdot\cdot,N/2$$

$n_c$= index of frequency at maximum $s(f_n)$

and $s_e(f_n)$ denotes the proposed empirical spreding parameter. This form of the equation is an extension of that suggested by Sand (1979), as presented in Eq.(2.43-1). The determination of $A_{LR}$ and $B_{LR}$ also utilizes a least square error analysis, which is presented in Appendix A.2.

Under some circumstances it may be appropriate to choose a constant value for the spreading parameter on the left side of $s_c$. It has been observed in many data sets of this study that the behavior of spreading parameter on the left side of fc may be approximated by a constant $.8s_c$ for the stochastic/deterministic approach and a constant $.9s_c$ for the geometric approach. Hence, Eq.(3.15) becomes

$$s_e(f_n)=A_L=\begin{cases}.8\ s_c, & \text{for stochastic/deterministic approach}\\ .9\ s_c, & \text{for geometric approach}\end{cases}$$

$$B_L = 0, \qquad \text{for } f_n < f_c \tag{3.16}$$

The two parameter power function is still utilized for the spreading parameter utilizing two power functions on each side of $s_c$ and will be referred to as the two-sided spreading parameter model. The proposed spreading parameter utilizing a constant on the left side of $s_c$ and a power function on the right side of $s_c$ will be referred to as the one-sided spreading parameter model.

A third-order polynominal function of frequency,

$$\phi_{poly}(f_n) = c_o + c_1 f_n + c_2 f_n^2 + c_3 f_n^3 \tag{3.17}$$

is proposed to model the central angle. This equation allows for a relative maximum or minimum in $\phi_o(f_n)$ as observed from many data sets associated with this study. Let $\phi_{oe}(f_n)$ denote the empirically proposed central angle function. Then

$$\phi_{oe}(f_n) = \phi_{poly}(f_n) \tag{3.18}$$

The coefficients $c_o$, $c_1$, $c_2$, and $c_3$, of Eq.(3.17) are determined by a least square error analysis, weighted with the frequency spectrum energy level appropriate to each frequency. The weighting procedure emphasizes central angle behavior near the spectral peak. A detailed presentation of this least square error analysis appears in Appendix A.3.

As a first approximation, a weighted main direction, defined as

$$\phi_{main} = \frac{\sum_{n=1}^{N} \phi_o(f_n) E(f_n)}{\sum_{n=1}^{N} E(f_n)} \tag{3.19}$$

may be employed to represent the directional spreading central angle. Then a constant value is proposed for the central angle function

$$\phi_{oe}(f_n)=\phi_{main} \tag{3.20}$$

The error associated with either empirical central angle function is evaluated as

$$\varepsilon_{rms,\phi_o}=\sqrt{\frac{\sum_{n=1}^{N}[\phi_{oe}(f_n)-\phi_o(f_n)]^2E(f_n)}{\sum_{n=1}^{N}E(f_n)}} \tag{3.21}$$

Both Eqs.(3.17) and (3.19) are utilized for the empirical central angle function in the data analysis.

## 3.5 Systematic Analysis of the Estimated Directional Spectrum

An estimation of the smoothed directional spectrum is based upon Eq.(2.37) utilizing three smoothed frequency dependent functions: the one-dimensional spectrum, the spreading parameter and central angle. In a discrete formula, this smoothed directional spectrum can be expressed as

$$E(f_n,\phi_m)=E(f_n)\frac{2^{2s(f_n)-1}}{\pi}\frac{\Gamma^2[s(f_n)+1]}{\Gamma[2s(f_n)+1]}\cos^{2s(f_n)}[\frac{\phi_m-\phi_o(f_n)}{2}] \tag{3.22}$$

where

$$f_n=n\Delta f, \qquad n=1,2,\cdots,N'$$

$$\phi_m=m\Delta\phi, \qquad m=1,2,\cdots,M'$$

The frequency interval, $\Delta f=1/T$, has been referred as the fundamental frequency in Finite Fourier Transformation procedures. The direction interval, $\Delta\phi$, has been chosen as $1^o$ or $2\pi/360$ radians in data analysis in this study. $M'$ and $N'$ (both integers) are the total number of discrete directions and frequencies, respectively, which are uniformly

spaced on the direction and frequency axes.

In general, the integer N′ has a maximum value of N/2 where N is the total number of data points on the wave property record utilized in the Fourier transformation. The spectral density can be computed up to a frequency of $N'\Delta f$, where N′ is less than N/2, if the spectral density of higher frequencies is not of interest. As a practical consideration, an upper limit should be set for N′ to avoid high frequency signals from sources other than surface waves. For example, with a measurement system installed near the ocean bottom, the Fourier coefficients associated with high frequencies should be ignored because these high frequency components may be caused by turbulence and electronic or mechanical noise rather than water surface waves. Accordingly, spectral density analysis should be truncated at the deep-water wave frequency (Ippen, 1966) for wave sensors located at the sea bed.

The deep-water wave is usually defined in ocean engineering as

$$\tanh(kh)>0.9962, \text{ or } kh>\pi$$

Hence, substituting this relation into the linear wave theory dispersion equation, Eq.(2.2), yields

$$(2\pi f)^2=gk\cdot\tanh(kh)=gk>g\frac{\pi}{h}, \quad \text{or } f>\sqrt{\frac{g}{4\pi h}}$$

Then

$$f_{N'}=N'\Delta f=\sqrt{\frac{g}{4\pi h}} \tag{3.23}$$

is interpreted as the upper limit of frequencies considered in wave spectrum analysis. At this frequency, $f_{N'}$, the sea bed is exposed to less than 9% of the water surface wave motion. This may be demonstrated by evaluating p(t) and V(t) at the sea surface and sea bed in Eqs.(2.8-2,3) with $kh=\pi$. It is concluded that $f_{N'}$ is a function of h. For h=60 (ft), $f_{N'}$=.2 (Hz); for h=200 (ft), $f_{N'}$=.11 (Hz). Ocean waves often

reveal significant energy levels near 0.1 (Hz). In order to sense this wave motion at the sea bed the wave measurement system should be located in a water depth less than 250 feet.

Linear wave theory can be used to demonstrate that deep water breaking waves are limited to high frequency spectral densities which are proportional to the inverse fifth power of frequency. That is (Roll and Fischer, 1956) $E(f) \propto f^{-5}$ at high frequencies. As a result, beyond the frequency $f_{N'}$, spectral densities and, therefore, wave amplitudes rapidly attenuate with increasing frequency. Thus, it is reasonable not to include these high frequency spectral densities in wave spectrum estimates.

Summarizing, the proposed directional spectrum is based on Eq.(2.37) and is expressed in discrete form as

$$E_e(f_n,\phi_m)=E_J(f_n)\frac{2^{2s_e(f_n)-1}}{\pi}\frac{\Gamma^2[s_e(f_n)+1]}{\Gamma[2s_e(f_n)+1]}\cos^{2s_e(f_n)}[\frac{\phi_m-\phi_{oe}(f_n)}{2}] \tag{3.24}$$

where

$f_n=n\Delta f, \qquad n=1,2,\cdots,N'$

$\phi_m=m\Delta\phi, \qquad m=1,2,\cdots,M'$

$N'$ is defined by Eq.(3.23),

$M'$ is limited in this study to 360, or $\Delta\phi=1^o$,

$E_J(f_n)$ is defined by Eq.(3.13)

$s_e(f_n)$ is defined by Eq.(3.15)

$\phi_{oe}(f_n)$ is defined by Eq.(3.18) or (3.20).

However, N´ has no limitation in applications of this model since one can extrapolate directional spectrum from the proposed functions, $E_J(f_n)$ , $s_e(f_n)$ and $\phi_{oe}(f_n)$, outside the range indicated by Eq.(3.23). Finally, the root mean square error between the proposed empirical directional spectrum and smoothed directional spectrum is defined as

$$\varepsilon_{rms,2\text{-}D} = \frac{\sqrt{\sum_{n=1}^{N'}\sum_{m=1}^{M'}[E_e(f_n,\phi_m)-E(f_n,\phi_m)]^2}}{\sum_{n=1}^{N'}\sum_{m=1}^{M'}E(f_n,\phi_m)} \qquad (3.25)$$

The statistical values collected from this proposed directional s spectrum are total spectral energy, dominant frequency and direction at the spectral peak and magnitude of the spectral peak. A flow chart summarizing directional spectrum calculation in this study appears in Fig. 3.3. A computer listing of the program used to perform these digital calculation is presented in Appendix C.

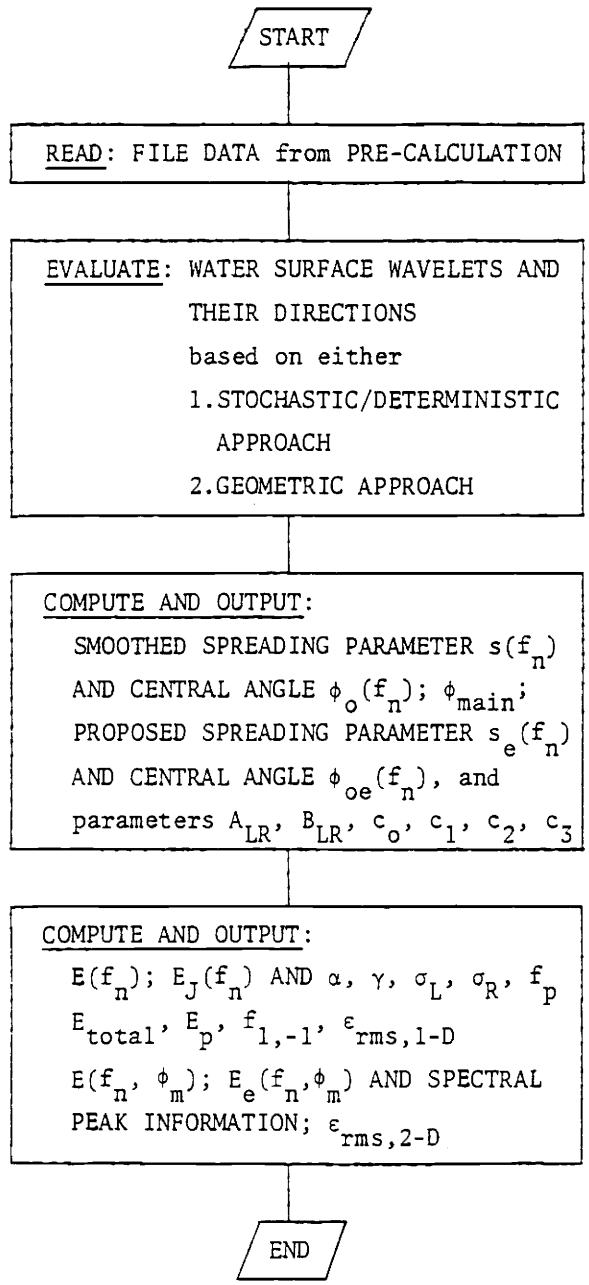


FIG. 3.3 Flow chart of directional wave spectrum estimates

# 4. DATA ANALYSIS

## 4.1 Introduction

This chapter contains a summary of numerical results of analyzed data from offshore Coos Bay, Oregon. Alternative solution methods are examined and evaluated. In Section 4.2, seasonal samples of wave properties are interpreted and a Kolmogorov-Smirnov goodness of fit test is introduced to characterize the statistical behavior of seasonal unsteady current measurements. In Section 4.3, a standard sample length is selected to provide reproducible directional spectrum results. In Section 4.4, the validity of the data collecting system is checked by analyzing simultaneously recorded samples from different depths at the same horizontal location. The resulting directional wave properties are compared with respect to the applied method. Also, directional wave properties evaluated in the time domain are compared with related properties evaluated in the frequency domain. Since wave spectra with high energy content are usually of interest in analyzing wave property behavior, significant data sets of samples which contain high wave energy are selected from the seasonal measurements. Graphical outputs of directional spectra are available from our computational system; example illustrations of real ocean data are presented. Tabular summaries of directional wave properties obtained from the geometric approach are presented for significant seasonal data sets. Seasonal variations in directional spectrum behavior are discussed. Section 4.5 is a parametric study of the proposed empirical equation coefficients. A correlation study is conducted, comparing the coefficient of the spreading parameter power function to the total energy integrated over all frequencies and directions. Section 4.6 discusses directional wave simulation. A wave simulation method is presented. Directional wave spectrum properties solved from a simulated wave sample are compared to known directional wave spectrum properties.

## 4.2 Seasonal Behavior of Measured Samples

Real ocean data have been measured from offshore Coos Bay, Oregon, area for this research project during August 1982, October 1982 and March 1983. Recorded data include instantaneous measurements of pressure and magnetic east and north water particle velocity components. Burst sampling, Neil Brown, Inc., acoustic current meters were employed for wave property measurements. The meters were located near the sea floor at sites with water depths ranging from 60 feet to 200 feet. Wave property samples were collected enery four hours with sample durations of 8.55 or 17.1 minutes, and sample rates of one record per second. A tabular summary of sample length, total samples measured each season, approximate depth of measurement site, meter identification number, and seasonal mean square velocity, is presented in Table 4.1.

TABLE 4.1 Summary of measured wave property samples

| Month, Year | Depth (ft) | Meter No. | Sample Length (sec) | Total samples $\nu$ | $\overline{V^2_{rms}}$ $(ft/s)^2$ |
|---|---|---|---|---|---|
| August, 1982 | 183 | 24 | 512 | 76 | .017 ±.014 |
| October, 1982 | 192 | 43* | 1024 | 11 | .052 ±.039 |
| October, 1982 | 192 | 25 | 512 | 70 | .082 ±.075 |
| March, 1983 | 60 | 26 | 512 | 55 | 1.21 ±.554 |

* The current sensor on meter number 43 is located 14' above the sea bottom; all other current sensors are located 4.3' above the sea bottom. The pressure sensor is located 3.4' above the current sensor on all meters. Due to electromic problems with meter 43 during October 1982, only 11 error free samples were recorded.

The seasonal mean square value of wave-induced horizontal velocity, $\overline{V^2_{rms}}$, is defined as

$$\overline{V^2_{rms}} = \frac{1}{\nu} \sum_{i=1}^{\nu} (V^2_{rms})_i = \frac{1}{\nu} \sum_{i=1}^{\nu} (\overline{V^2_t})_i = \frac{1}{\nu N} \sum_{i=1}^{\nu} \sum_{n=1}^{N} [u^2(t_n)+v^2(t_n)]_i \quad (4.1)$$

where

$$(V_{rms})_i = (\overline{V^2_t})^{\frac{1}{2}}_i \quad (4.2)$$

The index i indicates the i'th sample in a total $\nu$ samples per season, and $\overline{V^2_t}$ has been defined in Eq.(3.6). The mean square velocity quantifies the relative magnitide of unsteady currents.

Wave-induced current properties are of primary interest in this study. Consequently, the behavior of the root mean square velocity is analyzed first. Many previous random wave studies have demonstrated that the Rayleigh distribution function is a satisfactory model for representing the probability distribution of wave height (Kinsman, 1965). It is reasoned in this study that the root mean square velocity is proportional to the root mean square water surface elevation and that both of these quantities are proportional to the mean wave height. Thus, it is hypothesized that a Rayleigh distribution can be used to represent the probability distribution of $V_{rms}$. The Rayleigh distribution function of $V_{rms}$ can be expressed as

$$PDF(V_{rms}) = \frac{2V_{rms}}{\overline{V^2_{rms}}} \exp\left(-\frac{V^2_{rms}}{\overline{V^2_{rms}}}\right) = \frac{2V_{rms}}{V^2_{RMS}} \exp\left[-\left(\frac{V_{rms}}{V_{RMS}}\right)^2\right] \quad (4.3\text{-}1)$$

where $V_{RMS}=(\overline{V^2_{rms}})^{\frac{1}{2}}$, the root mean square value of $V_{rms}$, and $PDF(V_{rms})$ is the probability distribution function of $V_{rms}$. Now the hypothesis is examined using the Kolmogorov-Smirnov goodness of fit test, and samples in each season are regarded as a population in the test (Benjamin and Cornell, 1970). The Kolomogorov-Smirnov test is simply a comparison between the quantity

$$X_{max} = \text{maximum } |X_i|$$

$$= \text{maximum } |\text{observed cumulative distribution function} - \text{hypothesized cumulative distribution function}|_i$$

and

$$Y(\nu) = \begin{cases} 1.22/\sqrt{\nu}\,, & \alpha=0.1 \\ 1.36/\sqrt{\nu}\,, & \alpha=0.05 \\ 1.63/\sqrt{\nu}\,, & \alpha=0.01 \end{cases}$$

where $\nu$ is the population of sample in test, and $Y(\nu)$ is a $100(1-\alpha)\%$ confidence interval for $X_i$. If $X_{max}<Y(\nu)$ for a particular $\alpha$, the hypothesis is accepted by the test in a $100(1-\alpha)\%$ confidence interval. Otherwise, the hypotheses is rejected by the test.

The cumulative distribution function of $PDF(V_{rms})$ is

$$CDF(V_{rms}) = \int_0^{V_{rms}} PDF(V_{rms})\,dV_{rms} = 1-\exp\left[-\left(\frac{V_{rms}}{V_{RMS}}\right)^2\right] \qquad (4.3\text{-}2)$$

which is plotted versus the dimensionless parameter $V_{rms}/V_{RMS}$ in Fig. 4.1 as a continuous curve. The empirical cumulative probability distribution of $V_{rms}$ is then computed for samples in each season. Samples of August 1982, October 1982 (meter 25), and March 1983, are included in the test. Samples of October 1982, measured by meter 43, are not included in the test because of the limited sample population (only 11 samples). Thus, three empirical cumulative distribution curves are obtained and are plotted in Fig. 4.1. One may conclude from Fig. 4.1 that all three empirical curves are closely related to the hypothesized curve. The performance of Kolmogorov-Smirnov test indicates that the hypothesis is accepted for all three empirical curves at $\alpha=0.05$. Hence, the root mean square velocity data are modeled by the Rayleigh probability distribution function within a 95% confidence interval. The 95% confidence intervals in the test for each season's empirical curves are also indicated in Fig. 4.1. This analysis suggests that extreme seasonal wave conditions could be extrapolated by interpreting sample data with the

Rayleigh probabitity distribution function.

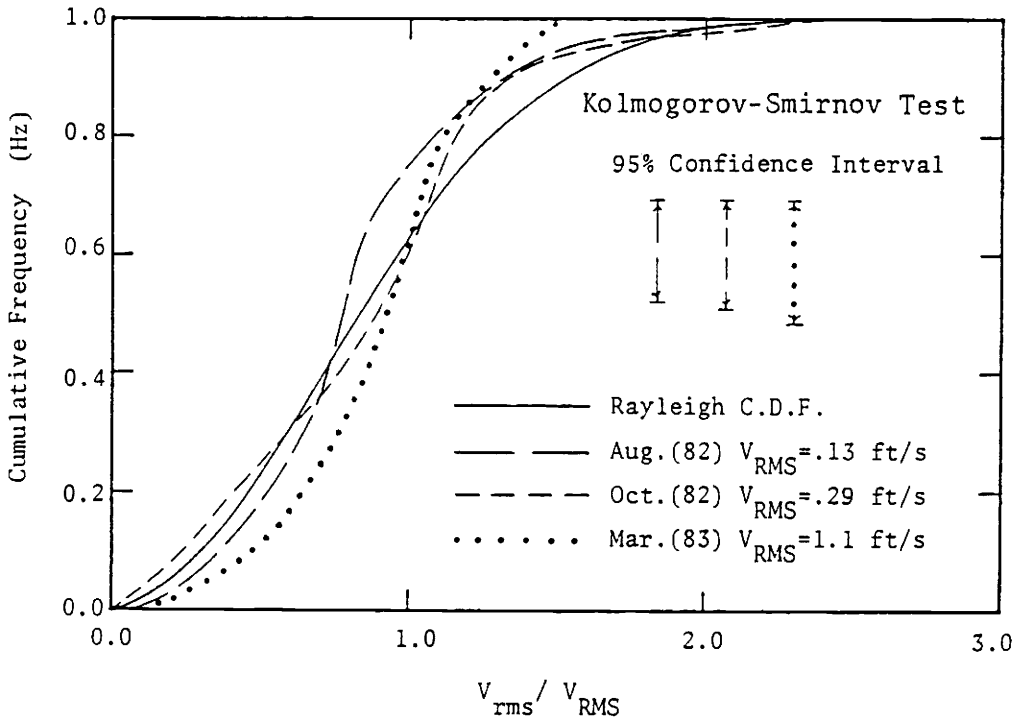


FIG. 4.1 C.D.F. of Rayleigh distribution and empirical C.D.F. of $V_{rms}/V_{RMS}$

## 4.3 Selection of a Sample Length for Spectral Analysis

For a stationary process, a long measurement record is desirable in spectral analysis in order to extract all possible frequency components of the measured process. However, for wave property measurements, a lengthy record allows contamination of wave states by tidal fluctuations, changes in wind and current patterns, etc. Thus, a shorter measurement record may be preferred to approximate a stationary process for ocean wave spectral analysis. Therefore, tradeoffs should be considered between long and short measurement records in order to obtain well behaved spectral results as well as low frequency component properties.

A satisfactory record length is to be determined for input data in directional spectral analysis. The procedure used to determine this record length is described as follows. Five October 1982, data sets from meter 43 are chosen for this study. These five data sets were chosen because each has a total record length of 1024 seconds, the maximum recorded in this study. The sample rate is one sample per second and the FFT algorithm requires a total number of data points equal to a integer power of 2. Therefore a record length of 1024 seconds allows us to monitor variation of wave property statistics evaluated from record halves (512 seconds) or quarters (256 seconds). It is hypothesized that the optimum sample length will be one which provides the least variation in wave property statistics. Thus, the optimum record length will be selected from alternative lengths of 256 ($2^8$) seconds, 512 ($2^9$) seconds and 1024 ($2^{10}$) seconds. It is assumed that any length greater than 1024 seconds (17.1 minutes) is contaminated by daily tides and variable wave conditions caused by winds and currents. Any length shorter than 256 seconds (4.27 minutes) can not evaluate wave periods longer than 256 seconds. Also, the fundamental frequency interval may not be small enough to discern the directional properties of ocean waves.

The samples of 512 seconds are retrieved from the first half, the second and third quarters, and the last half of 1024 seconds. The samples of 256 seconds are obtained by dividing 1024 seconds into four equi-spaced intervals (quarters). Another 256 seconds is retrieved from the contral part of 1024 seconds.

To check the accuracy of the measurement system, the resulting wave property statistics are compared with the statistics computed from simultaneously measured samples of 512 seconds, recorded by meter 25 which is located about 10 feet below meter 43. The wave property statistics evaluated in the time domain include mean current magnitude, $V_c$, and direction, $\phi_c$, mean square wave-induced velocity, $\overline{V_t^2}$, and the main propagation direction $\overline{\phi}$. The wave property statistics evaluated in the frequency domain include total wave spectral density, $E_{total}$, spectral peak of frequency spectrum, $E_p$, peak frequency, $f_p$, dimensionless fre-

quency, $f_{1,-1}$, critical spreading parameter, $s_c$, critical frequency, $f_c$, main propagation direction $\phi_{main}$, and the smoothed total velocity spectral density $\overline{V_f^2}$ at the sensor location. $\overline{V_f^2}$ is defined as

$$\overline{V_f^2} = \sum_{n=1}^{N'} E_{VV}(f_n) = \sum_{n=1}^{N'} K^2(f_n)E(f_n) \tag{4.4}$$

where $E_{VV}(f_n)=K^2(f_n)E(f_n)$ is the subsurface horizontal orbital velocity spectrum. The results of the October 21, 1982, data set are shown in Table 4.2 and 4.3. The initial time of each sample is also identified in these two tables. The results of the other four data sets are presented in Appendix B. In the frequency domain calculation, statistics are computed utilizing the three spectral analysis methods presented in this study. They are the one angle mode solution of the stochastic/deterministic approach, denoted as Sto./Det. approach$_1$ or S/D$_1$ in the following sections, the double angle mode solution of the stochastic/deterministic approach, denoted as Sto./Det. approach$_2$ or S/D$_2$ in the following sections, and the geometric approach, denoted as GEO. in the following sections.

TABLE 4.2 Sample statistics evaluated in the time domain

Date: October 21, 1982 Meter No. 43

| Length | Init. Time | $V_c$ | $\phi_c$ | $\overline{V_t^2}$ | $\overline{\phi}$ | Length | Init. Time | $V_c$ | $\phi_c$ | $\overline{V_t^2}$ | $\overline{\phi}$ |
|---|---|---|---|---|---|---|---|---|---|---|---|
| (sec) | | (ft/s) | (o) | $(ft/s)^2$ | (o) | (sec) | | (ft/s) | (o) | $(ft/s)^2$ | (o) |
| 1024 | 10:28 | .514 | -70 | .155 | 115 | 256 | 10:28 | .779 | -55 | .025 | 94 |
| 512 | 10:28 | .496 | -60 | .145 | 132 | 256 | 10:32 | .273 | -71 | .094 | 134 |
| 512* | 10:32 | .251 | -78 | .116 | 119 | 256* | 10:34 | .097 | -64 | .064 | 111 |
| 512 | 10:36 | .488 | -81 | .181 | 107 | 256 | 10:36 | .184 | -96 | .133 | 108 |
| 512** | 10:26 | .511 | -78 | .129 | 93 | 256 | 10:40 | .797 | -79 | .035 | 105 |

* central section of 1024 seconds

** data measured from meter 25

TABLE 4.3 Sample statistics evaluated in the frequency domain

Date: October 21, 1982 Meter No. 43

| Length (sec) | Init. Time | $E_{total}$ ($ft^2$) | $E_p$ ($ft^2 s$) | $f_p$ (Hz) | $f_{1,-1}$ (Hz) | $s_c$ | $f_c$ (Hz) | $\phi_{main}$ (o) | $\overline{v_f^2}$ $(ft/s)^2$ |
|---|---|---|---|---|---|---|---|---|---|
| | | | | STO./DET. APPROACH$_1$ | | | | | |
| 1024 | 10:28 | .077 | 7.2 | .059 | .069 | 39 | .053 | 64 | .033 |
| 512 | 10:28 | .082 | 6.0 | .059 | .068 | 17 | .055 | 56 | .038 |
| 512* | 10:32 | .056 | 7.5 | .059 | .066 | 4 | .051 | 79 | .023 |
| 512 | 10:36 | .061 | 3.9 | .059 | .067 | 8 | .057 | 57 | .023 |
| 512** | 10:26 | .075 | 4.0 | .059 | .068 | 28 | .051 | 41 | .015 |
| 256* | 10:34 | .057 | 2.6 | .059 | .064 | 5 | .062 | 68 | .017 |
| | | | | STO./DET. APPROACH$_2$ | | | | | |
| 1024 | 10:28 | .063 | 5.5 | .059 | .069 | 91 | .055 | 67 | .152 |
| 512 | 10:28 | .068 | 5.1 | .059 | .067 | 50 | .045 | 75 | .143 |
| 512* | 10:32 | .043 | 4.0 | .059 | .068 | 20 | .055 | 92 | .112 |
| 512 | 10:36 | .061 | 4.1 | .059 | .067 | 10 | .057 | 54 | .178 |
| 512** | 10:26 | .098 | 8.0 | .059 | .067 | 27 | .051 | 65 | .128 |
| 256* | 10:34 | .063 | 2.7 | .059 | .064 | 7 | .055 | 72 | .060 |
| | | | | GEOMETRIC APPROACH | | | | | |
| 1024 | 10:28 | .076 | 7.6 | .059 | .069 | 5.5 | .059 | 56 | .023 |
| 512 | 10:28 | .071 | 6.0 | .059 | .068 | 4.8 | .066 | 77 | .032 |
| 512* | 10:32 | .063 | 4.3 | .059 | .068 | 4.0 | .063 | 47 | .083 |
| 512 | 10:36 | .075 | 4.2 | .059 | .065 | 7.0 | .062 | 64 | .081 |
| 512** | 10:26 | .074 | 7.4 | .059 | .068 | 10. | .059 | 58 | .026 |
| 256* | 10:34 | .063 | 2.8 | .059 | .064 | 4.5 | .062 | 64 | .017 |

* central section of 1024 seconds, ** data measured from meter 25

A numerical stability study of wave property statistics for sample lengths of 256 and 512 seconds is first performed in the time domain for each of the five data sets. The mean and standard deviation for sample lengths of 256 and 512 seconds in each data set are computed and compared with the results from a 1024 second record length and a 512 second record from meter 25. These results are tabulated in Table 4.4 along with the date and initial time of each data set. The October 21, data indicates large standard deviations for all mean values. This is because the total wave energy content is small, i.e, about 5% of the wave energy content of the other four data sets. Hence, the resulting wave properties are sensitive to both physical and numerical disturbances. For the remaining four data sets, the standard deviations of the means are relatively samll. The standard deviations of the means for all 512 second records are smaller than those for the 256 second records. A graphical summary of the results appears in Fig. 4.2. The figure shows the relative variation of statistics $\overline{V_t^2}$ and $V_c$ for all five data sets by expressing $\overline{V_t^2}$ and $V_c$ of the 256 and 512 second records as ratios with respect to $\overline{V_t^2}$ and $V_c$ of the 1024 second record, respectively. $\overline{V_{t,1024}^2}$ and $V_{c,1024}$ denote the quantities $\overline{V_t^2}$ and $V_c$ of the 1024 second record for each data set in Fig. 4.2. Although both ratios, $\overline{V_t^2}/\overline{V_{t,1024}^2}$ and $V_c/V_{c,1024}$, are close to unity in a mean sense in Fig. 4.2, results from a record length of 256 seconds are more scattered than those from a record length of 512 seconds.

A stability study in the frequency domain is performed by comparing values of the total energy density and the peak energy density of the one-dimensional frequency spectrum, computed as dimensionless ratios relative to results from a 1024 second record length. The symbols $E_{p,1024}$ and $E_{total,1024}$ denote the peak and total energy density, respectively, of the 1024 second record. The mean value and standard deviation for these ratios are calculated for sample lengths of 512 seconds, measured by meter 43, utilizing the methods identified in Table 4.5. Also ratios are computed for samples from the central 256 seconds of the records from meter 43 and for samples of 512 seconds from meter 25; these are also shown in Table 4.5. The October 25, 10:52 data from meter 25 indi-

TABLE 4.4 Comparison of sample statistics in the time domain

Year: 1982 Meter No. 43

| Date, (init. time) | Length (sec) | $V_c$ (ft/s) | $\phi$ (o) | $\overline{V_t^2}$ $(ft/s)^2$ | $\phi$ (o) |
|---|---|---|---|---|---|
| Oct 21 | 1024 | .514 | -70 | .155 | 115 |
| (10:28) | 512 | .412±.139 | -73±11.3 | .147±.032 | 119±12.5 |
| | 512** | .511 | -78 | .129 | 93 |
| | 256 | .426±.336 | -73±15.6 | .070±.044 | 110±14.7 |
| Oct 23 | 1024 | .265 | -8 | .054 | 92 |
| ( 2:38) | 512 | .267±.009 | -6.7± 2.9 | .056±.003 | 94± 1.5 |
| | 512** | .392 | -6.7 | .065 | 84 |
| | 256 | .267±.019 | -7± 4.3 | .055±.010 | 91± 7.2 |
| Oct 24 | 1024 | 1.04 | -31 | .063 | 79 |
| (14:47) | 512 | 1.03±.010 | -31± 2.6 | .059±.008 | 80± 1.5 |
| | 512** | .736 | -56 | .070 | 78 |
| | 256 | 1.03±.030 | -31± 4.3 | .055±.003 | 81± 1.9 |
| Oct 25 | 1024 | .242 | 198 | .072 | 89 |
| ( 6:51) | 512 | .249±.031 | 199±10.8 | .068±.001 | 89± 3.0 |
| | 512** | .212 | 250 | .080 | 98 |
| | 256 | .250±.031 | 197±13.5 | .066±.019 | 91± 2.1 |
| Oct 25 | 1024 | .421 | -17 | .047 | 97 |
| (10:52) | 512 | .418±.011 | -17± 1.1 | .045±.002 | 96± 4.4 |
| | 512** | .468 | 193 | .043 | 72 |
| | 256 | .424±.006 | -16± 2.2 | .044±.007 | 96± 4.7 |

** data measured from meter 25

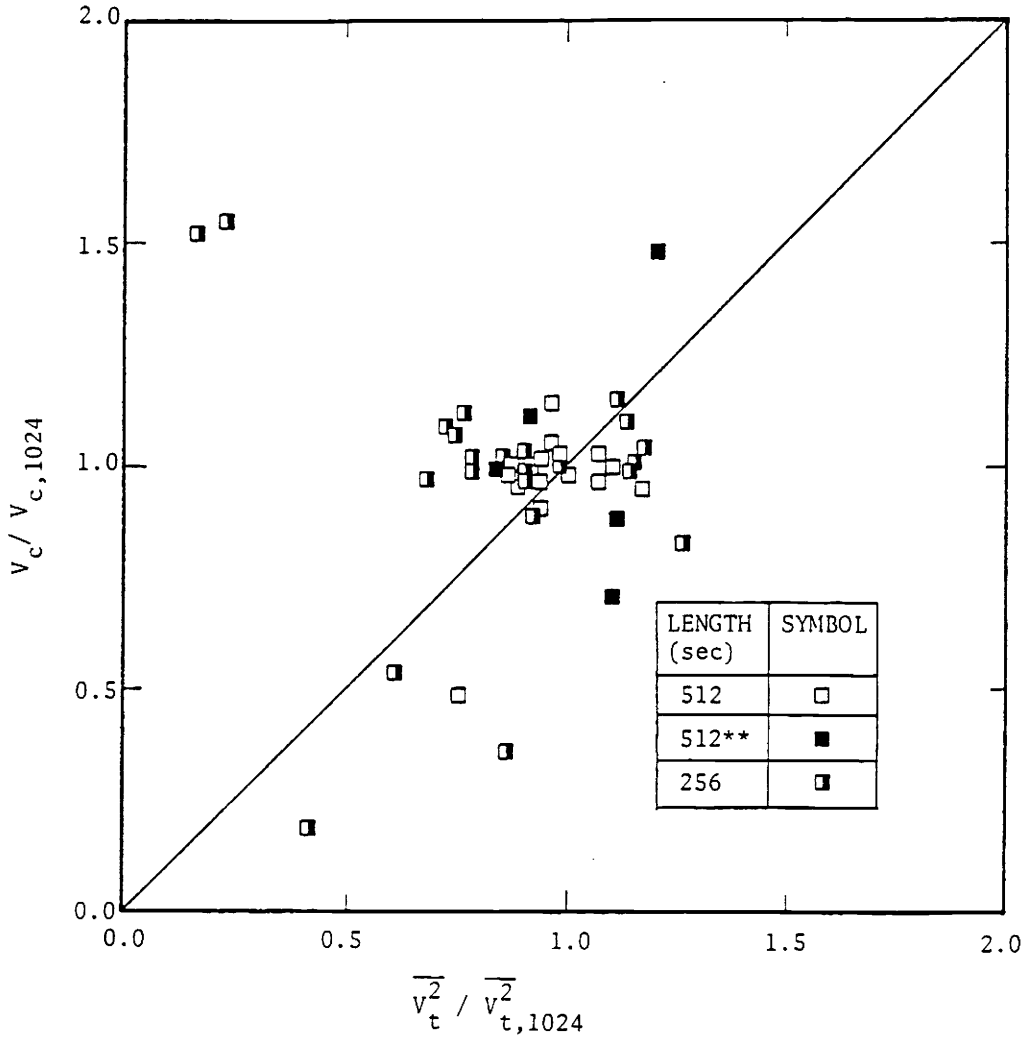


FIG. 4.2 Plot of dimensionless parameters $\frac{\overline{V_t^2}}{\overline{V_{t,1024}^2}}$ versus $\frac{V_c}{V_{c,1024}}$

** meter 25 data

cate ratios approaching three. This condition implies a strong, short term unsteady current occurring at the depth of meter 25 during this particular measuring period.

It is surprising that almost all ratios of $E_{total}/E_{total,1024}$ and $E_p/E_{p,1024}$ of the central 256 second records differ significantly from

TABLE 4.5 Comparison of ratios $E_{total}/E_{total,1024}$ and $E_p/E_{p,1024}$

Year: 1982 Meter No. 43

| Date, (init. time) | Length (sec) | $S/D_1$ $\frac{E_{total}}{E_{total,1024}}$ | $S/D_1$ $\frac{E_p}{E_{p,1024}}$ | $S/D_2$ $\frac{E_{total}}{E_{total,1024}}$ | $S/D_2$ $\frac{E_p}{E_{p,1024}}$ | GEO. $\frac{E_{total}}{E_{total,1024}}$ | GEO. $\frac{E_p}{E_{p,1024}}$ |
|---|---|---|---|---|---|---|---|
| Oct 21 | 512 | .86±.18 | .80±.25 | .91±.21 | .80±.11 | .92±.08 | .63±.14 |
| (10:28) | 512** | .97 | .55 | 1.56 | 1.45 | .97 | .96 |
| | 256 | .74 | .35 | 1.02 | .48 | .83 | .36 |
| Oct 23 | 512 | 1.08±.34 | .93±.10 | .95±.40 | .95±.10 | 1.07±.18 | .98±.10 |
| ( 2:38) | 512** | .91 | 1.02 | 1.62 | 1.18 | 1.00 | 1.12 |
| | 256 | 3.50 | 1.50 | 2.50 | 1.13 | 3.40 | 2.40 |
| Oct 24 | 512 | .93±.08 | .94±.08 | .92±.01 | .95±.11 | .93±.01 | .94±.13 |
| (14:47) | 512** | 1.05 | 1.09 | 1.56 | 2.00 | 1.03 | 1.08 |
| | 256 | 1.08 | .88 | 1.10 | .93 | 1.03 | .89 |
| Oct 25 | 512 | 1.12±.19 | .96±.08 | 1.16±.18 | .93±.06 | 1.03±.08 | .94±.06 |
| ( 6:51) | 512** | 1.22 | 1.17 | 1.64 | 1.47 | 1.14 | 1.10 |
| | 256 | .63 | .16 | .61 | .18 | .61 | .13 |
| Oct 25 | 512 | 1.09±.19 | 1.27±.30 | 1.00±.13 | 1.16±.27 | 1.13±.21 | 1.29±.31 |
| (10:52) | 512** | 2.70 | 2.60 | 3.96 | 3.80 | 2.40 | 2.30 |
| | 256 | 2.30 | .92 | 1.64 | .87 | 2.00 | 1.15 |

** data measured from meter 25

the means of the related ratios for 512 second records. This result is presented graphically as a plot of $E_{total}/E_{total,1024}$ versus $E_p/E_{p,1024}$ in Fig. 4.3. The standard deviations for each 512 second sample in Table 4.5 are relatively small value implying approximately stationary processes for this record length.

Numerical stability studies in both the time and frequency domains

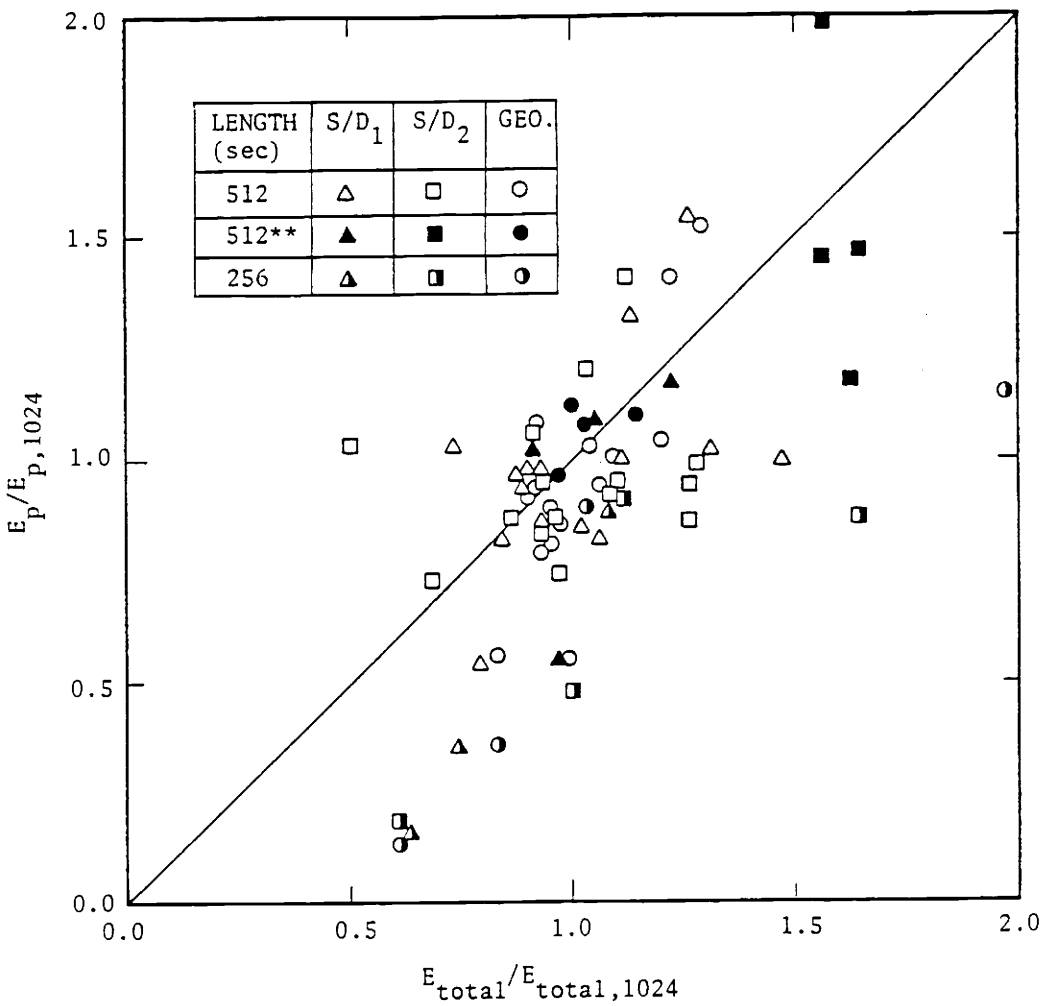


FIG. 4.3 Plot of dimensionless parameters $\frac{E_{total}}{E_{total,1024}}$ vs $\frac{E_p}{E_{p,1024}}$

** meter 25 data

show that wave property statistics estimated from a record length of 512 seconds are more reliable, less variable than those estimated from a record length of 256 seconds. Since 1024 second records are not generally available from the field measurements in this research project, 512 second data sets are selected as the optimum record length.

## 4.4 Comparisons of Results from Alternative Directional Spectrum Solution Methods

In this section, directional wave properties from the five data sets identified in Section 4.3 will be analyzed further to compare the behavior of the Stochastic/Deterministic one and double angle mode and geometric methods utilized in directional spectra analysis. This will be accomplished by comparing nearly simultaneous water surface spectrum predictions from two different current meters. These results will also be used as examples to compare wave property statistics in the time and frequency domains. Then, graphical examples of directional spectra output based on real ocean measured data will be presented for both smoothed spectra and proposed spectra.

### 4.4.1 Direct Comparison of Selected Numerical Results

Although the geometric approach has been shown to be theoretically superior to the Sto./Det. approach in Chapter 2, it is appropriate to compare numerical results to see if one method provides superior computations as well. This comparison will be facilitated by examining water surface spectrum predictions from two current meters separated by a ten foot vertical distance. One dimensional frequency spectra, critical spreading parameters and main propagation directions will be compared.

The same five data sets used in the numerical stability study in Section 4.3 will be the analyzed again. However, results from the data sets of October 21 with initial time 10:28 and of October 25 with initial time 10:52 are of less interest due to the previously mentioned small wave energy levels and unusual short duration unsteady currents, respectively. The ratios of total energy, $E_{total}/E_{total,1024}$, and peak energy, $E_p/E_{p,1024}$, for sample lengths of 512 seconds in Table 4.5 provide us with a comparison of one-dimensional spectrum results. Recall that the 512 second records were determined to be superior in Section 4.3. The results for meter 43 (upper meter) are presented in the first

row of each data set. The results from meter 25 (lower meter) are presented in the second row and identified with a double asterisk. The results from both meters should indicate the same one-dimensional spectrum estimates at the water surface because the same phenomenon is being sampled at different depths. The superior method should be indicated by the smallest difference between meters. An interpretation of the data from October 23,24, and 25 (6:51) reveals that the double angle mode solution of the stochastic/deterministic approach has the greatest differences between meters (<110%), the geometric approach has the samllest differences between meters (<17%), and the one angle mode solution of the stochastic/deterministic approach has an intermediate difference between meters (<31%). One could conclude that the geometric approach provides more reliable predictions of the water surface one-dimensional spectrum.

The directional wave properties used to compare the three methods are the critical spreading parameter, $s_c$, and the main direction, $\phi_{main}$, of the five data sets. The mean and standard deviation are calculated for these parameters for a sample length of 512 seconds, measured by meter 43, and are presented in Table 4.6. Also, values of $s_c$ and $\phi_{main}$ for sample record lengths of 512 seconds from meter 25 are presented in Table 4.6. Results from data sets of October 21 and 25 (10:52) are ignored in this comparison. For the remaining data sets, the maximum difference in main direction evaluated from separate current meters for methods $S/D_1$, $S/D_2$, and GEO. are $22^\circ$, $29^\circ$, and $18^\circ$, respectively (October 23 data set). The maximum difference in critical spreading parameters for methods $S/D_1$, $S/D_2$, and GEO. are 9.2, 11.0, and 6.7, respectively. One could conclude that the geometric approach provides more consistent predictions of directional information than the stochastic/deterministic approaches.

Figure 4.4 shows the variation of $s_c$ versus $\phi_{main}$ for the individual data sets (in Table 4.3 and Table B.2). No significant pattern is is revealed in this figure. In order to see whether these critical spreading parameters occur at consistent frequencies, values of $s_c$

TABLE 4.6 Comparison of $s_c$ and $\phi_{main}$

Year: 1982 Meter No. 43

| Date, (init. time) | Length (sec) | $S/D_1$ $s_c$ | $S/D_1$ $\phi_{main}$ (o) | $S/D_2$ $s_c$ | $S/D_2$ $\phi_{main}$ (o) | GEO. $s_c$ | GEO. $\phi_{main}$ (o) |
|---|---|---|---|---|---|---|---|
| Oct 21 | 1024 | 39.0 | 64 | 91.0 | 67 | 5.5 | 56 |
| (10:28) | 512 | 9.7±6.6 | 64±11 | 27.0±21. | 74±19 | 5.3±1.5 | 63±15 |
| | 512** | 28.0 | 41 | 27.0 | 65 | 10.0 | 58 |
| Oct 23 | 1024 | 29.0 | 92 | 32.0 | 99 | 7.6 | 90 |
| ( 2:38) | 512 | 10.0±2.6 | 95± 7 | 10.3±2.1 | 101± 9 | 4.7±0.6 | 90± 6 |
| | 512** | 14.0 | 73 | 10.0 | 72 | 8.0 | 72 |
| Oct 24 | 1024 | 12.0 | 75 | 16.0 | 77 | 3.8 | 73 |
| (14:47) | 512 | 15.6±2.1 | 74±11 | 13.3±3.2 | 74±11 | 3.3±0.3 | 72±13 |
| | 512** | 7.0 | 66 | 9.0 | 65 | 10.0 | 67 |
| Oct 25 | 1024 | 20.0 | 84 | 32.0 | 89 | 4.6 | 87 |
| ( 6:51) | 512 | 14.7±6.4 | 85± 2 | 20.0±2.6 | 95± 6 | 4.6±0.7 | 87± 2 |
| | 512** | 5.5 | 73 | 9.0 | 78 | 5.2 | 71 |
| Oct 25 | 1024 | 20.0 | 90 | 33.0 | 93 | 5.4 | 90 |
| (10:52) | 512 | 22.0±5.5 | 90± 1 | 16.7±5.5 | 100±10 | 4.0±1.7 | 85± 5 |
| | 512** | 43.0 | 81 | 31.0 | 82 | 23.0 | 76 |

** data measured from meter 25

versus $f_c$ are plotted in Fig.4.5. Ignoring the data of October 21 and 25 (10:52), the maximum difference in $f_c$ for methods $S/D_1$, $S/D_2$, and GEO. are .004 (Hz), .007 (Hz), and .002 (Hz), respectively. Therefore, less variability appears in the results of the geometric approach.

It should be pointed out that significant differences in values of $E_{total}$, $E_p$, $s_c$ and $\phi_{main}$ occur when comparing the results of one method

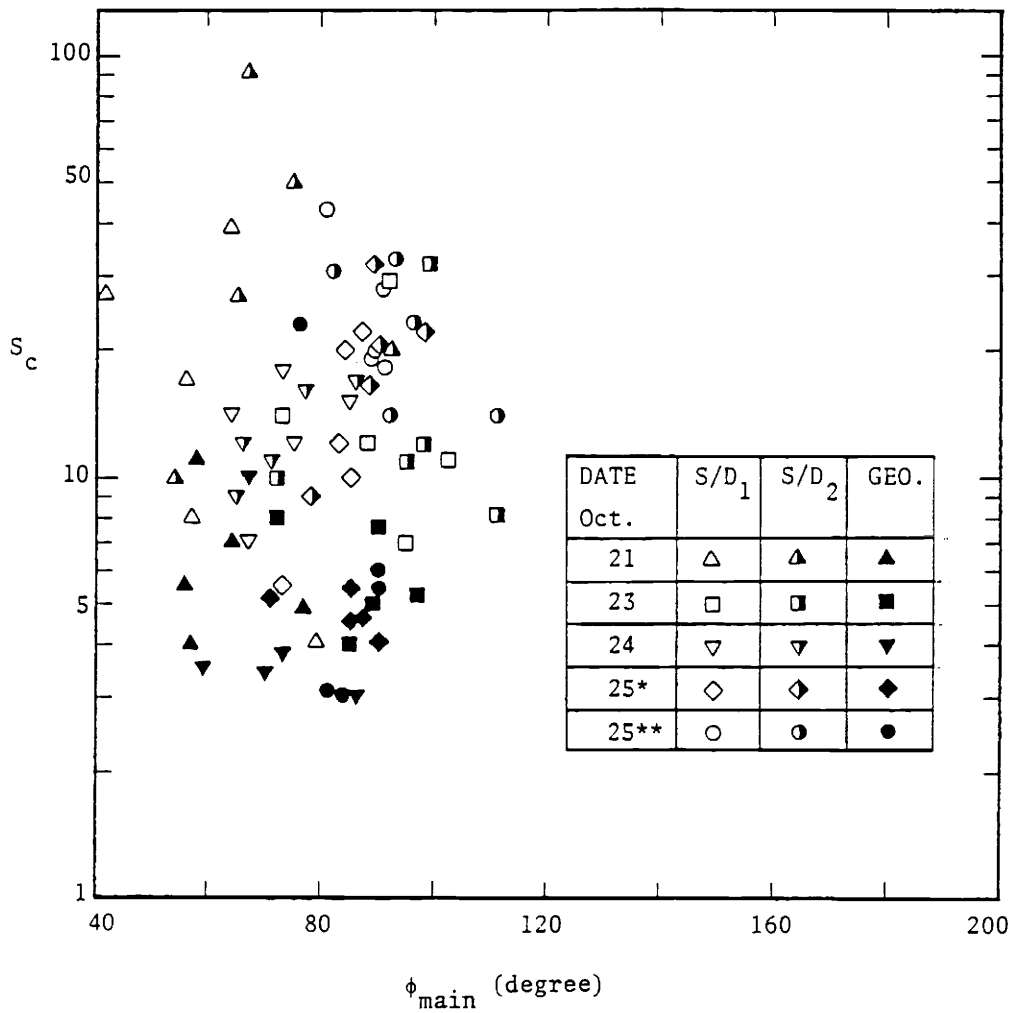


FIG. 4.4 Plot of $s_c$ versus $\phi_{main}$, * 6:51 data set, ** 10:52 data set

to the other. Hence, solutions obtained from one method cannot be used to approximate solutions obtained from another method. This is illustrated in Table 4.7 where a list of mean and standard deviation values for parameters $E_{total}$, $E_p$, $s_c$, and $\phi_{main}$ are presented for data sets from October 23,24, and 25 (6:51). The standard deviations reflect differences between three 512 second records, analyzed from the first half, last half, and second and third quarters of a 1024 second record. Note how relative means for the same sample vary from one method to another. The parameters $E_{total}$ and $E_p$ solved from $S/D_1$ differ from the

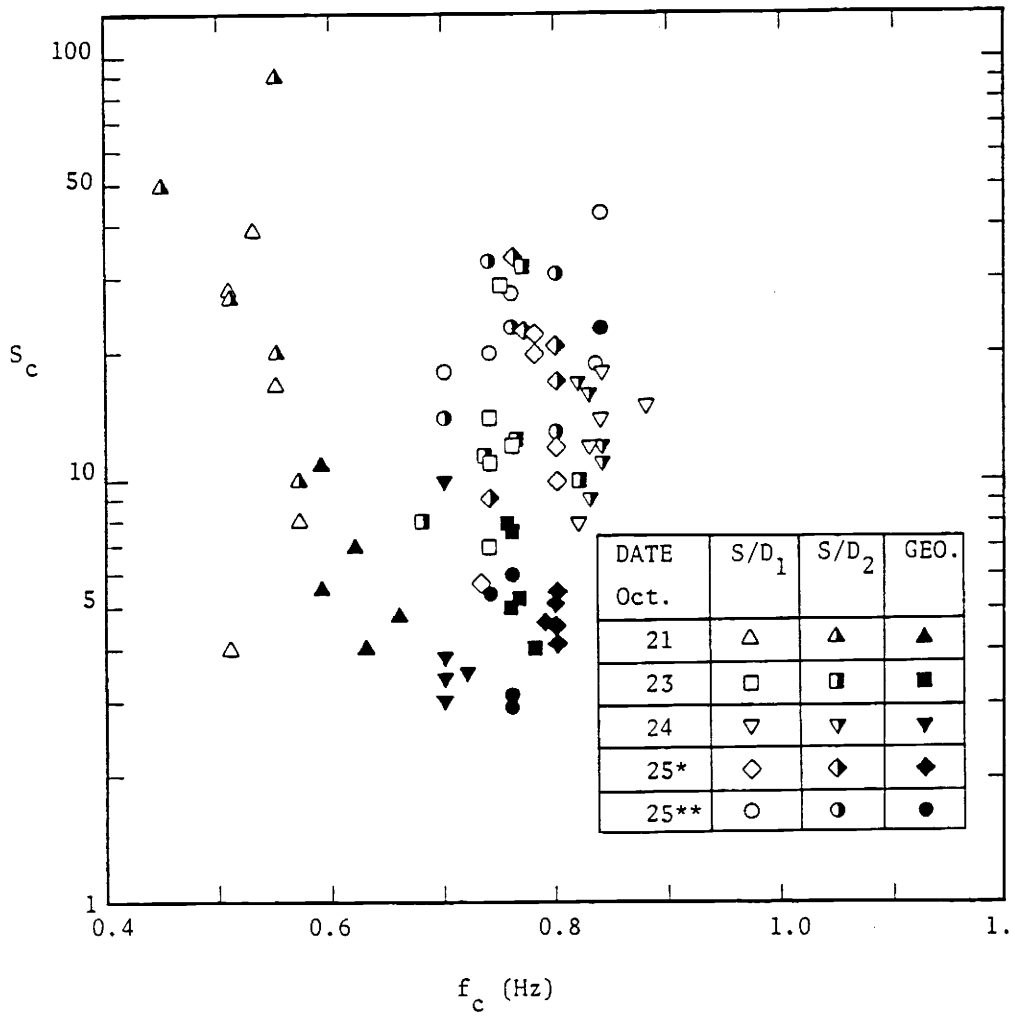


FIG. 4.5 Plot of $s_c$ versus $f_c$, * 6:51 data set, ** 10:52 data set

results of the GEO. method by 16% and 23%, or less. The values of $E_{total}$ and $E_p$ solved from $S/D_2$ are much smaller than those solved from either $S/D_1$ or GEO. The means of $\phi_{main}$ for the same sample are scattered with respect to the three methods. The maximum deviation about the mean of $\phi_{main}$ for the same sample is 11° (October 23, data). The values of $s_c$ solved from $S/D_1$ are fairly consistent with those solved from $S/D_2$; the maximum deviation about the mean being approximately five. The values of $s_c$ solved from GEO. are much samller than those solved from $S/D_1$ and $S/D_2$; this is illustrated in Figs. 4.4 and 4.5.

TABLE 4.7 The mean and standard deviation of $E_{total}$, $E_p$, $s_c$, and $\phi_{main}$

Year: 1982 Length: 512 (sec) Meter No. 43

| Date, (init. time) | | | $S/D_1$ | $S/D_2$ | GEO. |
|---|---|---|---|---|---|
| Oct 23 | $E_{total}$ | ($ft^2$) | 1.08±.34 | .60±.25 | 1.10±.12 |
| ( 2:38) | $E_p$ | ($ft^2s$) | 43.0±4.3 | 42.0±4.0 | 46.0±4.6 |
| | $s_c$ | | 10.0±2.6 | 10.3±2.1 | 4.7±0.6 |
| | $\phi_{main}$ | (o) | 95.0±7.0 | 101.±9.0 | 90.0±6.0 |
| Oct 24 | $E_{total}$ | ($ft^2$) | 1.23±.11 | .82±.01 | 1.43±.02 |
| (14:47) | $E_p$ | ($ft^2s$) | 56.0±4.6 | 34.0±4.0 | 69.0±9.5 |
| | $s_c$ | | 15.6±2.1 | 13.3±3.2 | 3.3±0.3 |
| | $\phi_{main}$ | (o) | 74.0±11. | 74.0±11. | 72.0±13. |
| Oct 25 | $E_{total}$ | ($ft^2$) | 1.76±.30 | 1.39±.21 | 1.78±.14 |
| ( 6:51) | $E_p$ | ($ft^2s$) | 96.0±9.3 | 75.0±4.5 | 102.±6.0 |
| | $s_c$ | | 14.7±6.4 | 20.0±2.6 | 4.6±0.7 |
| | $\phi_{main}$ | (o) | 85.0±2.0 | 95.0±6.0 | 87.0±2.0 |

The average critical spreading parameters solved from $S/D_1$ and $S/D_2$ for these three consecutive days' data are 13.5 and 14.5, respectively. However, the average value solved from GEO. is 4.2. Figure 2.5 indicates that smaller values of the spreading parameter, s, associated with the geometric method will yield broader directional spreading than that indicated by the stochastic/deterministic method. One may conclude from these results that computations from the geometric method are more consistent and , therefore, are superior in terms of reliability. Furthermore, if the geometric method is "correct", then significant errors may be associated with the stochastic/deterministic method. However, this analysis does not establish which method best approximates the actual, unknown, directional spectrum.

### 4.4.2 Directional Wave Properties Estimated in the Time and Frequency Domains

If one has records of water surface elevation, one can directly evaluate total water surface wave energy densities from both time and frequency domains.and immediately compare the results. However, with a current meter based measurement system, this comparison can only be done by evaluating subsurface mean square velocities, $\overline{V_t^2}$ and $\overline{V_f^2}$, as indicated by Eqs.(3.6) and (4.5), respectively. Similarly, directional properties must be compared utilizing subsurface time and frequency information.

According to Eq.(3.7-1), the accuracy of evaluating the main direction, $\overline{\phi}$, in the time domain is very much dependent on one's ability to guess the general direction of wave propagation. Our measurement system is located three miles offshore and all waves are assumed to propagate towards the coastline. A normal projection to the coastline is equal to $120^\circ$, relative to magnetic north. Hence, any velocity vector directed beyond $120^\circ \pm 90^\circ$ is assumed to correspond to a wave trough and is corrected by $180^\circ$. Since a perfect guess of this general propagation direction is nearly impossible, considerable differences may occur between the time domain main direction, $\overline{\phi}$, and the frequency domain main direction, $\phi_{main}$. The main direction, $\phi_{main}$, evaluated in the frequency domain is not affected by this directional ambiguity because pressure frequency components resolve troughs from crests in both the $S/D_1$ and GEO. methods. However, the estimation of $\phi_{main}$ in $S/D_2$ which excludes pressure data, may experience this direction ambiguity unless the pressure data is used to reference directions, in accordance with the discussion of Eq.(2.40-2).

The data sets identified in Table 4.5 have been analyzed to yield $\overline{\phi}$ and $\phi_{main}$. These are plotted on a scatter diagram in Fig. 4.6. The poor correlation of the October 21, data is because the wave heights were very low so the direction computations are limited by the resolving powers of the instrument and are subject to contamination by slight

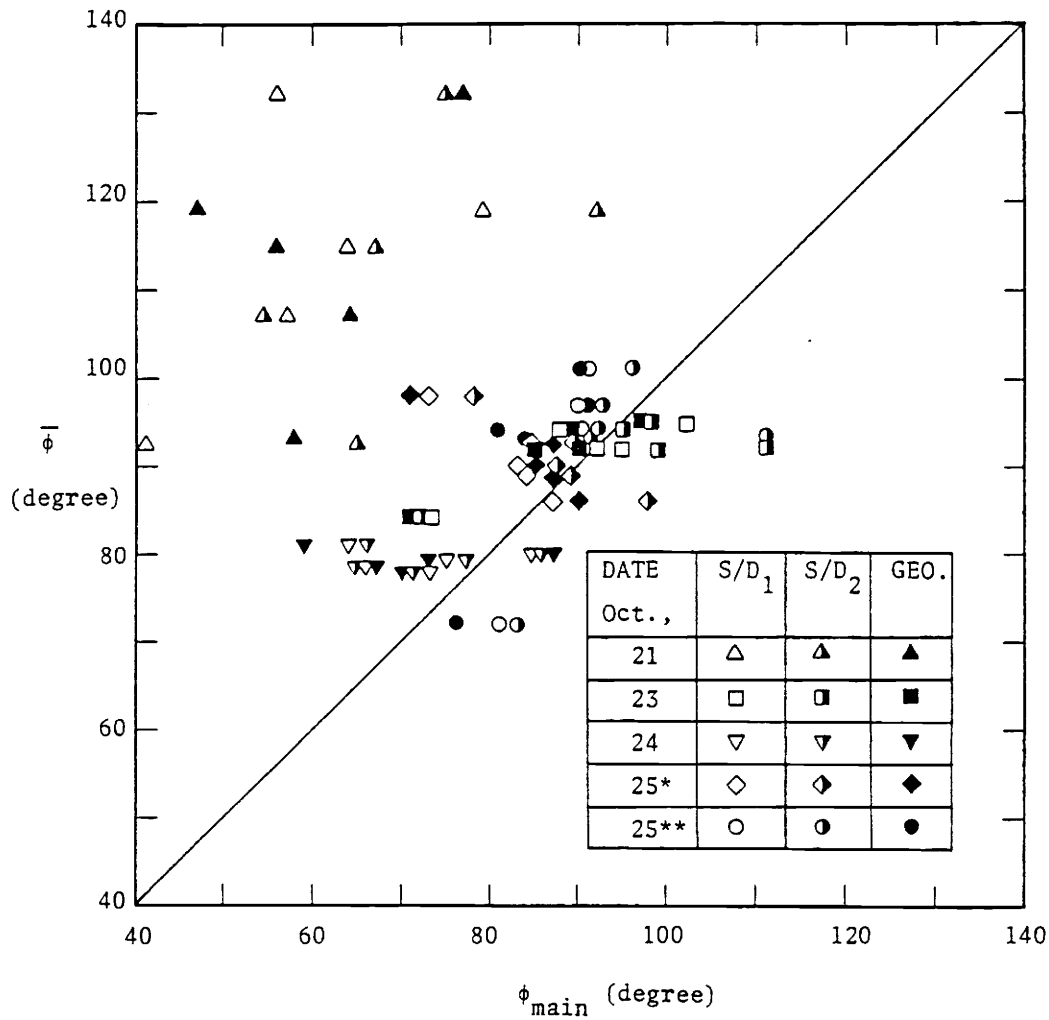


FIG. 4.6 Plot of main directions $\bar{\phi}$ versus $\phi_{main}$

electro-mechanical and/or hydraulic disturbances. On October 21, the main direction estimated from the frequency domain, $\phi_{main}$, is about 65 which is considerably different from the estimated shoreward direction of 120°. Less scatter is seen in Fig. 4.6 for the data of October 23, where $\phi_{main}$ is about 95°, and the maximum difference between $\bar{\phi}$ and $\phi_{main}$ is 12°.

The mean square velocities, $\overline{V_t^2}$ and $\overline{V_f^2}$, for the same five data sets are ploted in Fig. 4.7. The energy estimates of the method $S/D_2$ use

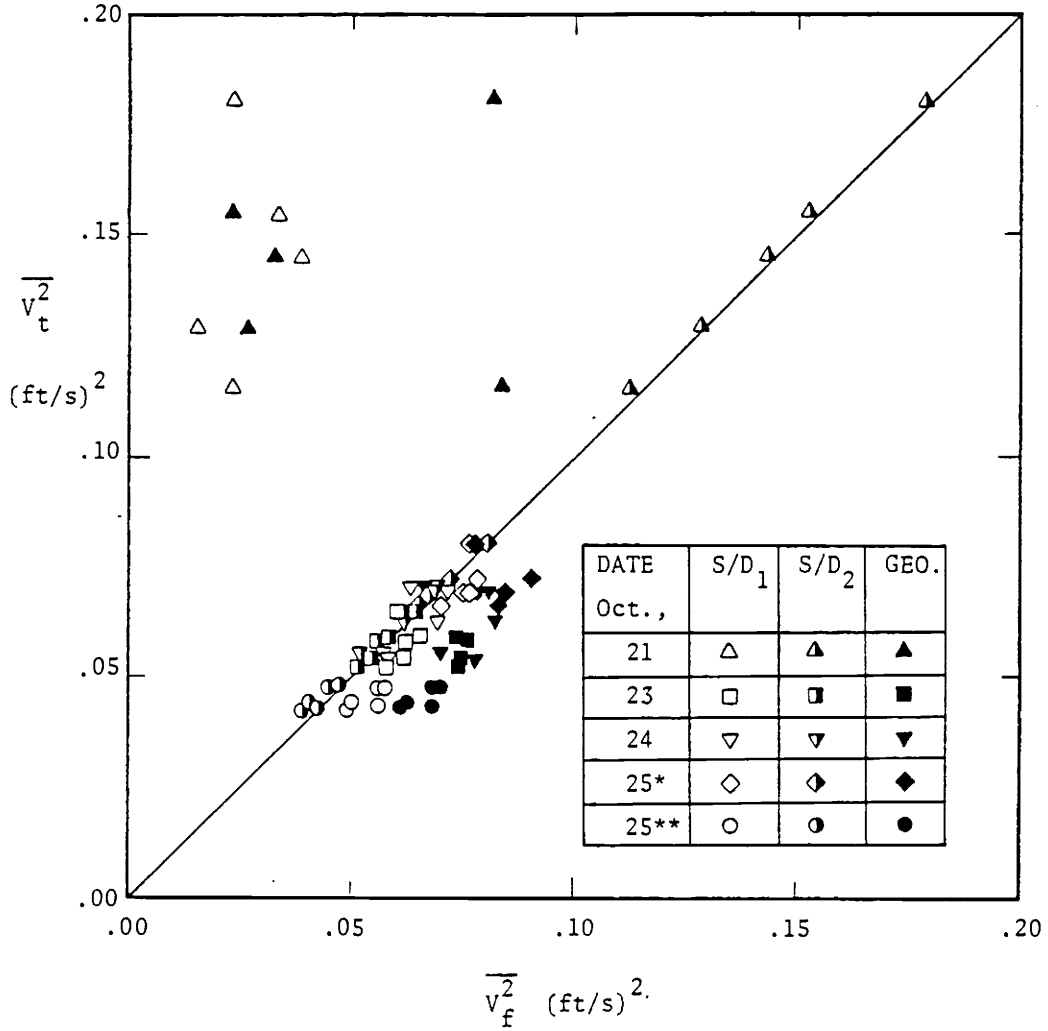


FIG. 4.7 Plot of mean square velocities $\overline{V_t^2}$ versus $\overline{V_f^2}$

Fourier coefficients which are directly transformed from the time series of measured wave properties. Consequently, the total energy density estimated from the frequency domain corresponds closely to the energy density estimated from the time domain except for the truncated high frequency components exceeding the deep water condition. Hence, all points based on S/D$_2$ fall along a 45$^\circ$ line in Fig. 4.7. The data of October 21 are extremely scattered again due to low wave conditions. The remaining four data sets correlate more closely in Fig. 4.7. However, differences between $\overline{V_t^2}$ and $\overline{V_f^2}$ can be significant for either the S/D$_1$ or GEO. methods.

The mean square velocity evaluated from the time domain generally under estimates the same quantity from the frequency domain by up to 14% for the $S/D_1$ method and 40% for the GEO. method. To explain this difference, two subsurface velocity fluctuations due to water surface wavelet pairs solved in a frequency interval are represented here in accordance with Eq.(2.69) from the GEO. method.

$$u_n(t)=A(\sigma_n)\cos(\sigma_n t-\theta_{an})\cos\phi_{an}+B(\sigma_n)\cos(\sigma_n t-\theta_{bn})\cos\phi_{bn}$$

$$v_n(t)=A(\sigma_n)\cos(\sigma_n t-\theta_{an})\sin\phi_{bn}+B(\sigma_n)\cos(\sigma_n t-\theta_{bn})\sin\phi_{bn}$$

where $\sigma_n=2\pi f_n$. The mean square velocity evaluated for this frequency $\sigma_n$ is

$$\overline{V_n^2}(t)=\overline{u_n^2(t)+v_n^2(t)}$$

$$=\frac{1}{2}[A^2(\sigma_n)+B^2(\sigma_n)]+A(\sigma_n)B(\sigma_n)\cos(\theta_{an}-\theta_{bn})\cos(\phi_{an}-\phi_{bn}) \qquad (4.5)$$

The frequency domain velocity energy density for the $A(\sigma_n)$ and $B(\sigma_n)$ wavelets in each frequency interval is simply

$$\frac{[A^2(\sigma_n)+B^2(\sigma_n)]}{2}$$

Equation (4.5) demonstrates that the mean square velocity in the time domain can not, in general, be equal to the velocity energy density in the frequency domain. However, for the stochastic/deterministic approach, $\theta_{an}-\theta_{bn}=90^\circ$ and the cross product term in Eq.(4.5) vanishes,

yielding an identity between the time and frequency domains. This solution is appropriate for the $S/D_2$ approach which utilizes only velocity data. However, the $S/D_1$ approach modifies the velocity amplitudes $A(\sigma_n)$ and $B(\sigma_n)$ with pressure data, violating the equality suggested by Eq. (4.5). Furthermore, it has been observed in this study that the two directions, $\phi_{an}$ and $\phi_{bn}$, solved from the GEO. approach are highly correlated and the difference between the two directions is usually smaller than $90^\circ$. Also, the difference between two phases, $\theta_{an}$ and $\theta_{bn}$, solved from the GEO. approach at each frequency is often larger than $90^\circ$. Therefore, the cross product term in Eq.(4.5) is negative and the mean square velocity in the time domain is reduced relative to the velocity energy density in the frequency domain. Consequently, $\overline{V_f^2}$ exceeds $\overline{V_t^2}$ for the geometric approach. This behavior is substantiated in Fig. 4.7.

### 4.4.3 Selection of Significant Data Sets

Utilizing a low energy content wave property record may confuse the interpretation of wave spectrum behavior, as shown for the data of October 21 in Section 4.4.1 and Section 4.4.2. Wave property measurements containing high wave energy, implying a significant wave state, are preferred in directional spectrum analysis. The parameter utilized to characterize significant data sets is the time domain mean square velocity, $\overline{V_t^2}$. Althrough $\overline{V_t^2}$ is not equal to $\overline{V_f^2}$, both quantities are proportional to the total wave energy content. Also $\overline{V_t^2}$ is the only parameter which can be simply calculated from velocity records in the time domain and associated with total wave energy content. For samples of October 1982, measured by meter 25, and March 1983 (see Table 4.1), 25% of each months samples with the highest $\overline{V_t^2}$ values are selected for spectral analysis. For samples of August 1982, the root mean square value of $\overline{V_t^2}$ shows a low average energy content for the entire month, $\overline{V_{rms}^2}=0.017\ (ft/s)^2$. Consequently, only the highest 10% of $\overline{V_t^2}$ values are utilized for spectral analysis in August 1982. For samples of October 1982, the sample population is so small that all 11 samples are

used in spectral analysis.

Tabular summaries of $E_{total}$ and $\overline{V_t^2}$ obtained from samples of significant data sets in October 1983 (meter 25) and March 1983 are presented in Table 4.8. These samples are thought to have sufficiently large energy densities to relate $E_{total}$ to $\overline{V_t^2}$. The tabular results suggest that $V_t^2$ can be an appropriate indicator for the total wave energy content. Figure 4.8 shows a plot of $E_{total}$ versus $\overline{V_t^2}/\overline{V_{rms}^2}$ for the significant data sets of October 1982 and March 1983.

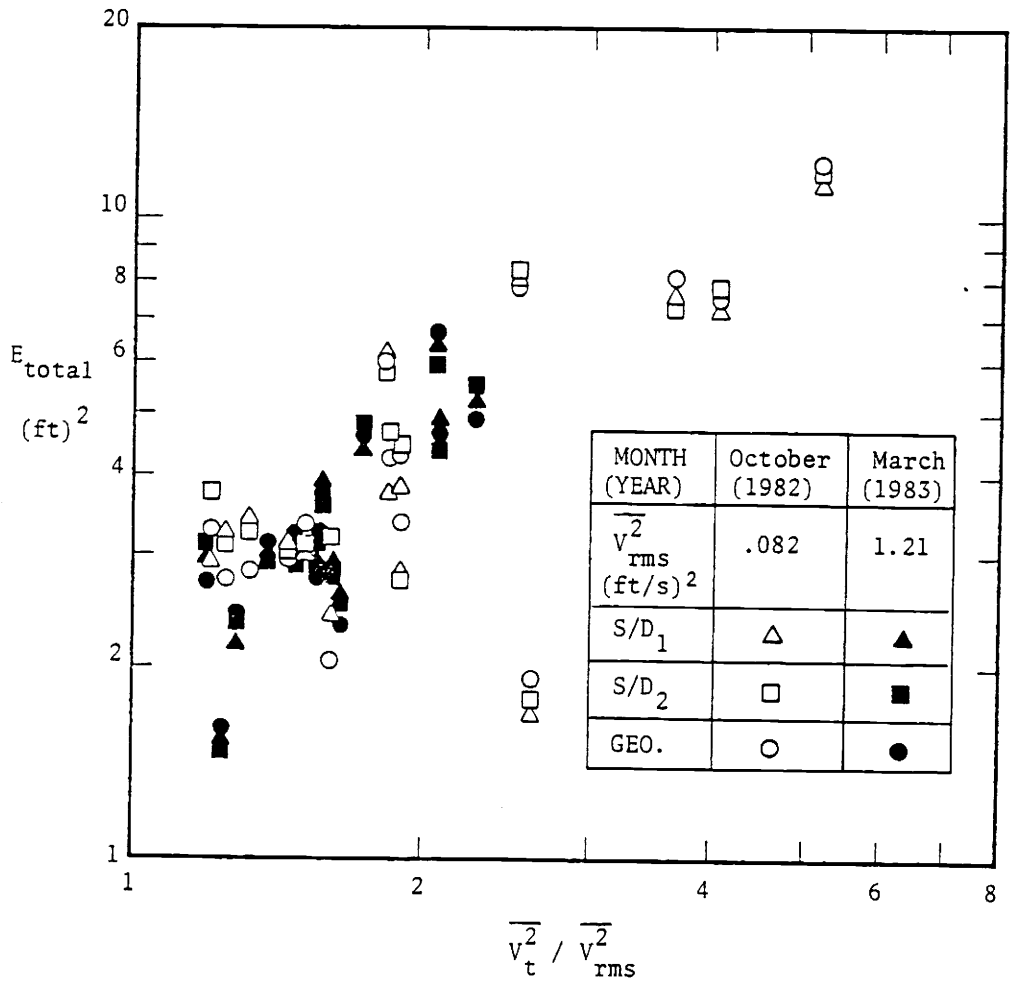


FIG. 4.8 Plot of $E_{total}$ versus $\overline{V_t^2}/\overline{V_{rms}^2}$

TABLE 4.8 Tabular summary of $E_{total}$ and $\overline{V_t^2}$

Month: March Year: 1983 Meter No. 26

| Date | Init. time | GEO. $E_{total}$ ($ft^2$) | $S/D_1$ $E_{total}$ ($ft^2$) | $S/D_2$ $E_{total}$ ($ft^2$) | $\overline{V_t^2}$ $(ft/s)^2$ | |
|---|---|---|---|---|---|---|
| 24 | 7:42 | 2.73 | 3.00 | 3.05 | 1.455 | |
| 24 | 13:34 | 4.87 | 5.27 | 5.42 | 2.753 | |
| 24 | 16:30 | 2.33 | 2.65 | 2.61 | 1.971 | |
| 24 | 19:26 | 3.14 | 2.96 | 2.87 | 1.776 | |
| 24 | 22:22 | 4.67 | 4.68 | 4.58 | 2.532 | |
| 25 | 1:18 | 3.73 | 3.79 | 3.67 | 1.905 | |
| 25 | 4:14 | 1.58 | 1.54 | 1.48 | 1.496 | |
| 25 | 7:10 | 2.74 | 2.87 | 2.76 | 1.917 | |
| 25 | 10:06 | 3.11 | 3.07 | 3.03 | 1.660 | |
| 25 | 13:02 | 3.18 | 3.13 | 3.10 | 1.894 | |
| 25 | 15:02 | 2.73 | 2.80 | 2.78 | 1.946 | |
| 25 | 18:54 | 2.43 | 2.19 | 2.39 | 1.560 | |
| 27 | 3:10 | 4.61 | 4.59 | 4.76 | 2.086 | |
| 27 | 6:06 | 6.49 | 6.48 | 5.97 | 2.525 | |

Month: October Year: 1982 Meter No. 25

| Date | Init. time | GEO. $E_{total}$ ($ft^2$) | $S/D_1$ $E_{total}$ ($ft^2$) | $S/D_2$ $E_{total}$ ($ft^2$) | $\overline{V_t^2}$ $(ft/s)^2$ | |
|---|---|---|---|---|---|---|
| 21 | 10:26 | .08 | .10 | .11 | .129 | |
| 22 | 2:30 | 6.03 | 5.92 | 4.51 | .151 | |
| 24 | 2:42 | 2.74 | 3.23 | 3.12 | .104 | |
| 26 | 2:54 | 2.83 | 3.41 | 3.24 | .110 | |
| 26 | 6:55 | 8.11 | 7.70 | 7.65 | .300 | |
| 26 | 10:56 | 7.54 | 7.47 | 7.78 | .331 | |
| 26 | 14:57 | 12.2 | 11.6 | 12.0 | .425 | |
| 27 | 3:00 | 4.38 | 3.82 | 4.26 | .155 | |
| 27 | 7:01 | 8.00 | 8.08 | 8.28 | .205 | |
| 27 | 11:02 | 1.92 | 1.75 | 1.82 | .215 | |
| 28 | 19:10 | 2.03 | 2.42 | 3.20 | .131 | |
| 28 | 23:11 | 3.34 | 3.02 | 3.13 | .124 | |
| 29 | 3:12 | 3.37 | 2.73 | 2.72 | .156 | |
| 29 | 7:13 | 3.29 | 2.91 | 3.76 | .099 | |
| 29 | 11:14 | 3.00 | 2.28 | 3.14 | .118 | |
| 31 | 19:28 | 4.29 | 3.78 | 4.70 | .152 | |

In Fig. 4.8, the increase of $\overline{V_t^2}/\overline{V_{rms}^2}$ is monotonic with $E_{total}$ for all three applied methods. Figure 4.8 also indicates how the total energy densities of the sample vary from one method to the other. The maximum difference in $E_{total}$ between the GEO. and $S/D_1$ methods is 22%, between the GEO. and $S/D_2$ methods is 55%, and between the $S/D_1$ and $S/D_2$ methods is 33%. Therefore, the one-dimensional spectrum may vary significantly depending on the method of analysis. Since the one-dimensional spectrum is a fundamental quantity in directional spectrum analysis, the appropriate method of analysis should be carefully chosen. The geometric method has been shown to be theoretically more satisfying and numerically more stable when compared to the other two methods. Consequently, the geometric method is regarded as a standard for comparing the results of other methods in the following sections.

### 4.4.4 Graphical presentation and Comparison of Directional Wave Spectrum Outputs

The computer system utilized in this study is equipped with a Tektronix, Model No. 4631, Hard Copy Unit, providing a variety of graphical outputs in response to user specified options in the directional spectrum software. A typical example of the available graphical outputs from a geometric method of analysis of the October 26, 1982, data set is shown in Figures 4.9 and 4.10. Each figure is composed of six sub-graphs. In Fig. 4.9, from left to right and from top to bottom, the sub-graphs include a proposed directional wave spectrum (plotted from the empirical equations representing the JONSWAP spectrum, spreading parameter and central angle), a smoothed directional wave spectrum, a one-dimensional wave spectrum, the distribution pattern of the spreading parameter, the frequency spectrum of the dominant (main) direction and the directional spectrum of the dominant (peak) frequency. In Fig. 4.10, from left to right and from top to bottom, the sub-graphs are a proposed directional velocity spectrum (plotted from the empirical equations), a smoothed directional velocity spectrum, a one-dimensional velocity spectrum, the distribution of central direction, the frequency velocity spectrum of the dominant direction and the direc-

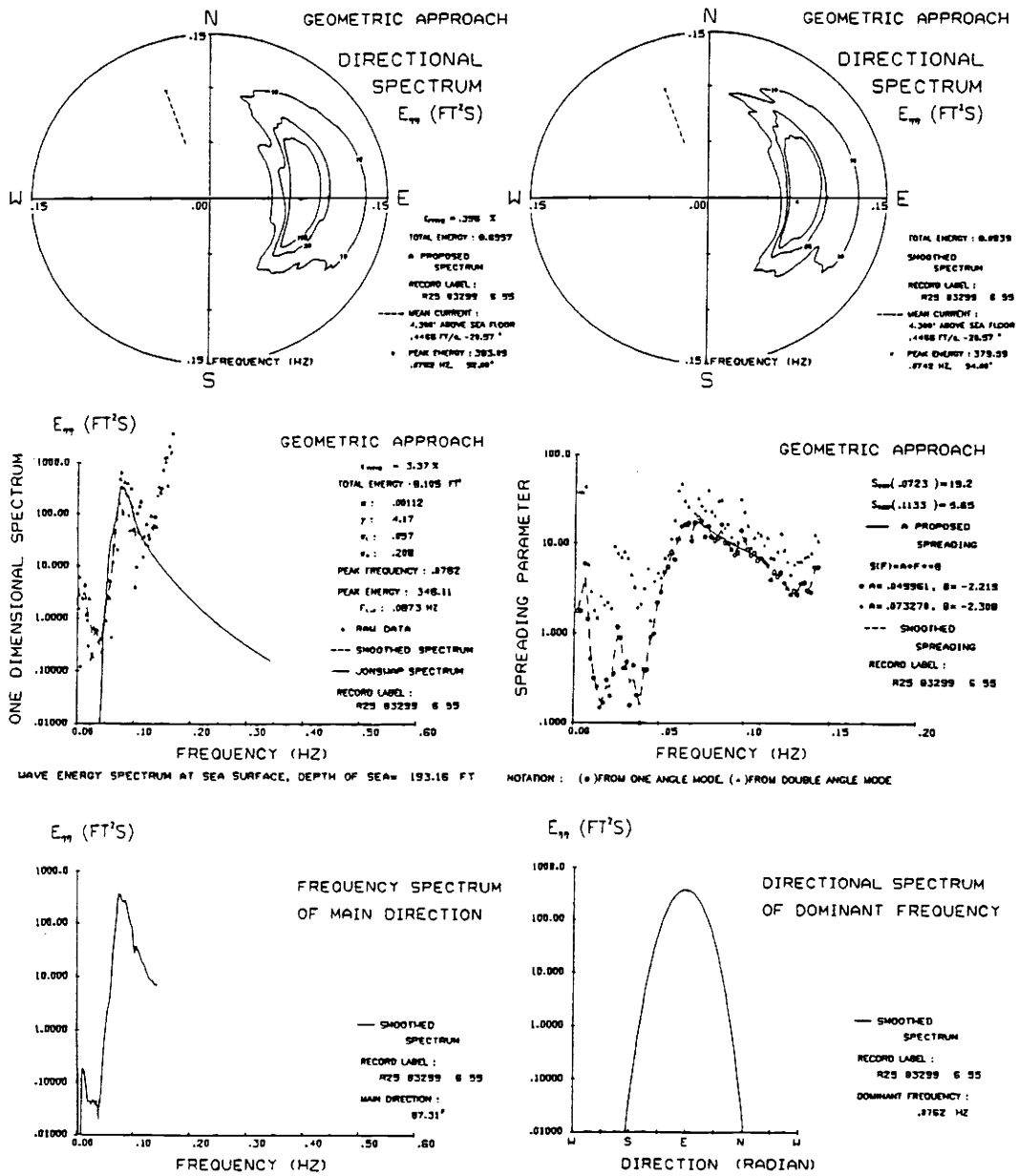


FIG. 4.9 Results of directional wave spectrum from the geometric approach

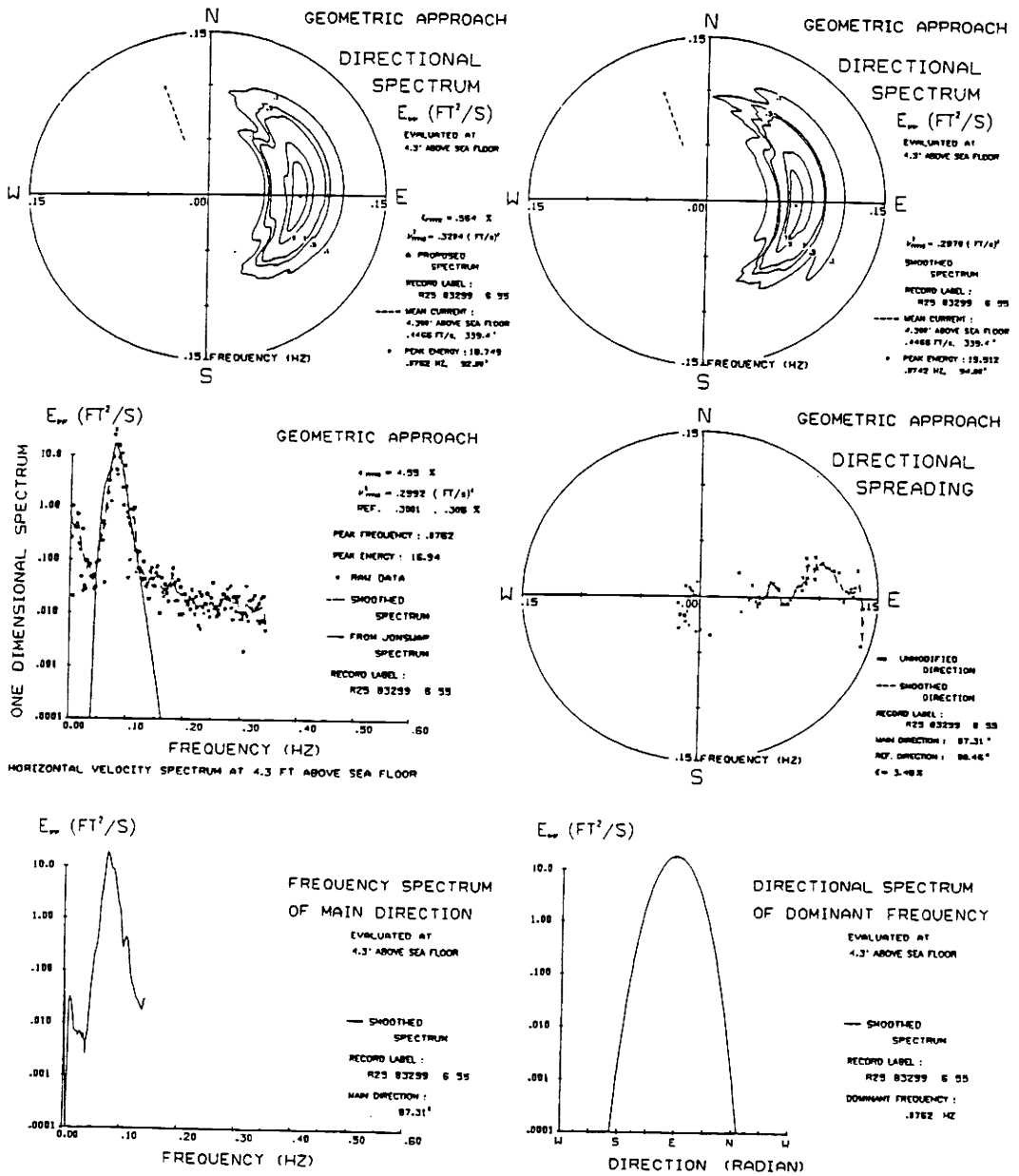


FIG. 4.10 Results of directional velocity spectrum from the geometric approach

tional velocity spectrum of the dominant frequency.

To examine the difference between the proposed directional spectrum and the smoothed raw data spectrum, the smoothed central angles (not the empirical central angle function) are utilized in the proposed directional spectrum in both Figs. 4.9 and 4.10. The error associated with the proposed models of the one-dimensional and the directional spectra compared to the smoothed raw data spectra have been evaluated in a root mean square sense, as specified in Eqs.(3.14) and (3.25), respectively. The errors as well as the total energy estimates are evaluated in a discrete form with a fundamental directional interval of $1^{\circ}$ and a fundamental frequency interval identical to that used in the FFT calculations. The errors are discussed later in this section.

The distribution of the spreading parameter with respect to frequency shows a maximum, $s_c$, near the spectral peak of the one-dimensional spectrum with decreasing values on both sides of $s_c$. One may notice that the spreading parameter maintains high values for a finite low frequency interval and then decreases rapidly to relatively low values at much lower frequencies. A decrease in the spreading parameter at low frequencies implies increased spreading of low frequency waves. This is contrary to what one would expect for waves coming from a single storm source. That is, long waves are relatively resistant to the dispersive effects of cross winds and currents, therefore, it is anticipated that low frequency waves are unidirectional. Accordingly, higher values of the spreading parameter should be associated with low frequency waves generated from the same origin. Evidently real ocean waves include low frequency waves arriving from a variety of sources, propagating in a variety of directions. The energy density levels at low frequencies are quite small so the absolute value of the spreading parameter in this frequency range does not significantly affect the overall energy distribution, evaluated in a mean square error sense.

The empirical equation for the spreading parameter utilized in the proposed directional spectra in both Figs. 4.9 and 4.10 has been

defined as a power function, as indicated in Eq.(3.15), for values to the right of $s_c$ and a constant, as indicated in Eq.(3.16), for values to the left of $s_c$. Normally, the spreading parameter power function to the right of $s_c$ covers an interval from the critical point, $f_c$, to the deep water frequency, indicated in Eq.(3.23). However, if the energy density drops by more than an order of magnitude prior to the deep water frequency, then the spreading parameter formula is evaluated over an abbreviated frequency range corresponding to the first relative minimum observed in the smoothed spreading parameter. The raw data one-dimensional spectrum (Fig. 4.9) indicates high energy density values at frequencies beyond the deep water wave condition. This occurs because a finite amount of energy remains in the velocity spectrum at high frequencies (Fig. 4.10) due to instrument noise. Then the inverse transfer function, Eq.(2.11) becomes very large at high frequencies, causing the calculated water surface elevation spectrum to become proportionately large. Clearly, this is a result of the numerical procedure, not an indication of wave activity at the water surface. Consequently, raw data beyond the deep water frequency should be ignored.

The graphical outputs from the same sample utilizing the $S/D_1$ and $S/D_2$ methods are shown in Figs. 4.11, 4.12, 4.13 and 4.14. The spreading parameter distribution from $S/D_1$ is closely related to the distribution from $S/D_2$ except at low frequencies where long wave effects become significant. However, both distribution curves of the spreading parameter solved from $S/D_1$ and $S/D_2$ differ greatly from the one solved from GEO.

A tabular summary comparing the three methods for the October 26 data is presented in Table 4.9. Results include total energy estimated from the smoothed and proposed directional spectra, spectral peak values, five JONSWAP parameters, two parameters of the spreading parameter power function to the right of $s_c$, and main directions evaluated in the time and frequency domains. According to Table 4.9, the root mean square errors for the proposed directional water surface elevation

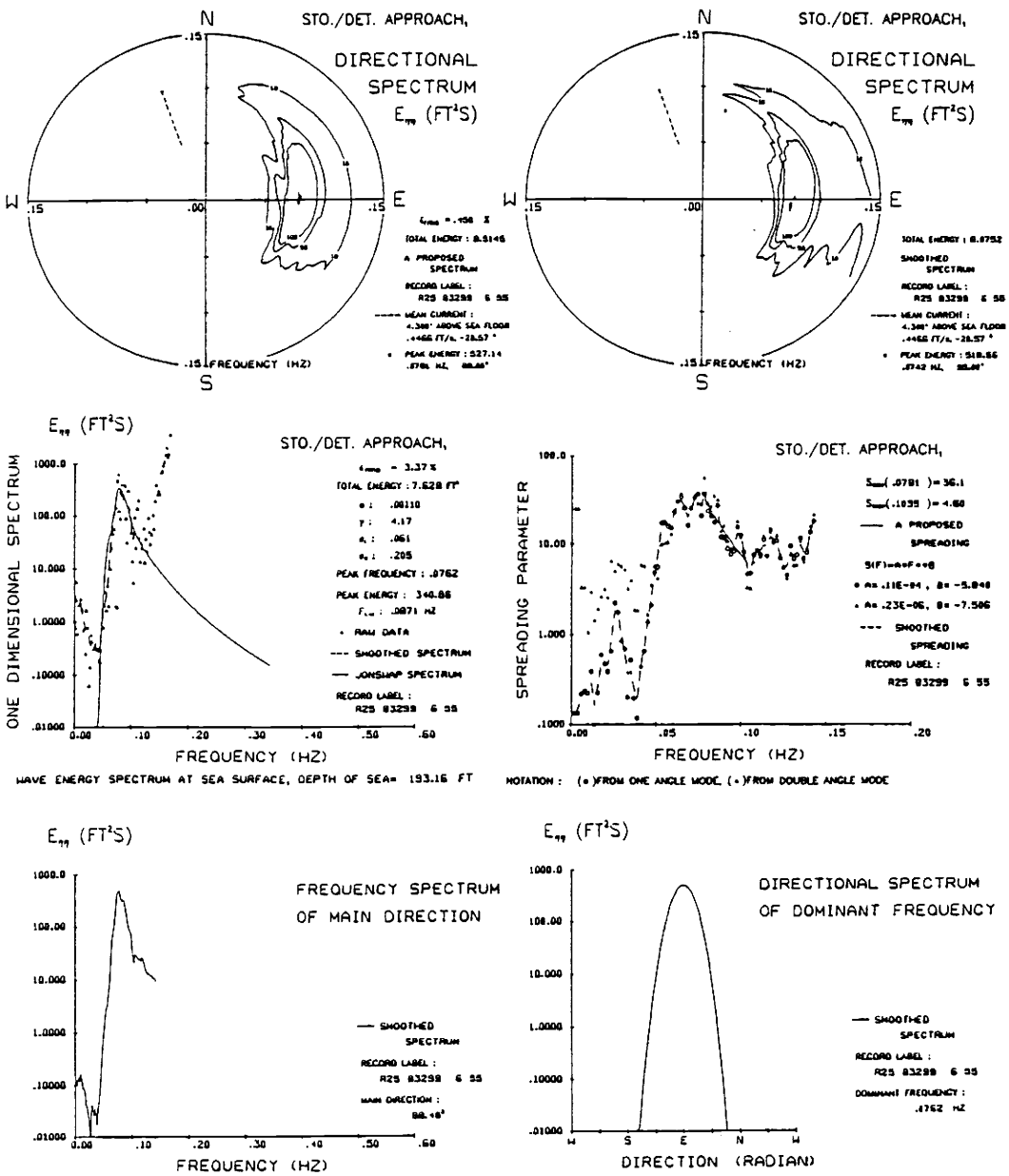


FIG. 4.11 Results of directional wave spectrum from the stochastic/deterministic approach one angle mode solution

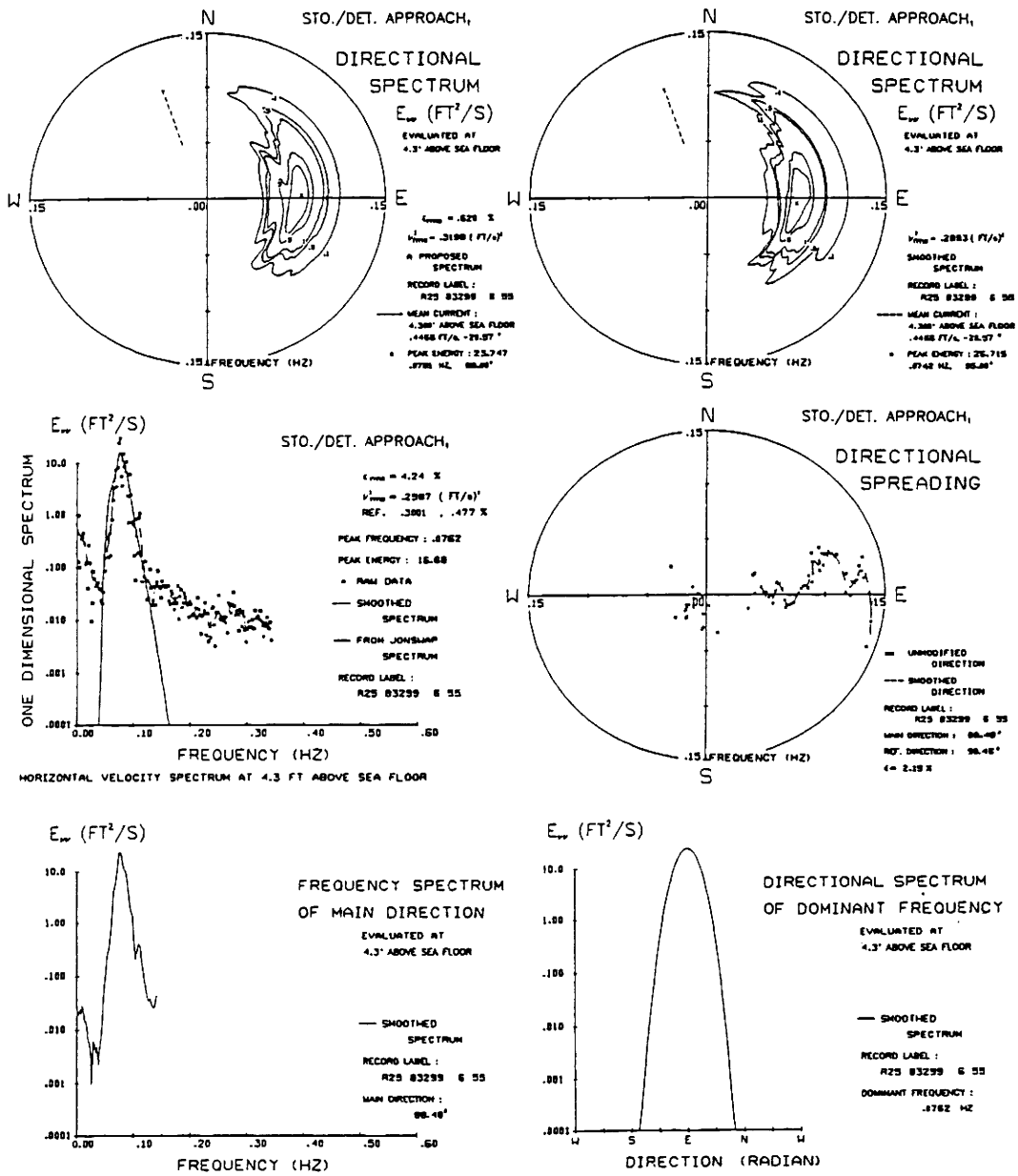


FIG. 4.12 Results of directional velocity spectrum from the stochastic/deterministic approach one angle mode solution

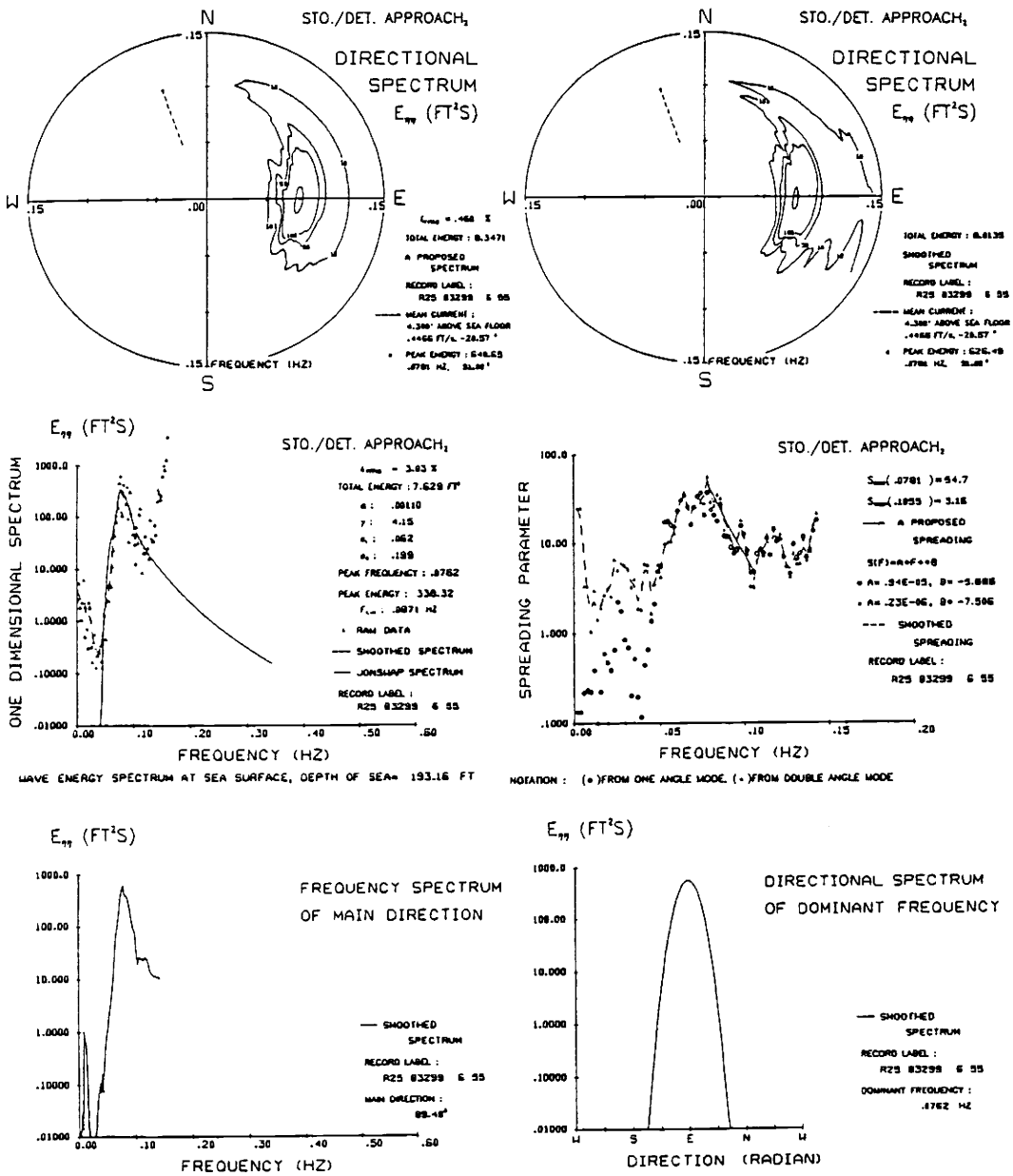


FIG. 4.13 Results of directional wave spectrum from the stochastic/deterministic approach double angle mode solution

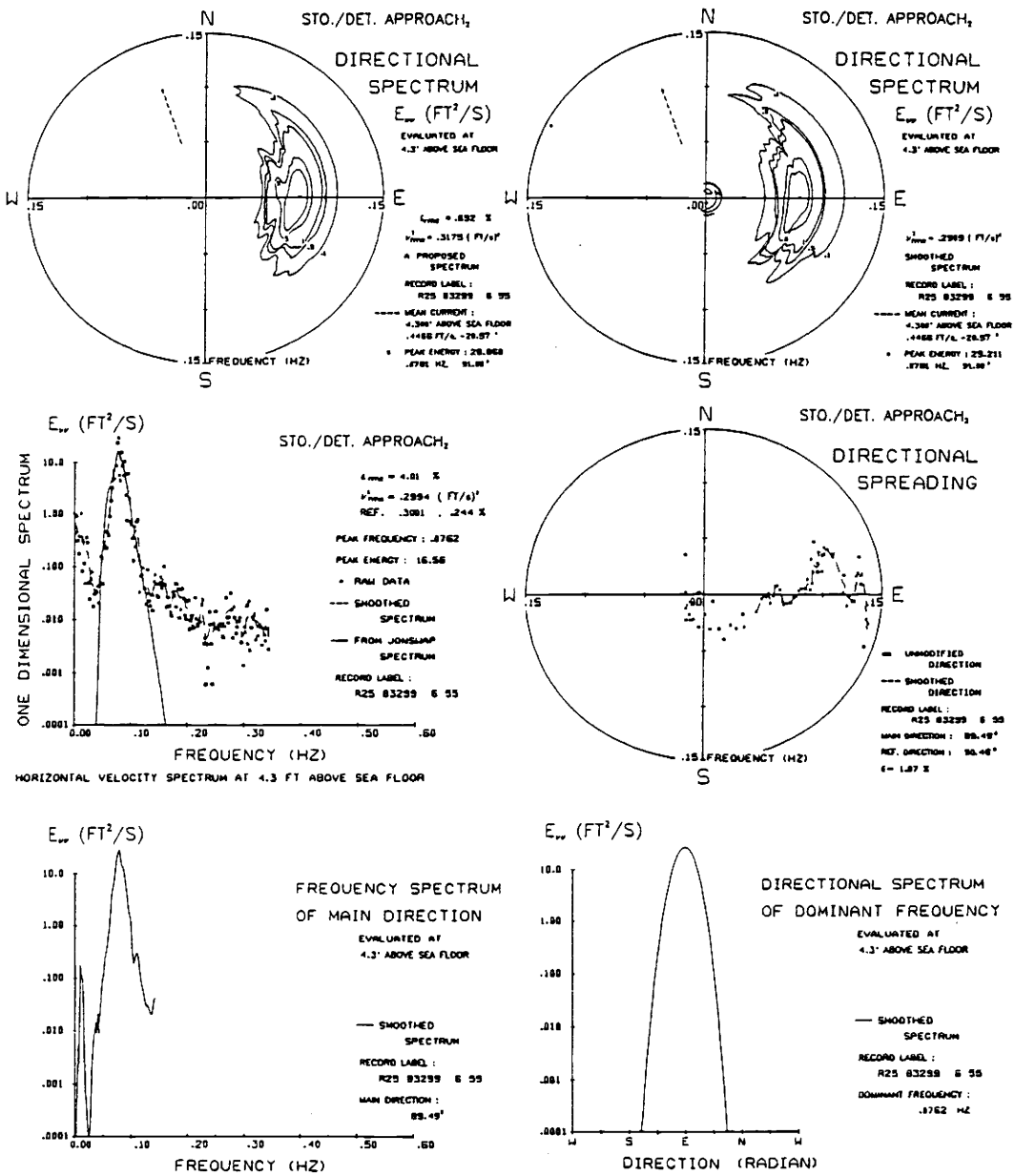


FIG. 4.14 Results of directional velocity spectrum from the stochastic/deterministic approach double angle mode solution

TABLE 4.9 Directional spectra summary

Date: Oct 26, 1982 Init. time: 6:55 Water depth: 193.2 (ft)

Mean current( 4.3 ft above bottom): .45 (ft/s), -20.6 (o) $\overline{V_t^2}$= .30 $(ft/s)^2$, $\bar{\phi}$= 90.5 (o)

ONE DIMENSIONAL WATER SURFACE WAVE ENERGY SPECTRUM

| | smoothed spectrum | JONSWAP spectrum | | | | | | | | |
|---|---|---|---|---|---|---|---|---|---|---|
| | $E_{total}$ $(ft^2)$ | $E_{total}$ $(ft^2)$ | $E_p$ $(ft^2 s)$ | $f_p$ (Hz) | $10^3\alpha$ | $\gamma$ | $\sigma_L$ | $\sigma_R$ | $\epsilon_{rms}$ (%) | $f_{1,-1}$ (Hz) |
| GEO. | 8.094 | 8.11 | 346 | .0762 | 1.12 | 4.17 | .057 | .208 | 3.37 | .0873 |
| $S/D_1$ | 8.075 | 7.63 | 341 | .0762 | 1.10 | 4.17 | .061 | .205 | 3.37 | .0871 |
| $S/D_2$ | 8.014 | 7.63 | 338 | .0762 | 1.10 | 4.15 | .062 | .199 | 3.03 | .0871 |

PROPOSED DIRECTIONAL WATER SURFACE WAVE ENERGY SPECTRUM

| | $E_{total}$ $(ft^2)$ | $E_p$ $(ft^2 s)$ | $f_p$ (Hz) | $\phi_p$ (o) | $\epsilon_{rms}$ (%) | $\phi_{main}$ (o) | $s_c$ | $f_c$ (Hz) | $A_R$ | $B_R$ |
|---|---|---|---|---|---|---|---|---|---|---|
| GEO. | 8.656 | 383 | .0762 | 92 | .40 | 87.3 | 19.2 | .0723 | $.50\ 10^{-1}_{-4}$ | -2.219 |
| $S/D_1$ | 8.514 | 527 | .0781 | 89 | .45 | 88.5 | 36.1 | .0781 | $.11\ 10^{-6}$ | -5.840 |
| $S/D_2$ | 8.347 | 641 | .0781 | 91 | .46 | 89.5 | 54.7 | .o781 | $.23\ 10^{-}$ | -7.506 |

SMOOTHED $E_{VV}(f)$

| | $E_{total}$ $(ft/s)^2$ |
|---|---|
| GEO. | .287 |
| $S/D_1$ | .289 |
| $S/D_2$ | .291 |

PROPOSED $E_{VV}(f)$

| | $E_{total}$ $(ft/s)^2$ | $E_p$ $(ft^2/s)$ | $f_p$ (Hz) | $\epsilon_{rms}$ (%) |
|---|---|---|---|---|
| GEO. | .299 | 16.9 | .0762 | 4.6 |
| $S/D_1$ | .299 | 16.7 | .0762 | 4.2 |
| $S/D_2$ | .299 | 16.6 | .0762 | 4.0 |

PROPOSED $E_{VV}(f,\phi)$

| | $E_{total}$ $(ft/s)^2$ | $E_p$ $(ft^2/s)$ | $f_p$ (Hz) | $\phi_p$ (o) | $\epsilon_{rms}$ (%) |
|---|---|---|---|---|---|
| GEO. | .320 | 18.7 | .0762 | 92 | .56 |
| $S/D_1$ | .320 | 23.7 | .0781 | 89 | .62 |
| $S/D_2$ | .318 | 28.9 | .0781 | 91 | .69 |

spectrum or velocity spectrum are small, less than 1%, for all three solution methods. Also, the root mean square errors associated with the proposed one-dimensional spectra are all less than 5%. However, the total energy densities estimated from the proposed water surface elevation spectrum and velocity spectrum may have errors up to 6% and 10%, respectively, of the smoothed directional wave spectrum and velocity spectrum.

Differences between the two-sided spreading parameter power function and one-sided power function are illustrated in Fig. 4.15. Alternative spreading function formulae are discussed in Section 3.4.2. The spreading parameter distributions are shown in the lower right hand corner of the figure. Water surface elevation directional spectra are presented on the left, velocity directional spectra are presented on the right. Smoothed raw data results appear in the center row while the one-dided and two-sided spreading function results are presented in the first and third rows, respectively. Smoothed raw data central angle distributions rather than empirical distributions were utilized for the proposed directional spectra in Fig. 4.15. A summary of total energy densities estimated from the smoothed directional spectra and from the alternative proposed directional spectra are tabulated in Table 4.10. Root mean square errors associated with alternative spreading functions are also listed. Both graphical and tabular results

TABLE 4.10 Total energy densities and root mean square errors of directional spectra for alternative spreading function representations

| | smoothed spectra | proposed spectra | | | |
|---|---|---|---|---|---|
| | | $s_{1\text{-side}}$* | | $s_{2\text{-side}}$** | |
| | $E_{total}$ | $E_{total}$ | $\varepsilon_{rms,2\text{-D}}$ | $E_{total}$ | $\varepsilon_{rms,2\text{-D}}$ |
| $E(f,\phi)$ | 8.094 $(ft^2)$ | 8.656 | .40 | 8.655 | .39 |
| $E_{VV}(f,\phi)$ | .2870 $(ft/s)^2$ | 0.320 | .56 | 0.320 | .53 |

* $A_L$=15.340 , $B_L$=0.000, $A_R$=.050, $B_R$=-2.22

** $A_L$=.23×$10^7$, $B_L$=4.435, $A_R$=.050, $B_R$=-2.22

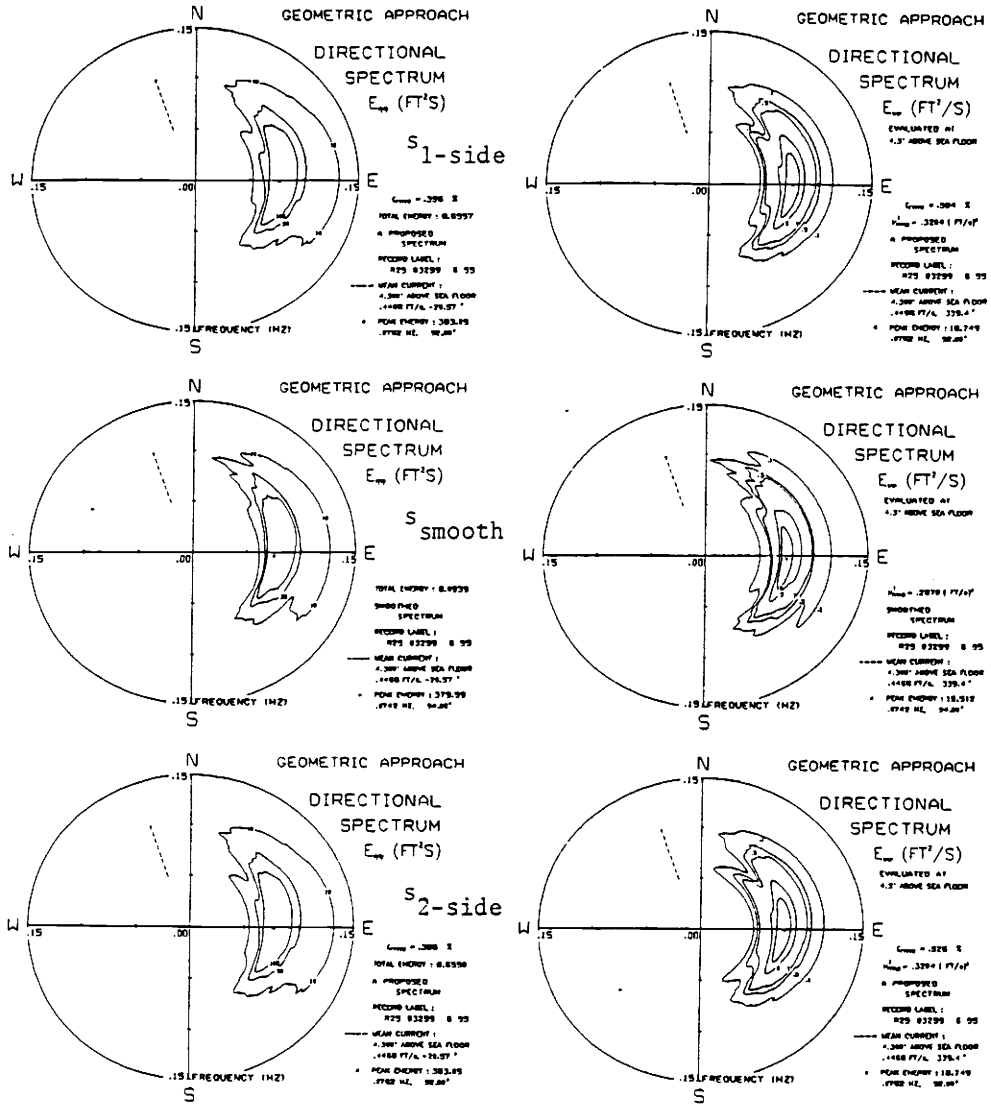


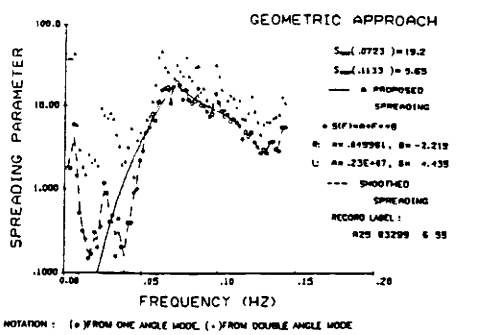


FIG. 4.15 Comparison of directional spectra for alternative spreading function representations

indicate little difference between the one-sided and two-sided spreading functions in the proposed directional spectrum models.

The main direction, $\phi_{main}$, and the third-order polynominal function , $\phi_{poly}$, are considered as alternatives in the proposed directional spectrum model. The two-sided spreading parameter power functions are utilized in comparing the two models. The resulting graphical outputs are shown in Fig. 4.16. The cental angle distribution with respect to frequency appears in the lower right hand corner of the figure; both raw data and the polynomial function are shown. The geometric approach is used to solve for water surface elevation directional spectra on the left and velocity directional spectra on the right. The smoothed raw data is graphed in the center row while the results for the proposed central angle represented as a contant, $\phi_{main}$, appear in the top row and the polynomial function results appear in the bottom row. Both functions smooth the results relative to the raw data. The $\phi_{main}$ results are symmetric about a constant $\phi_{main}$. The polynomial central angle results are symmetric about a central angle which varies with frequency, providing a more realistic appearance to the directional spectra. However, root mean square errors associated with both methods, tabulated in Table 4.11, are less than 1%. The polynomial central angle results are somewhat better than the constant central angle results and should be used for improved graphical presentations. However, a constant central

TABLE 4.11 Total energy densities and root mean square errors of directional spectra for alternative central angle representations

| | smoothed spectra | proposed spectra | | | |
|---|---|---|---|---|---|
| | | $\phi_{main}$ * | | $\phi_{poly}$ ** | |
| | $E_{total}$ | $E_{total}$ | $\epsilon_{rms,2\text{-}D}$ | $E_{total}$ | $\epsilon_{rms,2\text{-}D}$ |
| $E(f,\phi)$ | 8.094 $(ft^2)$ | 8.695 | .68 | 8.652 | .52 |
| $E_{VV}(f,\phi)$ | 0.287 $(ft/s)^2$ | 0.320 | .73 | 0.320 | .59 |

** $\phi_{main}=87.31$

** $\phi_{poly}=90.00+1419.6f_n-28536.8f_n^2+128392.0f_n^3$

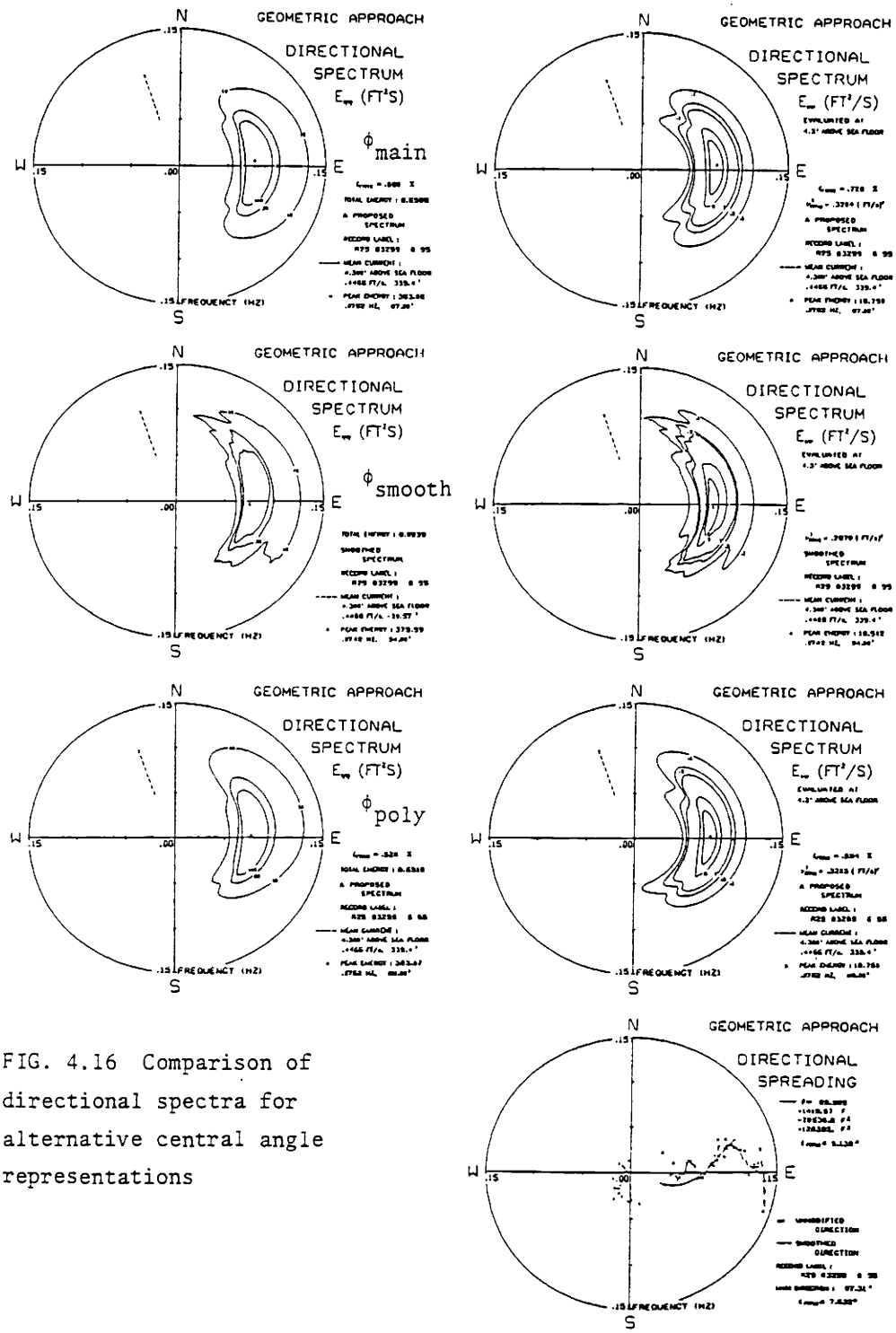


FIG. 4.16 Comparison of directional spectra for alternative central angle representations

angle equal to $\phi_{main}$ appears to provide a satisfactory representation of directional spectrum energy density.

## 4.5 Parametric Analysis

Empirical equations have been proposed to represent the water surface elevation directional spectrum as dicussed in Section 3.4. The directional spectrum is summarized by Eq.(3.24), the latter requiring frequency dependent relationships for the one-dimensional frequency spectrum, the spreading parameter and the central angle of wave propagation. The one-dimensional frequency spectrum is represented by the five parameter JONSWAP spectrum, defined in Eq.(3.13). The frequency dependent spreading parameter is defined by a two-sided exponential relationship in Eq.(3.15). A polynomial form for the frequency dependent central angle of wave propagation is defined in Eq.(3.17). Ten wave records with the highest energy levels were selected to analyze via the geometric method to obtain least squares best fit values to the empirical parameters. The results are summarized in Table 4.12, along with root mean square errors between the empirical directional spectra and the smoothed raw data spectra. Note that all errors are less than 2%, indicating that the the empirical formulae can provide reasonable precision as well as efficiency in quantifying directional spectrum properties.

All significant data sets identified in Section 4.4.3 have been analyzed via the geometric method to obtain abbreviated versions of the least squares best fit empirical parameters. The abbreviated empirical formulations use the one-sided spreading parameter, Eqs.(3.15) and (3.16), and a constant central angle equal to $\phi_{main}$, (Eq. 3.20). Results are tabulated in Table 4.13. Again, root mean square errors for the empirical spectra are less than 2% relative to the smoothed raw data spectra, suggesting that the abbreviated empirical formulations are also quite useful for quantifying wave directional spectrum properties.

In Table 4.13 the average values and standard deviations of the

TABLE 4.12 Empirical directional water surface elevation spectrum summary for ten high energy data sets

| Date | Init. time | Depth (ft) | $f_p$ (Hz) | $10^4\alpha$ | $\gamma$ | $\sigma_L$ | $\sigma_R$ | $A_L$ | $B_L$ | $f_c$ (Hz) | $A_R$ | $B_R$ | $\phi_{main}$ (o) | $10^{-1}c_o$ | $10^{-2}c_1$ | $10^{-3}c_2$ | $10^{-4}c_3$ | $\epsilon_{rms,2\text{-}D}$ (%) |
|---|---|---|---|---|---|---|---|---|---|---|---|---|---|---|---|---|---|---|
| 8/ 5/82 | 20:11 | 179.5 | .088 | 6.40 | 4.37 | .037 | .101 | $.126\times10^{4}$ | 1.22 | .074 | $.770\times10^{-1}$ | -2.02 | 80.9 | 9.0 | -12.13 | 20.20 | -8.47 | .85 |
| 10/24/82 | 6:45 | 185.9 | .082 | 5.53 | 4.07 | .033 | .030 | $.720\times10^{6}$ | 3.55 | .069 | $.512\times10^{-2}$ | -2.41 | 71.9 | 9.0 | -14.43 | 38.52 | -28.31 | 1.39 |
| 10/25/82 | 6:51 | 185.8 | .078 | 4.60 | 3.70 | .019 | .028 | $.300\times10^{8}$ | 5.53 | .064 | $.357\times10^{-5}$ | -5.44 | 87.0 | 9.0 | -19.54 | 57.29 | -41.16 | 1.58 |
| 10/26/82 | 6:55 | 193.2 | .076 | 11.2 | 4.17 | .057 | .208 | $.230\times10^{7}$ | 4.44 | .072 | $.500\times10^{-1}$ | -2.22 | 87.3 | 9.0 | 14.20 | -28.54 | 12.84 | .52 |
| 10/26/82 | 14:57 | 192.2 | .084 | 22.0 | 4.00 | .225 | .189 | $.360\times10^{12}$ | 9.08 | .078 | $.170\times10^{-2}$ | -3.81 | 98.3 | 9.0 | -5.00 | 19.57 | -14.72 | .57 |
| 10/27/82 | 7:01 | 192.9 | .088 | 30.0 | 4.38 | .050 | .048 | $.400\times10^{5}$ | 2.87 | .076 | $.314\times10^{-3}$ | -4.44 | 104.7 | 9.0 | -15.37 | 47.06 | -31.27 | .64 |
| 3/24/83 | 13:34 | 56.52 | .059 | 3.50 | 3.98 | .048 | .058 | $.660\times10^{9}$ | 5.56 | .062 | $.700\times10^{-4}$ | -5.25 | 98.1 | 9.0 | 6.75 | -13.01 | 6.70 | 1.38 |
| 3/25/83 | 1:18 | 58.73 | .064 | 3.84 | 2.93 | .070 | .086 | $.280\times10^{11}$ | 7.19 | .064 | $.800\times10^{-7}$ | -7.51 | 96.0 | 9.0 | 4.46 | -7.88 | 3.74 | .76 |
| 3/25/83 | 13:02 | 57.58 | .072 | 1.38 | 11.4 | .210 | .167 | $.120\times10^{10}$ | 6.24 | .057 | $.184\times10^{-0}$ | -1.80 | 91.8 | 9.0 | .71 | -2.71 | 2.40 | 1.57 |
| 3/27/83 | 3:10 | 57.82 | .072 | 7.70 | 2.68 | .088 | .103 | $.700\times10^{6}$ | 3.19 | .068 | $.105\times10^{-5}$ | -6.64 | 95.7 | 9.0 | 6.75 | -9.03 | 1.87 | .67 |

TABLE 4.13 Empirical directional water surface elevation spectrum summary for all significant data sets

Month: August Year: 1982 Meter No. 24 Meter height above bottom: 4.3 (ft)

| Date | Init. time | Depth (ft) | $f_p$ (Hz) | $10^4\alpha$ | $\gamma$ | $\sigma_L$ | $\sigma_R$ | $\theta_{main}$ (°) | $A_L$ ($B_L$=0) | $f_c$ (Hz) | $A_R$ | $B_R$ | $\varepsilon_{rms,2\text{-}D}$ (%) |
|---|---|---|---|---|---|---|---|---|---|---|---|---|---|
| 5 | 8:11 | 177.4 | .0703 | .181 | 4.14 | .080 | .108 | 78.5 | 5.15 | .0684 | $.116\times10^{-8}$ | -3.17 | .75 |
| 6 | 4:11 | 180.3 | .0644 | .017 | 7.35* | .123 | .125 | 81.0 | 11.57 | .0664 | $.227\times10^{-1}$ | -8.28 | .54 |
| 6 | 20:11 | 179.5 | .0879 | 6.40 | 4.37 | .037 | .101 | 80.9 | 13.26 | .0742 | $.770\times10^{-1}$ | -2.02 | .86 |
| 7 | 0:11 | 182.0 | .0938 | 7.55 | 4.17 | .055 | .048 | 75.2 | 11.95 | .0801 | $.153\times10^{-3}$ | -2.68 | .97 |
| 9 | 8:11 | 178.4 | .0918 | 1.99 | 6.07 | .251 | .095 | 96.9 | 13.56 | .0762 | $.850\times10^{-9}$ | -3.80 | .64 |
| 9 | 12:11 | 179.7 | .0957 | 5.65 | 3.92 | .068 | .056 | 92.8 | 19.38 | .0957 | $.401\times10^{-8}$ | -10.53 | 1.19 |
| 13 | 0:11 | 178.5 | .0644 | .025 | 3.97 | .090 | .059 | 83.3 | 4.94 | .0840 | $.688\times10^{-}$ | -8.28 | .97 |
| Average | | | .0812 | | 4.44 | .100 | .085 | 84.1 | | .0778 | | -5.54 | |
| ±Std.Dev. | | | ±.0142 | | ±.81 | ±.072 | ±.030 | ±7.86 | | ±.0101 | | ±4.00 | |

* not include in average

Month: October Year: 1982 Meter No. 25 Meter height above bottom: 4.3 (ft)

| | | | | | | | | | | | | | |
|---|---|---|---|---|---|---|---|---|---|---|---|---|---|
| 21 | 10:26 | 192.0 | .0586 | .072 | 3.57 | .060 | .043 | 46.8 | 29.40 | .0508 | $.277\times10^{-9}_{1}$ | -7.01 | .72 |
| 22 | 2:30 | 193.2 | .0938 | 31.4 | 3.65 | .048 | .058 | 14.0 | 6.33 | .0879 | $.154\times10^{}$ | -.626 | .56 |
| 24 | 2:42 | 191.6 | .0859 | 8.60 | 3.95 | .132 | .076 | 58.3 | 13.84 | .0703 | $.140^{-5}$ | -1.77 | .60 |
| 26 | 2:54 | 190.8 | .0918 | 4.50 | 10.29* | .193 | .117 | 71.0 | 9.08 | .0742 | $.290\times10^{}$ | -3.98 | .71 |
| 26 | 6:55 | 193.2 | .0762 | 11.2 | 4.17 | .057 | .208 | 87.3 | 15.34 | .0723 | $.050^{-10}$ | -2.22 | .68 |
| 26 | 10:56 | 193.1 | .0703 | 6.01 | 4.52 | .061 | .517 | 87.2 | 38.21 | .0664 | $.361\times10^{-2}$ | -8.55 | .95 |
| 26 | 14:57 | 192.2 | .0840 | 22.0 | 4.00 | .225 | .189 | 98.3 | 25.33 | .0781 | $.170\times10^{-5}$ | -3.81 | .65 |
| 27 | 3:00 | 190.6 | .0879 | 19.6 | 3.66 | .045 | .059 | 108.1 | 11.68 | .0879 | $.450\times10^{-5}$ | -4.18 | .69 |
| 27 | 7:01 | 192.9 | .0879 | 30.0 | 4.38 | .050 | .048 | 104.7 | 23.32 | .0781 | $.314\times10^{-5}$ | -4.44 | .67 |
| 27 | 11:02 | 200.3 | .0840 | 3.30 | 4.43 | .040 | .423 | 106.9 | 7.06 | .0820 | $.630\times10^{-7}$ | -3.77 | .58 |
| 28 | 19:10 | 202.0 | .0898 | 10.0 | 4.35 | .036 | .022 | 95.4 | 2.45 | .0742 | $.132\times10^{-2}$ | -5.59 | .66 |
| 28 | 23:11 | 200.9 | .0879 | 13.9 | 3.51 | .045 | .051 | 96.1 | 2.60 | .0762 | $.880\times10^{-6}$ | -2.25 | .48 |
| 29 | 3:12 | 200.0 | .0859 | 13.0 | 3.80 | .044 | .058 | 89.4 | 2.75 | .0762 | $.170\times10^{-2}$ | -4.82 | .44 |
| 29 | 7:13 | 201.8 | .0977 | 14.7 | 5.84 | .087 | .062 | 77.6 | 2.70 | .0898 | $.690\times10^{-8}$ | -2.52 | .51 |
| 29 | 11:14 | 203.7 | .0859 | 9.80 | 4.06 | .068 | .053 | 80.0 | 4.85 | .0703 | $.848\times10^{-1}$ | -5.90 | .72 |
| 31 | 19:28 | 198.7 | .0859 | 5.70 | 8.97* | .125 | .134 | 123.0 | 10.07 | .0723 | $.845\times10^{}$ | -1.86 | .75 |
| Average | | | .0846 | | 4.14 | .082 | .132 | 84.0 | | .0752 | | -3.96 | |
| ±Std.Dev. | | | ±.0094 | | ±.59 | ±.057 | ±.143 | ±26.8 | | ±.0095 | | ±2.10 | |

* not include in average

TABLE 4.13 (continued) Empirical directional water surface elevation spectrum summary for all significant data sets

Month: October Year: 1982 Meter No. 43 Meter height above bottom: 14. (ft)

| Date | Init. time | Depth (ft) | $f_p$ (Hz) | $10^4\alpha$ | $\gamma$ | $\sigma_L$ | $\sigma_R$ | $\phi_{main}$ (o) | $A_L$ ($B_L$=0) | $f_c$ (Hz) | $A_R$ | $B_R$ | $\epsilon_{rms,2\text{-}D}$ (%) |
|---|---|---|---|---|---|---|---|---|---|---|---|---|---|
| 19 | 18:18 | 182.9 | .0840 | .130 | 21.33* | .195 | .049 | 82.8 | 3.01 | .0781 | $.790\times10^{-13}$ | -10.50 | .65 |
| 21 | 2:26 | 185.8 | .0927 | 1.10 | 2.78 | .027 | .016 | 88.1 | 2.15 | .0518 | $.172^{-7}$ | -.888 | .59 |
| 21 | 10:28 | 184.5 | .0586 | .062 | 3.77 | .059 | .043 | 88.0 | 2.43 | .0566 | $.720\times10^{-7}$ | -4.47 | .93 |
| 21 | 18:30 | 184.4 | .0811 | .120 | 9.46* | .041 | .115 | 60.6 | 3.24 | .0576 | $.440\times10^{-13}$ | -4.77 | 1.86 |
| 23 | 2:38 | 184.9 | .0859 | 4.28 | 4.50 | .025 | .040 | 90.4 | 4.76 | .0762 | $.730\times10^{-10}$ | -10.53 | .89 |
| 23 | 14:41 | 186.4 | .0937 | .780 | 20.78* | .100 | .105 | 59.0 | 2.49 | .0790 | $.104\times10^{-2}$ | -8.55 | 1.14 |
| 24 | 6:45 | 185.9 | .0820 | 5.53 | 4.07 | .033 | .030 | 71.9 | 2.87 | .0693 | $.512\times10^{-6}$ | -2.41 | 1.31 |
| 24 | 14:47 | 185.6 | .0840 | .760 | 21.00* | .145 | .066 | 70.2 | 3.28 | .0723 | $.290\times10^{-9}$ | -4.47 | .74 |
| 25 | 2:50 | 183.7 | .0830 | 5.40 | 3.91 | .019 | .026 | 92.7 | 3.04 | .0811 | $.760\times10^{-7}$ | -7.01 | .56 |
| 25 | 6:51 | 185.8 | .0781 | 4.60 | 3.70 | .019 | .028 | 87.0 | 9.70 | .0644 | $.357\times10^{-2}$ | -5.44 | 1.54 |
| 25 | 10:52 | 185.2 | .0742 | 1.39 | 4.10 | .044 | .043 | 90.3 | 3.41 | .0664 | $.171\times10^{-2}$ | -2.84 | .48 |
| Average | | | .0816 | | 3.83 | .063 | .051 | 80.1 | | .0679 | | -5.62 | |
| ±Std.Dev. | | | ±.0095 | | ±.53 | ±.057 | ±.032 | ±12.4 | | ±.0101 | | ±3.05 | |

* not include in average

Month: March Year: 1983 Meter No. 26 Meter height above bottom: 4.3 (ft)

| | | | | | | | | | | | | | |
|---|---|---|---|---|---|---|---|---|---|---|---|---|---|
| 24 | 7:42 | 61.25 | .0586 | 1.68 | 4.38 | .063 | .090 | 89.1 | 24.53 | .0547 | $.670\times10^{-2}_{-6}$ | -2.86 | 1.32 |
| 24 | 13:34 | 56.52 | .0586 | 3.50 | 3.98 | .048 | .058 | 98.1 | 132.1 | .0625 | $.700\times10^{-10}$ | -5.25 | 1.05 |
| 24 | 16:30 | 57.14 | .0644 | 2.81 | 2.99 | .044 | .044 | 102.4 | 50.91 | .0625 | $.606\times10^{-2}$ | -8.28 | .83 |
| 24 | 19:26 | 59.91 | .0625 | 2.86 | 2.88 | .059 | .094 | 95.5 | 35.41 | .0606 | $.575\times10^{-5}$ | -3.15 | .92 |
| 24 | 22:22 | 60.45 | .0645 | 3.48 | 4.06 | .076 | .164 | 94.0 | 44.50 | .0645 | $.633\times10^{-9}$ | -4.11 | .68 |
| 25 | 1:18 | 58.73 | .0645 | 3.84 | 2.93 | .070 | .086 | 96.0 | 63.47 | .0644 | $.800\times10^{-1}$ | -7.51 | .76 |
| 25 | 4:14 | 58.85 | .0644 | 1.32 | 4.06 | .069 | .114 | 90.4 | 19.89 | .0606 | $.331\times10^{-9}$ | -2.32 | .83 |
| 25 | 7:10 | 61.00 | .0664 | 3.33 | 3.99 | .047 | .073 | 92.6 | 36.49 | .0703 | $.115\times10^{-1}$ | -8.28 | .94 |
| 25 | 10:06 | 60.87 | .0684 | 3.10 | 4.05 | .080 | .118 | 94.3 | 25.94 | .0664 | $.548\times10^{-2}$ | -2.31 | .57 |
| 25 | 13:02 | 57.58 | .0723 | 1.38 | 11.35* | .210 | .167 | 91.8 | 29.17 | .0566 | .184 | -1.80 | 1.54 |
| 25 | 15:02 | 55.96 | .0762 | 5.20 | 3.95 | .072 | .058 | 97.3 | 24.08 | .0742 | .147 | -2.00 | .58 |
| 25 | 18:54 | 58.63 | .0723 | 2.66 | 4.26 | .083 | .201 | 99.6 | 22.26 | .0684 | $.777^{-7}$ | -1.29 | .71 |
| 27 | 3:10 | 57.82 | .0723 | 7.70 | 2.68 | .088 | .103 | 95.7 | 51.34 | .0684 | $.105\times10^{-2}$ | -6.64 | .86 |
| 27 | 6:06 | 58.02 | .0742 | 11.7 | 3.85 | .055 | .065 | 88.5 | 19.45 | .0703 | .667 | -1.31 | 1.57 |
| Average | | | .0670 | | 3.70 | .076 | .102 | 94.7 | | .0646 | | -4.08 | |
| ±Std.Dev. | | | ±.0057 | | ±.59 | ±.041 | ±.046 | ±4.0 | | ±.0055 | | ±2.61 | |

* not include in average

JONSWAP parameters have been evaluated for the significant seasonal data sets. These average values do not reflect the mean JONSWAP parameter values obtained during the Joint North Sea Wave Project ($\gamma$=3.3, $\sigma_L$=.07, $\sigma_R$=.09) (Hasselmann et al., 1975). This is because the referenced JONSWAP values were evaluated under well-behaved wind conditions, implying the existence of a single or dominant wind fetch and duration. It is generally believed that a dominant storm will generate a wave spectrum with a single spectral peak. The JONSWAP spectrum appears to be able to represent a large range of single-peaked spectral shapes. However many wave spectra evaluated in the present study have two or more spectral peaks, implying the presence of waves from two or more storm sources. The JONSWAP spectrum may not be precisely applicable to those spectra which contain two or more peaks, consequently the resulting JONSWAP parameters deviate from standard values.

The average values of $B_R$ from the significant seasonal data sets in Table 4.13 are not equal to -2.7 as suggested by Eq.(2.43-1). Also, the standard deviations of these average values are large, contradicting the existence of a single constant power as shown in Eq.(2.43-1). However, this variability in $B_R$ may be due to the superposition of many wave systems generated from many storms. To substantiate this hypothesis, parameter values from single peaked spectra are examined.

An examination of the graphs of one-dimensional frequency spectra from the available significant data sets reveals very few single peaked spectra. As a compromise, single storm wave spectra have been approximated as those with low secondary peaks at higher frequencies. It is reasoned that relatively small, secondary peaks may be generated by local winds or nonlinear wave interactions. The effects of the secondary peak have been minimized by terminating the analysis of spectral properties at a frequency less than that associated with the secondary peak.

Spectral properties of the dominant peak have been evaluated via the $S/D_1$, $S/D_2$ and GEO. methods for the appropriate significant seasonal data sets. Tabular summaries of spectral properties $E_{total}$, $E_p$, $f_p$,

TABLE 4.14 Numerical behavior of directional wave properties
—— GEOMETRIC APPROACH

| Date | Init. time | $E_{total}$ ($ft^2$) | $E_p$ ($ft^2 s$) | $f_p$ (Hz) | $10^4\alpha$ | $\gamma$ | $\sigma_L$ | $\sigma_R$ | $f_{1,-1}$ (Hz) | $10^8 A_R$ | $B_R$ | $10^8 A_{Ro}$ | $A_{R1}$ |
|---|---|---|---|---|---|---|---|---|---|---|---|---|---|
| 3/27/83 | 6:06 | 6.488 | 382.5 | .0742 | 11.7 | 3.85 | .055 | .065 | .0852 | 4.356 | -8.275 | 2.426 | 29.94 |
| 10/27/82 | 7:01 | 5.406 | 476.9 | .0879 | 32.8 | 4.00 | .048 | .047 | .1010 | 1.940 | -8.275 | 1.123 | 3.262 |
| 3/27/83 | 3:10 | 3.288 | 199.0 | .0723 | 33.0 | 3.48 | .088 | .104 | .0833 | 1.388 | -8.275 | .7686 | 11.53 |
| 3/25/83 | 1:18 | 2.909 | 192.0 | .0644 | 3.86 | 2.91 | .070 | .088 | .0746 | .9970 | -8.275 | .5377 | 20.64 |
| 10/26/82 | 10:56 | 2.894 | 302.1 | .0703 | 8.20 | 3.33 | .056 | .047 | .0816 | .4420 | -8.55 | .5043 | 8.95 |
| 10/26/82 | 6:55 | 2.660 | 346.1 | .0762 | 9.78 | 4.77 | .061 | .108 | .0860 | .7170 | -8.275 | .4019 | 4.58 |
| 3/25/83 | 7:10 | 2.244 | 195.8 | .0664 | 3.32 | 4.00 | .047 | .067 | .0765 | .0031 | -10.525 | .7580 | 23.40 |
| 10/29/82 | 3:12 | 1.678 | 201.3 | .0860 | 13.1 | 3.79 | .044 | .047 | .0994 | .1810 | -8.55 | .2046 | .679 |
| 10/25/82 | 2:50 | 1.396 | 102.8 | .0830 | 5.44 | 3.91 | .019 | .026 | .0982 | .1660 | -8.55 | .6795 | .694 |
| 10/24/82 | 6:45 | 1.025 | 115.2 | .0820 | 5.49 | 4.10 | .033 | .030 | .0959 | 8.640 | -7.012 | .2093 | .948 |
| 10/25/82 | 6:51 | .8441 | 110.2 | .0781 | 4.34 | 3.88 | .019 | .031 | .0924 | .3400 | -8.275 | .1916 | 3.15 |
| 10/27/82 | 11:02 | .7871 | 66.18 | .0840 | 3.24 | 4.48 | .041 | .081 | .0961 | .0033 | -10.525 | .4968 | 2.20 |
| 10/25/82 | 10:52 | .4011 | 43.46 | .0781 | 1.67 | 3.97 | .044 | .062 | .0897 | 1.623 | -7.506 | .1287 | 1.o2 |
| 8/ 5/82 | 8:11 | .1530 | 8.286 | .0703 | .180 | 4.14 | .078 | .108 | .0793 | .0633 | -8.55 | .0723 | 1.64 |
| 10/21/82 | 10:26 | .0639 | 7.108 | .0586 | .074 | 3.47 | .059 | .043 | .0680 | .0857 | -8.275 | .0452 | 3.82 |
| 10/21/82 | 18:30 | .0527 | 6.180 | .0810 | .330 | 3.43 | .026 | .047 | .0953 | .0866 | -8.55 | .0982 | .470 |
| 10/21/82 | 10:28 | .0505 | 9.055 | .0586 | .076 | 4.31 | .023 | .032 | .0691 | .0141 | -8.55 | .0141 | 1.192 |
| 10/21/82 | 2:26 | .0253 | 3.424 | .0586 | .030 | 4.18 | .038 | .045 | .0682 | .0118 | -8.55 | .0136 | .949 |
| Average ±Std.Dev. | | | | | | 3.89 ±.44 | .048 ±.020 | .060 ±.027 | | | -8.52 ±.83 | | |

TABLE 4.15 Numerical behavior of directional wave properties
—— STO./DET. APPROACH$_1$

| Date | Init. time | $E_{total}$ ($ft^2$) | $E_p$ ($ft^2 s$) | $f_p$ (Hz) | $10^4\alpha$ | $\gamma$ | $\sigma_L$ | $\sigma_R$ | $f_{1,-1}$ (Hz) | $10^8 A_R$ | $B_R$ | $10^8 A_{Ro}$ | $A_{R1}$ |
|---|---|---|---|---|---|---|---|---|---|---|---|---|---|
| 3/27/83 | 6:06 | 6.482 | 380.0 | .0742 | 11.7 | 3.84 | .055 | .067 | .0852 | .0254 | -10.525 | 4.923 | 60.60 |
| 10/27/82 | 7:01 | 5.886 | 483.7 | .0879 | 3.41 | 3.91 | .048 | .045 | .1010 | 4.900 | -8.275 | 2.835 | 8.240 |
| 10/26/82 | 6:55 | 4.284 | 340.8 | .0762 | 12.1 | 3.81 | .060 | .073 | .0872 | .0075 | -10.525 | 1.378 | 13.95 |
| 10/26/82 | 10:56 | 4.243 | 295.8 | .0703 | 8.30 | 3.22 | .056 | .044 | .0818 | 1.480 | -8.550 | 1.690 | 29.54 |
| 3/27/83 | 3:10 | 3.828 | 197.7 | .0703 | 6.42 | 2.78 | .066 | .144 | .0815 | 8.213 | -8.275 | 4.519 | 81.16 |
| 10/22/82 | 2:30 | 3.779 | 298.4 | .0938 | 32.3 | 3.52 | .048 | .051 | .1083 | 5.905 | -8.275 | 3.467 | 5.57 |
| 3/25/83 | 1:18 | 3.343 | 191.5 | .0644 | 3.73 | 3.00 | .072 | .094 | .0744 | 3.280 | -8.275 | 1.770 | 69.50 |
| 3/25/83 | 7:10 | 2.273 | 197.3 | .0664 | 3.30 | 4.06 | .048 | .069 | .0764 | 1.130 | -8.55 | 1.294 | 40.40 |
| 3/25/83 | 10:06 | 2.220 | 160.5 | .0683 | 3.11 | 4.05 | .077 | .110 | .0773 | 1.945 | -8.275 | 1.063 | 29.90 |
| 3/25/83 | 15:58 | 2.149 | 155.0 | .0762 | 5.25 | 3.98 | .073 | .062 | .0865 | .0075 | -10.525 | 1.377 | 14.90 |
| 3/24/83 | 19:26 | 1.917 | 168.2 | .0625 | 3.04 | 2.77 | .062 | .094 | .0727 | 4.780 | -7.506 | .3038 | 14.40 |
| 10/28/82 | 23:11 | 1.913 | 166.2 | .0879 | 11.6 | 3.95 | .049 | .050 | .1012 | .5750 | -8.55 | .6493 | 1.86 |
| 10/25/82 | 10:52 | .3822 | 40.85 | .0781 | 1.63 | 3.83 | .047 | .054 | .0897 | 8.978 | -7.506 | .7120 | 5.67 |
| 10/19/82 | 18:18 | .1513 | 10.35 | .0840 | .510 | 4.45 | .136 | .021 | .0925 | 2.480 | -7.888 | .5446 | 3.34 |
| 8/ 5/82 | 8:11 | .1465 | 8.846 | .0703 | .175 | 4.56 | .083 | .079 | .0788 | .1600 | -8.55 | .1827 | 4.37 |
| 10/21/82 | 10:26 | .0596 | 7.194 | .0586 | .076 | 3.45 | .059 | .046 | .0679 | .0172 | -8.55 | .0198 | 1.68 |
| 10/21/82 | 10:28 | .0503 | 8.468 | .0586 | .073 | 4.24 | .022 | .032 | .0692 | .0322 | -8.55 | .0371 | 2.69 |
| Average | | | | | | 3.73 | .062 | .067 | | | -8.66 | | |
| ±Std.Dev. | | | | | | ±.53 | ±.024 | ±.030 | | | ±.95 | | |

TABLE 4.16 Numerical behavior of directional wave properties
—— STO./DET. APPROACH$_2$

| Date | Init. time | $E_{total}$ ($ft^2$) | $E_p$ ($ft^2 s$) | $f_p$ (Hz) | $10^4\alpha$ | $\gamma$ | $\sigma_L$ | $\sigma_R$ | $f_{1,-1}$ (Hz) | $10^8 A_R$ | $B_R$ | $10^8 A_{Ro}$ | $A_{R1}$ |
|---|---|---|---|---|---|---|---|---|---|---|---|---|---|
| 10/26/82 | 6:55 | 4.603 | 338.3 | .0762 | 12.0 | 3.80 | .061 | .079 | .0871 | 3.230 | -8.275 | 1.810 | 17.90 |
| 10/27/82 | 7:01 | 4.404 | 496.5 | .0879 | 35.1 | 3.90 | .052 | .044 | .1010 | 3.970 | -8.275 | 2.297 | 6.67 |
| 3/27/83 | 3:10 | 4.197 | 201.7 | .0703 | 6.72 | 2.71 | .068 | .146 | .0816 | 9.850 | -8.275 | 5.420 | 28.20 |
| 10/22/82 | 2:30 | 3.337 | 225.8 | .0939 | 21.7 | 3.96 | .055 | .053 | .1073 | 5.905 | -8.275 | 3.467 | 6.04 |
| 3/25/83 | 1:18 | 3.165 | 184.0 | .0644 | 3.66 | 2.94 | .072 | .093 | .0744 | 3.620 | -8.275 | 1.953 | 76.00 |
| 3/24/83 | 19:26 | 2.927 | 162.3 | .0625 | 2.91 | 2.83 | .059 | .094 | .0727 | .6340 | -8.275 | .3398 | 16.10 |
| 3/24/83 | 16:30 | 2.606 | 140.3 | .0644 | 2.81 | 2.92 | .093 | .046 | .0742 | .5280 | -8.55 | .6056 | 24.30 |
| 3/25/83 | 10:06 | 2.197 | 157.4 | .0683 | 3.05 | 4.05 | .079 | .111 | .0773 | 12.55 | -7.506 | .8805 | 24.70 |
| 10/29/82 | 3:12 | 2.132 | 152.8 | .0762 | 5.18 | 3.98 | .073 | .063 | .0865 | 1.200 | -8.55 | 1.365 | 14.81 |
| 10/28/82 | 23:11 | 1.973 | 164.3 | .0860 | 12.4 | 3.27 | .039 | .038 | .1006 | .1810 | -8.55 | .2647 | .614 |
| 10/27/82 | 11:02 | 1.736 | 160.3 | .0879 | 13.4 | 3.30 | .045 | .044 | .1023 | 3.070 | -8.275 | 1.776 | 4.626 |
| 10/25/82/ | 6:51 | .9898 | 76.21 | .0840 | 3.77 | 4.44 | .040 | .090 | .0962 | .0270 | -10.525 | 4.071 | 17.97 |
| 10/25/82 | 10:52 | .5860 | 79.96 | .0781 | 3.30 | 3.70 | .019 | .028 | .0926 | .9380 | -8.55 | 1.066 | 6.489 |
| 10/19/82 | 18:18 | .3978 | 2.904 | .0781 | .890 | 4.98 | .072 | .093 | .0876 | .9830 | -8.275 | .5540 | 5.387 |
| 8/ 5/82 | 8:11 | .1358 | 7.485 | .0703 | .167 | 4.06 | .083 | .086 | .0794 | .6510 | -8.55 | .7423 | 16.68 |
| 10/21/82 | 10:28 | .0348 | 6.512 | .0586 | .061 | 3.90 | .024 | .031 | .0694 | .0740 | -8.55 | .0853 | 6.038 |
| Average | | | | | | 3.67 | .058 | .071 | | | -8.47 | | |
| ±Std.Dev. | | | | | | ±.63 | ±.021 | ±.033 | | | ±.60 | | |

$\alpha$, $\gamma$, $\sigma_L$, $\sigma_R$, $f_{1,-1}$, $A_R$ and $B_R$ are expressed in Tables 4.14, 15, 16. In these tables, the samples are ordered from large values of $E_{total}$ to small values. Average values and standard deviations are calculated for $\gamma$, $\sigma_L$, $\sigma_R$, and $B_R$, for each method of analysis. A list of these average values and standard deviations appears in Table 4.17.

TABLE 4.17 Means and Standard Deviations of Parameters $\gamma$, $\sigma_L$, $\sigma_R$, $B_R$

| Method | $\gamma$ | $\sigma_L$ | $\sigma_R$ | $B_R$ |
|---|---|---|---|---|
| GEO. | 3.89±.44 | .048±.02 | .060±.027 | -8.52±.83 |
| $S/D_1$ | 3.73±.53 | .062±.024 | .067±.030 | -8.66±.95 |
| $S/D_2$ | 3.67±.63 | .058±.021 | .071±.033 | -8.47±.060 |

The mean JONSWAP parameters obtained here are somewhat diffenent from those obtained from the North Sea Project (Hasselmann et al., 1975 ). This may be due to meteorological and oceanographical conditions which are unique to the two different ocean systems. Neverthless, the JONSWAP spectrum parameter mean values expressed in Table 4.17 for the geometric approach are deemed most appropriate to model one-dimensional frequency spectra for single storm wave systems in the offshore Coos Bay, Oregon, area.

Averages of $B_R$ obtained from the various methods are relatively consistent and all have small standard deviations. Thus, a constant value of -8.5, from the geometric method, is proposed for the power in Eq.(2.43-1), instead of a value of -2.7 which was utilized by S.E. Sand (1979). Hence, Eq.(2.43-1) because

$$s_e(f_n)=A_{R1}\left(\frac{f_n}{f_{1,-1}}\right)^{-8.5} \tag{4.6}$$

An alternative form for the right side spreading parameter function is proposed as

$$s_e(f_n)=A_{Ro}(f_n)^{-8.5} \tag{4.7}$$

The parameters $A_{R1}$ and $A_{Ro}$ are calculated relative to this constant value for $B_R$ by a regression procedure which evaluates the spreading parameter at the peak frequency utilizing Eq.(3.15) and then returns the values $A_{R1}$ and $A_{Ro}$ utilizing Eqs.(4.6) and (4.7), respectively. Chosing the spreading parameter at the peak frequency, $f_p$, rather than at the critical frequency, $f_c$, is thought to be a more significant value for regressing $A_{R1}$ and $A_{Ro}$. The regressed values of $A_{R1}$ and $A_{Ro}$ are also expressed in Tables 4.14, 15, 16 for each method.

Both parameters $A_{Ro}$ and $A_{R1}$ tend to decrease with decreasing $E_{total}$ and $E_p$. The statistical correlations among these parameters are calculated and expressend in Table 4.18. The tabular results demonstrate that the parameters $E_{total}$ and $A_{Ro}$ have the highest positive correlation, a value of unity being a perfect correlation.

TABLE 4.18 Correlations among parameters $E_{total}$, $E_p$, $A_{Ro}$, $A_{R1}$

| | GEO. | | $S/D_1$ | | $S/D_2$ | |
|---|---|---|---|---|---|---|
| | $A_{Ro}$ | $A_{R1}$ | $A_{Ro}$ | $A_{R1}$ | $A_{Ro}$ | $A_{R1}$ |
| $E_{total}$ | .85 | .64 | .78 | .39 | .44 | .39 |
| $E_p$ | .68 | .46 | .67 | .30 | .31 | .06 |

A graph of $E_{total}$ versus $A_{Ro}$ is presented in Figure 4.17, including results obtained from the GEO., $S/D_1$, $S/D_2$ methods. The points associated with $S/D_2$ are more scattered. The points associated with both the GEO. and $S/D_1$ methods are more well behaved and may be approximated by straight lines in Figure 4.17. The function

$$A_{Ro}=C(E_{total})^D \tag{4.8}$$

indicates a straight line on log-log scaled paper and is utilized here to present an empirical relationship between $A_{Ro}$ and $E_{total}$. Parameters C and D of Eq.(4.8) are determined utilizing a least square best fit

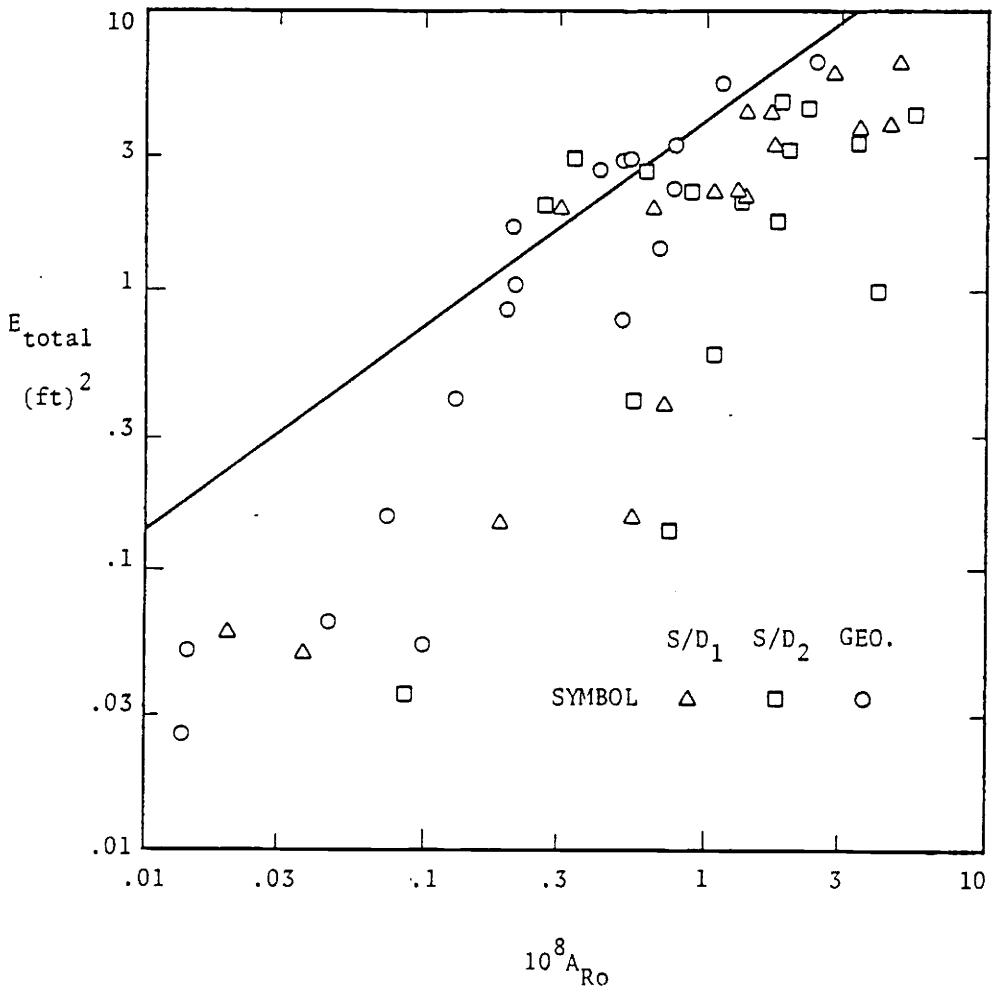


FIG. 4.17 Correlation study of $E_{total}$ and $A_{Ro}$

procedure which is similar to the one used in determining the parameters $A_R$ and $B_R$ for the spreading parameter power function expressed by Eq.(3.15). The resulting parameters for the three methods of analysis provide the following equations

TABLE 4.19 Empirical spreading parameter coefficient equations

| Method | Equation | Correlation |
|---|---|---|
| GEO. | $A_{Ro}=1.5*10^{-9}(E_{total})^{1.396}$ | .85 |
| $S/D_1$ | $A_{Ro}=5.1*10^{-9}(E_{total})^{1.131}$ | .78 |
| $S/D_2$ | $A_{Ro}=1.24*10^{-8}(E_{total})^{.47}$ | .44 |

where $E_{total}$ is the total wave energy density with a unit of $ft^2$. The equation for the geometric appropach is graphed through the data in Fig. 4.17.

The proposed spreading parameter function of Eq.(4.7) may now be, expressed empirically as

$$s_e(f_n)=C(E_{total})^D(f_n)^{-8.5} \tag{4.9}$$

However, Eq.(4.9) is suitable only for wave systems generated by a single storm event in the region offshore of Coos Bay, Oregon.

The main direction of wave propagation is shown to vary from $80^\circ$ in October to $95^\circ$ in March; see Table 4.13. One may use these seasonally variable values to approximate the central angle of wave propagation in Eq.(3.20). Also, the mean JONSWAP parameters from Table 4.17 may be used to approximate the frequency spectrum shape. The total spectral energy, $E_{total}$, and peak frequency, $f_p$, may be obtained from traditional hindcasting procedures for a specific design storm wind velocity, fetch and duration. With $E_{total}$ and $f_p$ known, along with the results of Table 4.17, the JONSWAP spectrum is specified. Similarily, the spreading parameter is specified by Eq.(4.9). Now one can predict the water surface elevation directional spectrum for offshore Coos Bay, Oregon by substituting these specific results into Eq.(3.24).

## 4.6 Directional Wave Simulation Study

Random wave simulation produces wave property records directly from a designed wave spectrum, called a target spectrum. Only the statistics of the wave property can be reproduced, not the originally measured records. That is, the wave properties are reproduced in a statistical sense by utilizing the wave simulation method (Borgman, 1969).

The concept of a directional wave simulation algorithm comes from

a physical interpretation of the directional spectrum as discussed in Section 2.2. An infinitestimal amplitude wavelet may be thought of as contributing energy to a small interval of frequency and direction. The entire spectrum can then be thought of as the sum of the contributions from a large number of wavelets. Each of these wavelets may have its amplitude evaluated from Eq.(2.51), or

$$a_{mn} = \sqrt{2E(f_n,\phi_m)\Delta f_n \Delta\phi_m} \tag{4.10}$$

where $a_{mn}$ denotes the amplitude of a wavelet within a frequency interval $\Delta f_n$ and a direction interval $\Delta\phi_m$. More specifically, a wavelet which has an amplitude $a_{mn}$ is regarded as an independent small wave with wave frequency $f_n$ and propagation direction $\phi_m$. The surface wave profile then may be represented by the sum of those small, independent wavelets, or

$$\eta(x,y,t) = \sum_{n=1}^{N} \sum_{m=1}^{M} a_{mn} \cos(k_n x\cos\phi_m + k_n y\sin\phi_m - 2\pi f_n t + \theta_{mn}) \tag{4.11}$$

Since each small wave is assumed to be independent of others, the phase $\theta_{mn}$ is assumed to be uniformly and randomly distributed over the interval $(0, 2\pi)$. Hence, various other wave properties can be described simply by transferring Eq.(4.11) to the desired wave properties in accordance with linear wave theory.

Wave simulation from a one-dimensional frequency spectrum is a simplified model of directional wave simulation. By dropping out the direction index and symbols from Eqs.(4.10) and (4.11), a wave simulation model associated with the frequency spectrum is obtained.

The validity of a wave simulation model is usually tested by evaluating a spectrum from the simulated wave properties and comparing the results with the target spectrum. The wave simulation model associated with a frequency spectrum usually has no difficulty returning the spectral properties of the target spectrum. However, the results obtained from directional wave simulation are usually poorly correlated with

the target directional spectrum. The main reason is that the phases of individual wave frequency components can be nicely described as random variables. However, phases of waves with the same frequency but different directions may not be appropriately represented by a uniform distribution over the interval (0, $2\pi$), that is, wave directional components of the same fequency may have related phases.

Poor results from directional wave simulation have been obtained by many investigators in the past. A procedure utilized to improve directional wave simulation results is to look the mean values and standard deviations of spectral properties of many simulation runs. Since each run of many simulations is assumed to be independent of other runs, the mean values and standard deviations of wave properties of many runs allow one to identify the intervals in which the theoretically true values are most likely located. This procedure is referred as the Maximum Likelihood Method in statistics (Goda, 1981).

In order to see how directional wave simulation results vary with respect to individual methods of analysis a target directional spectrum is utilized here to generate 15 subsurface pressure and velocity records which are then analyzed by the computational system. The resulting mean values and standard deviations of $E_{total}$, $E_p$, $\varepsilon_{rms,1\text{-}D}$, JONSWAP parameters, $f_{1,-1}$, $s_c$, $f_c$, $B_L$, $B_R$, $\phi_{main}$ and $\varepsilon_{rms,\phi_o}$ are expressed in Table 4.20. The same information for the target directional wave spectrum is also indicated in Table 4.20, providing a constant spreading parameter, $.9s_c$, for values to the left of $s_c$ and a constant direction, $15^o$, for all central angles.

One may notice that the mean values of $E_{total}$, $E_p$, $\alpha$ and $s_c$ obtained from $S/D_1$ and $S/D_2$ are considerably larger than the values assigned to the target spectrum. Also the standard deviations are much larger those obtained from GEO. For other parameters expressed in Table 4.20 the related mean values and standard deviations are approximately equal for all methods. Nevertheless, the geometric approach produces less biased means, smaller standard deviations, and smaller errors.

the target directional spectrum. The main reason is that the phases of individual wave frequency components can be nicely described as random variables. However, phases of waves with the same frequency but different directions may not be appropriately represented by a uniform distribution over the interval $(0, 2\pi)$, that is, wave directional components of the same fequency may have related phases.

Poor results from directional wave simulation have been obtained by many investigators in the past. A procedure utilized to improve directional wave simulation results is to look the mean values and standard deviations of spectral properties of many simulation runs. Since each run of many simulations is assumed to be independent of other runs, the mean values and standard deviations of wave properties of many runs allow one to identify the intervals in which the theoretically true values are most likely located. This procedure is referred as the Maximum Likelihood Method in statistics (Mendenhall et al., 1981).

In order to see how directional wave simulation results vary with respect to individual methods of analysis a target directional spectrum is utilized here to generate 15 subsurface pressure and velocity records which are then analyzed by the computational system. The resulting mean values and standard deviations of $E_{total}$, $E_p$, $\varepsilon_{rms,1\text{-}D}$, JONSWAP parameters, $f_{1,-1}$, $s_c$, $f_c$, $B_L$, $B_R$, $\phi_{main}$ and $\varepsilon_{rms,\phi_o}$ are expressed in Table 4.20. The same information for the target directional wave spectrum is also indicated in Table 4.20, providing a constant spreading parameter, $.9s_c$, for values to the left of $s_c$ and a constant direction, $15^o$, for all central angles.

One may notice that the mean values of $E_{total}$, $E_p$, $\alpha$ and $s_c$ obtained from $S/D_1$ and $S/D_2$ are considerably larger than the values assigned to the target spectrum. Also the standard deviations are much larger those obtained from GEO. For other parameters expressed in Table 4.20 the related mean values and standard deviations are approximately equal for all methods. Nevertheless, the geometric approach produces less biased means, smaller standard deviations, and smaller errors.

TABLE 4.20 Maximum likelihood resolution of directional wave simulation

Sample population: 15 Water Depth: 63.36 (ft)

| | $E_{total}$ | $E_p$ | $f_p$ | $\alpha$ | $\gamma$ | $\sigma_L$ | $\sigma_R$ | $\epsilon_{rms,1\text{-}D}$ | $f_{1,-1}$ |
|---|---|---|---|---|---|---|---|---|---|
| | ($ft^2$) | (ft2s) | (Hz) | | | | | | (Hz) |
| Target spectrum | 5.636 | 279.9 | .0703 | .00062 | 4.08 | .081 | .095 | 0.00 | .0793 |
| GEO. | 6.325 ±2.184 | 307.3 ±117.1 | .0721 ±.0033 | .00079 ±.00031 | 4.05 ±.68 | .088 ±.067 | .071 ±.036 | 6.85 ±2.68 | .0798 ±.0037 |
| $S/D_1$ | 6.733 ±2.841 | 360.1 ±163.0 | .0703 ±.0036 | .00084 ±.00036 | 3.92 ±.65 | .069 ±.066 | .090 ±.090 | 7.54 ±2.19 | .0785 ±.0031 |
| $S/D_2$ | 6.707 ±2.807 | 338.5 ±178.5 | .0706 ±.0038 | .00085 ±.00037 | 3.94 ±.80 | .074 ±.064 | .087 ±.088 | 7.46 ±2.42 | .0785 ±.0029 |

| | $A_L$ | $B_L$ | $s_c$ | $f_c$ | $A_R$ | $B_R$ | $\phi_{main}$ | $\epsilon_{rms,\phi_o}$ |
|---|---|---|---|---|---|---|---|---|
| | | | | (Hz) | | | (o) | (o) |
| Target spectrum | 48.7 | .0 | 54.1 | .0742 | .00115 | -4.136 | 15.0 | 0.0 |
| GEO. | 10977 ±20298 | .0177 ±1.851 | 55.3 ±17.2 | .0752 ±.0043 | .110 ±.417 | -4.859 ±2.338 | 15.5 ±4.1 | 3.42 ±1.30 |
| $S/D_1$ | 3753780 ±14528176 | .0477 ±1.480 | 95.3 ±67.3 | .0719 ±.0059 | .045 ±.142 | -4.686 ±2.128 | 15.1 ±4.2 | 3.53 ±1.46 |
| $S/D_2$ | 3753780 ±14528176 | .0480 ±1.478 | 89.9 ±68.3 | .0721 ±.0064 | .033 ±.108 | -4.852 ±2.057 | 15.1 ±4.3 | 4.13 ±1.37 |

The mean values of $A_L$, $A_R$ differ significantly from the target values in Table 4.20. This is because slight changes in $B_L$ or $B_R$ cause considerable changes in $A_L$ or $A_R$. It should be noted that resulting mean values of $B_R$ for all three methods do not differ appreciably from $B_R$ of the target spectrum. This suggests that the simulated distribution curves of the spreading parameter to the right of $s_c$ approximately parallel the distribution curves of the target spectrum spreading parameter. Also, small mean values of $B_L$ for all three methods imply that the simulated spreading parameters to the left of $s_c$ can be approximately represented by constant values. However, the simulated distribution curves of spreading parameters obtained from both $S/D_1$ and $S/D_2$ are very biased relative to the target spectrum distribution curve. This is indicated by the resulting critical spreading parameters, $s_c$, which differ from the target $s_c$ by approximately 40%. Also, the standard deviations are about 75% of the means for the $S/D_1$ and $S/D_2$ methods. The critical spreading parameter, $s_c$, from the geometric approach, however, differs from the target $s_c$ by 2% and has a standard deviation of about 30% of the mean $s_c$.

It is concluded that wave simulation results do not validate any method. However, the geometric method yields the smallest errors for wave simulation tests examined in this study.

# 5. CONCLUSIONS

## 5.1 Summary

This study has examined directional wave spectrum analysis based upon a single point measurement system. The input data required for spectral analysis are simultaneous records of wave-induced dynamic pressure and horizontal orbital velocity. The directional spectrum estimate is obtained by expanding the one-dimensional frequency spectrum into a two-dimensional spectrum by means of an angular distribution function. This angular distribution function is usually normalized, single-peaked, and symmetric with respect to a central direction. The angular distribution function utilized in this study is a square-cosine-power function. The power is called the spreading parameter and a main direction associated with the peak at each frequency is called the central angle of propagation. Both the spreading parameter and central angle may vary with frequency. The directional wave spectrum is simply expressed as a product of the one-dimensional frequency spectrum and the normalized angular distribution function. Hence, directional wave spectrum analysis reduces to an evaluation of the one-dimensional frequency spectrum, spreading parameter and central angle of wave propagation.

Two previously developed methods, stochastic and deterministic approaches, have been reviewed and restudied. By expressing an estimation to the one-dimensional frequency spectrum in a more general sense, the two methods are shown to yield identical solutions to the directional wave spectrum. In order to improve directional resolutions obtained from the combined stochastic/deterministic approach, a new method, the geometric approach, has been developed as part of this research effort. The geometric approach matches Fourier transformed wave properties to frequency dependent wavelet pairs in each frequency interval. The amplitude, direction and phase of each wavelet are uniquely specified by equating kinematic and dynamic properties for each frequency component. Wavelets evaluated in each

frequency interval do not have an artificially imposed phase constraint in the geometric approach as they have in the stochastic/deterministic approach, providing a more realistic model to represent the directional properties of ocean random waves.

Inspection of directional properties obtained from real ocean data reveals that numerically more stable results are obtained from the geometric approach than from the stochastic/deterministic approach. Directional behavior based upon an analysis of simulated data also indicate that improved results are obtained from the geometric approach.

## 5.2 Conclusions

Several conclusions relating to this work are summarized in the following paragraphs.

(1) The principle of the wavelet concept in both the geometric approach and the stochastic/deterministic approach is that the propagating directions and amplitudes can be solved by matching velocities and/or pressures for wavelets in each frequency interval. The wavelet amplitudes are then used to estimate the directional distribution of wave energy density in each frequency interval. As a result, a finite number of wavelets solved in a frequency interval are used to estimate the behavior of a continuous distribution of wavelets in that frequency interval. One would expect that the directional properties obtained from the one angle mode solutions would be more accurate than those obtained from the double angle mode solutions. However, directional properties obtained from both the one angle mode and double angle mode solutions are fairly consistent with one another for either the geometric approach or stochastic/deterministic approach as observed in this research.

(2) Estimating the main propagating direction, $\overline{\phi}$, from velocity

records in the time domain is complicated by not knowing if a specific velocity measurement is associated with a wave trough or crest. However, this same calculation in the frequency domain can utilize pressure measurements to circumvent this difficulty.

(3) The variance of a time series of wave-induced horizontal velocity, $\overline{V_t^2}$, is identical to the sum of all frequency components of the horizontal velocity spectrum, $\overline{V_f^2}$, from a stochastic/deterministic approach, Double Angle Mode solution, as indicated by Parseval's theorem. However, $\overline{V_t^2}$ is not identical to $\overline{V_f^2}$ for both the stochastic/deterministic approach one angle mode solution and the geometric approach. However, the geometric approach does precisely observe the kinematic and dynamic relationships required to obtain the correct velocity and pressure spectra.

(4) A record length of 512 seconds, digitized every second, was found as an optimum size for directional spectrum input data. Results obtained from consecutively recorded samples of 512 seconds in length show a gradual variation in spectral property, indicating a non-stationary process.

(5) An empirical directional spectrum formula has been proposed which utilizes a JONSWAP one-dimensional frequency spectrum, a cosine squared spreading function, a spreading parameter which is inversely proportional to a power of frequency, and a central angle of wave propagation which is represented by a third-order polynomial function of frequency. Parameters evaluated from a least squares best fit procedure provide directional spectrum predictions with root mean square errors less than 2% of the smoothed raw data spectrum.

(6) The mean JONSWAP parameters obtained here, $\gamma$=3.9, $\sigma_L$=.048, $\sigma_R$ =.06, from a geometric approach are based on a single peaked spectrum approximation. The standard deviations of these mean JONSWAP parameters are small, suggesting that they should be appropriate for

characterizing spectra at the measurement site located offshore of Coos Bay, Oregon. This spectrum has a sharper peak than that associated with North Sea waves.

## 5.3 Future Studies

Further studies related to this work are suggested as follows:

(1) Discrepancies between frequency and time domain variances for directional wave properties need to be resolved theoretically and numerically.

(2) Alternative angular distribution functions should be proposed based upon dimensional analysis of real ocean wave data.

(3) More high quality, simultaneous wave measurements are required to check the repeatability of various directional spectrum calculations.

REFERENCES

1. Barber, M. F. 1954. "Finding the Direction of Travel of Sea Waves", Nature, 174, pp. 1048-1050.

2. Benjamin, J. R., and Cornell C. A. 1970. "Probability, Statistics, and Decision for Civil Engineers", McGraw-Hill Book Co., New York, pp. 466-469.

3. Borgman, L. E. 1969. "Ocean Wave Simulation for Engineering Design", Journ. Waterways and Harbors Division, ASCE., WW4, pp. 557-583.

4. Bowden, K. F., and White, R. A. 1966. "Measurements of the Orbital Velocities of Sea Waves and Their Use in Determining the Directional Spectrum", Geophys. Journ. Royal Astron. Soc., Vol. 12, pp. 33-54.

5. Brighan, E. O. 1954. "The Fast Fourier Transform", Prentice-Hall, Inc., Englewood Cliffs, New Jersey, pp. 50-90.

6. Cartwright, D. E. 1962. "Waves, Analysis and Statistics", The Sea, Vol. 1, pp. 567-568.

7. Cartwright, D. E. 1963. "The Use of Directional Spectra in Studying Output of a Wave Recorder on a Moving Ship", Ocean Wave Spectra, Proc. of a Conf., pp. 203-218.

8. Cartwright, D. E., and Smith, N. D. 1964. "Buoy Techniques for Obtaining Directional Wave Spectra", Buoy Technology, Washington, D.C., Marine Tech. Soc., pp. 112-121.

9. Forristall, G. Z., Ward, E. G., Cardone, V. J., and Borgman, L. E. 1978. "The Directional Spectra and Kinematics of Surface Gravity Wave in Tropical Storm DELIA", Journ. Phys. Oceanography, Vol. 8, pp. 888-909.

10. Hasselmann, K., Ross, D. B., Müller, P., and Sell, W. 1975. "A parametric Wave Prediction Model", Journ. Phys. Oceanography, Vol. 6, pp. 200-228.

11. Ippen, A. T. 1966. "Estuary and Coastline Hydrodynamics", McGraw-Hill Book Co., New York, pp. 20-56.

12. Jenkins, G. M., and Watts, D. G. 1968. "Spectral Analysis and its Applications", Holden-Day Series in Time Series Analysis, Holden-Day, Inc., pp. 209-277.

13. Kinsman, B. 1965. "Wind Waves", Prentice-Hall, Inc., Englewood Cliffs, New Hersey, pp. 330-487.

14. Longuet-Higgins, M. S. 1962. "The Directional Spectrum of Ocean

Waves and Processes of Wave Generation", Royal Sec. London, A 265, pp. 286-315.

15. Longuet-Higgins, M. S., Cartwright, D. E., and Smith, N. D. 1963. "Observations of the Directional Spectrum of Sea Waves Using the Motions of a Floating Buoy", Ocean Wave Spectra, Proc. of a Conf., pp. 111-132.

16. Lundgren, H., and Sand, S. E. 1979. "Natural Wave Trains: Description and Reproduction", Proc. 16th Coastal Engrg. Conf., Hanburg, ASCE, pp. 312-319.

17. Mendenhall W., Scheaffer R. L., and Wackerly D. D. 1981. "Mathematical Statistics with Applications", pp. 361-367.

18. Mitsuyasu, H. 1969. "A Study on the Interaction between Water Waves and Winds (2)", Proc. 14th Japan. Conf. Coastal Engrg., Japan, Japanese Soc. Civil Engrg., pp. 39-44.

19. Mitsuyasu, H., Tasai, F., Mizuno, S., Ohkusu, M., Honda, T., and Rikiishi, K. 1975. "Observations of the Directional Spectrum of Ocean Waves Using a Cloverleaf Buoy", Journ. Oceanography, Vol. 5, pp. 750-760.

20. Nagata, Y. 1964. "The Statistics Properties of Orbital Wave Motions and Their Application for the Measurement of Directional Wave Spectra", Journ. Oceanography, Soc. of Japan., Vol. 19, NO. 4, pp. 1-14.

21. Otnes, R. K., and Enochson, L. 1978. "Applied Time Series Analysis : Basic Techniques", New York, Wiley, Vol. 1, pp. 246-254.

22. Roll, H. U., and Fischer G. 1956. "Eine Kritische Bemerkung Zum Neumann-Spectrum des Seeganges", Deut. Hydrog. Zeits., 9:9-14.

23. Rye, H., and Svee, R. 1976. "Parametric Representation of a Wind-Wave Field", New York, Wiley, Vol. 1, pp. 246-254.

24. Sand, S. E. 1979. "Three-dimensional Deterministic Structure of Ocean Waves", Inst. Hydrodyn. and Hydr. Engrg., Tech. Univ. Denmark, Series paper, 24, xi-177.

25. Sand, S. E. 1981. "Short and Long Wave Directional Spectra", Directional Wave Spectra Applications, Proc. of Conf., Univ. of Calif. Berkeley, ECOR, pp. 103-115.

26. Thomson, W. T. 1972. "Theory of Vibration with Applications", Prentice-Hall, Inc., Englewood Cliffs, New Jersey, pp. 333-364.

# APPENDICES

Appendix A - Summary of Least Square Analysis

A.1 JONSWAP Spectrum

$$E_J(f_n)=\frac{\alpha g^2}{(2\pi)^4 f_n^5}\gamma^{\beta}\exp[-\frac{5}{4}(\frac{f_p}{f_n})^4] \tag{A.1}$$

where

$$\beta=\exp[-\frac{(f_n-f_p)^2}{2\sigma_{LR}^2 f_p^2}]$$

$$\sigma_{LR}=\begin{cases}\sigma_L, & \text{for } f_n\leq f_p\\ \sigma_R, & \text{for } f_n>f_p\end{cases} \qquad n=1,2,\cdot\cdot,n_p,\cdot\cdot,N'$$

$n_p$= index of frequency at maximum $E(f_n)$

$f_p$= frequency at maximum $E(f_n)$

The parameters are determined by minimizing the root-mean-square error $\varepsilon_{rms,1\text{-}D}$, defined in Eq.(3.14), between the actual one-dimensional frequency spectrum $E(f_n)$ and the proposed JONSWAP spectrum $E_J(f_n)$. Taking the derivatives of $\varepsilon_{rms,1\text{-}D}$ with respect to $\alpha$, $\gamma$, $\sigma_L$, $\sigma_R$ and equating them to zero, four equations can be obtained and expressed as follows:

$$\alpha\sum_{n=1}^{N'}\frac{g^2\gamma^{2\beta}}{(2\pi)^4 f_n^{10}}\exp[-\frac{5}{2}(\frac{f_p}{f_n})^4]=\sum_{n=1}^{N'}E(f_n)\frac{\gamma^{\beta}}{f_n^5}\exp[-\frac{5}{4}(\frac{f_p}{f_n})^4] \tag{A.2}$$

$$\alpha\sum_{n=1}^{N'}\frac{g^2\beta\gamma^{2\beta-1}}{(2\pi)^4 f_n^{10}}\exp[-\frac{5}{2}(\frac{f_p}{f_n})^4]=\sum_{n=1}^{N'}E(f_n)\frac{\beta\gamma^{\beta-1}}{f_n^5}\exp[-\frac{5}{4}(\frac{f_p}{f_n})^4] \tag{A.3}$$

$$\alpha \sum_{n=1}^{n_p} \frac{g^2 \beta_L \gamma^{2\beta_L}}{(2\pi)^4 f_n^{10}} (f_n - f_p)^2 \exp[-\frac{5}{2}(\frac{f_p}{f_n})^4]$$

$$= \sum_{n=1}^{n_p} E(f_n) \frac{\beta_L \gamma^{\beta_L}}{f_n^5} (f_n - f_p)^2 \exp[-\frac{5}{4}(\frac{f_p}{f_n})^4] \qquad (A.4)$$

$$\alpha \sum_{n=n_p}^{N'} \frac{g^2 \beta_R \gamma^{2\beta_R}}{(2\pi)^4 f_n^{10}} (f_n - f_p)^2 \exp[-\frac{5}{2}(\frac{f_p}{f_n})^4]$$

$$= \sum_{n=n_p}^{N'} E(fn) \frac{\beta_R \gamma^{\beta_R}}{f_n^5} (f_n - f_p)^2 \exp[-\frac{5}{4}(\frac{f_p}{f_n})^4] \qquad (A.5)$$

In order to solve these non-linear equations, a numerical iteration procedure is utilized. The spectral peak is previously known and provided by the actual spectrum. Thus

$$\gamma = \frac{(2\pi)^4 f_p^2}{\alpha g^2} \exp(\frac{5}{4}) E(f_p) \qquad (A.6)$$

To start the numerical iteration, initial conditions are assigned, by experience, as

$$\alpha = 4, \quad .004 \leq \sigma_L \leq 4, \quad .004 \leq \sigma_R \leq 4 \qquad (A.7)$$

The initial value $\gamma$ is evaluated by Eq.(A.6). Then, $\sigma_L$ and $\sigma_R$ are calculated from Eqs.(A.4) and (A.5), respectively, utilizing the Bisection method. The Bisection method is a procedure which is used to approximate a root of the function $F(x)$ in a known interval. Suppose that $F(x)$ has a unique root between $x_1$ and $x_2$, there must exist the relationship $F(x_1)F(x_2)$ 0. Let $x_o=(x_1+x_2)/2$; if $F(x_1)F(x_o)<0$, there must be a root between $x_1$ and $x_o$. Otherwise, if $F(x_1)F(X_o)>0$, there must be a root between $x_2$ and $x_o$. Thus, one may reiterate the procedure until the resulting root converges in a satisfactorally small interval.

By using $\sigma_L$ and $\sigma_R$ solved from the Bisection method, two solutions of $\alpha$ can be obtained from Eqs.(A.2) and (A.3), respectively. Taking the average of the two values of $\alpha$ and replacing this average value into Eq.(A.6), one may evaluate a new $\gamma$. Therefore, one may reiterate the entire procedure until an acceptable closure error is obtained.

A.2 Two Parameter Power Function of Spreading Parameter

$$s_e(f_n)=A_{LR}f_n^{B_{LR}} \tag{A.8}$$

where

$$(A_{LR},B_{LR})=\begin{cases}(A_L,B_L), & \text{for } f_n<f_c\\ (A_R,B_R), & \text{for } f_n\geq f_c\end{cases} \qquad n=1,2,\cdot\cdot,n_c,\cdot\cdot,N'$$

$n_c$= index of frequency at maximum $s(f_n)$

The parameters defined in Eq.(A.8) are determined by minimizing the root-mean-square error between the actual spreading parameter $s(f_n)$ and the proposed spreading parameter function $s_e(f_n)$. This root-mean-square error is defined as

$$\varepsilon_{rms,s}=\frac{\sqrt{\sum_{n=n_1}^{n_2}[s_e(f_n)-s(f_n)]^2}}{\sum_{n=n_1}^{n_2}s(f_n)} \tag{A.9}$$

where

$n_1$, $n_2$= 1, $n_c$ to the left of the critical point

$n_1$, $n_2$= $n_c$,$N'$ to the right of the critical point

Taking the derivatives of $\varepsilon_{rms,s}$ with respect to $A_{LR}$, $B_{LR}$ and equating them to zero, two equations can be obtained and expressed as follows:

$$A_{LR}=\sum_{n=n_1}^{n_2} s(f_n)f_n^{B_{LR}}/\sum_{n=n_1}^{n_2} f_n^{2B_{LR}} \tag{A.10}$$

$$A_{LR}=\sum_{n=n_1}^{n_2} s(f_n)f_n^{B_{LR}}\ln(f_n)/\sum_{n=n_1}^{n_2} f_n^{2B_{LR}}\ln(fn) \tag{A.11}$$

By equating Eq.(A.10) to Eq.(A.11), the Bisection method can be again employed to solve $B_{LR}$. Then, $A_{LR}$ can be obtained by replacing the resulting $B_{LR}$ into either Eq.(A.10) or Eq.(A.11). The initial condition for $B_{LR}$ is

$$-40\leq B_R\leq -0.1, \quad -40\leq B_L\leq 40 \tag{A.12}$$

A.3 Third-order Polynomial Function of Central Angle

$$\phi_{oe}(f_n)= c_o+c_1f_n+c_2f_n^2+c_3f_n^3 \tag{A.13}$$

The parameters in Eq.(A.13) can be determined by minimizing the root-mean-square error $\epsilon_{rms,\phi_o}$, defined in Eq.(3.21), with respect to each of $c_o$, $c_1$, $c_2$ and $c_3$. That is,

$$\sum_{n=1}^{N'}[c_o+c_1f_n+c_2f_n^2+c_3f_n^3]E(f_n)=\sum_{n=1}^{N'}\phi_o(f_n)E(f_n) \tag{A.14}$$

$$\sum_{n=1}^{N'}[c_o+c_1f_n+c_2f_n^2+c_3f_n^3]f_nE(f_n)=\sum_{n=1}^{N'}\phi_o(f_n)f_nE(f_n) \tag{A.15}$$

$$\sum_{n=1}^{N'}[c_o+c_1f_n+c_2f_n^2+c_3f_n^3]f_n^2E(f_n)=\sum_{n=1}^{N'}\phi_o(f_n)f_n^2E(f_n) \tag{A.16}$$

$$\sum_{n=1}^{N'}[c_o+c_1f_n+c_2f_n+c_3f_n]f_n^3E(f_n)=\sum_{n=1}^{N'}\phi_o(f_n)f_n^3E(f_n) \tag{A.17}$$

The parameters, $c_o$, $c_1$, $c_2$, and $c_3$, can be then solved from these four linear equations.

# Appendix B - Statistics of Ocean Waves Evaluated in the Time and Frequency Domains

## B.1 Statistics Evaluated in the Time Domain

TABLE B.1 Summary of statistics evaluated in the time domain

Date: October 23, 1982 Meter No. 43

| Length | Init. Time | $V_c$ | $\phi_c$ | $\overline{V_t^2}$ | $\overline{\phi}$ | Length | Init. Time | $V_c$ | $\phi_c$ | $\overline{V_t^2}$ | $\overline{\phi}$ |
|---|---|---|---|---|---|---|---|---|---|---|---|
| (sec) | | (ft/s) | (o) | $(ft/s)^2$ | (o) | (sec) | | (ft/s) | (o) | $(ft/s)^2$ | (o) |
| 1024 | 2:38 | .265 | -8 | .054 | 92 | 256 | 2:38 | .283 | -9 | .040 | 88 |
| 512 | 2:38 | .273 | -5 | .053 | 92 | 256 | 2:42 | .265 | -2 | .061 | 95 |
| 512* | 2:42 | .272 | -5 | .058 | 94 | 256* | 2:44 | .276 | -4 | .062 | 97 |
| 512 | 2:46 | .256 | -10 | .058 | 95 | 256 | 2:46 | .277 | -7 | .063 | 96 |
| 512** | 2:36 | .392 | -67 | .065 | 84 | 256 | 2:50 | .235 | -13 | .050 | 80 |

* central section of 1024 seconds

** data measured from meter 25

TABLE B.1 (continued) Summary of statistics evaluated in the time domain

Date: October 24, 1982 Meter No. 43

| Length | Init. Time | $V_c$ | $\phi_c$ | $\overline{V_t^2}$ | $\overline{\phi}$ | Length | Init. Time | $V_c$ | $\phi_c$ | $\overline{V_t^2}$ | $\overline{\phi}$ |
|---|---|---|---|---|---|---|---|---|---|---|---|
| (sec) | | (ft/s) | (o) | $(ft/s)^2$ | (o) | (sec) | | (ft/s) | (o) | $(ft/s)^2$ | (o) |
| 1024 | 14:47 | 1.04 | -31 | .063 | 79 | 256 | 14:47 | 1.07 | -39 | .057 | 80 |
| 512 | 14:47 | 1.04 | -34 | .069 | 78 | 256 | 14:51 | 1.01 | -29 | .057 | 79 |
| 512* | 14:51 | 1.02 | -30 | .054 | 81 | 256* | 14:53 | 1.00 | -29 | .056 | 80 |
| 512 | 14:55 | 1.04 | -29 | .055 | 80 | 256 | 14:55 | 1.03 | -30 | .056 | 80 |
| 512** | 14:45 | .736 | -56 | .070 | 78 | 256 | 14:59 | 1.06 | -30 | .049 | 84 |

* central section of 1024 seconds

** data measured from meter 25

TABLE B.1 (continued) Summary of statistics evaluated in the time domain

Date: October 25, 1982 Meter No. 43

| Length | Init. Time | $V_c$ | $\phi_c$ | $\overline{V_t^2}$ | $\overline{\phi}$ | Length | Init. Time | $V_c$ | $\phi_c$ | $\overline{V_t^2}$ | $\overline{\phi}$ |
|---|---|---|---|---|---|---|---|---|---|---|---|
| (sec) | | (ft/s) | (o) | $(ft/s)^2$ | (o) | (sec) | | (ft/s) | (o) | $(ft/s)^2$ | (o) |
| 1024 | 6:51 | .242 | 198 | .072 | 89 | 256 | 6:51 | .202 | 174 | .091 | 91 |
| 512 | 6:51 | .216 | 187 | .067 | 86 | 256 | 6:55 | .235 | 195 | .049 | 88 |
| 512* | 6:55 | .253 | 202 | .069 | 90 | 256* | 6:57 | .261 | 201 | .054 | 93 |
| 512 | 6:59 | .277 | 208 | .069 | 92 | 256 | 6:59 | .272 | 207 | .055 | 93 |
| 512** | 6:49 | .212 | 250 | .080 | 98 | 256 | 7:03 | .278 | 206 | .080 | 90 |

* central section of 1024 seconds

** data measured from meter 25

TABLE B.1 (continued) Summary of statistics evaluated in the time domain

Date: October 25, 1982 Meter No. 43

| Length | Init. Time | $V_c$ | $\phi_c$ | $\overline{V_t^2}$ | $\overline{\phi}$ | Length | Init. Time | $V_c$ | $\phi_c$ | $\overline{V_t^2}$ | $\overline{\phi}$ |
|---|---|---|---|---|---|---|---|---|---|---|---|
| (sec) | | (ft/s) | (o) | $(ft/s)^2$ | (o) | (sec) | | (ft/s) | (o) | $(ft/s)^2$ | (o) |
| 1024 | 10:52 | .421 | -17 | .047 | 97 | 256 | 10:52 | .428 | -17 | .043 | 93 |
| 512 | 10:52 | .431 | -16 | .044 | 94 | 256 | 10:56 | .431 | -15 | .046 | 92 |
| 512* | 10:56 | .421 | -16 | .043 | 93 | 256* | 10:58 | .424 | -15 | .040 | 96 |
| 512 | 11:00 | .414 | -18 | .047 | 101 | 256 | 11:00 | .419 | -15 | .037 | 95 |
| 512 | 10:50 | .468 | 193 | .043 | 72 | 256 | 11:04 | .417 | -20 | .054 | 104 |

* central section of 1024 seconds

** data measured from meter 25

## B.2 Statistics Evaluated in the Frequency Domain

TABLE B.2 Summary of statistics evaluated in the frequency domain

Date: October 23, 1982 Meter No. 43

| Length (sec) | Init. Time | $E_{total}$ ($ft^2$) | $E_p$ ($ft^2 s$) | $f_p$ (Hz) | $f_{1,-1}$ (Hz) | $s_c$ | $f_c$ (Hz) | $\phi_{main}$ (o) | $\overline{V_f^2}$ $(ft/s)^2$ |
|---|---|---|---|---|---|---|---|---|---|
| | | | | STO./DET. APPROACH$_1$ | | | | | |
| 1024 | 2:38 | 1.00 | 46 | .077 | .088 | 29 | .075 | 92 | .061 |
| 512 | 2:38 | 1.47 | 46 | .088 | .101 | 7 | .074 | 95 | .057 |
| 512* | 2:42 | .84 | 38 | .076 | .087 | 12 | .076 | 88 | .065 |
| 512 | 2:46 | .93 | 45 | .076 | .087 | 11 | .074 | 102 | .062 |
| 512** | 2:36 | .91 | 47 | .078 | .088 | 14 | .074 | 73 | .060 |
| 256* | 2:44 | 3.49 | 69 | .094 | .114 | 8 | .078 | 93 | .051 |
| | | | | STO./DET. APPROACH$_2$ | | | | | |
| 1024 | 2:38 | .63 | 44 | .077 | .088 | 32 | .076 | 99 | .054 |
| 512 | 2:38 | .32 | 46 | .080 | .091 | 8 | .068 | 111 | .053 |
| 512* | 2:42 | .80 | 38 | .078 | .091 | 11 | .074 | 95 | .058 |
| 512 | 2:46 | .69 | 42 | .076 | .086 | 12 | .076 | 98 | .058 |
| 512** | 2:36 | 1.02 | 52 | .078 | .089 | 10 | .082 | 72 | .064 |
| 256* | 2:44 | 1.56 | 50 | .082 | .091 | 10 | .078 | 114 | .062 |
| | | | | GEOMETRIC APPROACH | | | | | |
| 1024 | 2:38 | 1.03 | 48 | .077 | .089 | 7.6 | .076 | 90 | .075 |
| 512 | 2:38 | 1.24 | 49 | .080 | .093 | 4.0 | .078 | 85 | .074 |
| 512* | 2:42 | 1.00 | 41 | .076 | .088 | 5.0 | .076 | 89 | .073 |
| 512 | 2:46 | 1.07 | 49 | .076 | .088 | 5.2 | .076 | 97 | .074 |
| 512** | 2:36 | 1.01 | 53 | .078 | .088 | 8.0 | .076 | 72 | .063 |
| 256* | 2:44 | 3.52 | 112 | .094 | .114 | 3.5 | .078 | 95 | .055 |

* central section of 1024 seconds, ** data measured from meter 25

TABLE B.2 (continued) Summary of statistics evaluated in the frequency domain

Date: October 24, 1982 Meter No. 43

| Length (sec) | Init. Time | $E_{total}$ ($ft^2$) | $E_p$ ($ft^2 s$) | $f_p$ (Hz) | $f_{1,-1}$ (Hz) | $s_c$ | $f_c$ (Hz) | $\phi_{main}$ (o) | $\overline{v_f^2}$ $(ft/s)^2$ |
|---|---|---|---|---|---|---|---|---|---|
| | | | | STO./DET. APPROACH$_1$ | | | | | |
| 1024 | 14:47 | 1.32 | 60 | .084 | .084 | 12 | .083 | 75 | .069 |
| 512 | 14:47 | 1.19 | 59 | .086 | .088 | 18 | .084 | 73 | .071 |
| 512* | 14:51 | 1.35 | 51 | .084 | .093 | 14 | .084 | 64 | .058 |
| 512 | 14:55 | 1.15 | 59 | .084 | .089 | 15 | .088 | 85 | .056 |
| 512** | 14:45 | 1.39 | 66 | .086 | .092 | 7 | .084 | 66 | .063 |
| 256* | 14:53 | 1.43 | 53 | .082 | .092 | 37 | .082 | 64 | .064 |
| | | | | STO./DET. APPROACH$_2$ | | | | | |
| 1024 | 14:47 | .89 | 36 | .084 | .083 | 16 | .083 | 77 | .063 |
| 512 | 14:47 | .81 | 38 | .086 | .089 | 11 | .084 | 71 | .068 |
| 512* | 14:51 | .83 | 30 | .084 | .093 | 12 | .084 | 66 | .054 |
| 512 | 14:55 | .83 | 34 | .084 | .091 | 17 | .082 | 86 | .054 |
| 512** | 14:45 | 1.39 | 71 | .086 | .092 | 9 | .086 | 65 | .069 |
| 256* | 14:53 | .98 | 33 | .082 | .092 | 25 | .082 | 64 | .056 |
| | | | | GEOMETRIC APPROACH | | | | | |
| 1024 | 14:47 | 1.54 | 73 | .084 | .086 | 3.8 | .070 | 73 | .082 |
| 512 | 14:47 | 1.42 | 69 | .086 | .089 | 3.4 | .070 | 70 | .080 |
| 512* | 14:51 | 1.46 | 59 | .084 | .094 | 3.5 | .072 | 59 | .074 |
| 512 | 14:55 | 1.42 | 78 | .084 | .090 | 3.0 | .070 | 86 | .077 |
| 512** | 14:45 | 1.60 | 78 | .084 | .088 | 10. | .070 | 67 | .068 |
| 256* | 14:53 | 1.60 | 65 | .082 | .092 | 3.6 | .070 | 65 | .067 |

* central section of 1024 seconds, ** data measured from meter 25

TABLE B.2 (continued) Summary of statistics evaluated in the frequency domain

Date: October 25, 1982 Meter No. 43

| Length (sec) | Init. Time | $E_{total}$ ($ft^2$) | $E_p$ ($ft^2 s$) | $f_p$ (Hz) | $f_{1,-1}$ (Hz) | $s_c$ | $f_c$ (Hz) | $\phi_{main}$ (o) | $\overline{V_f^2}$ $(ft/s)^2$ |
|---|---|---|---|---|---|---|---|---|---|
| | | | | STO./DET. APPROACH$_1$ | | | | | |
| 1024 | 6:51 | 1.57 | 97 | .078 | .093 | 20 | .078 | 84 | .078 |
| 512 | 6:51 | 1.46 | 85 | .078 | .091 | 22 | .078 | 87 | .070 |
| 512* | 6:55 | 1.75 | 100 | .088 | .092 | 12 | .080 | 83 | .076 |
| 512 | 6:59 | 2.06 | 102 | .088 | .098 | 10 | .080 | 85 | .075 |
| 512** | 6:49 | 1.91 | 116 | .078 | .091 | 5.5 | .078 | 73 | .077 |
| 256* | 6:57 | .99 | 17 | .090 | .104 | 41 | .059 | 97 | .060 |
| | | | | STO./DET. APPROACH$_2$ | | | | | |
| 1024 | 6:51 | 1.19 | 80 | .078 | .092 | 32 | .077 | 89 | .072 |
| 512 | 6:51 | 1.14 | 70 | .078 | .090 | 22 | .078 | 98 | .067 |
| 512* | 6:55 | 1.50 | 75 | .088 | .097 | 17 | .080 | 87 | .067 |
| 512 | 6:59 | 1.52 | 79 | .088 | .098 | 21 | .080 | 90 | .070 |
| 512** | 6:49 | 1.95 | 117 | .078 | .091 | 9 | .078 | 78 | .080 |
| 256* | 6:57 | .72 | 14 | .078 | .094 | 42 | .059 | 98 | .052 |
| | | | | GEOMETRIC APPROACH | | | | | |
| 1024 | 6:51 | 1.72 | 108 | .078 | .092 | 4.6 | .079 | 87 | .090 |
| 512 | 6:51 | 1.63 | 96 | .078 | .091 | 4.1 | .080 | 90 | .082 |
| 512* | 6:55 | 1.82 | 102 | .088 | .092 | 5.4 | .080 | 85 | .084 |
| 512 | 6:59 | 1.90 | 108 | .088 | .092 | 4.5 | .080 | 87 | .081 |
| 512** | 6:49 | 1.97 | 117 | .078 | .091 | 5.2 | .080 | 71 | .078 |
| 256* | 6:57 | 1.05 | 14 | .066 | .081 | 8.0 | .066 | 95 | .067 |

* central section of 1024 seconds, ** data measured from meter 25

# Appendix C - Computer Program Listing

## C.1 Pre-calculation: Program PRECAL

```
      PROGRAM PRECAL(INPUT,OUTPUT,DATA1,DATA2,DATA3,TAPE6=DATA1,TAPE8=
     1 DATA2,TAPE10=DATA3)
C  ---THIS PROGRAM IS USED TO CALCULATE FOURIER COEFFICIENTS OF WAVE DATA THROUGH FFT---
C  ---NOTICE THAT THE DISTANCE FROM METERS TO WATER SURFACE SHOULD BE LESS THEN 220 FT---
C  ---ALWAYS CHECK THE INPUT FORMAT FOR [DATA1] BEFORE DEBUGGING THE PROGRAM---
C  ---[DATA1] IS USED TO INPUT ORIGINAL FILTERED TAPE RECORDER DATA---
C  ---[DATA2] IS USED TO OUTPUT FREQUENCY DOMAIN DATA FROM FFT CALCULATION---
C  ---[DATA3] IS USED TO INPUT OR OUTPUT WAVE INDUCED VELOCITIES AND DYNAMIC PRESSURE---
C  ---REMARK [A] IS USED FOR INPUT FILE WITHOUT H1 VALUE(USUALLY 81 DATA)---
C  ---REMARK [B] IS USED FOR INPUT FILE WITH H1 VALUE(USUALLY 82,83 DATA)---
C      CHARACTER DATE*75
       CHARACTER*10 M(4)
       DIMENSION RECORD(3300),V(1100),D(1100),P(1100)
       DIMENSION PR(512),VB(512),DB(512)
       DATA VI,DI,PI,DEGREE/.0,.0,.0,57.29578/
       DATA M(1),M(3)/'R',' 83'/                                          [B]
C ***************************************************************************
C *---PART I: INPUT INFORMATION FOR RIGHT PROGRAM---                        *
C ***************************************************************************
C      PRINT 1000
C1000 FORMAT(/"-----CHECK IF THE INPUT FORMAT FOR [DATA1] IS CORRECT,
C     1"/"=====INPUT DATE AND TIME INFORMATION (FORMAT IS A75).")
C      READ(*,1005) DATE
C1005 FORMAT(A75)
C ***************************************************************************
C *---PART II: READ DATA OF VELOCITY,DIRECTION AND PRESSURE---               *
C ***************************************************************************
C      PRINT 1019
C1019 FORMAT(1X/"=====INPUT 0 IF [DATA1] IS READY FOR INPUT."/ "=====OR
C     1INPUT 1 IF [DATA3] IS READY FOR INPUT.")
C      READ*,K
C
C      IF(K.EQ.0) THEN
C      PRINT 1017                                                         [A]
C1017 FORMAT(/"=====INPUT H1(FT): DISTANCE FROM CURRENTMETER TO FLOOR.")  [A]
C      READ*,H1                                                           [A]
C      PRINT 1002
C1002 FORMAT(1X/"-----THE RECORD IS DIGITIZED AT EVERY ONE SECOND."
C     1 /"=====INPUT THE LENGTH OF RECORD IN SECOND (FORMAT IS I5).")
       READ*,LL
C      PRINT 1004,LL
C1004 FORMAT(1X/"=====RECORD LENGTH=",I5,1X,"SECONDS.")
C  ---NOTE THAT FOUR CONTINUOUS DATA FORMATED IN ONE LINE IN REFILED MAGNETIC TAPE---
C  ---DIRECTION IS IN CLOCKWISE COORDINATE WITH NORTH BEING ZERO---
       L1=LL*3
C      READ(6,1003) M(1),M(2),M(3),DEPTH,M(4),(RECORD(I),I=1,L1)          [A]
C1003 FORMAT(3X,A1,1X,A2,4X,A3/37X,F8.2/18X,A9,2X,3(4F7.2,2X)/(29X,3      [A]
C     1(4F7.2,2X)))                                                      [A]
       READ(6,1003) M(2),H1,DEPTH,M(4),(RECORD(I),I=1,L1)                 [B]
 1003 FORMAT(/22X,A2,13X,F8.2,20X,F8.2/4X,A9,2X,2(4F7.2,2X),4F8.3         [B]
     1/(15X,2(4F7.2,2X),4F8.3))                                         [B]
       I1=1
       I2=I1+3
       L2=LL*2-8
       DO 1006 J=0,L2,8
       DO 1007 I=I1,I2
       V(I)=RECORD(I+J)
       D(I)=RECORD(I+J+4)
C  ---V(I): WAVE INDUCED PARTICLE VELOCITIES(CM/S)---
C  ---D(I): DIRECTION OF PARTICLE VELOCITIES(DEGREE)---
       RADIAN=(90-D(I))*0.017453293
C  ---WHERE 0.017453293=3.141592654/180, CHANGING DEGREE TO RADIANS---
       D(I)=V(I)*SIN(RADIAN)
       V(I)=V(I)*COS(RADIAN)
C  ---V(I) BECOMES VELOCITY IN X DIRECTION (+:EAST & -:WEST)---
C  ---D(I) BECOMES VELOCITY IN Y DIRECTION (+:NORTH & -:SOUTH)---
       P(I)=RECORD(I+J+8)
C  ---P(I): WAVE INDUCED DYNAMIC PRESSURE(PSI)---
       VI=VI+V(I)
       DI=DI+D(I)
       PI=PI+P(I)
 1007 CONTINUE
       I1=I
       I2=I1+3
 1006 CONTINUE
```

```
      VI=VI/LL
      DI=DI/LL
      PI=PI/LL
      H2=PI*2.25
      H0=H2+3.4167
      IF(ABS(H0-H1).GT.5.0) PRINT*,'CHECK H1'
      IF(H0+4.3.GT.DEPTH) DEPTH=H0+4.3
      H1=DEPTH-H0
      H2=H1+3.4167
C     DEPTH=(V1*VI+DI*DI+12.9*PI)*0.174375+H2
C  ---ABOVE EQUATION CAN NOT BE USED TO COMPUTE DEPTH SINCE CURRENT OF SURFACE IS UNKNOWN---
C     DEPTH=(DEPTH+4.5+PI*2.25+H2)/2.
C  ---THE NUMBER 4.5 FT APPEARED ABOVE IS THE SENSOR LOCATED ON THE BOTTON OF BOAT---
C  ---WHERE 2.25 IS CONTANT TO CONVERT PRESSURE(PSI) TO DEPTH(FT)---
      VI=VI*.3937
      DI=DI*.3937
      SUM=.0
      C=.0
      CC=.0
      WRITE(*,1013)
 1013 FORMAT(1X/"*****GUESS & INPUT A MAIN DIRECTION (DEGREE, 0=NORTH)"
     1/"     OF WAVE PROPAGATION.")
      READ*,ANGLE
      ANGLE=90.-ANGLE
      DO 1008 I=1,LL
      V(I)=V(I)*.3937-VI
      D(I)=D(I)*.3937-DI
C  ---SUBTRACT CURRENT FROM VELOCITY DATA, V(I) & D(I) BECOME WAVE INDUCED VELOCITIES---
C  ---CHANGING UNIT OF VELOCITY FROM (CM/S) TO (IN/S)---
      ALL=V(I)*V(I)+D(I)*D(I)
      SUM=SUM+ALL
      R=SQRT(ALL)
      TEMP=ATAN2(D(I),V(I))*DEGREE
      H0=ABS(TEMP-ANGLE)
      IF(H0.GT.90..AND.H0.LT.270.) THEN
      IF(ABS(TEMP+180.-ANGLE).LT.90.) THEN
      TEMP=TEMP+180.
      ELSE
      TEMP=TEMP-180.
      END IF
      ELSE IF(H0.GE.270.) THEN
      IF(ANGLE.GT.90.) TEMP=TEMP+360.
      IF(ANGLE.LE.-90.) TEMP=TEMP-360.
      END IF
      C=C+R*TEMP
      CC=CC+R
      P(I)=P(I)-PI
C  ---P(I) BECOMES WAVE INDUCED DYNAMIC PRESSURE (PSI)---
 1008 CONTINUE
      SUM=SUM/LL/144.
      CC=90.-C/CC
      VI=VI/12.
      DI=DI/12.
      C=SQRT(VI*VI+DI*DI)/12.
      DI=90.-ATAN2(DI,VI)*DEGREE
      PRINT 1014, M(1),M(2),M(3),M(4),H1,H2,DEPTH,C,DI,PI,CC,SUM
 1014 FORMAT(1X/"-----BURST METER NUMBER AND RECORD DATE FOR FILE DATA="
     1,A1,A2,A3,A9,"."/"-----CURRENTMETER IS",F6.1," (FT) ABOVE SEA FLOO
     1R."/"-----PRESSURE GAGE IS",F6.1," (FT) ABOVE SEA FLOOR."/
     1 "-----WATER DEPTH FROM SEA BOTTOM TO SUL IS",F7.2,"(FT)."/
     1 "*****MAGNITUDE OF MEAN CURRENT=",F9.4," (FT/S)."/
     1 "*****DIRECTION OF MEAN CURRENT=",F9.4," (DEGREE, 0=NORTH)."/
     1 "*****AVERAGE PRESSURE IN THE RECORDS=",F9.4," (PSI)."/
     1 "*****WEIGHTED MEAN DIRECTION=",F9.4," (DEGREE, 0=NORTH)."/
     1 "VARIANCE OF HORI. VELOCITY(W/O CURRENT)=",F9.4," (FT/S)**2")
      VI=C
C     END IF
C
C ***************************************************************************
C *---PART III: RUNNING FFT TECHNIQUE AMONG DIFFERENT WAVE PROPERTIES---      *
C ***************************************************************************
C     PRINT 1018
C1018 FORMAT(1X/"-----THE FFT APPLIED LATER WILL BE BASED ON 2 ALGORITHM
C    1."/"*****INPUT N PREPARED FOR APPLING FFT LATER (FORMAT IS FREE*).
C    1"/"-----REQUIRE THAT N=2**IP IS THE LEAST VALUE THAT IS GE. TO THE
C    1 DATA PERIOD." / "-----FOR EXAMPLE: DATA PERIOD=250 POINTS, N=2**8
C    1=256 POINTS (MAX. N=2**9=512 POINTS).")
C     READ*,N
      N=LL
C     N=256
C     IF(ABS(512-LL).LT.50) N=512
C     IF(ABS(1024-LL).LT.50) N=1024
C  ---THE CHARACTERS "IP" INDICATES "POWER" OF BASE 2---
C
C     IF(K.EQ.0) THEN
```

```
      IF(N.LE.LL) GO TO 1023
      L1=LL+1
      DO 1024 I=L1,N
      V(I)=0.0
      D(I)=0.0
 1024 P(I)=0.0
 1023 CONTINUE
C     WRITE(10,1015) M(1),M(2),M(3),M(4),DEPTH,VI,DI,PI,(V(I),D(I),P(I)
C    1,I=1,N)
C1015 FORMAT(1X/A1,A2,A3,A9,4F8.3/(9(F11.7,2X)))
C
C     ELSE
C     READ(10,1021)M(1),M(2),H1,DEPTH,VI,DI,PI,CC,SUM,(V(I),D(I),P(I)
C    1,I=1,N)
C1021 FORMAT(1X/A10,A5,7F9.4/(9(F11.7,2X)))
C     END IF
C
      CALL ORBIT(P,PB,N)
      CALL ORBIT(V,VB,N)
      CALL ORBIT(D,DB,N)
      NH=N/2
      K=0
      NH0=NH/1.2
      FREQ2=SQRT(2.5/(DEPTH-H1))
C  ---IN A DISTANCE 'DEPTH-H1' BELOW WATER SURFACE, ONE MAY SENSE 4.3%
C     OF WAVE MOTION AT SURFACCE IN ACORDANCE WITH LINEAR WAVE THORY---
      IF(FREQ2.GT..5) PRINT*,'CHEAK DEEP'
      LJ=FREQ2*FLOAT(N)
      IF(NH0.LT.LJ) NH0=LJ
      IF(NH0.GT.NH) NH0=NH
      IF(K.EQ.0) WRITE(8,1020)N,NH0,M(1),M(2),M(3),M(4),H1,DEPTH,VI,DI,
     1PI,CC,SUM,(P(I),PB(I),V(I),VB(I),D(I),DB(I),I=1,NH0)
C     IF(K.EQ.1) WRITE(8,1022)N,NH0,M(1),M(2),H1,DEPTH,VI,DI,PI,CC,SUM
C    1,(P(I),PB(I),V(I),VB(I),D(I),DB(I),I=1,NH0)
 1020 FORMAT(1X/2I5/A1,A2,A3,A9,7F9.4/(10E12.6))
C1022 FORMAT(1X/2I5/A10,A5,7F9.4/(10E12.6))
C     PRINT 1001,DATE
C1001 FORMAT(1X/"*****DATE AND TIME= ",A/)
      STOP
      END
C
C ***************************************************************************
C *---PART X: COLLECTION OF SUBROUTINES AND BLOCK DATA---                     *
C ***************************************************************************
      SUBROUTINE ORBIT(T1,T2,N)
      DIMENSION T1(N),T2(N)
      COMPLEX X(2048)
      DO 10 I=1,N
   10 X(I)=CMPLX(T1(I),.0)
      CALL COOLEY(X,N,1,1)
      NH=N/2
      DO 20 I=1,NH
      NN=N-I+1
      T1(I)=2.*REAL(X(NN))
   20 T2(I)=2.*AIMAG(X(NN))
      RETURN
      END
C
      SUBROUTINE COOLEY(X,N,INV,KIND)
C  ---COOLEY-TUKEY METHOD BASE 2 FFT ALGORITHM; FROM R.K.BINES & L.ENOCHSON---
C  ---"APPLIED TIME SERIES ANALYSIS: BASIC TECHNIQUES"(1978) V.1 PP.246-254---
C  ---N: N=2**IP, NUMBER OF COMPLEX VALUES FOR RUNNING FFT BASED ON 2 ALGORITHM---
C  ---INV: EQUALED 1 FOR FORWARD FFT, EQUALED -1 FOR INVERSE FFT---
C  ---KIND: EQUALED 1 FOR FIRST KIND TYPE, EQUALED 3 FOR THIRD KIND TYPE---
C  ---X(I) IS A COMPLEX VARIABLE ARRAY USED TO INPUT & OUTPUT FFT INFORMATION---
      DIMENSION X(N),CS(2),MSK(13)
      COMPLEX X,CXCS,HOLD,XA
      EQUIVALENCE (CXCS,CS)
      IF(KIND.EQ.3) KIND=-1
      IN=N
      DO 5 I=2,15
      IN=IN/2
      IF(IN.LE.2) GO TO 10
    5 CONTINUE
   10 IP=I
      ZZ=-6.283185306*INV/FLOAT(N)
      MSK(1)=N/2
      DO 15 I=2,IP
   15 MSK(I)=MSK(I-1)/2
      NN=N
      MM=2
      DO 45 LAYER=1,IP
      NN=NN/2
      II=NN
C  ---INITIAL NW=0 HERE---
```

```
      DO 20 J=1,NN
      II=II+1
      IJ=II-NN
      XA=X(II)
      X(II)=X(IJ)-XA
   20 X(IJ)=X(IJ)+XA
      DO 25 LOC=2,IP
      LL=-MSK(LOC)
      IF(LL) 30,35,25
   25 NW=LL
   30 NW=MSK(LOC)
      GO TO 40
   35 NW=MSK(LOC+1)
   40 DO 400 I=3,MM,2
      II=NN*I
      W=FLOAT(NW)*ZZ
      CS(1)=COS(W)
      CS(2)=SIN(W)
      DO 200 J=1,NN
      II=II+1
      IJ=II-NN
      XA=CXCS*X(II)
      X(II)=X(IJ)-XA
  200 X(IJ)=X(IJ)+XA
      DO 250 LOC=2,IP
      LL=NW-MSK(LOC)
      IF(LL) 300,350,250
  250 NW=LL
  300 NW=MSK(LOC)+NW
      GO TO 400
  350 NW=MSK(LOC+1)
  400 CONTINUE
   45 MM=MM*2
      NW=0
      DO 80 I=1,N
      NW1=NW+1
      HOLD=X(NW1)
      IF(NW1-I) 60,55,50
   50 X(NW1)=X(I)
      IF(INV.EQ.KIND) X(NW1)=X(I)/FLOAT(N)
   55 X(I)=HOLD
      IF(INV.EQ.KIND) X(I)=HOLD/FLOAT(N)
   60 DO 65 LOC=1,IP
      LL=NW-MSK(LOC)
      IF(LL) 70,75,65
   65 NW=LL
   70 NW=MSK(LOC)+NW
      GO TO 80
   75 NW=MSK(LOC+1)
   80 CONTINUE
      RETURN
      END
EOI ENCOUNTERED.
```

## C.2 Directional Spectrum Estimation: the stochastic/deterministic approach, Program STOCH

```
      PROGRAM STOCH(INPUT,OUTPUT,DATA2,DATA4,TAPE6=DATA2,TAPE8=DATA4)
C  ---CAUTION: BEFORE RUNNING THIS PROGRAM, 'LIBRARY(COMPLOT)' & 'SETTL(100)' MUST BE CALLED---
C  ---CAUTION: FFT POINTS M.LE.1024, CHANGE DIM. IF ONE INCREASES M---
C  ---CAUTION: 0 DIRECTS TOWARD TO EAST FOR MATH, BUT TO NORTH FOR OUTPUT---
C  ---[DATA2] IS USED TO INPUT FORWARD FFT DATA, COMPUTED FROM <FUNDA>---
C  ---[DATA4] ARE USED TO COLLECT DESIRED OUTPUT FROM FORMATED @TAPE8---
      CHARACTER*10 LX(2),LY(2),LX1(2),LY1(2),LX2(2),LY2(2),ST(2),LX21
      CHARACTER*3 LX3,LY3,LX4,LY4,LX10,LY10,LX18,LZ,LZ1,LZ2,LZ4,LZ5
      CHARACTER*10 LX5(2),LY5(6),LX6,LY6(6),LX7,LY7(6),LX11(2),LY14(3)
      CHARACTER*10 LX8,LY8(3),LX9,LY9,M(2),LX15,LY15,LX16,LY16,LY21(2)
      CHARACTER*10 LX14,LY11(2),LX12(3),LY12(3),LX13(2),LY13(3),LX25(3)
      CHARACTER*10 LX17,LY17(7),LY18(2),LX19(2),LY19,LX20(3),LY20(3)
      CHARACTER*10 LZ3(2),LX22,LY22(2),LX23,LY23(2),LX24,LY24(3),LY25(2)
      CHARACTER*10 LX26,LZ6,LZ7,LZ8,LZ9,LZ10,LX30,ST2(2)
      DIMENSION P(720),PB(720),V(720),VB(720),D(720),DB(720)
      DIMENSION T33(720),T12(720),RECORD(720),D1(720),D2(720),FS(100)
      DIMENSION S1(720),S2(720),V1A(720),V1B(720),V2A(720),V2B(720)
      DIMENSION XX(7,14,2),YY(7,14,2),IXY(7),XL(10),YL(10),IK3(4),A(4,5)
      COMMON /DATA10/ FREQ(720),T13(720),T23(720),WP(720),WK(720),FREQ1
     1,FREQ2,ALFA,GA,PEAKF,LL,IPEAK,IDPEAK,IIPEAK,K,A1,ICPEAK,L1
      DATA LX,LY,LX18/'FREQUENCY','(HZ)','E>?M?N <(F','T^2S)','C2'/
      DATA LX1,LY1/'E&>?MTH !<','(FT^2/S)','SPREADING','PARAMETER'/
      DATA LX2,LY2/'RECORD LAB','EL >.<','E&>?G?B !<','(FT^2S)'/
      DATA LX3,LX4,LY3,LY4,LX14,LZ/'E','W','M','S','FROM','100'/
      DATA LX5,LX6,LX7/'DIRECTIONA','L','SPECTRUM','UNMODIFIED'/
      DATA LY5,LX13/'WAVE ENERG','Y SPECTRUM',' AT SEA SU','RFACE, DEP',
     1 'TH OF SEA=','         FT','FT/>S<, ','     ^0'/
      DATA LY6,LX12/'HORIZONTAL',' AMPLITUDE',' SPECTRUM ',' AT 4.3 FT ',
     1 'ABOVE SEA ','FLOOR','---@>*!< M','EAN CURREN','T >.<'/
      DATA LY7,LY12/'HORIZONTAL',' VELOCITY ','SPECTRUM A','T 4.3 FT A',
     1 'BOVE SEA F','LOOR','   @>-<! A','BOVE SEA F','LOOR'/
      DATA LX8,LY8,LY22,LY25/'SMOOTHED','ONE DIMENS','IONAL SPEC','TRUM'
     1,'SPC?R?I?T(',',       )=','S?D?E?E?P(',',       )=','/
      DATA LZ5,LX9,LY9,LY19/'&Z','RAW DATA','JONSWAP','A PROPOSED'/
      DATA LX10,LY10,LY13/'---','XXX',' ','   --------','@>*!<'/
      DATA LX11,LY11/'PEAK FREQU','ENCY >.<','PEAK ENERG','Y >.<'/
      DATA LX15,LX16,LY18/'&>A! .<','&>R!<?L> .',',S(F)*A=F**','B'/
      DATA LY15,LY16,LX19/'&>C! .<','&>R!<?R> .',',A=       ',',' B='/
      DATA LY14,LX17/'MAIN DIREC','TION >.<',',        ^0','C1 AND C2'/
      DATA LY17/'NOTATION >',',.<   (  )F','ROM ONE AN','GLE MODE, ',
     1 '(  )FROM D','OUBLE ANGL','E MODE'/
      DATA LX20,LY20,ST/'TOTAL ENER','GY >.<',',    FT^2','FT?T,T-T? '
     1,'>.<','  HZ','STO./DET. ','APPROACH?!'/
      DATA LZ3,LZ4,LX23,LX24,LZ2/'HZ,       ',',  ^0','0','(RADIAN)'
     1,'=       @(','OF'/
      DATA LY23,LY24/'EVALUATED','AT','DOMINANT F','REQUENCY >',',.<'/
      DATA LZ1,LX25,LZ7/'500','REF. DIREC','TION >.',',       ^0','L>.<'/
      DATA LX21,LX22,LY21/'&>M^2',')>RMS<','=        (',' FT/>S<)^2'/
      DATA LX26,LZ6,ST2/'',      @(','R>.<','STO./DET.','APPROACH?2'/
      DATA A,LZ8,LZ9,LZ10,LX30/20*.0,'3','2','+','&>Y!<='/
      DATA CPI,DEGREE,RN,DMEAN,ESDA/3.14159265,57.29578,.0174532,.0,.0/
      DATA FS/ 1.00000,1.33333,1.60000,1.82857,2.03175,2.21645,2.38695,
     1 2.54608,2.69585,2.83773,2.97286,3.10212,3.22620,3.34569,3.46106,
     1 3.57271,3.68097,3.78614,3.88847,3.98817,4.08545,4.18046,4.27335,
     1 4.36428,4.45334,4.54066,4.62634,4.71045,4.79309,4.87433,4.95424,
     1 5.03288,5.11031,5.18658,5.26175,5.33586,5.40895,5.48107,5.55225,
     1 5.62253,5.69195,5.76053,5.82830,5.89529,5.96153,6.02704,6.09185,
     1 6.15597,6.21943,6.28226,6.34446,6.40605,6.46706,6.52750,6.58739,
     1 6.64673,6.70556,6.76386,6.82168,6.87900,6.93585,6.99224,7.04818,
     1 7.10368,7.15874,7.21339,7.26763,7.32146,7.37490,7.42796,7.48064,
     1 7.53295,7.58490,7.63650,7.68775,7.73866,7.78924,7.83950,7.88943,
     1 7.93905,7.98836,8.03737,8.08608,8.13450,8.18263,8.23048,8.27806,
     1 8.32536,8.37240,8.41917,8.46569,8.51195,8.55796,8.60372,8.64924,
     1 8.69453,8.73958,8.78440,8.82899,8.87335/
      DATA XL,YL/.0,.333,.5,.667,.8,.857,.889,.909,.952,.98,10*1./
      DATA CPI2,VLARGE,ESDB,GA,XX/6.2831853,.0,.0,4.,196*1./
      DATA IPNOW,EDEP,ADEP/0,.0,.0001/
      PRINT 5040
 5040 FORMAT(1X/"-----THE PROGRAM WILL FIRST COMPUTE THE INFORMATION FOR
     1 SPREADING USE,"/"-----THEN, IT WILL COMPUTE ONE DIMENSION CASE,"/
     1"-----FINALLY IT WILL DRAW THE DIRECTIONAL SPECTRUM.")
      READ(6,5068) N
 5068 FORMAT(1X/I5)
      NH=N/2
      NH1=NH/1.45
```

```
      READ(6,5050)N(1),N(2),H1,DEPTH,VI,DI,PI,S,SV,(P(I),PB(I),V(I),
     1 VB(I),D(I),DB(I),I=1,NH1)
 5050 FORMAT(A10,A5,7F9.4/(10E12.6))
      IF(DEPTH.LT.140.) EDEP=2.
      IF(EDEP.GT.1.) ADEP=.01
      PRINT 5028
 5028 FORMAT(/"=====INPUT 1 WILL BE BASED ON U,V,P DATA,"
     1/"=====OR INPUT 2 WILL BE BASED ON U,V DATA.")
      READ*,NOTE
      NH2=NH/3.5
      NH3=NH2-3
      NH6=NH/2.5
      NH5=NH6+1
      FREQ1=1./FLOAT(N)
      PII=SQRT(VI*VI+DI*DI)
      DII=90.-ATAN2(DI,VI)*DEGREE
      IF(DII.LT..0) DII=DII+360.
C  ---PII & DII ARE THE MAGNITUDE AND DIRECTION OF CURRENT AT H1(FT)' ABOVE SEA FLOOR---
C ***************************************************************************
C *---PART IV: CALCULATE ONE DIMENSIONAL SPECTRUM---                          *
C ***************************************************************************
      L1=N/32
      IF(L1.LT.4) L1=4
      FREQ2=SQRT(2.56/DEPTH)
C  ---FREQUENCY FREQ2(HZ) CIRCUMSCRIBES DEEP WATER WAVES, WAVE LENGTH<2*DEPTH---
      L3=FREQ2/FREQ1
      IDEEP=L3
      ENH=FLOAT(N)/288.
C  ---ENH=FLOAT(N)/144./2. COEF. USED TO COMPUTE ENERGY IN POSITIVE FREQUENCY---
C  ---ALSO UNIT CHANGES FROM IN*IN TO FT*FT---
      CALL TRANS(DEPTH,H1,NH1)
C
      DO 5001 I=1,NH1
      B=SQRT(V(I)*V(I)+D(I)*D(I))
      C=SQRT(VB(I)*VB(I)+DB(I)*DB(I))
      IF(NOTE.EQ.1) THEN
      RECORD(I)=(ABS(P(I))*B+ABS(PB(I))*C)/UP(I)*ENH
C  ---RECORD(I) IS EXPRESSED IN A BEST ESTIMATE IN ABOVE FORM---
C  ---RECORD(I) IS RAW DATA OF 1-D HORI. VELOCITY SPECTRUM @ H1(FT) ABOVE SEA FLOOR---
      V2A(I)=(B*B+C*C)*ENH
      ELSE
      RECORD(I)=(B*B+C*C)*ENH
      V2A(I)=(ABS(P(I))*B+ABS(PB(I))*C)/UP(I)*ENH
      END IF
 5001 CONTINUE
      IF(NOTE.EQ.1) THEN
      CALL SMOOTH(N,T12,RECORD,NH5,0,1)
      CALL SMOOTH(N,T33,V2A,NH5,0,1)
      ELSE
      CALL SMOOTH(N,T33,RECORD,NH5,0,1)
      CALL SMOOTH(N,T12,V2A,NH5,0,1)
      END IF
      DO 5047 I=1,NH5
      IF(I.LE.L1.OR.I.GE.L3) GO TO 5027
      IF(RECORD(I).LE.VLARGE) GO TO 5027
      VLARGE=RECORD(I)
      IPEAK=I
 5027 CONTINUE
      IF(NOTE.EQ.1) THEN
      B=ENH*T12(I)/RECORD(I)/UP(I)
      C=ENH*T33(I)/V2A(I)
      ELSE
      B=ENH*T12(I)/V2A(I)/UP(I)
      C=ENH*T33(I)/RECORD(I)
      END IF
      T13(I)=(V(I)*P(I)+VB(I)*PB(I))*B
      T23(I)=(D(I)*P(I)+DB(I)*PB(I))*B
      V1A(I)=(V(I)*D(I)+VB(I)*DB(I))*C
 5047 V1B(I)=(V(I)*V(I)+VB(I)*VB(I)-D(I)*D(I)-DB(I)*DB(I))*C
      IF(L3.LT.NH2) L3=NH2
      IF(L3-IPEAK.GT.20) L3=IPEAK+20
C     WRITE(*,7) H1,(RECORD(I),I=1,30)
C   7 FORMAT(1X/"-----OUTPUT VELOCITY SPECTRUM AT ",F6.1,"' ABOVE SEA FLO
C    1OR,"/(9F8.3))
C ***************************************************************************
C *---PART V: CALCULATE SPREADING PARAMETER AND DIRECTIONAL SPREADING---      *
C ***************************************************************************
      PRINT 5014
 5014 FORMAT(1X/"=====INPUT 3 WILL AVERAGE THREE FREQUENCY DATA,"/
     1"=====OR INPUT 4 WILL AVERAGE FOUR FREQUENCY DATA,"/
     1"=====OR INPUT 5 WILL AVERAGE FIVE FREQUENCY DATA."/
     1"-----DOUBLE THE VALUE OF INPUT WILL CALCULATE BEST-FIT CURVE"/
     1"     OF SPREADING PARAMETER IN EITHER SIDE OF PEAK POINT.")
      READ*,INTO
```

```
      IF(INTO.GE.6) IPNOV=1
      IF(INTO.GE.6) INTO=INTO/2
      DO 5054 I=2,NH6
      B=T23(I)+T23(I-1)+T23(I+1)
      C=T13(I)+T13(I-1)+T13(I+1)
      TEMP=T12(I)+T12(I-1)+T12(I+1)
      BB=2.*(V1A(I)+V1A(I+1)+V1A(I-1))
      CC=V1B(I)+V1B(I+1)+V1B(I-1)
      VARY=T33(I)+T33(I-1)+T33(I+1)
      IF(INTO.EQ.4.AND.I.LT.NH6) THEN
      B=B+T23(I+2)
      C=C+T13(I+2)
      TEMP=TEMP+T12(I+2)
      BB=BB+2.*V1A(I+2)
      CC=CC+V1B(I+2)
      VARY=VARY+T33(I+2)
      ELSE IF(INTO.EQ.5.AND.I.LT.NH6.AND.I.GT.2) THEN
      B=B+T23(I+2)+T23(I-2)
      C=C+T13(I+2)+T13(I-2)
      TEMP=TEMP+T12(I+2)+T12(I-2)
      BB=BB+2.*(V1A(I+2)+V1A(I-2))
      CC=CC+V1B(I+2)+V1B(I-2)
      VARY=VARY+T33(I+2)+T33(I-2)
      END IF
      S1(I)=SQRT(B*B+C*C)/TEMP
      D1(I)=ATAN2(B,C)
      S2(I)=SQRT(BB*BB+CC*CC)/VARY
      D2(I)=ATAN2(BB,CC)/2.
      IF(ABS(D2(I)-D1(I)).LT.1.75) GO TO 5054
      IF(D2(I).LT.D1(I)) D2(I)=D2(I)+CPI
      IF(ABS(D2(I)-D1(I)).GT.1.75) D2(I)=D2(I)-CPI
 5054 CONTINUE
      L2=IPEAK-L1/2
      S1(1)=S1(2)
      S2(1)=S2(2)
      D1(1)=D1(2)
      D2(1)=D2(2)
      DO 5016 I=1,NH6
      IF(S1(I).GT..999) S1(I)=.999
 5016 IF(S2(I).GT..999) S2(I)=.999
      CALL PLOTYPE(1)
      CALL BAUD(1200)
      CALL SIZE(7.5,5.625)
C  ---THE FOLLOWING 80 LINES CAN BE DELETED IF NOT NEEDED---
C
      PRINT 5060
 5060 FORMAT(//"=====INPUT THE NUMBER TO OUTPUT CORRESPONDING FIGURES,"/
     1"-----SPREADING PARAMETER & PROPAGATION DIRECTION - FREQUENCY,"/
     1"-----CODE=1 GIVES THE COMPARISON FROM ONE & DOUBLE ANGLE RESULTS,
     1"/"-----CODE=2 WILL SHOW THE FINAL SOLUTION ONLY.")
      READ*,JMODE
      IF(JMODE.EQ.2) GO TO 5061
      CALL ERASE
      CALL SCALE(25.,4.,1.1,1.,0.,-.1)
      CALL AXISL(0.,.2,.0,.0,1.,.0,.05,.1,4,0,1,2,1.,1.,.1,0)
      CALL VECTORS
      CALL PLOT(.0,1.,0,0)
      CALL PLOT(.2,1.,1,0)
      CALL PLOT(.2,0.,1,0)
      CALL SYMBOL(.06,-.14,.0,.15,15,LX)
      CALL SYMBOL(-.025,.33,90.,.16,9,LX17)
      CALL SYMBEL(-.03,-.24,.0,.1,68,LY17)
      CALL POINTS
      CALL PLOT(.0185,-.23,1,17)
      CALL PLOT(.107,-.23,1,3)
C  ---DRAW S1 AND S2 VERSE FREQUENCY FIGURES---
      CALL LINE(FREQ,S1,17,NH6)
      CALL LINE(FREQ,S2,3,NH6)
      CALL TEKPAUS
      CALL ERASE
      CALL SCALE(4.4,4.,1.8,.9,0.,-.1)
      CALL AXISL(.0,1.,.0,.0,1.,.0,.1,.1,0,0,2,2,1.,1.,.1,0)
C  ---DRAW S1-S2 PICTURE AS C1-C2 RELATION---
      DO 5044 I=L2,L3
      J=I-L2+1
      T12(J)=S1(I)
 5044 T33(J)=S2(I)
      CALL POINTS
      CALL LINE(T12,T33,1,J)
      CALL LINE(XL,YL,6,10)
      CALL NUMBER(.0,1.02,.0,.085,3,.0)
      CALL NUMBER(.333,1.02,.0,.085,3,.5)
      CALL NUMBER(.5,1.02,.0,.085,3,1.)
      CALL NUMBER(.667,1.02,.0,.085,3,2.)
```

```
      CALL NUMBER(.78,1.02,.0,.085,3,4.)
      CALL SYMBOL(.909,1.02,.0,.085,2,LZ)
      CALL SYMBOL(.98,1.02,.0,.085,2,LZ1)
      CALL SYMBOL(.2,1.04,.0,.12,1,LX6)
      DO 5045 I=1,51
      T12(I)=.02*FLOAT(I-1)
 5045 T33(I)=6./(2.-T12(I))-3.-2.*T12(I)
      CALL VECTORS
      CALL LINE(T12,T33,0,51)
      CALL PLOT(1.,.0,1,0)
      CALL PLOT(1.,1.,0,0)
      CALL PLOT(0.,1.,1,0)
      CALL SYMBOL(.7,-.12,.0,.12,2,LX17)
      CALL SYMBOL(-.22,.71,.0,.12,2,LX18)
      CALL TEKPAUS
      CALL ERASE
      CALL SCALE(25.,.63662,1.1,1.5,0.,-CPI)
      CALL AXISL(.0,.2,0.,-CPI,CPI,-CPI,.05,CPI,4,3,1,0,1.,1.,.1,0)
      CALL PLOT(.0,CPI,0,0)
      CALL PLOT(.2,CPI,1,0)
      CALL PLOT(.2,-CPI,1,0)
      CALL SYMBOL(.05,-4.1,.0,.15,15,LX)
      CALL SYMBOL(-.033,-2.4,90.,.15,11,LX5)
      CALL SYMBOL(-.026,.65,90.,.15,9,LY1)
      CALL NUMBER(-.028,-3.1,.0,.1,6,-180.0)
      CALL NUMBER(-.025,-1.57,.0,.1,5,-90.0)
      CALL NUMBER(-.019,.0,.0,.11,3,.0)
      CALL NUMBER(-.025,1.55,.0,.1,5,90.0)
      CALL NUMBER(-.029,3.10,.0,.1,6,180.0)
      CALL SYMBEL(-.03,-4.8,.0,.1,68,LY17)
      CALL POINTS
      CALL PLOT(.018,-4.71,1,28)
      CALL PLOT(.106,-4.71,1,20)
C  ---DRAW D1 AND D2 DATA SHOWING WAVE PROPAGATION DIRECTION---
      CALL LINE(FREQ,D1,28,NH6)
      CALL LINE(FREQ,D2,20,NH6)
      CALL TEKPAUS
 5061 CONTINUE
C
C
      DO 5033 I=1,NH2
      IF(NOTE.EQ.2) D1(I)=D2(I)
      C=1.-S1(I)
      UP(I)=S1(I)/C
      C=1.-S2(I)
      B=(1.5*S2(I)+.5)/C
 5033 T13(I)=B+SQRT(B*B+2.*S2(I)/C)
C  ---UP(I) AND T13(I) ARE SPREADING PARAMETERS FROM ONE AND DOUBLE ANGLE MODE---
C
      IF(L3-IPEAK.LT.L1) L3=IPEAK+L1+L1/2
      IF(L3.GT.NH2) L3=NH2
      IDPEAK=L3-L1/2
      IF(NOTE.EQ.1) VARY=UP(IDPEAK)
      IF(NOTE.EQ.2) VARY=T13(IDPEAK)
      DO 5049 I=IDPEAK,L3
      IF(NOTE.EQ.1.AND.UP(I).GE.VARY) GO TO 5049
      IF(NOTE.EQ.2.AND.T13(I).GE.VARY) GO TO 5049
      IDPEAK=I
      IF(NOTE.EQ.1) VARY=UP(I)
      IF(NOTE.EQ.2) VARY=T13(I)
 5049 CONTINUE
C
      TEMP=FREQ(IDPEAK)
      LL=IPEAK+L1/3
      ICPEAK=L2
C  ---CRITICAL FREQUENCY INDEX INDICATES HIGHEST SPREADING PARAMETER---
      IF(NOTE.EQ.1) VLARGE=UP(ICPEAK)
      IF(NOTE.EQ.2) VLARGE=T13(ICPEAK)
      DO 5006 I=ICPEAK,LL
      IF(NOTE.EQ.1.AND.UP(I).LE.VLARGE) GO TO 5006
      IF(NOTE.EQ.2.AND.T13(I).LE.VLARGE) GO TO 5006
      ICPEAK=I
      IF(NOTE.EQ.1) VLARGE=UP(I)
      IF(NOTE.EQ.2) VLARGE=T13(I)
 5006 CONTINUE
      PEAKF=FREQ(ICPEAK)
C
      MOD=1
C
 5020 X1=-5.
      X2=-.1
      IF(MOD.EQ.2.AND.IPNOW.EQ.1) X1=.1
      IF(MOD.EQ.2.AND.IPNOW.EQ.1) X2=20.
      CALL LST(FF2,X2,MOD)
 5063 CALL LST(FF1,X1,MOD)
```

```
      XN=100000.*FF1*FF2
      IF(XN.GT..0) THEN
      X1=X1-3.
      IF(MOD.EQ.2.AND.IPNOW.EQ.1.AND.X1.GT.-7.) GO TO 5063
      IF(MOD.EQ.2.AND.IPNOW.EQ.1) GO TO 5080
      IF(X1.GT.-40.) GO TO 5063
 5080 X=.0
      A1=.0
      GO TO 5056
      END IF
      DO 5057 I=1,22
      X=(X1+X2)/2.
      CALL LST(FF,X,MOD)
      XN=100000.*FF*FF1
      IF(XN.LE..0) THEN
      X2=X
      FF2=FF
      ELSE
      X1=X
      FF1=FF
      END IF
      IF(ABS(FF)-1.E-10) 5056,5056,5057
 5057 CONTINUE
 5056 IF(MOD.EQ.2) GO TO 5018
      MOD=2
      CALL ERASE
C ***************************************************************************
C *---PART V1: DRAWING APPLIED SPREADING PARAMETER IN LOG. SCALE---          *
C ***************************************************************************
      IF(NOTE.EQ.1) CALL SMOOTH(N,S1,WP,NM2,ICPEAK,3)
      IF(NOTE.EQ.2) CALL SMOOTH(N,S1,T13,NM2,ICPEAK,3)
      CALL SCALE(25.,1.3,1.1,1.06,.0,-1.)
      CALL AXISL(.0,.2,.0,-1.,2.,-1.,.05,1.,4,0,1,0,1.,1.,.1,0)
      DO 6069 I=1,NM2
      IF(S1(I).LT..1) VB(I)=-1.
      IF(WP(I).LT..1) T12(I)=-1.
      IF(T13(I).LT..1) D(I)=-1.
      IF(S1(I).GE..1) VB(I)=ALOG10(S1(I))
      IF(T13(I).GE..1) D(I)=ALOG10(T13(I))
 6069 IF(WP(I).GE..1) T12(I)=ALOG10(WP(I))
      CALL POINTS
      IF(IPNOW.EQ.0) THEN
      CALL PLOT(.168,.53,1,27)
      CALL PLOT(.168,.31,1,19)
      ELSE
      IF(NOTE.EQ.1) CALL PLOT(.168,.75,1,27)
      IF(NOTE.EQ.2) CALL PLOT(.168,.75,1,19)
      CALL SYMBEL(.16,.5,.0,.09,4,LZ6)
      CALL SYMBEL(.16,.28,.0,.09,4,LZ7)
      END IF
      CALL POINTS
      CALL PLOT(.009,-1.64,1,27)
      CALL PLOT(.098,-1.64,1,19)
      CALL LINE(FREQ,T12,27,NM2)
      CALL LINE(FREQ,D,19,NM2)
      CALL DASHES
      CALL LINE(FREQ,VB,0,NM2)
      CALL VECTORS
      IF(X.NE.0.) THEN
      IF(IPNOW.EQ.0.AND.NOTE.NE.1) GO TO 5084
      INTO=0
      DO 6071 I=NM2,1,-1
      IF(I.GE.ICPEAK) S2(I)=A1*FREQ(I)**X
 6071 IF(I.LT.ICPEAK) S2(I)=.8*S2(ICPEAK)
      DO 6066 I=ICPEAK,IDPEAK
      J=I-ICPEAK+1
      DB(J)=FREQ(I)
      IF(S2(I).LT..1) VB(J)=-1.
 6066 IF(S2(I).GE..1) VB(J)=ALOG10(S2(I))
      CALL LINE(DB,VB,0,J)
      END IF
 5084 XL(1)=.17
      XL(2)=.183
      YL(1)=1.19
      YL(2)=1.19
      CALL SYMBOL(.05,-1.4,.0,.15,15,LX)
      CALL SYMBOL(-.026,-.7,90.,.15,20,LY1)
      CALL SYMBEL(-.038,-1.67,.0,.1,68,LY17)
      CALL NUMBER(-.024,-1.03,.0,.1,6,.1000)
      CALL NUMBER(-.024,-.03,.0,.1,6,1.000)
      CALL NUMBER(-.024,.97,.0,.1,6,10.00)
      CALL NUMBER(-.024,1.97,.0,.1,6,100.0)
      IF(NOTE.EQ.1) CALL SYMBEL(.12,2.,.0,.15,20,ST)
      IF(NOTE.EQ.2) CALL SYMBEL(.12,2.,.0,.15,20,ST2)
      CALL SYMBEL(.173,1.64,.0,.107,19,LY22)
```

```
      CALL NUMBER(.185,1.64,.0,.09,6,PEAKF)
      CALL NUMBER(.215,1.64,.0,.09,5,VLARGE)
      CALL SYMBEL(.173,1.4,.0,.102,19,LY25)
      CALL NUMBER(.185,1.4,.0,.09,6,TEMP)
      CALL NUMBER(.215,1.4,.0,.09,5,VARY)
      CALL SYMBOL(.191,1.16,.0,.09,10,LY19)
      CALL SYMBOL(.2,.96,.0,.09,9,LY1)
      CALL SYMBOL(.173,.72,.0,.09,11,LY18)
      CALL SYMBOL(.173,.5,.0,.09,14,LX19)
      CALL NUMBER(.179,.5,.0,.09,8,A1)
      CALL NUMBER(.226,.5,.0,.09,6,X)
      CALL SYMBOL(.17,.03,.0,.104,3,LX10)
      CALL SYMBOL(.191,.03,.0,.09,8,LX8)
      CALL SYMBOL(.2,-.17,.0,.09,9,LY1)
      CALL SYMBEL(.173,-.37,.0,.09,16,LX2)
      CALL SYMBOL(.187,-.57,.0,.09,15,M)
      GO TO 5020
 5018 CALL SYMBOL(.173,.28,.0,.09,14,LX19)
      CALL NUMBER(.179,.28,.0,.09,8,A1)
      CALL NUMBER(.226,.28,.0,.09,6,X)
      IF(IPNOW.EQ.1.AND.X.NE.0.) THEN
      II=ICPEAK-1
      DO 5081 I=1,II
 5081 S2(I)=A1*FREQ(I)**X
      DO 5082 I=1,II
      IF(S2(I).LT..1) VB(I)=-1.
 5082 IF(S2(I).GE..1) VB(I)=ALOG10(S2(I))
      CALL LINE(FREQ,VB,0,II)
      GO TO 5083
      END IF
      IF(NOTE.EQ.2.AND.X.NE..0) THEN
      INTO=0
      DO 6051 I=NH2,1,-1
      IF(I.GE.ICPEAK) S2(I)=A1*FREQ(I)**X
 6051 IF(I.LT.ICPEAK) S2(I)=.8*S2(ICPEAK)
      DO 6052 I=ICPEAK,IDPEAK
      J=I-ICPEAK+1
      DB(J)=FREQ(I)
      IF(S2(I).LT..1) VB(J)=-1.
 6052 IF(S2(I).GE..1) VB(J)=ALOG10(S2(I))
      CALL LINE(DB,VB,0,J)
      END IF
 5083 CALL LINE(XL,YL,0,2)
      CALL TEKPAUS
      CALL ERASE
      IF(INTO.NE.0) THEN
      DO 6053 I=NH2,1,-1
      IF(I.GE.ICPEAK) S2(I)=.00003/FREQ(I)**5
 6053 IF(I.LT.ICPEAK) S2(I)=.8*S2(ICPEAK)
      END IF
C *************************************************************************
C *---PART VII: DRAWING APPLIED DIRECTIONAL SPREADING IN POLAR COORDINATES---  *
C *************************************************************************
      PRINT 303
  303 FORMAT(/"*****INPUT 1 WILL SET PROPOSED DIRECTION AS SMOOTHED DIRE
     1TION,"/"*****OR INPUT 2 TO SET MAIN DIRECTION IN PROPOSED SPECTRUM,
     1"/"*****OR INPUT 3 TO SET BEST-FIT-CURVE IN PROPOSED SPECTRUM.")
      READ*,JUMP
      CALL ERASE
      DO 6067 I=L1,NH2
      ESDA=ESDA+RECORD(I)
 6067 DMEAN=DMEAN+D1(I)*RECORD(I)
      DDMEAN=DMEAN/ESDA
      IF(JUMP.NE.2) THEN
      CALL SCALE(17.4,16.,.42,.42,.0,.0)
      CALL ORIGIN(3.03,2.83)
      CALL POINTS
      END IF
      T12(1)=DDMEAN
      DO 6065 I=2,NH2
      IF(JUMP.NE.2) THEN
      X=FREQ(I)*COS(D1(I))
      Y=FREQ(I)*SIN(D1(I))
      CALL PLOT(X,Y,1,1)
      END IF
      T12(I)=D1(I)
 6065 IF(I.GT.L2.AND.ABS(T12(I)-T12(I-1)).GE..9) T12(I)=T12(I-1)
     1*.7+T12(I)*.3
      DMEAN=DDMEAN*DEGREE
      CALL SMOOTH(N,D1,T12,NH2,0,2)
C  ---WHERE D1(I) IS A SMOOTHED DIRECTIONAL SPREADING---
      IF(JUMP.EQ.2) GO TO 304
      IF(JUMP.EQ.3) THEN
      II=IDEEP
      IF(II.GT.NH3) II=NH3
```

```
      CALL SMOOTH(N,WP,RECORD,II,0,2)
      DO 301 I=L1,II
      A(1,1)=A(1,1)+WP(I)
      BB=WP(I)*FREQ(I)
      A(1,2)=A(1,2)+BB
      BB=BB*FREQ(I)
      A(1,3)=A(1,3)+BB
      BB=BB*FREQ(I)
      A(1,4)=A(1,4)+BB
      BB=BB*FREQ(I)
      A(2,4)=A(2,4)+BB
      BB=BB*FREQ(I)
      A(3,4)=A(3,4)+BB
      A(4,4)=A(4,4)+BB*FREQ(I)
      CC=WP(I)*(D1(I)-DDMEAN)
      A(1,5)=A(1,5)+CC
      CC=CC*FREQ(I)
      A(2,5)=A(2,5)+CC
      CC=CC*FREQ(I)
      A(3,5)=A(3,5)+CC
  301 A(4,5)=A(4,5)+CC*FREQ(I)
      X12=A(1,1)
      A(2,1)=A(1,2)
      A(2,2)=A(1,3)
      A(2,3)=A(1,4)
      A(3,1)=A(1,3)
      A(3,2)=A(2,3)
      A(3,3)=A(2,4)
      A(4,1)=A(1,4)
      A(4,2)=A(2,4)
      A(4,3)=A(3,4)
      DO 405 I=1,4
      DO 405 J=1,5
  405 A(I,J)=A(I,J)/A(I,1)
      DET=1.
      DO 411 K=1,4
      BIG=ABS(A(K,K))
      KKK=K
      DO 410 KK=K,4
      IF(BIG-ABS(A(KK,K))) 409,410,410
  409 BIG=ABS(A(KK,K))
      KKK=K
  410 CONTINUE
      DO 408 JJ=K,5
      BOXX=A(K,JJ)
      A(K,JJ)=A(KKK,JJ)
  408 A(KKK,JJ)=BOXX
      DET=DET*A(K,K)
      IF(DET-.0) 413,412,413
  412 PRINT*,'DET.=.0'
      STOP
  413 K1=K+1
      DO 414 J=K1,5
      A(K,J)=A(K,J)/A(K,K)
      IF(K-N.EQ.0) GO TO 411
      DO 415 I=K1,4
  415  A(I,J)=A(I,J)-A(I,K)*A(K,J)
  414 CONTINUE
  411 CONTINUE
      XL(4)=A(4,5)
      K=4
  417 SIGNN=.0
      DO 416 J=K,4
  416 SIGNN=SIGNN+A(K-1,J)*XL(J)
      XL(K-1)=A(K-1,5)-SIGNN
      K=K-1
      IF(K.EQ.1) GO TO 418
      GO TO 417
  418 Z1=XL(1)+DDMEAN
      Z2=XL(2)
      Z3=XL(3)
      Z4=XL(4)
      DO 302 I=1,NH2
  302 D2(I)=Z1+Z2*FREQ(I)+Z3*FREQ(I)*FREQ(I)+Z4*FREQ(I)**3
C  ---D2(I) IS THE BEST-FIT-CURVE FOR PROPOSED DIRECTION---
      Z1=90.-Z1*DEGREE
      Z2=-Z2*DEGREE
      Z3=-Z3*DEGREE
      Z4=-Z4*DEGREE
      BB=.0
      CC=.0
      DO 305 I=L1,II
      J=I-L1+1
      D(J)=FREQ(I)*COS(D2(I))
      T33(J)=FREQ(I)*SIN(D2(I))
      CC=CC+(D1(I)-DDMEAN)**2*WP(I)
```

```
  305 BB=BB+(D1(I)-D2(I))**2*WP(I)
      BB=SQRT(BB/X12)*DEGREE
      CC=SQRT(CC/X12)*DEGREE
      XL(1)=.151
      XL(2)=.168
      YL(1)=.078
      YL(2)=.078
      CALL VECTORS
      CALL LINE(D,T33,0,J)
      CALL LINE(XL,YL,0,2)
      CALL SYMBEL(.173,.075,.0,.105,6,LX30)
      CALL NUMBER(.187,.075,.0,.08,7,Z1)
      CALL SYMBOL(.2145,.065,.0,.08,1,LX)
      IF(Z2.GT.0.) CALL SYMBOL(.17,.065,.0,.08,1,LZ10)
      CALL NUMBER(.17,.065,.0,.08,8,Z2)
      CALL SYMBOL(.2145,.055,.0,.08,1,LX)
      CALL SYMBOL(.22,.058,.0,.065,1,LZ9)
      IF(Z3.GT.0.) CALL SYMBOL(.17,.055,.0,.08,1,LZ10)
      CALL NUMBER(.17,.055,.0,.08,8,Z3)
      CALL SYMBOL(.2145,.045,.0,.08,1,LX)
      CALL SYMBOL(.22,.048,.0,.065,1,LZ8)
      IF(Z4.GT.0.) CALL SYMBOL(.17,.045,.0,.08,1,LZ10)
      CALL NUMBER(.17,.045,.0,.08,8,Z4)
      CALL SYMBEL(.173,.03,.0,.11,2,LZ5)
      CALL SYMBEL(.179,.0283,.0,.09,4,LX22)
      CALL SYMBOL(.195,.03,.0,.1,1,LX24)
      CALL SYMBOL(.229,.033,.0,.05,1,LZ2)
      CALL NUMBER(.2,.03,.0,.08,6,BB)
      CALL SYMBEL(.173,-.145,.0,.11,2,LZ5)
      CALL SYMBEL(.179,-.1467,.0,.09,4,LX22)
      CALL SYMBOL(.195,-.145,.0,.1,1,LX24)
      CALL SYMBOL(.229,-.142,.0,.05,1,LZ2)
      CALL NUMBER(.2,-.145,.0,.08,6,CC)
      END IF
      S=90.-S
      DM=90.-DMEAN
      R=100.*ABS(DM-S)/S
      L4=L1+L1/2
      DO 6068 I=L4,NH2
      II=I-L4+1
      D(II)=FREQ(I)*COS(D1(I))
 6068 T33(II)=FREQ(I)*SIN(D1(I))
      CALL DASHES
      CALL LINE(D,T33,0,II)
      INTO=1
      GO TO 7062
 6072 CALL SYMBOL(.13,.095,.0,.18,9,LY1)
      CALL SYMBEL(.15,-.0545,.0,.05,3,LY10)
      CALL SYMBOL(.17,-.055,.0,.08,10,LX7)
      CALL SYMBOL(.19,-.065,.0,.08,9,LX5)
      CALL SYMBOL(.15,-.08,.0,.09,3,LX10)
      CALL SYMBOL(.17,-.08,.0,.08,8,LX8)
      CALL SYMBOL(.19,-.09,.0,.08,9,LX5)
      CALL SYMBEL(.15,-.105,.0,.08,16,LX2)
      CALL SYMBOL(.176,-.115,.0,.08,15,R)
      CALL SYMBEL(.15,-.13,.0,.08,30,LY14)
      CALL NUMBER(.215,-.13,.0,.08,6,DM)
      IF(JUMP.EQ.1) THEN
      CALL SYMBEL(.15,-.145,.0,.08,29,LX25)
      CALL NUMBER(.215,-.145,.0,.08,6,S)
      CALL SYMBEL(.15,-.16,.0,.11,2,LZ5)
      CALL SYMBEL(.155,-.16,.0,.08,10,LX24)
      CALL NUMBER(.161,-.16,.0,.08,5,B)
      END IF
      CALL TEXPAUS
      CALL ERASE
  304 CONTINUE
C
      IF(ABS(H1-4.3).GT..5)  L5=0
      DO 5043 I=1,NH1
      IF(L5.EQ.0) RECORD(I)=RECORD(I)*(COSH(WK(I)*4.333)/COSH(WK(I)*
     1H1))**2
C  ---RECORD(I) IS RAW DATA OF HORI. VELOCITY SPECTRUM @  4.3'---
 5043 DB(I)=RECORD(I)/FREQ(I)**2/39.47842
C  ---39.47842=(CPI2)**2---
C  ---DB(I) IS RAW DATA OF HORI. AMPLITUDE SPECTRUM @ 4.3' ABOVE SEA FLOOR---
C
      DO 5041 I=1,NH1
      VB(I)=DB(I)*(SINH(WK(I)*DEPTH)/COSH(WK(I)*4.333))**2
C  ---VB(I) IS RAW DATA OF WAVE ENERGY SPECTRUM AT SEA SURFACE---
      IF(VB(I).GE.2500.) GO TO 5042
 5041 CONTINUE
C
 5042 MINN=I-1
```

```
      K=MINN-1.5*L1
      IF(IDEEP.GE.MINN) IDEEP=MINN
      MAX=(IPEAK+K)/2
      IF(MAX-IPEAK.GT.L1) MAX=IPEAK+L1
      CALL SMOOTH(N,UP,VR,IDEEP,0,1)
      IIPEAK=IPEAK
      VLARGE=UP(IIPEAK)
      MAX=MAX+L1/3
      DO 5038 J=L2,MAX
      IF(UP(J).LE.VLARGE) GO TO 5038
      VLARGE=UP(J)
      IIPEAK=J
 5038 CONTINUE
      MM=K
      IF(K.GT.IIPEAK+L1*2) MM=IIPEAK+L1*2.3
      WRITE(*,5053) VLARGE,IIPEAK,UP(MM),MM,(UP(I),I=L2,MM)
 5053 FORMAT(/////////"-----CHECK 1-D. WATER SURFACE ENERGY HERE,"/"-----
     1INDEX OF PEAK ENERGY",F7.2," SHOWN HERE IS",I3,","/"-----INDEX OF
     1UPPER BOUND",F7.2," IS",I3,","/ "-----SMOOTHED ENERGY SERIES NEAR
     1PEAK ARE SHOWN AS FOLLOWS,"/(9F8.2))
      PRINT 7067
 7067 FORMAT(/"=====INPUT NEW INDEX FOR UPPER BOUND TO CONTINUE,"/"=====
     1OR INPUT 0 TO STOP THE PROGRAM,"/"=====OR INPUT 1 WILL RESET INDEX
     1 FOR DESIRED PEAK AND UPPER BOUND.")
      READ*,MOD
      IF(MOD.EQ.0) STOP
      IF(MOD.EQ.1) THEN
      READ*,IIPEAK,MOD
      VLARGE=UP(IIPEAK)
      END IF
      K=MOD
      XN=1.
      X2=10.
      PEAKF=FREQ(IIPEAK)
      CALL ERASE
      IF(K.LE.IIPEAK+3) PRINT*,'IIPEAK=',IIPEAK,', K=',K
      IF(K.LE.IIPEAK) STOP
C
      Y=.6641874
      LL=.62*IIPEAK
      IF(K.GT.IIPEAK+LL) K=IIPEAK+LL
C  ---LL WILL HELP AVOIDING THE OVERFLOW IN EXP---
      DO 120 I=LL,K
      C=EXP((PEAKF/FREQ(I))**4*1.25)*FREQ(I)**5
      T13(I)=Y/C/C
  120 T23(I)=UP(I)/C
      P(IIPEAK)=1.
      ALFA=VLARGE*PEAKF**5*3.490343/Y/GA
      MM=1
  130 MAX=1
  160 X1=.0038
      X2=4.
      IF(MAX.EQ.1) CALL LSM(FF1,X1,MAX)
      IF(MAX.EQ.1) B=FF1
      IF(MAX.EQ.2) FF1=B
  110 CALL LSM(FF2,X2,MAX)
      XN=100000.*FF1*FF2
      IF(XN.GT..0) THEN
      X2=X2+2.
      IF(X2.LE.10.) GO TO 110
      PA=.0
      PC=.0
      ALFA=.0081
      GA=1.
      DO 7055 I=IIPEAK,MM1
      TEMP=PEAKF/FREQ(I)
      V(I)=TEMP**5*EXP(1.25*(1.-TEMP**4))*VLARGE
C  ---USE P-M SPECTRUM TO EXTRAPOLATE THE TAIL OF RAW DATA OF WAVE ENERGY DENSITY---
 7055 UP(I)=V(I)
      DO 7056 I=1,IIPEAK
      TEMP=PEAKF/FREQ(I)
      A2=1.25*(1.-TEMP**4)
      IF(I.GE.IPEAK) V(I)=UP(I)
      IF(I.LT.IPEAK) V(I)=.0
 7056 IF(I.LT.IPEAK.AND.A2.GE.-670.) V(I)=TEMP**5*EXP(A2)*VLARGE
      GO TO 220
      END IF
      DO 140 I=1,15
      X=(X1+X2)/2.
      CALL LSM(FF,X,MAX)
      XN=100000.*FF*FF1
      IF(XN.LE..0) THEN
      X2=X
      FF2=FF
```

```
      ELSE
      X1=X
      FF1=FF
      END IF
      IF(ABS(FF)-1.E-8) 150,150,140
  140 CONTINUE
  150 IF(MAX.EQ.1) PA=X
      IF(MAX.EQ.2) PC=X
      MAX=MAX+1
      IF(MAX.LE.2) GO TO 160
      Z1=.0
      Z2=.0
      Z3=.0
      Z4=.0
      DO 170 I=LL,K
      TEMP=PC
      IF(I.LT.IIPEAK) TEMP=PA
      P(I)=(1./EXP(((FREQ(I)-PEAKF)/PEAKF/TEMP)**2/26.))**13
C  ---WHERE .36788=1/EXP---
      C=GA**P(I)
      Z1=Z1+T13(I)*C*C
      Z2=Z2+T23(I)*C
      Z3=Z3+T13(I)*P(I)*C*C/GA
  170 Z4=Z4+T23(I)*P(I)*C/GA
      Z1=Z2/Z1
      Z2=Z4/Z3
      ALFA=(Z1+Z2)/2.
      GA=VLARGE*PEAKF**5*3.490343/Y/ALFA
      IF(ABS((Z1-Z2)/Z1).LE..01) GO TO 180
      MM=MM+1
      IF(MM.LE.15) GO TO 130
  180 MAX=FLOAT(IIPEAK)*(1.+125.*PC)
      DO 190 I=LL,MM1
      IF(I.LE.K) V(I)=ALFA*Y/FREQ(I)**5/EXP((PEAKF/FREQ(I))**4*1.25)
     !*GA**P(I)
C  ---V(I) IS AN APPLIED JONSWAP SPECTRUM AT SEA SURFACE---
      IF(I.GT.K.AND.I.LE.MAX) THEN
      P(I)=(1./EXP(((FREQ(I)-PEAKF)/PEAKF/PC)**2/26.))**13
      V(I)=ALFA*Y/FREQ(I)**5/EXP((PEAKF/FREQ(I))**4*1.25)*GA**P(I)
      END IF
      IF(I.GT.MAX) V(I)=V(MAX)
  190 IF(I.GT.IDEEP) WP(I)=V(I)
C  ---USE JONSWAP TO EXTRAPOLATE THE TAIL PART OF RAW DATA OF WAVE ENERGY SPECTRUM---
      VALUE=FLOAT(IIPEAK)*(1.-125.*PA)+1.
      DO 5034 I=1,LL
      A2=(PEAKF/FREQ(I))**4*1.25
      IF(A2.GT.740.) THEN
      V(I)=.0
      ELSE
      V(I)=.0
      IF(I.GT.VALUE)P(I)=(1./EXP(((FREQ(I)-PEAKF)/PEAKF/PA)**2/26.))**13
      IF(I.GT.VALUE)V(I)=ALFA*Y/FREQ(I)**5/EXP(A2)*GA**P(I)
      END IF
 5034 CONTINUE
  220 B2=.0
      B3=.0
      ESDA=.0
      DO 7063 I=1,MM1
C     IF(I.LT.IIPEAK.AND.V(I).LT.WP(1)) V(I)=WP(1)
C     IF(I.LE.IIPEAK) B2(I)=V(I)
C  ---B2(I) KEEPS THE ORIGINAL FRONT PART OF JONSWAP---
      ESDA=ESDA+RECORD(I)
      B2=B2+FREQ(I)*V(I)
 7063 B3=B3+V(I)/FREQ(I)
      VMS=ESDA*FREQ1
      B2=SQRT(B2/B3)
      B=.0
      DO 5065 I=L1,IDPEAK
      ESDB=ESDB+V(I)
 5065 B=B+(V(I)-WP(I))**2
      TOT=ESDB*FREQ1
      ERR1=100.*SQRT(B)/ESDB
      DO 7064 I=1,MM2
      IF(S1(I).GT.1000.) S1(I)=1000.
      IF(S2(I).GT.1000.) S2(I)=1000.
C  ---ASSUME THAT SPREADING PARAMETER WILL BE NEVER ACCESSES 50.---
      IS=INT(S1(I))
      IF(IS.EQ.0) THEN
      T13(I)=S1(I)
      ELSE
      IF(IS.LT.100) T13(I)=FS(IS)+(S1(I)-IS)*(FS(IS+1)-FS(IS))
      IF(IS.GE.100) T13(I)=8.87335+.022*(S1(I)-100.)
      END IF
      IS=INT(S2(I))
```

```
      IF(IS.EQ.0) THEN
      T23(I)=S2(I)
      ELSE
      IF(IS.LT.100) T23(I)=FS(IS)+(S2(I)-IS)*(FS(IS+1)-FS(IS))
      IF(IS.GE.100) T23(I)=8.87335+.022*(S2(I)-100.)
      END IF
 7064 CONTINUE
C  ---T13 & T23 REPRESENT G(S)*CPI AS SHOWN IN THEORITICAL SOLUTION---
C ***************************************************************************
C *---PART VIII: DRAWING ONE DIMENSIONAL KINEMATIC SPECTRUM IN LOG. SCALE---   *
C ***************************************************************************
      PRINT 5032
      READ*,MODE
C  ---MODE=1 : WILL CALCULATE HORIZONTAL VELOCITY SPECTRUM AT 4.3 FT ABOVE SEA BUTTOM---
C  ---MODE=2 : WILL CALCULATE HORIZONTAL AMPLITUDE SPECTRUM AT 4.3 FT ABOVE SEA BUTTOM---
C  ---MODE=3 : WILL CALCULATE WAVE ENERGY SPECTRUM AT SEA SURFACE---
      IF(MODE.EQ.4) GO TO 7072
C
C  ---ONCE CALCULATION THROUGH THIS LINE WILL DISCONNECT WITH ABOVE PART---
C
 5048 PRINT 5035
 5035 FORMAT(/// "=====INPUT 1 TO DRAW ONE DIMENSIONAL SPECTRUM,"/"=====
     1OR INPUT 2 TO DRAW DIRECTIONAL SPECTRUM.")
      READ*,JMODE
      IF(JMODE.EQ.2)  THEN
      IF(MODE.EQ.3) GO TO 5046
      GO TO 5052
      END IF
      CALL ERASE
C
      IF(MODE.NE.3) GO TO 5029
      CALL SCALE(8.3,.76,1.1,1.,.0,-2.)
      CALL AXISL(.0,.6,.0,-2.,3.,-2.,.1,1.,1,0,1,0,1.,1.,.1,0)
      CALL SYMBOL(-.1,-3.08,.0,.1,60,LY5)
      CALL NUMBER(.579,-3.08,.0,.1,7,DEPTH)
      CALL SYMBEL(-.05,3.65,.0,.18,17,LY2)
      DO 5037 J=1,MINN
      IF(VB(J).LT..01) T12(J)=-2.
 5037 IF(VB(J).GE..01) T12(J)=ALOG10(VB(J))
      CALL POINTS
      CALL LINE(FREQ,T12,19,MINN)
      CALL PLOT(.47,-.19,1,19)
 5046 DO 5036 J=1,NH1
      PB(J)=WP(J)
      IF(JMODE.EQ.1) THEN
      IF(PB(J).LT..01.AND.J.LE.IDEEP) T12(J)=-2.
      IF(PB(J).GE..01.AND.J.LE.IDEEP) T12(J)=ALOG10(PB(J))
      IF(V(J).LT..01) T33(J)=-2.
      IF(V(J).GE..01) T33(J)=ALOG10(V(J))
      END IF
 5036 P(J)=V(J)
      IF(JMODE.EQ.2) GO TO 7060
      PEAKF=FREQ(IIPEAK)
      VLARGE=V(IIPEAK)
      XL(1)=.452
      XL(2)=.482
      YL(1)=-1.
      YL(2)=-1.
      CALL VECTORS
      CALL LINE(XL,YL,0,2)
      CALL LINE(FREQ,T33,0,NH1)
      CALL DASHES
      CALL LINE(FREQ,T12,0,IDEEP)
      CALL SYMBOL(-.1,-2.,90.,.15,24,LY8)
      CALL SYMBOL(.18,-2.68,.0,.15,15,LX)
      CALL NUMBER(-.088,2.95,.0,.1,7,1000.0)
      CALL NUMBER(-.088,1.95,.0,.1,7,100.00)
      CALL NUMBER(-.088,.95,.0,.1,7,10.000)
      CALL NUMBER(-.088,-.05,.0,.1,7,1.0000)
      CALL NUMBER(-.088,-1.05,.0,.1,7,0.1000)
      CALL NUMBER(-.088,-2.05,.0,.1,7,0.0100)
      IF(NOTE.EQ.1) CALL SYMBEL(.36,3.3,.0,.15,20,ST)
      IF(NOTE.EQ.2) CALL SYMBEL(.36,3.3,.0,.15,20,ST2)
      CALL SYMBEL(.5,2.86,.0,.11,2,LZ5)
      CALL SYMBEL(.511,2.83,.0,.08,4,LX22)
      CALL SYMBEL(.555,2.86,.0,.09,10,LX24)
      CALL NUMBER(.57,2.86,.0,.088,5,ERR1)
      CALL SYMBEL(.46,2.5,.0,.09,29,LX20)
      CALL NUMBER(.583,2.5,.0,.09,6,TOT)
      CALL SYMBEL(.5,2.14,.0,.09,7,LX15)
      CALL NUMBER(.545,2.14,.0,.09,7,ALFA)
      CALL SYMBEL(.5,1.82,.0,.09,7,LY15)
      CALL NUMBER(.545,1.82,.0,.09,5,GA)
```

```
      CALL SYMBEL(.5,1.5,.0,.09,10,LX16)
      CALL NUMBER(.545,1.5,.0,.09,5,PA)
      CALL SYMBEL(.5,1.18,.0,.09,10,LY16)
      CALL NUMBER(.545,1.18,.0,.09,5.PC)
      CALL SYMBEL(.46,.84,.0,.09,18,LX11)
      CALL NUMBER(.615,.84,.0,.09,6.PEAKF)
      CALL SYMBEL(.46,.44,.0,.09,15,LY11)
      CALL NUMBER(.59,.44,.0,.09,7,VLARGE)
      CALL SYMBEL(.5,.14,.0,.09,27,LY20)
      CALL NUMBER(.546,.14,.0,.09,6,R2)
      CALL SYMBOL(.495,-.26,.0,.09,9,LX9)
      CALL SYMBOL(.45,-.66,.0,.09,3,LX10)
      CALL SYMBOL(.495,-.66,.0,.09,8.LX8)
      CALL SYMBOL(.605,-.66,.0,.09,8,LX6)
      CALL SYMBOL(.495,-1.06,.0,.09,10,LY9)
      CALL SYMBOL(.588,-1.06,.0,.09,8,LX6)
      CALL SYMBEL(.46,-1.46,.0,.09,16,LX2)
      CALL SYMBOL(.496,-1.71,.0,.09,15,M)
      CALL TEKPAUS
C
      IF(MODE.EQ.3) GO TO 7060
 5029 CALL SCALE(8.3,.76,1.1,1.,0.0,-4.)
      CALL AXISL(.0,.6,.0,-4.,1.,-4.,.1,1.,1,0,1,0,1.,1.,.1,0)
      IF(MODE.EQ.1) THEN
      CALL SYMBOL(-.1,-5.08,.0,.1,55,LY7)
      CALL SYMBEL(-.05,1.65,.0,.18,18,LX1)
      CALL SYMBEL(.504,.26,.0,.105,5,LX21)
      CALL SYMBEL(.55,.25,.0,.1,20,LY21)
      CALL SYMBEL(.517,.22,.0,.08,5,LX22)
      CALL NUMBER(.561,.25,.0,.088,6,VMS)
      B=100.*ABS(SV-VMS)/VMS
      CALL SYMBOL(.504,-.05,.0,.09,4,LX25)
      CALL NUMBER(.56,-.05,.0,.088.6,SV)
      CALL SYMBEL(.64,-.05,.0,.1,10,LX26)
      CALL NUMBER(.65,-.05,.0,.088,5,B)
      ELSE
      CALL SYMBOL(-.1,-5.08,.0,.1,56,LY6)
      CALL SYMBEL(-.05,1.65,.0,.18,15,LY)
      END IF
 5052 IF(MODE.EQ.1) CALL SMOOTH(N,PB,RECORD,NH1,0,1)
      IF(MODE.EQ.2) CALL SMOOTH(N,PB,DB,NH1,0,1)
      PEAKF=FREQ(IPEAK)
      VLARGE=.0
      DO 5031 I=1,NH1
      IF(MODE.EQ.1) THEN
      IF(I.LE.IPEAK)P(I)=V(I)*RECORD(I)/VB(I)
      IF(I.GT.IPEAK)P(I)=V(I)*(COSH(WK(I)*4.333)*FREQ(I)*CPI2/SINH(WK(I)
     1*DEPTH))**2
      IF(JMODE.EQ.1.AND.RECORD(I).LT.ADEP) T12(I)=-4.
      IF(JMODE.EQ.1.AND.RECORD(I).GE.ADEP)T12(I)=ALOG10(RECORD(I))-EDEP
      ELSE
      IF(I.LE.IPEAK)P(I)=V(I)*DB(I)/VB(I)
      IF(I.GT.IPEAK) P(I)=V(I)*(COSH(WK(I)*4.333)/SINH(WK(I)*DEPTH))**2
      IF(JMODE.EQ.1.AND.DB(I).LT.ADEP) T12(I)=-4.
      IF(JMODE.EQ.1.AND.DB(I).GE.ADEP)T12(I)=ALOG10(DB(I))-EDEP
      END IF
      IF(JMODE.EQ.1) THEN
      IF(P(I).LT.ADEP) D(I)=-4.
      IF(PB(I).LT.ADEP) T33(I)=-4.
      IF(P(I).GE.ADEP) D(I)=ALOG10(P(I))-EDEP
      IF(PB(I).GE.ADEP) T33(I)=ALOG10(PB(I))-EDEP
      END IF
      IF(I.LT.L1.AND.I.GT.NH5) GO TO 5031
      IF(P(I).LT.VLARGE) GO TO 5031
      VLARGE=P(I)
      II=I
 5031 CONTINUE
      PEAKF=FREQ(II)
      IF(JMODE.EQ.2) GO TO 7060
      IF(MODE.EQ.1) THEN
      B=.0
      ESDB=.0
      DO 5066 I=L1,IDPEAK
      ESDB=ESDB+P(I)
 5066 B=B+(P(I)-PB(I))**2
      ERR2=100.*SQRT(B)/ESDB
      CALL SYMBEL(.504,.65,.0,.11,2,LZ5)
      CALL SYMBEL(.517,.62,.0,.08,4,LX22)
      CALL SYMBEL(.55,.65,.0,.1,10,LX24)
      CALL NUMBER(.561,.65,.0,.088,5,ERR2)
      END IF
      CALL POINTS
      CALL LINE(FREQ,T12,17,NH1)
      CALL PLOT(.47,-1.29,1,17)
```

```
      CALL DASHES
      CALL LINE(FREQ,T33,0,NH1)
      XL(1)=.452
      XL(2)=.482
      YL(1)=-2.4
      YL(2)=-2.4
      CALL VECTORS
      CALL LINE(XL,YL,0,2)
      CALL LINE(FREQ,B,0,NH1)
      CALL SYMBOL(-.08,-4.,90.,.15,24,LY8)
      CALL SYMBOL(.18,-4.68,0.0,0.15,15,LX)
      IF(EDEP.LT.1.) CALL NUMBER(-.07,-4.05,.0,.1,6,.0001)
      IF(EDEP.LT.1.) CALL NUMBER(-.07,-3.05,.0,.1,5,.001)
      IF(EDEP.LT.1.) CALL NUMBER(-.07,-2.05,.0,.1,5,.010)
      IF(EDEP.LT.1.) CALL NUMBER(-.07,-1.05,.0,.1,5,.100)
      IF(EDEP.LT.1.) CALL NUMBER(-.07,-.05,.0,.1,5,1.00)
      IF(EDEP.LT.1.) CALL NUMBER(-.07,.95,.0,.1,5,10.0)
      IF(EDEP.GE.1.) CALL NUMBER(-.07,-4.05,.0,.1,5,.010)
      IF(EDEP.GE.1.) CALL NUMBER(-.07,-3.05,.0,.1,5,.100)
      IF(EDEP.GE.1.) CALL NUMBER(-.07,-2.05,.0,.1,5,1.00)
      IF(EDEP.GE.1.) CALL NUMBER(-.07,-1.05,.0,.1,5,10.0)
      IF(EDEP.GE.1.) CALL NUMBER(-.07,-.05,.0,.1,5,100.)
      IF(EDEP.GE.1.) CALL NUMBER(-.07,.95,.0,.1,6,1000.)
      IF(NOTE.EQ.1) CALL SYMBEL(.36,1.3,.0,.15,20,ST)
      IF(NOTE.EQ.2) CALL SYMBEL(.36,1.3,.0,.15,20,ST2)
      CALL SYMBEL(.46,-.55,.0,.09,18,LX11)
      CALL NUMBER(.615,-.55,.0,.09,6,PEAKF)
      CALL SYMBEL(.46,-.95,.0,.09,15,LY11)
      CALL NUMBER(.59,-.95,.0,.09,6,VLARGE)
      CALL SYMBOL(.495,-1.35,.0,.09,9,LX9)
      CALL SYMBOL(.45,-1.76,.0,.09,3,LX10)
      CALL SYMBOL(.495,-1.76,.0,.09,8,LX8)
      CALL SYMBOL(.54,-2.06,.0,.09,8,LX6)
      CALL SYMBOL(.495,-2.46,.0,.09,4,LX14)
      CALL SYMBOL(.553,-2.46,.0,.09,10,LY9)
      CALL SYMBOL(.54,-2.76,.0,.09,8,LX6)
      CALL SYMBEL(.46,-3.16,.0,.09,16,LX2)
      CALL SYMBOL(.496,-3.46,.0,.09,15,M)
      CALL TEKPAUS
C
C ***************************************************************************
C *---PART IX: DRAWING DIRECTIONAL SPECTRUM IN THREE DIMENSION SPACE---      *
C ***************************************************************************
C  ---THIS PART WILL BE MORE FLEXIBLE AS APPLIED TO SMOOTHED DIRECTIONAL SPECTRUM---
 7060 CONTINUE
C  ---THE FOLLOWING 137 LINE CAN BE DELETED IF IT IS NOT INTENDED TO HAVE---
C
C
      IF(MODE.EQ.2.OR.JMODE.EQ.2) GO TO 7057
      BDEP=.01
      IF(MODE.EQ.1.AND.DEPTH.LT.140.) BDEP=1.
      CALL ERASE
      IF(MODE.EQ.1) CALL SCALE(8.3,.76,1.1,1.,.0,-2.)
      DO 7058 I=1,NH2
      COSDA=COS((DDMEAN-D1(I))/2.)**2
      TEMP=ALOG10(COSDA)*S1(I)
      IF(TEMP.GE.-120.) T12(I)=PB(I)*T13(I)/CP1*COSDA**S1(I)
      IF(TEMP.LT.-120.) T12(I)=PB(I)*T13(I)/CP1*1.E-120
      IF(MODE.EQ.1) T12(I)=T12(I)*100.
      IF(T12(I).LT.BDEP) THEN
      T12(I)=-2.
      ELSE
      T12(I)=ALOG10(T12(I))
      IF(BDEP.GE..5) T12(I)=T12(I)-2.
      END IF
 7058 CONTINUE
      XL(1)=.498
      XL(2)=.528
      YL(1)=.1
      YL(2)=.1
      IF(MODE.EQ.3) THEN
      CALL SYMBEL(-.05,3.65,.0,.18,17,LY2)
      CALL SYMBOL(.18,-2.68,.0,.15,15,LX)
      CALL NUMBER(-.088,2.95,.0,.1,7,1000.0)
      CALL NUMBER(-.088,1.95,.0,.1,7,100.00)
      CALL NUMBER(-.088,.95,.0,.1,7,10.000)
      CALL NUMBER(-.088,-.05,.0,.1,7,1.0000)
      CALL NUMBER(-.088,-1.05,.0,0.1,7,.1000)
      CALL NUMBER(-.088,-2.05,.0,.1,7,0.0100)
      ELSE
      CALL SYMBEL(-.05,3.65,.0,.18,18,LX1)
      CALL SYMBOL(.18,-2.68,.0,.15,15,LX)
      IF(BDEP.LT..5) CALL NUMBER(-.07,-2.05,.0,.1,6,.0001)
      IF(BDEP.LT..5) CALL NUMBER(-.07,-1.05,.0,.1,5,.001)
      IF(BDEP.LT..5) CALL NUMBER(-.07,-.05,.0,.1,5,.010)
```

```
      IF(BDEP.LT..5) CALL NUMBER(-.07,.95,.0,.1,5,.100)
      IF(BDEP.LT..5) CALL NUMBER(-.07,1.95,.0,.1,5,1.00)
      IF(BDEP.LT..5) CALL NUMBER(-.07,2.95,.0,.1,5,10.0)
      IF(BDEP.GE..5) CALL NUMBER(-.07,-2.05,.0,.1,5,.010)
      IF(BDEP.GE..5) CALL NUMBER(-.07,-1.05,.0,.1,5,.100)
      IF(BDEP.GE..5) CALL NUMBER(-.07,-.05,.0,.1,5,1.00)
      IF(BDEP.GE..5) CALL NUMBER(-.07,.95,.0,.1,5,10.0)
      IF(BDEP.GE..5) CALL NUMBER(-.07,1.95,.0,.1,5,100.)
      IF(BDEP.GE..5) CALL NUMBER(-.07,2.95,.0,.1,6,1000.)
      CALL SYMBOL(.504,1.67,.0,.09,12,LY23)
      CALL NUMBER(.495,1.37,.0,.085,4,4.3)
      CALL SYMBEL(.511,1.37,.0,.09,24,LY12)
      END IF
      CALL AXISL(.0,.6,.0,-2.,3.,-2.,.1,1.,1,0,1,0,1.,1.,.1,0)
      CALL LINE(FREQ,T12,0,NH2)
      CALL LINE(XL,YL,0,2)
      CALL SYMBOL(.393,2.6,.0,.15,9,LX)
      CALL SYMBOL(.594,2.6,.0,.15,8,LX6)
      CALL SYMBOL(.393,2.07,.0,.15,2,LZ2)
      CALL SYMBOL(.4515,2.07,.0,.15,14,LY14)
      CALL SYMBOL(.54,.04,.0,.09,8,LX8)
      CALL SYMBOL(.585,-.26,.0,.09,8,LX6)
      CALL SYMBEL(.504,-.66,.0,.09,16,LX2)
      CALL SYMBOL(.54,-.96,.0,.09,15,M)
      CALL SYMBEL(.504,-1.36,.0,.09,18,LY14)
      CALL NUMBER(.585,-1.66,.0,.085,6,DM)
      CALL SYMBOL(.648,-1.57,.0,.06,1,LZ4)
      CALL TEKPAUS
      CALL ERASE
C
      IF(MODE.EQ.1) IPNOW=IPEAK
      IF(MODE.EQ.3) IPNOW=IIPEAK
      DO 7059 I=1,120
      C=FLOAT(I)*3.*RN-CPI
      COSDA=COS((C-D1(IPNOW))/2.)**2
      TEMP=ALOG10(COSDA)*S1(IPNOW)
      IF(TEMP.GE.-120.) T12(I)=VLARGE*T13(IPNOW)/CPI*COSDA**S1(IPNOW)
      IF(TEMP.LT.-120.) T12(I)=VLARGE*T13(IPNOW)/CPI*1.E-120
      IF(MODE.EQ.1) T12(I)=T12(I)*100.
      T33(I)=FLOAT(I)/300.
      IF(T12(I).LT.BDEP) THEN
      T12(I)=-2.
      ELSE
      T12(I)=ALOG10(T12(I))
      IF(BDEP.GE..5) T12(I)=T12(I)-BDEP
      END IF
7059  CONTINUE
      IF(MODE.EQ.3) THEN
      CALL SYMBEL(-.05,3.65,.0,.18,17,LY2)
      CALL NUMBER(-.088,2.95,.0,.1,7,1000.0)
      CALL NUMBER(-.088,1.95,.0,.1,7,100.00)
      CALL NUMBER(-.088,.95,.0,.1,7,10.000)
      CALL NUMBER(-.088,-.05,.0,.1,7,1.0000)
      CALL NUMBER(-.088,-1.05,.0,0.1,7,.1000)
      CALL NUMBER(-.088,-2.05,.0,.1,7,0.0100)
      ELSE
      CALL SYMBEL(-.05,3.65,.0,.18,18,LX1)
      IF(BDEP.LT..5) CALL NUMBER(-.07,-2.05,.0,.1,6,.0001)
      IF(BDEP.LT..5) CALL NUMBER(-.07,-1.05,.0,.1,5,.001)
      IF(BDEP.LT..5) CALL NUMBER(-.07,-.05,.0,.1,5,.010)
      IF(BDEP.LT..5) CALL NUMBER(-.07,.95,.0,.1,5,.100)
      IF(BDEP.LT..5) CALL NUMBER(-.07,1.95,.0,.1,5,1.00)
      IF(BDEP.LT..5) CALL NUMBER(-.07,2.95,.0,.1,5,10.0)
      IF(BDEP.GE..5) CALL NUMBER(-.07,-2.05,.0,.1,5,.010)
      IF(BDEP.GE..5) CALL NUMBER(-.07,-1.05,.0,.1,5,.100)
      IF(BDEP.GE..5) CALL NUMBER(-.07,-.05,.0,.1,5,1.00)
      IF(BDEP.GE..5) CALL NUMBER(-.07,.95,.0,.1,5,10.0)
      IF(BDEP.GE..5) CALL NUMBER(-.07,1.95,.0,.1,5,100.)
      IF(BDEP.GE..5) CALL NUMBER(-.07,2.95,.0,.1,6,1000.)
      CALL SYMBOL(.504,1.67,.0,.09,12,LY23)
      CALL NUMBER(.495,1.37,.0,.085,4,4.3)
      CALL SYMBEL(.511,1.37,.0,.09,24,LY12)
      END IF
      CALL AXISL(.0,.4,.0,-2.,3.,-2.,.05,1.,1,0,0,0,1.,1.,.1,0)
      CALL LINE(T33,T12,0,120)
      CALL LINE(XL,YL,0,2)
      CALL SYMBOL(-.006,-2.26,.0,.11,1,LX4)
      CALL SYMBOL(.094,-2.26,.0,.11,1,LY4)
      CALL SYMBOL(.194,-2.26,.0,.11,1,LX3)
      CALL SYMBOL(.294,-2.26,.0,.11,1,LY3)
      CALL SYMBOL(.394,-2.26,.0,.11,1,LX4)
      CALL SYMBOL(.09,-2.72,.0,.15,9,LX5)
      CALL SYMBOL(.294,-2.72,.0,.15,8,LX23)
      CALL SYMBOL(.336,2.6,.0,.15,11,LX5)
      CALL SYMBOL(.5646,2.6,.0,.15,8,LX6)
```

```
      CALL SYMBOL(.336,2.07,.0,.15,2,LZ2)
      CALL SYMBOL(.3945,2.07,.0,.15,18,LY24)
      CALL SYMBOL(.54,.04,.0,.09,8,LX8)
      CALL SYMBOL(.585,-.26,.0,.09,8,LX6)
      CALL SYMBEL(.504,-.66,.0,.09,16,LX2)
      CALL SYMBOL(.54,-.96,.0,.09,15,M)
      CALL SYMBEL(.504,-1.36,.0,.09,22,LY24)
      CALL NUMBER(.6,-1.66,.0,.085,6,PEAKF)
      CALL SYMBOL(.678,-1.66,.0,.088,2,LZ3)
      CALL TEKPAUS
 7057 CONTINUE
C
C
      CALL ERASE
      CALL SCALE(17.4,16.,.42,.42,.0,.0)
      PRINT 7069
      READ*, JMODE
      GO TO (7068,7068,7071,7072) JMODE
 7068 PRINT 7061, MODE
 7061 FORMAT(1X/"*****INPUT CONSTANT, CMODE, FOR RANGING THE CONTOURS."/
     1"-----CMODE=1. WILL COVER 1,4,10,40,100,400,700,1000."/"-----CMODE
     1 IS THE VALUE 10**INTEGER, RANGE: (1,4....,1000)*CMODE."/"-----FOR
     1 EXAMPLE: CMODE=.1 COVERS (.1,.4,1,4,...,100)."/"-----GUIDE: CMODE
     1=.1,1.,10. RESPECT TO MODE=1,2,3. MODE=",I1," NOW.")
      READ*,CMODE
      PRINT 800
  800 FORMAT(/"*****INPUT ANGULAR INTERVAL (DEG.) FOR ITERATIVE COMPUTAT
     1ION." /"-----GUIDE: 4 FOR ROUGH DRAW, OR LESS FOR SHARP VIEW.")
      READ*,NH3
      VLARGE=.002+.0002*NH3
      R=.0
      SUM=.0
      ALL=.0
      PRINT 7074
 7074 FORMAT(1X/"*****INPUT NUMBER OF POINT-INCREMENT IN FREQUENCY INDEX
     1."/"-----E.G. INPUT 3 WILL SKIP 2 POINTS, ETC."/"-----GUIDE: INPUT
     1 1 FOR N.LE.256, INPUT (N/256)*2 FOR N.GT.256.")
      READ*,NH4
      FREQ2=FLOAT(NH4)*FREQ1
      CALL ERASE
      CALL ORIGIN(3.03,2.83)
      DO 7070 I=2,NH2,NH4
      IF(JMODE.EQ.1) THEN
      T12(I)=T13(I)/CMODE/CPI*PB(I)
      ELSE
      T33(I)=T23(I)/CMODE/CPI*P(I)
      IF(I.GE.L1.AND.I.LE.IDPEAK) T12(I)=T13(I)/CMODE/CPI*PB(I)
      END IF
 7070 CONTINUE
C  ---P(I) IS THE PROPOSED JONSWAP SPECTRUM, AND PB(I) IS THE SMOOTHED DATA---
      MIN=INT(DMEAN)-90
      MAX=2*INT(DMEAN)-MIN
C
      DO 7065 J=MIN,MAX,NH3
      C=FLOAT(J)
      BIG=C*RN
      COSJ=COS(BIG)
      SINJ=SIN(BIG)
      ESDA=1.E-7
      DO 200 JJ=1,7
  200 IXY(JJ)=0
C
      IF(JMODE.EQ.2.AND.JUMP.EQ.2) COSDA=COS((BIG-DMEAN)/2.)**2
      DO 7066 I=2,NH2,NH4
      IF(JMODE.EQ.1.OR.JUMP.EQ.1) COSDA=COS((BIG-D1(I))/2.)**2
      IF(JMODE.EQ.2.AND.JUMP.EQ.3) COSDA=COS((BIG-D2(I))/2.)**2
      IF(JMODE.EQ.1) THEN
      TEMP=ALOG10(COSDA)*S1(I)
      IF(TEMP.GE.-120.) ESDB=T12(I)*COSDA**S1(I)
      IF(TEMP.LT.-120.) ESDB=T12(I)*1.E-120
      ELSE
      TEMP=ALOG10(COSDA)*S2(I)
      IF(TEMP.GE.-120.) ESDB=T33(I)*COSDA**S2(I)
      IF(TEMP.GE.-120..AND.I.GE.L1.AND.I.LE.IDPEAK) L2=10
      IF(L2.EQ.10) BOXX=COS((BIG-D1(I))/2.)**2
      IF(L2.EQ.10) SUM=SUM+(ESDB-T12(I)*BOXX**S1(I))**2
      IF(TEMP.LT.-120.) ESDB=T33(I)*1.E-120
      END IF
      ALL=ALL+ESDB
      IF(ESDA.LT.1..AND.ESDB.LT.1.) GO TO 7066
      IF(ESDA.GT.1000..AND.ESDB.GT.1000.) GO TO 7066
      IF(I.LT.IPEAK-10.OR.I.GT.IPEAK+10) GO TO 700
      IF(C.LT.DMEAN-20..OR.C.GT.DMEAN+20.) GO TO 700
      IF(ESDB.GT.R) THEN
      R=ESDB
```

```
      L3=I
      CC=C
      END IF
C  ---WHERE ESDB IS THE DISCRETE DIRECTIONAL SPECTRUM OF INTERESTED WAVE PROPERTY---
  700 L00=INT(ESDA)
      L11=INT(ESDB)
      IF(L00.GE.1.AND.L00.LE.4) THEN
      L00=1
      ELSE IF(L00.GE.5.AND.L00.LE.9) THEN
      L00=2
      ELSE IF(L00.GE.10.AND.L00.LE.49) THEN
      L00=3
      ELSE IF(L00.GE.50.AND.L00.LE.99) THEN
      L00=4
      ELSE IF(L00.GE.100.AND.L00.LE.499) THEN
      L00=5
      ELSE IF(L00.GE.500.AND.L00.LE.999) THEN
      L00=6
      ELSE IF(L00.GE.1000) THEN
      L00=7
      END IF
      IF(L11.GE.1.AND.L11.LE.4) THEN
      L11=1
      ELSE IF(L11.GE.5.AND.L11.LE.9) THEN
      L11=2
      ELSE IF(L11.GE.10.AND.L11.LE.49) THEN
      L11=3
      ELSE IF(L11.GE.50.AND.L11.LE.99) THEN
      L11=4
      ELSE IF(L11.GE.100.AND.L11.LE.499) THEN
      L11=5
      ELSE IF(L11.GE.500.AND.L11.LE.999) THEN
      L11=6
      ELSE IF(L11.GE.1000) THEN
      L11=7
      END IF
      LLL=L11
      L2=1
      IF(L11-L00) 10,7066,20
   10 L11=L00
      L00=LLL
      L2=0
   20 L00=L00+1
      IF(L11.GT.11) L11=11
      DO 100 K=L00,L11
      IF(K.EQ.1.OR.K.EQ.3.OR.K.EQ.5.OR.K.EQ.7) KMODE=10**(K/2)
      IF(K.EQ.2.OR.K.EQ.4.OR.K.EQ.6) KMODE=5.*10**(K/2-1)
      TEMP=FREQ(I)-ABS((KMODE-ESDB)/(ESDA-ESDB))*FREQ2
      K1=IXY(K)+1
      IF(K1.GT.14) GO TO 100
      K2=1
      IF(XX(K,K1,1).NE.1.) K2=2
      XX(K,K1,K2)=TEMP*COSJ
      YY(K,K1,K2)=TEMP*SINJ
C  ---K: "MEMORY CODE" FOR TRACING THE RELATIVE CONTOURS---
C  ---K1: "ORDER CODE" FOR CONNECTING PRESENT(I) & LAST(I-1)-RUN CONTOUR LOCATION---
C  ---K2: "ITERATION CODE", K2=1 FOR LAST-RUN, K2=2 FOR PRESENT RUN---
      IXY(K)=K1
      IF(K2.NE.2) GO TO 100
   30 XL(1)=XX(K,K1,1)
      XL(2)=XX(K,K1,2)
      YL(1)=YY(K,K1,1)
      YL(2)=YY(K,K1,2)
      X12=SQRT(XL(2)*XL(2)+YL(2)*YL(2))-SQRT(XL(1)*XL(1)+YL(1)*YL(1))
      IF(ABS(X12).LT.VLARGE) GO TO 300
      IF(X12) 40,300,50
   40 DO 60 L=13,K1,-1
      XX(K,L+1,1)=XX(K,L,1)
   60 YY(K,L+1,1)=YY(K,L,1)
      XX(K,K1,1)=XX(K,K1,2)
      YY(K,K1,1)=YY(K,K1,2)
      GO TO 30
   50 MM=K1+1
      DO 70 II=MM,14
      XL(1)=XX(K,II,1)
      IF(XL(1).EQ.1.) GO TO 400
      YL(1)=YY(K,II,1)
      X12=SQRT(XL(2)*XL(2)+YL(2)*YL(2))-SQRT(XL(1)*XL(1)+YL(1)*YL(1))
      IF(ABS(X12).LT.VLARGE) THEN
      DO 80 LL=1,13
      XX(K,K1+LL,1)=XX(K,II+LL,1)
      YY(K,K1+LL,1)=YY(K,II+LL,1)
      IF(II+LL.GE.14) XX(K,14,1)=1.
   80 IF(XX(K,K1+LL,1).EQ.1.) GO TO 300
      END IF
   70 CONTINUE
```

```
      GO TO 400
  300 IF(L2.EQ.1) GO TO 90
      IF(I.LE.L1) GO TO 90
      L5=J-60
      L4=J-15
      NH5=J+25
      IF(L5.LT.NH3.AND.L5.GE.0) GO TO 91
      IF(L4.LT.NH3.AND.L4.GE.0) GO TO 91
      IF(NH5.LT.NH3.AND.NH5.GE.0) GO TO 91
      GO TO 90
   91 VALUE=FLOAT(KMODE)*CMODE
      IF(K.EQ.2.OR.K.EQ.4.OR.K.EQ.6) IPNOW=1
      IF(IPNOW.EQ.1.AND.FREQ(I).LT..12.AND.ABS(C-D1(I)*DEGREE).LT
     1.17.) GO TO 90
      X=XL(2)-.0025
      Y=YL(2)-.0015
      Y1=YL(2)-.006
      INTO=INT(VALUE)
      IF(INTO.GE.1) THEN
      IF(INTO.EQ.1) CALL SYMBOL(X,Y,.0,.06,1,LZ)
      IF(INTO.EQ.5) CALL SYMBOL(X,Y1,.0,.06,1,LZ1)
      IF(INTO.EQ.10) CALL SYMBOL(X,Y,.0,.06,2,LZ)
      IF(INTO.EQ.50) CALL SYMBOL(X,Y1,.0,.06,2,LZ1)
      IF(INTO.EQ.100) CALL SYMBOL(X,Y,.0,.06,3,LZ)
      IF(INTO.EQ.500) CALL SYMBOL(X,Y1,.0,.06,3,LZ1)
      GO TO 400
      END IF
      NUM=INT(ABS(ALOG10(VALUE*1.2)))+3
      X=X-.001
      IF(IPNOW.EQ.1) Y=Y1
      CALL NUMBER(X,Y,.0,.06,NUM,VALUE)
      GO TO 400
   90 CALL LINE(XL,YL,0,2)
  400 XX(K,K1,1)=XX(K,K1,2)
      YY(K,K1,1)=YY(K,K1,2)
  100 CONTINUE
 7066 ESDA=ESDB
      DO 500 K=1,7
      KK=IXY(K)+1
      DO 500 K1=KK,14
      XX(K,K1,1)=1.
  500 CONTINUE
 7065 CONTINUE
      DO 600 K=1,7
      KK=IXY(K)
      DO 600 K1=1,KK
      XX(K,K1,1)=1.
  600 CONTINUE
      INTO=2
      C=FREQ(L3)
      X=C*COS(CC*RN)
      Y=C*SIN(CC*RN)
      CC=90.-CC
      SUM=100.*SQRT(SUM)/ALL
      ALL=ALL*FREQ2*NH4*RN*CMODE
      B=B*CMODE
      TEMP=90.-DII
      CALL SYMBOL(X,Y,.0,.05,1,LY10)
      CALL SYMBEL(.0,-.0045,TEMP,.09,25,LY13)
      CALL SYMBOL(.138,.095,0.,.18,8,LY6)
      IF(MODE.EQ.1) THEN
      CALL SYMBEL(.158,.07,.0,.18,18,LX1)
      CALL SYMBEL(.168,-.038,.0,.105,5,LX21)
      CALL SYMBEL(.172,-.04,.0,.08,4,LX22)
      CALL SYMBEL(.186,-.038,.0,.08,20,LY21)
      CALL NUMBER(.19,-.038,.0,.08,6,ALL)
      END IF
      IF(MODE.EQ.2) CALL SYMBEL(.158,.07,.0,.18,15,LY)
      IF(MODE.EQ.3) THEN
      CALL SYMBEL(.158,.07,.0,.18,17,LY2)
      CALL SYMBEL(.168,-.038,.0,.08,15,LX20)
      CALL NUMBER(.222,-.038,.0,.08,7,ALL)
      ELSE
      CALL SYMBOL(.165,.053,.0,.08,12,LY23)
      CALL SYMBEL(.167,.041,.0,.08,25,LY12)
      CALL NUMBER(.16,.041,.0,.077,4,4.3)
      END IF
 7062 CALL AXISL(-.15,.15,0.,-.15,.15,0.,.05,.05,0,0,0,0,1.,1.,.1,0)
      CALL CIRCLE(0.,0.,0.,90.,.15,.15,.1)
      CALL CIRCLE(0.,0.,98.,180.,.15,.15,.1)
      CALL CIRCLE(0.,0.,185.,261.,.15,.15,.1)
      CALL CIRCLE(0.,0.,290.,355.,.15,.15,.1)
      CALL SYMBOL(.159,-.006,.0,.2,1,LX3)
      CALL SYMBOL(-.168,-.006,.0,.2,1,LX4)
      CALL SYMBOL(-.0038,.158,0.,.2,1,LY3)
      CALL SYMBOL(-.0038,-.171,.0,.2,1,LY4)
```

```
      CALL SYMBOL(.11,.12,0.,.18,11,LX5)
      CALL NUMBER(.131,-.01,0.,.1,4,.15)
      CALL NUMBER(-.157,-.01,0.,.1,4,.15)
      CALL NUMBER(-.022,-.01,.0,.107,4,.00)
      CALL NUMBER(-.024,.145,0.,.1,4,.15)
      CALL NUMBER(-.024,-.150,0.,.1,4,.15)
      CALL SYMBOL(.0043,-.151,0.,.1,14,LX)
      IF(NOTE.EQ.1) CALL SYMBEL(.08,.158,.0,.15,20,ST)
      IF(NOTE.EQ.2) CALL SYMBEL(.08,.158,.0,.15,20,ST2)
      IF(INTO.EQ.1) GO TO 6072
      IF(JMODE.EQ.1) THEN
      CALL SYMBOL(.168,-.055,.0,.08,8,LX8)
      ELSE
      CALL SYMBEL(.18,-.021,.0,.11,2,LZ5)
      CALL SYMBEL(.184,-.023,.0,.08,4,LX22)
      CALL SYMBEL(.201,-.021,.0,.09,10,LX24)
      CALL NUMBER(.205,-.021,.0,.08,5.SUM)
      CALL SYMBOL(.168,-.055,.0,.08,10,LY19)
      END IF
      CALL SYMBOL(.19,-.065,.0,.08,8,LX6)
      CALL SYMBEL(.1418,-.1038,.0,.08,25,LX12)
      CALL SYMBEL(.1789,-.1166,.0,.08,25,LY12)
      CALL NUMBER(.1645,-.1166,.0,.075,6,H1)
      CALL SYMBEL(.194,-.1276,.0,.08,19,LX13)
      CALL NUMBER(.1653,-.1276,.0,.075,6,PII)
      CALL NUMBER(.215,-.1276,.0,.075,6,DII)
      CALL SYMBOL(.154,-.1422,.0,.05,1,LY10)
      CALL SYMBEL(.168,-.1426,.0,.08,15,LY11)
      CALL NUMBER(.219,-.1426,.0,.08,7,B)
      CALL NUMBER(.1653,-.1536,.0,.075,6,C)
      CALL NUMBER(.212,-.1536,.0,.075,6,CC)
      CALL SYMBEL(.194,-.1536,.0,.08,15,LZ3)
      CALL SYMBEL(.168,-.08,.0,.08,16,LX2)
      CALL SYMBOL(.18,-.0908,.0,.08,15,H)
      CALL TEKPAUS
      CALL ERASE
      PRINT 7069
 7069 FORMAT(/"========================================"/
     1      /     /"=====INPUT 1 TO DRAW AN SMOOTHED SPECTRUM,"/"=====OR
     1 INPUT 2 TO DRAW A PROPOSED SPECTRUM,"/"=====OR INPUT 3 TO EXECUTE
     1 THE PROGRAM IN OTHER MODE."    /"=====OR INPUT 4 TO TERMINATE THE
     1 EXECUTION OF THIS PROGRAM.")
      READ*, JMODE
      GO TO (7068,7068,7071,7072) JMODE
 7071 PRINT 5032
 5032 FORMAT(/"========================================"/
     1      /    /"=====INPUT MODE CODE,"/"-----MODE=1 RUN A HORIZONTAL
     1 VELOCITY SPECTRUM (4.3' ABOVE SEA FLOOR)"/"-----MODE=2 RUN A HORI
     1ZONTAL AMPLITUDE SPECTRUM (4.3' ABOVE SEA FLOOR)"/ "-----MODE=3 WI
     1LL RUN A WAVE ENERGY SPECTRUM AT SEA SURFACE,  "/"-----MODE=4 WILL
     1 TERMINATE THE PROGRAM.")
      READ*, MODE
      IF(MODE.NE.4) GO TO 5048
      STOP
 7072 END
C
C ***************************************************************************
C *---PART X: COLLECTION OF SUBROUTINES AND BLOCK DATA---                     *
C ***************************************************************************
      SUBROUTINE TRANS(DEPTH,H1,MH)
      COMMON /DATA10/ FREQ(720),T13(720),T23(720),WP(720),WK(720),FREQ1
     1,FREQ2,ALFA,GA,PEAKF,LL,IPEAK,IIPEAK,IIIPEAK,K,A1,ICPEAK,L1
      FREQ3=FREQ2/6.
C  ---FREQ3(HZ) CIRCUMSCRIBES SHALLOW WATERWAVES---
      WK(MH+1)=.1
      H2=H1+3.4167
C  ---3.4167(FT) IS THE DISTANCE BETWEEN CURRENT-METER AND PRESSURE GAUGE---
      DO 130 I=MH,1,-1
      FREQ(I)=FLOAT(I)*FREQ1
      IF(FREQ(I).GT.FREQ2) THEN
      WK(I)=FREQ(I)*FREQ(I)*1.2270286
C  ---1.2270286=(CPI2)**2/32.174---
      WP(I)=.0058855*COSH(WK(I)*H2)/COSH(WK(I)*H1)/FREQ(I)
C  ---.0058855=(UNIT WEIGHT OF SEA WATER)/CPI2=(64./12**3 PSI)/CPI2---
      ELSE IF(FREQ(I).LE.FREQ3) THEN
      WK(I)=FREQ(1)*SQRT(1.2270286/DEPTH)
      WP(I)=.0058855*WK(I)*DEPTH/FREQ(I)
      ELSE
C  ---CONSIDER THE INTERMEDIATE WATER CONDITION---
      XX=WK(I+1)*DEPTH
      WH=FREQ(I)*FREQ(I)*DEPTH*1.2270286
      TANHH=TANH(XX)
      DO 170 J=1,10
      DH=(WH-XX*TANHH)/(TANHH+XX/COSH(XX)**2)
      XX=DH+XX
      TANHH=TANH(XX)
      IF(ABS(DH/XX).LT..005) GO TO 150
```

```
  170 CONTINUE
  150 WK(I)=XX/DEPTH
      WK(I)=XX/DEPTH
      WP(I)=.0058855*TANHH*COSH(WK(I)*H2)/COSH(WK(I)*H1)/FREQ(I)
      END IF
  130 CONTINUE
      RETURN
      END
C
      SUBROUTINE SMOOTH(NN,S2,S1,MH,ICPEAK,MOD)
      DIMENSION S1(MH),S2(MH)
C  ---USING BARTLETT WINDOW: I=2M/3, BASEWIDTH=2/M (HZ)------
C     N(SEC)   M(SEC)   D.O.F.   80% C.I.
C      256      128       6      (.58)(2.6)
C      512      128      12      (.65)(1.8)
C     1024      128      24      (.72) (1.5)
      IF(NN.GE.1024) MOD=4
      S2(1)=(S1(1)+S1(2))/2.
      S2(MH)=(S1(MH-1)+S1(MH))/2.
      GO TO (5,20,40,70) MOD
    5 S2(2)=(S1(1)+S1(3))/3.25+S1(2)/2.6
      S2(3)=(S1(2)+S1(4))/3.25+S1(3)/2.6
      NS=MH-3
      IF(NN.EQ.512) THEN
      DO 10 I=4,NS
   10 S2(I)=(S1(I-3)+S1(I+3))/36.+(S1(I-2)+S1(I+2))/9.+(S1(I-1)+S1(I+1))
     1/4.5+S1(I)/3.6
      S2(NS+1)=(S1(NS)+S1(NS+2))/3.25+S1(NS+1)/2.6
      S2(MH-1)=(S1(MH-2)+S1(MH))/3.25+S1(MH-1)/2.6
      ELSE
      NS=MH-1
      DO 11 I=2,NS
   11 S2(I)=(S1(I-1)+S1(I+1))/4.5+S1(I)/1.8
      END IF
      RETURN
   20 NS=MH-1
      DO 30 I=2,NS
   30 S2(I)=S1(I-1)*.2+S1(I)*.6+S1(I+1)*.2
      RETURN
   40 NS=ICPEAK-1
      DO 50 I=2,NS
   50 S2(I)=S1(I-1)*.2+S1(I)*.6+S1(I+1)*.2
      NS=ICPEAK+1
      II=MH-1
      DO 60 I=NS,II
   60 S2(I)=S1(I-1)*.2+S1(I)*.6+S1(I+1)*.2
      S2(ICPEAK)=S1(ICPEAK)
      RETURN
   70 S2(2)=(S1(1)+S1(3))/3.05+S1(2)/2.9
      S2(3)=(S1(1)+S1(5))/5.625+(S1(2)+S1(4))/4.737+S1(3)/4.5
      S2(4)=(S1(2)+S1(6))/5.625+(S1(3)+S1(5))/4.737+S1(4)/4.5
      S2(5)=(S1(3)+S1(7))/5.625+(S1(4)+S1(6))/4.737+S1(5)/4.5
      S2(6)=(S1(4)+S1(8))/5.625+(S1(5)+S1(7))/4.737+S1(6)/4.5
      NS=MH-6
      DO 80 I=7,NS
   80 S2(I)=(S1(I-6)+S1(I+6))*.0125+(S1(I-5)+S1(I+5))*.0306+
     1(S1(I-4)+S1(I+4))*.0562+(S1(I-3)+S1(I+3))*.0853+
     1(S1(I-2)+S1(I+2))*.1123+(S1(I-1)+S1(I+1))*.1318+S1(I)*.1388
      S2(NS+1)=(S1(NS-1)+S1(NS+3))/5.625+(S1(NS)+S1(NS+2))/4.737
     1+S1(NS+1)/4.5
      S2(NS+2)=(S1(NS)+S1(NS+4))/5.625+(S1(NS+1)+S1(NS+3))/4.737
     1+S1(NS+2)/4.5
      S2(NS+3)=(S1(NS+1)+S1(NS+5))/5.625+(S1(NS+2)+S1(NS+4))/4.737
     1+S1(NS+3)/4.5
      S2(NS+4)=(S1(NS+2)+S1(MH))/5.625+(S1(NS+3)+S1(NS+5))/4.737
     1+S1(NS+4)/4.5
      S2(NS+5)=(S1(NS+4)+S1(MH))/3.05+S1(NS+5)/2.9
      RETURN
      END
C
      SUBROUTINE LSM(AIM,X,MAX)
      COMMON /DATA10/ FREQ(720),T13(720),T23(720),WP(720),WK(720),FREQ1
     1,FREQ2,ALFA,GA,PEAKF,LL,IPEAK,IDPEAK,IIPEAK,K,A1,ICPEAK,L1
      Z1=.0
      Z2=.0
      IA=LL
      IB=K
      IF(MAX.EQ.1) IB=IIPEAK
      IF(MAX.EQ.2) IA=IIPEAK
      DO 10 I=IA,IB
      BATA=(1./EXP(((FREQ(I)-PEAKF)/PEAKF/X)**2/26.))**13
      TEMP=GA**BATA
      C=BATA*TEMP*(FREQ(I)-PEAKF)**2
      Z1=Z1+T13(I)*C*TEMP
   10 Z2=Z2+T23(I)*C
      AIM=ALFA*Z1-Z2
      RETURN
      END
```

```
C
      SUBROUTINE LST(AIM,X,M)
      DIMENSION P(720)
      COMMON /DATA10/ FREQ(720),T13(720),T23(720),UP(720),UK(720),FREQ1
     1,FREQ2,ALFA,GA,PEAKF,LL,IPEAK,IDPEAK,IIPEAK,K,A1,ICPEAK,L1
      Z1=0.
      Z2=0.
      Z3=0.
      Z4=0.
      IF(IIPEAK.EQ.0.OR.M.EQ.1) THEN
      IA=ICPEAK
      IB=IDPEAK
      ELSE
      IA=1
      IB=ICPEAK
      END IF
      DO 10 I=IA,IB
      IF(IIPEAK.EQ.0) THEN
      IF(M.EQ.1) P(I)=UP(I)
      IF(M.EQ.2) P(I)=T13(I)
      IF(P(I).GT.P(ICPEAK)) P(I)=P(ICPEAK)
      ELSE IF(IIPEAK.EQ.1) THEN
      P(I)=UP(I)
      IF(M.EQ.1.AND.P(I).GT.P(ICPEAK)) P(I)=P(ICPEAK)
      ELSE
      P(I)=T13(I)
      IF(M.EQ.1.AND.P(I).GT.P(ICPEAK)) P(I)=P(ICPEAK)
      END IF
      B=FREQ(I)**X
      C=B*ALOG(FREQ(I))
      Z1=Z1+P(I)*B
      Z2=Z2+P(I)*C
      Z3=Z3+B*B
   10 Z4=Z4+B*C
      A1=Z1/Z3
      AIM=A1-Z2/Z4
      RETURN
      END
 EOI ENCOUNTERED.
/
```

## C.3 Directional Spectrum Estimation: the geometric approach, Program GEOME

```
      PROGRAM GEOME(INPUT,OUTPUT,DATA2,DATA4,TAPE6=DATA2,TAPE8=DATA4)
C  ---CAUTION: BEFORE RUNNING THIS PROGRAM, 'LIBRARY(COMPLOT)' & 'SETTL(100)' MUST BE CALLED---
C  ---CAUTION: FFT POINTS M.LE.1024, CHANGE DIM. IF ONE INCREASES M---
C  ---CAUTION: 0 DIRECTS TO EAST FOR MATH, BUT TO NORTH FOR OUTPUT---
C  ---(DATA2) IS USED TO INPUT FORWARD FFT DATA, COMPUTED FROM <FUNDA>---
C  ---(DATA4) ARE USED TO COLLECT DESIRED OUTPUT FROM FORMATED NTAPE8---
      CHARACTER*10 LX(2),LY(2),LX1(2),LY1(2),LX2(2),LY2(2),BE(2),LX21
      CHARACTER*3 LX3,LY3,LX4,LY4,LY10,LY10,LX18,LZ,LZ1,LZ2,LZ4,LZ5
      CHARACTER*10 LX5(2),LY5(6),LX6,LY6(6),LX7,LY7(6),LX11(2),LY14(3)
      CHARACTER*10 LX8,LY8(3),LX9,LY9,M(2),LX15,LY15,LX16,LY16,LY21(2)
      CHARACTER*10 LX14,LY11(2),LX12(3),LY12(3),LX13(2),LY13(3),LX25(3)
      CHARACTER*10 LX17,LY17(7),LY18(2),LX19(2),LY19,LX20(3),LY20(3)
      CHARACTER*10 LZ3(2),LX22,LY22(2),LX23,LY23(2),LX24,LY24(3),LY25(2)
      CHARACTER*10 LX26,LZ6,LZ7,LZ8,LZ9,LZ10,LX30
      DIMENSION PR(720),VR(720),PP(720),V(720),D(720)
      DIMENSION T33(720),T13(720),T12(720),T23(720)
      DIMENSION S1(720),S2(720),P1(720),P2(720),RECORD(720),FS(100)
      DIMENSION XX(7,14,2),YY(7,14,2),IXY(7),XL(10),YL(10),IK3(4),A(4,5)
      COMMON /DATA10/ FREQ(720),TA(720),TR(720),P(720),VP(720),VR(720)
     1,FREQ1,FREQ2,ALFA,GA,PEAKF,LL,IPEAK,IDPEAK,IIPEAK,K,A1,ICPEAK,L1
      DATA LX,LY,LX18/'FREQUENCY','(HZ)','E>**N ((F','T**2S)','C2'/
      DATA LX1,LY1/'E&>**N ((','(FT**2/S)','SPREADING','PARAMETER'/
      DATA LX2,LY2/'RECORD LAB','EL >.((','E&>**G ((','(FT**2S)'/
      DATA LX3,LX4,LY3,LY4,LX14,LZ/'E','V','M','S','FROM','100'/
      DATA LX5,LX6,LX7/'DIRECTIONA','L','SPECTRUM','UNMODIFIED'/
      DATA LY5,LX13/'WAVE ENERG','Y SPECTRUM',' AT SEA SU','RFACE, DEP',
     1 'TH OF SEA=','        FT','FT/)S(',',','      '0'/
      DATA LY6,LX12/'HORIZONTAL',' AMPLITUDE',' SPECTRUM ','AT 4.3 FT ',
     1 'ABOVE SEA ','FLOOR','---@>*!( M','EAN CURREN','T >.((/
      DATA LY7,LY12/'HORIZONTAL',' VELOCITY ','SPECTRUM A','T 4.3 FT A',
     1 'BOVE SEA F','LOOR',' @>-(! A','BOVE SEA F','LOOR'/
      DATA LX8,LY8,LY22,LY25/'SMOOTHED','ONE DIMENS','IONAL SPEC','TRUM'
     1,'S?C?R?I?T(',',        )=','S?D?E?E?R(',',        )=*/
      DATA LZ5,LX9,LY9,LY19/'&Z','RAW DATA','JONSWAP','A PROPOSED'/
      DATA LX10,LY10,LY13/'---','XXX',' ',',  --------','@>*!('/
      DATA LX11,LY11/'PEAK FREQU','ENCY >.((','PEAK ENERG','Y >.((/
      DATA LX15,LX16,LY18/'&>AI .((','&>RI(?L> .(','S(F)=A**F**','B'/
      DATA LY15,LY16,LX19/'&>C! .((','&>R!(?R) .(','A=       ',',' B=*/
      DATA LY14,LX17/'MAIN DIREC','TION >.((','        '0','C1 AND C2'/
      DATA LY17/'NOTATION >','.(   (  )F','ROM ONE AN','GLE MODE, ',
     1'(  )FROM D','OUBLE ANGL','E MODE'/
      DATA LX20,LY20,GE/'TOTAL ENER','GY >.((','    FT**2','/FT**2-S1 '
     1,'>.((',' HZ','GEOMETRIC ','APPROACH'/
      DATA LZ3,LZ4,LX23,LX24,LZ2/'HZ,       ',' '0','0','(RADIAN)'
     1,'=       @(','OF'/
      DATA LY23,LY24/'EVALUATED','AT','DOMINANT F','REQUENCY >','.(('/
      DATA LX21,LX22,LY21/'&>M**2','>RMS((','=         (',' FT/)S(**2'/
      DATA LX26,LZ6,LZ7/'',       @(','R>.((','LX.(('/
      DATA LZ1,LX25/'500','REF. DIREC','TION >.((','       '0'/
      DATA A,LZ8,LZ9,LZ10,LX30/20*.0,'3','2','4','&SY!<=*/
      DATA CPI,DEGREE,PM,DMEAN,ESDA/3.14159265,57.29578,.0174532,.0,.0/
      DATA FS/ 1.00000,1.33333,1.60000,1.82857,2.03175,2.21645,2.38695,
     1 2.54608,2.69585,2.83773,2.97286,3.10212,3.22620,3.34569,3.46106,
     1 3.57271,3.68097,3.78614,3.88847,3.98817,4.08545,4.18046,4.27335,
     1 4.36428,4.45334,4.54066,4.62634,4.71045,4.79309,4.87433,4.95424,
     1 5.03288,5.11031,5.18658,5.26175,5.33586,5.40895,5.48107,5.55225,
     1 5.62253,5.69195,5.76053,5.82830,5.89529,5.96153,6.02704,6.09185,
     1 6.15597,6.21943,6.28226,6.34446,6.40605,6.46706,6.52750,6.58739,
     1 6.64673,6.70556,6.76386,6.82168,6.87900,6.93585,6.99224,7.04818,
     1 7.10368,7.15874,7.21339,7.26763,7.32146,7.37490,7.42796,7.48064,
     1 7.53295,7.58490,7.63650,7.68775,7.73866,7.78924,7.83950,7.88943,
     1 7.93905,7.98836,8.03737,8.08608,8.13450,8.18263,8.23048,8.27806,
     1 8.32536,8.37240,8.41917,8.46569,8.51195,8.55796,8.60372,8.64924,
     1 8.69453,8.73958,8.78440,8.82899,8.87335/
      DATA YL,YL/.0,.33,.5,.66,.8,.857,.889,.909,.952,.98,10*1./
      DATA CPI2,VARY,ULARGE,ESDB,GA,XX/6.2831853,.0,.0,.0,4.,196*1./
      DATA IIPEAK,TEMP,IPNOW,EDEP,ADEP/0.,0.,0,.0,.0001/
      PRINT 5040
5040  FORMAT(1X/"-----THE PROGRAM WILL FIRST COMPUTE THE INFORMATION FOR
     1 SPREADING USE,"/"-----THEN, IT WILL COMPUTE ONE DIMENSION CASE,"/
     1"-----FINALLY IT WILL DRAW THE DIRECTIONAL SPECTRUM.")
      READ(6,5068) M
5068  FORMAT(1X/I5)
      MM=M/2
      MM1=MM/1.45
```

```
      READ(6,5050)M(1),M(2),M1,DEPTH,V1,D1,PI,S,SV,(P(I),PB(I),V(I)
     1,VB(I),D(I),DB(I),I=1,NM1)
 5050 FORMAT(A10,A5,7F9.4/(10F12.6))
      AA=S
      IF(DEPTH.LT.140.) EDEP=2.
      IF(EDEP.GT.1.) ADEP=.01
      NM2=NM/3.5
      NM3=NM2-3
      NM4=NM/2.5
      NM5=NM4+1
      FREQ1=1./FLOAT(N)
      PII=SQRT(V1*V1+D1*D1)
      DII=90.-ATAN2(D1,V1)*DEGREE
      IF(DII.LT..0) DII=DII+360.
C  ---PII & DII ARE THE MAGNITUDE AND DIRECTION OF CURRENT AT M1(FT) ABOVE SEA FLOOR---
C ***************************************************************************
C *---PART IV: CALCULATE ONE DIMENSIONAL SPECTRUM---                          *
C ***************************************************************************
      L1=N/32
      IF(L1.LT.4) L1=4
      FREQ2=SQRT(2.56/DEPTH)
C  ---FREQUENCY FREQ2 CIRCUMSCRIBES DEEP WATER WAVES, WAVE LENGTH=2*DEPTH---
      L3=FREQ2/FREQ1
      IDEEP=L3
      ENH=FLOAT(N)/288.
C  ---ENH=FLOAT(N)/144./2. : USED TO COMPUTE ENERGY IN POSITIVE FREQUENCY---
C  ---ALSO THE UNIT CHANGES FROM IN**IN TO FT**FT---
      CALL TRANS(DEPTH,M1,NM1)
C
      DO 5001 I=1,NM1
      S1(I)=P(I)/UP(I)
      S2(I)=PB(I)/UP(I)
C  ---UP(I) : TRANSFER PRESSURE DATA(PSI) @ M2' TO VELOCITY DATA(IN/S) @ M1'---
      B=(V(I)*S2(I)-VB(I)*S1(I))**2+(D(I)*S2(I)-DB(I)*S1(I))**2
      C=(V(I)*DB(I)-D(I)*VB(I))**2
      BB=V(I)*V(I)+D(I)*D(I)
      CC=VB(I)*VB(I)+DB(I)*DB(I)
      VALUE=ABS((B-C)/C)
      IF(VALUE.LT..07) GO TO 5010
      TEMP=(BB+B-S1(I)*S1(I)*C)/(B-C)
      VARY=(CC+B-S2(I)*S2(I)*C)/(B-C)
 5010 T23(I)=.0
      IF(VALUE.LT..05.OR.TEMP.LT..0.OR.VARY.LT..0) T23(I)=5.
      IF(T23(I).LE.1.) THEN
      TA(I)=(S1(I)+SQRT(TEMP))/2.
      TB(I)=S1(I)-TA(I)
      T13(I)=(S2(I)+SQRT(VARY))/2.
      T33(I)=S2(I)-T13(I)
      D1(I)=(TB(I)*TB(I)+T33(I)*T33(I))*ENH
      D2(I)=(T13(I)*T13(I)+TA(I)*TA(I))*ENH
      ELSE
      TA(I)=ATAN2(D(I),V(I))
      TB(I)=ATAN2(DB(I),VB(I))
      IF(P(I).LT..0) TA(I)=TA(I)+CPI
      IF(PB(I).LT..0) TB(I)=TB(I)+CPI
      D1(I)=ABS(S1(I))*SQRT(BB)*ENH
      D2(I)=ABS(S2(I))*SQRT(CC)*ENH
      END IF
 5001 RECORD(I)=D1(I)+D2(I)
C  ---RECORD(I) IS RAW DATA OF 1-D HORI. VELOCITY SPECTRUM @ M1(FT) ABOVE SEA FLOOR---
      CALL SMOOTH(N,UP,RECORD,NM5,0,1)
      DO 5047 I=1,NM5
      T12(I)=UP(I)/RECORD(I)
      IF(I.LE.L1.OR.I.GE.L3) GO TO 5027
      IF(UP(I).LE.ULARGE) GO TO 5027
      ULARGE=UP(I)
      IPEAK=I
 5027 CONTINUE
      IF(T23(I).GT.1.) THEN
      TEMP=D1(I)*T12(I)
      VARY=D2(I)*T12(I)
      GO TO 5005
      END IF
      DC=TA(I)
      CC=TB(I)
      DS=T13(I)
      CS=T33(I)
      TEMP=D1(I)*T12(I)
      VARY=D2(I)*T12(I)
C
      MOD=0
      MODE=0
      JMODE=0
      R=DS*CC-DC*CS
      IF(R.EQ..0) MOD=1
```

```
      IF(MOD.EQ.1) GO TO 5024
      A1=(DS*D(I)-DC*DB(I))/B
      B1=(DS*V(I)-DC*VB(I))/B
      A2=(CC*DB(I)-CS*D(I))/B
      B2=(CC*VB(I)-CS*V(I))/B
      IF(ABS(A1).GT.1..OR.ABS(A2).GT.1..OR.ABS(B1).GT.1..OR.ABS(
     1B2).GT.1.) MOD=1
      IF(MOD.EQ.1) GO TO 5024
      TA(I)=ATAN2(A1,B1)
      TB(I)=ATAN2(A2,B2)
      C=CC*COS(TA(I))+DC*COS(TB(I))
 5024 DC=CC
      CC=S1(I)-DC
      B=DS*CC-DC*CS
      IF(B.EQ..0) MODE=1
      IF(MODE.EQ.1.AND.MOD.EQ.1) GO TO 5023
      IF(MODE.EQ.1) GO TO 5005
      A1=(DS*D(I)-DC*DB(I))/B
      B1=(DS*V(I)-DC*VB(I))/B
      A2=(CC*DB(I)-CS*D(I))/B
      B2=(CC*VB(I)-CS*V(I))/B
      IF(ABS(A1).GT.1..OR.ABS(A2).GT.1..OR.ABS(B1).GT.1..OR.ABS(
     1B2).GT.1.) MODE=1
      IF(MODE.EQ.1.AND.MOD.EQ.1) GO TO 5023
      IF(MODE.EQ.1) GO TO 5005
      D1(I)=ATAN2(A1,B1)
      D2(I)=ATAN2(A2,B2)
      IF(MOD.EQ.1) GO TO 5000
      VALUE=CC*COS(D1(I))+DC*COS(D2(I))
      IF(ABS(C-V(I)).LE.ABS(VALUE-V(I))) GO TO 5005
 5000 TA(I)=D1(I)
      TB(I)=D2(I)
      TEMP=(CC*CC+CS*CS)*EMM*T12(I)
      VARY=(DS*DS+DC*DC)*EMM*T12(I)
 5005 P(I)=TEMP*COS(TA(I))+VARY*COS(TB(I))
      PB(I)=TEMP*SIN(TA(I))+VARY*SIN(TB(I))
      T33(I)=TEMP*COS(2.*TA(I))+VARY*COS(2.*TB(I))
      T13(I)=TEMP*SIN(2.*TA(I))+VARY*SIN(2.*TB(I))
      GO TO 5047
 5023 IF(I.EQ.1) THEN
      P(1)=.00001
      PB(1)=.00001
      T33(1)=.00001
      T13(1)=.00001
      UP(1)=.00001
      GO TO 5047
      END IF
      P(I)=P(I-1)
      PB(I)=PB(I-1)
      T33(I)=T33(I-1)
      T13(I)=T13(I-1)
      UP(I)=UP(I-1)
 5047 CONTINUE
      IF(L3.GT.NM2) L3=NM2
C     WRITE(*,7) (RECORD(I),I=1,30)
C   7 FORMAT(1X/"-----OUTPUT VELOCITY SPECTRUM AT H!' ABOVE SEA FLOOR,
C    1"/(9F8.3))
C ***************************************************************************
C *---PART V: CALCULATE SPREADING PARAMETER AND DIRECTIONAL SPREADING---     *
C ***************************************************************************
      PRINT 5015
 5015 FORMAT(1X/"=====INPUT 3 WILL AVERAGE THREE FREQUENCY DATA."/
     1"=====OR INPUT 4 WILL AVERAGE FOUR FREQUENCY DATA."/
     1"=====OR INPUT 5 WILL AVERAGE FIVE FREQUENCY DATA."/
     1"-----DOUBLE THE VALUE OF INPUT WILL CALCULATE BEST-FIT CURVE"/
     1"     OF SPREADING PARAMETER IN EITHER SIDE OF PEAK POINT.")
      READ*,INIU
      IF(INIU.GE.6) IPNOW=1
      IF(INIU.GE.6) INIO=INIO/2
      A1=P(1)+P(2)
      B1=PB(1)+PB(2)
      A2=T33(1)+T33(2)
      B2=T13(1)+T13(2)
      M=UP(1)+UP(2)
      D1(1)=SQRT(A1*A1+B1*B1)/M
      TA(1)=ATAN2(B1,A1)
      TB(1)=ATAN2(B2,A2)/2.
      IF(ABS(TB(1)-TA(1)).LT.1.75) GO TO 5999
      IF(TB(1).LT.TA(1)) TB(1)=TB(1)+CPI
      IF(ABS(TB(1)-TA(1)).GT.1.75) TB(1)=TB(1)-CPI
 5999 D2(1)=A2/B/COS(TB(1)*2.)
      DO 5054 I=2,NM6
      A1=P(I)+P(I+1)+P(I-1)
      B1=PB(I)+PB(I+1)+PB(I-1)
```

```
      A2=T33(I)+T33(I+1)+T33(I-1)
      B2=T13(I)+T13(I+1)+T13(I-1)
      B=WP(I)+WP(I+1)+WP(I-1)
      IF(INTO.EQ.4.AND.I.LT.NH6) THEN
      A1=A1+P(I+2)
      B1=B1+PB(I+2)
      A2=A2+T33(I+2)
      B2=B2+T13(I+2)
      B=B+WP(I+2)
      ELSE IF(INTO.EQ.5.AND.I.LT.NH6.AND.I.GT.3) THEN
      A1=A1+P(I-2)+P(I+2)
      B1=B1+PB(I-2)+PB(I+2)
      A2=A2+T33(I-2)+T33(I+2)
      B2=B2+T13(I-2)+T13(I+2)
      B=B+WP(I-2)+WP(I+2)
      END IF
      D1(I)=SQRT(A1*A1+B1*B1)/B
      TA(I)=ATAN2(B1,A1)
      TB(I)=ATAN2(B2,A2)/2.
      IF(ABS(TB(I)-TA(I)).LT.1.75) GO TO 5054
      IF(TB(I).LT.TA(I)) TB(I)=TB(I)+CPI
      IF(ABS(TB(I)-TA(I)).GT.1.75) TB(I)=TB(I)-CPI
 5054 D2(I)=A2/B/COS(TB(I)*2.)
C  ---D1,TA ARE SINGLE-ANGLE MODE. D2,TB ARE DOUBLE-ANGLE MODE---
      DO 5017 I=NH2,NH6
      IF(D1(I).GT..999) D1(I)=.999
 5017 IF(D2(I).GT..999) D2(I)=.999
      KSIMU=NH2
      PRINT 900
  900 FORMAT(/"=====INPUT 1 WILL OUTPUT DATA FOR SIMULATION USE LATER,
     1"/"=====OR INPUT 0 WILL NOT OUTPUT DATA FOR SIMULATION USE.")
      READ*,K
      IF(K.EQ.1) KSIMU=NH6
      DO 5051 I=1,KSIMU
      IF(D1(I).GT..999) D1(I)=.999
      C=1.-D1(I)
      P(I)=D1(I)/C
C  ---P(I) IS THE SPREADING PARAMETER CALCULATED FROM SINGLE-ANGLE MODE---
      IF(D2(I).GT..999) D2(I)=.999
      C=1.-D2(I)
      B=(1.5*D2(I)+.5)/C
 5051 WP(I)=B+SQRT(B*B+2.*D2(I)/C)
C  ---WP(I) IS THE SPREADING PARAMETER CALCULATED FROM DOUBLE-ANGLE MODE---
C
      L2=IPEAK-L1/2
      IF(L3-IPEAK.LT.L1) L3=IPEAK+L1+L1/2
      IF(L3.GT.NH2) L3=NH2
      IDPEAK=L3-L1/2
      VARY=P(IDPEAK)
      DO 5049 I=IDPEAK,L3
      IF(P(I).GE.VARY) GO TO 5049
      IDPEAK=I
      VARY=P(I)
 5049 CONTINUE
C
      TEMP=FREQ(IDPEAK)
      LL=IPEAK+L1/3
      ICPEAK=L2
C  ---CRITICAL FREQUENCY INDEX INDICATES HIGHEST SPREADING PARAMETER---
      VLARGE=P(ICPEAK)
      DO 5006 I=ICPEAK,LL
      IF(P(I).LE.VLARGE) GO TO 5006
      ICPEAK=I
      VLARGE=P(I)
 5006 CONTINUE
      PEAKF=FREQ(ICPEAK)
C
      CALL PLOTYPE(1)
      CALL BAUD(1200)
      CALL SIZE(7.5,5.625)
C  ---THE FOLLOWING 80 LINES CAN BE DELETED IF NOT NEEDED---
C
      PRINT 5060
 5060 FORMAT(//"=====INPUT CODE NUMBER TO OUTPUT CORRESPONDING FIGURES,
     1"/"-----SPREADING PARAMETER & PROPAGATION DIRECTION & FREQUENCY,"/
     1"-----CODE=1 WILL SHOW THE DETAIL COMPUTATION THROUGH FIGURES,"
     1/"-----CODE=2 WILL SHOW THE OPTIMAL SOLUTION ONLY.")
      READ*,JMODE
      IF(JMODE.EQ.2) GO TO 5061
      CALL ERASE
      CALL SCALE(25.,4.,1.1,1.,0.,-.1)
      CALL AXISL(0.,.2,.0,.0,1.,.0,.05,.1,4,0,1,2,1.,1.,.1,0)
      CALL VECTORS
```

```
      CALL PLOT(.0,1.,0,0)
      CALL PLOT(.2,1.,1,0)
      CALL PLOT(.2,0.,1,0)
      CALL SYMBOL(.06,-.14,.0,.15,15,LX)
      CALL SYMBOL(-.025,.33,90.,.16,9,LY17)
      CALL SYMBEL(-.03,-.24,.0,.1,65,LY17)
      CALL POINTS
      CALL PLOT(.0342,-.23,1,17)
      CALL PLOT(.1412,-.23,1,3)
C  ---DRAW D1,D2-FREQUENCY FIGURES---
      CALL LINE(FREQ,D1,17,NN6)
      CALL LINE(FREQ,D2,3,NN6)
      CALL TEKPAUS
      CALL ERASE
      CALL SCALE(4.4,4.,1.8,.9,0.,-.1)
      CALL AXISL(.0,1.,.0,.0,1.,.0,.1,.1,0,0,2,2,1.,1.,.1,0)
C  ---DRAW D1-D2 PICTURE AS C1-C2 RELATION---
      DO 5044 I=L2,L3
      J=I-L2+1
      T12(J)=D1(I)
 5044 T33(J)=D2(I)
      CALL POINTS
      CALL LINE(T12,T33,J,1)
      CALL LINE(XL,YL,8,10)
      CALL NUMBER(.0,1.02,.0,.085,3,.0)
      CALL NUMBER(.333,1.02,.0,.085,3,.5)
      CALL NUMBER(.5,1.02,.0,.085,3,1.)
      CALL NUMBER(.667,1.02,.0,.085,3,2.)
      CALL NUMBER(.78,1.02,.0,.085,3,4.)
      CALL SYMBOL(.909,1.02,.0,.085,2,LZ)
      CALL SYMBOL(.98,1.02,.0,.085,2,LZ1)
      CALL SYMBOL(.2,1.04,.0,.12,1,LX6)
      DO 5045 I=1,51
      T12(I)=.02*FLOAT(I-1)
 5045 T33(I)=6./(2.-T12(I))-3.-2.*T12(I)
      CALL VECTORS
      CALL LINE(T12,T33,0,51)
      CALL PLOT(1.,.0,1,0)
      CALL PLOT(1.,1.,0,0)
      CALL PLOT(0.,1.,1,0)
      CALL SYMBEL(-.1,-.2,.0,.12,9,LY17)
      CALL SYMBOL(.7,-.12,.0,.12,2,LX17)
      CALL SYMBOL(-.22,.71,.0,.12,2,LX18)
      CALL TEKPAUS
      CALL ERASE
      CALL SCALE(25.,.63662,1.1,1.5,0.,-CP1)
      CALL AXISL(.0,.2,0.,-CP1,CP1,-CP1,.05,CP1,4,3,1,0,1.,1.,.1,0)
      CALL PLOT(.0,CP1,0,0)
      CALL PLOT(.2,CP1,1,0)
      CALL PLOT(.2,-CP1,1,0)
      CALL SYMBOL(.05,-4.1,.0,.15,15,LX)
      CALL SYMBOL(-.033,-2.4,90.,.15,11,LX5)
      CALL SYMBOL(-.028,.65,90.,.15,9,LY1)
      CALL NUMBER(-.028,-3.1,.0,.1,6,-180.0)
      CALL NUMBER(-.025,-1.57,.0,.1,5,-90.0)
      CALL NUMBER(-.019,.0,.0,.11,3,.0)
      CALL NUMBER(-.025,1.55,.0,.1,5,90.0)
      CALL NUMBER(-.029,3.10,.0,.1,6,180.0)
      CALL SYMBOL(-.03,-4.8,.0,.1,65,LY17)
      CALL POINTS
      CALL PLOT(.0342,-4.7,1,28)
      CALL PLOT(.1412,-4.7,1,20)
C  ---DRAW TA,TB DATA SHOWING WAVE PROPAGATION DIRECTION---
      CALL LINE(FREQ,TA,28,NN6)
      CALL LINE(FREQ,TB,20,NN6)
      CALL TEKPAUS
 5061 CONTINUE
C
C
      MOD=1
 5055 X1=-5.
      X2=-.1
      IF(MOD.EQ.2.AND.IPNOW.EQ.1) X1=.1
      IF(MOD.EQ.2.AND.IPNOW.EQ.1) X2=20.
      CALL LST(FF2,X2,MOD)
 5063 CALL LST(FF1,X1,MOD)
      XN=100000.*FF1*FF2
      IF(XN.GT..0) THEN
      X1=X1-3.
      IF(MOD.EQ.2.AND.IPNOW.EQ.1.AND.X1.GT.-7) GO TO 5063
      IF(MOD.EQ.2.AND.IPNOW.EQ.1) GO TO 5080
      IF(X1.GT.-40.) GO TO 5063
 5080 X=.0
```

```
      A1=.0
      GO TO 5056
      END IF
      DO 5057 I=1,22
      X=(X1+X2)/2.
      CALL LST(FF,X,MOD)
      XN=100000.*FF*FF1
      IF(XN.LE..0) THEN
      X2=X
      FF2=FF
      ELSE
      X1=X
      FF1=FF
      END IF
      IF(ABS(FF)-1.E-10) 5056,5056,5057
 5057 CONTINUE
 5056 IF(MOD.GE.2) GO TO 5018
      MOD=2
      CALL ERASE
C ***************************************************************************
C *---PART V1: DRAWING APPLIED SPREADING PARAMETER IN LOG. SCALE---          *
C ***************************************************************************
      CALL SMOOTH(N,S1,P,KSIMU,ICPEAK,3)
      CALL SCALE(25.,1.3,1.1,1.06,.0,-1.)
      CALL AXISL(.0,.2,.0,-1.,2.,-1.,.05,1.,4,0,1,0,1.,1.,.1,0)
      DO 6069 I=1,NN2
      IF(S1(I).LT..1) V8(I)=-1.
      IF(P(I).LT..1) T12(I)=-1.
      IF(UP(I).LT..1) D(I)=-1.
      IF(S1(I).GE..1) V8(I)=ALOG10(S1(I))
      IF(UP(I).GE..1) D(I)=ALOG10(UP(I))
 6069 IF(P(I).GE..1) T12(I)=ALOG10(P(I))
      CALL POINTS
      IF(IPNOW.EQ.0) THEN
      CALL PLOT(.168,.53,1,27)
      CALL PLOT(.168,.31,1,19)
      ELSE
      CALL PLOT(.168,.75,1,27)
      CALL SYMBEL(.16,.5,.0,.09,3,LZ6)
      CALL SYMBEL(.16,.28,.0,.09,3,LZ7)
      END IF
      CALL POINTS
      CALL PLOT(.009,-1.64,1,27)
      CALL PLOT(.098,-1.64,1,19)
      CALL LINE(FREQ,T12,27,NN2)
      CALL LINE(FREQ,D,19,NN2)
      CALL DASHES
      CALL LINE(FREQ,V8,0,NN2)
      CALL VECTORS
      IF(X.EQ..0) INTO=10
      IF(INTO.NE.10) THEN
      DO 6071 I=KSIMU,1,-1
      IF(I.GE.ICPEAK) S2(I)=A1*FREQ(I)**X
 6071 IF(I.LT.ICPEAK) S2(I)=.9*S2(ICPEAK)
      DO 6066 I=ICPEAK,IPPEAK
      J=I-ICPEAK+1
      D2(J)=FREQ(I)
      IF(S2(I).LT..1) D1(J)=-1.
 6066 IF(S2(I).GE..1) D1(J)=ALOG10(S2(I))
      CALL LINE(D2,D1,0,J)
      END IF
      XL(1)=.17
      XL(2)=.183
      YL(1)=1.19
      YL(2)=1.19
      CALL SYMBOL(.05,-1.4,.0,.15,15,LX)
      CALL SYMBOL(-.028,-.7,90.,.15,20,LY1)
      CALL SYMBEL(-.038,-1.67,.0,.1,66,LY17)
      CALL NUMBER(-.024,-1.03,.0,.1,6,.1000)
      CALL NUMBER(-.024,-.03,.0,.1,6,1.000)
      CALL NUMBER(-.024,.97,.0,.1,6,10.00)
      CALL NUMBER(-.024,1.97,.0,.1,6,100.0)
      CALL SYMBOL(.12,2.,.0,.15,20,BE)
      CALL SYMBEL(.173,1.64,.0,.107,19,LY22)
      CALL NUMBER(.185,1.64,.0,.09,6,PEAKF)
      CALL NUMBER(.215,1.64,.0,.09,5,VLARGE)
      CALL SYMBEL(.173,1.4,.0,.102,19,LY25)
      CALL NUMBER(.185,1.4,.0,.09,6,TEMP)
      CALL NUMBER(.215,1.4,.0,.09,5,VARY)
      CALL SYMBOL(.191,1.16,.0,.09,10,LY19)
      CALL SYMBOL(.2,.96,.0,.09,9,LT1)
      CALL SYMBOL(.173,.72,.0,.09,11,LY18)
      CALL SYMBOL(.173,.5,.0,.09,14,LX19)
```

```
      CALL NUMBER(.179,.5,.0,.09,8,A1)
      CALL NUMBER(.226,.5,.0,.09,6,X)
      CALL SYMBOL(.17,.03,.0,.104,3,LX10)
      CALL SYMBOL(.191,.03,.0,.09,8,LX8)
      CALL SYMBOL(.2,-.17,.0,.09,9,LY1)
      CALL SYMBEL(.173,-.37,.0,.09,16,LX2)
      CALL SYMBOL(.187,-.57,.0,.09,15,M)
      IF(IPNOW.EQ.1) IIPEAK=1
C  ---THIS STEP IS USED IN SUBROUTINE   LST---
      GO TO 5055
 5018 CALL SYMBOL(.173,.28,.0,.09,14,LX19)
      CALL NUMBER(.179,.28,.0,.09,8,A1)
      CALL NUMBER(.226,.28,.0,.09,6,X)
      IF(IPNOW.EQ.1.AND.X.NE..0) THEN
      II=ICPEAK-1
      DO 5081 I=1,II
 5081 S2(I)=A1*FREQ(I)**X
      DO 5082 I=1,II
      IF(S2(I).LT..1) D1(I)=-1.
 5082 IF(S2(I).GE..1) D1(I)=ALOG10(S2(I))
      CALL LINE(FREQ,D1,0,II)
      GO TO 5083
      END IF
      IF(INTO.EQ.10.AND.X.NE..0) THEN
      DO 6051 I=KSIMU,1,-1
      IF(I.GE.ICPEAK) S2(I)=A1*FREQ(I)**X
 6051 IF(I.LT.ICPEAK) S2(I)=.9*S2(ICPEAK)
      DO 6052 I=ICPEAK,IPPEAK
      J=I-ICPEAK+1
      D2(J)=FREQ(I)
      IF(S2(I).LT..1) D1(J)=-1.
 6052 IF(S2(I).GE..1) D1(J)=ALOG10(S2(I))
      CALL LINE(D2,D1,0,J)
      END IF
 5083 CALL LINE(XL,YL,0,2)
      CALL TEKPAUS
      CALL ERASE
      IF(INTO.EQ.10.AND.X.EQ..0) THEN
      DO 6053 I=KSIMU,1,-1
      IF(I.GE.ICPEAK) S2(I)=.00003/FREQ(I)**5
 6053 IF(I.LT.ICPEAK) S2(I)=.9*S2(ICPEAK)
      END IF
C ***************************************************************************
C *---PART VII: DRAWING APPLIED DIRECTIONAL SPREADING IN POLAR COORDINATES---  *
C ***************************************************************************
      PRINT 303
  303 FORMAT(/"=====INPUT 1 WILL SET PROPOSED DIRECTION AS SMOOTH DIRECT
     1ION,"/"=====OR INPUT 2 TO SET MAIN DIRECTION IN PROPOSED SPECTRUM,
     1"/"=====OR INPUT 3 TO SET BEST-FIT-CURVE IN PROPOSED SPECTRUM.")
      READ*,JUMP
      CALL ERASE
      DO 6067 I=L1,NM2
      ESDA=ESUM+RECORD(I)
 6067 DMEAN=DMEAN+TA(I)*RECORD(I)
      DDMEAN=DMEAN/ESDA
      IF(JUMP.NE.2) THEN
      CALL SCALE(17.4,16.,.42,.42,.0,.0)
      CALL ORIGIN(3.03,2.83)
      CALL POINTS
      END IF
      T12(1)=DDMEAN
      DO 6065 I=2,NM2
      IF(JUMP.NE.2) THEN
      X=FREQ(I)*COS(TA(I))
      Y=FREQ(I)*SIN(TA(I))
      CALL PLOT(X,Y,1,1)
      END IF
      T12(I)=TA(I)
 6065 IF(I.GT.L2.AND.ABS(T12(I)-T12(I-1)).GE..2) T12(I)=T12(I-1)
     1*.7+T12(I)*.3
      DMEAN=DDMEAN*DEGREE
      CALL SMOOTH(N,D1,T12,NM2,0,2)
C  ---WHERE D1(I) IS A SMOOTHED DIRECTIONAL SPREADING---
      IF(JUMP.EQ.2) GO TO 304
      IF(JUMP.EQ.3) THEN
      II=IDEEP
      IF(II.GT.NM3) II=NM3
      CALL SMOOTH(N,UP,RECORD,II,0,2)
      DO 301 I=L1,II
      A(1,1)=A(1,1)+UP(I)
      BB=UP(I)*FREQ(I)
      A(1,2)=A(1,2)+BB
      BB=BB*FREQ(I)
      A(1,3)=A(1,3)+BB
```

```
      BB=BB*FREQ(I)
      A(1,4)=A(1,4)+BB
      BB=BB*FREQ(I)
      A(2,4)=A(2,4)+BB
      BB=BB*FREQ(I)
      A(3,4)=A(3,4)+BB
      A(4,4)=A(4,4)+BB*FREQ(I)
      CC=UP(I)*(D1(I)-DDMEAN)
      A(1,5)=A(1,5)+CC
      CC=CC*FREQ(I)
      A(2,5)=A(2,5)+CC
      CC=CC*FREQ(I)
      A(3,5)=A(3,5)+CC
  301 A(4,5)=A(4,5)+CC*FREQ(I)
      X12=A(1,1)
      A(1,1)=A(1,2)
      A(1,2)=A(1,3)
      A(1,3)=A(1,4)
      A(2,1)=A(1,3)
      A(2,2)=A(2,3)
      A(2,3)=A(2,4)
      A(4,1)=A(1,4)
      A(4,2)=A(2,4)
      A(4,3)=A(3,4)
      DO 405 I=1,4
      DO 405 J=1,5
  405 A(I,J)=A(I,J)/A(I,1)
      DET=1.
      DO 411 K=1,4
      BIG=ABS(A(K,K))
      KKK=K
      DO 410 KK=K,4
      IF(BIG-ABS(A(KK,K))) 409,410,410
  409 BIG=ABS(A(KK,K))
      KKK=K
  410 CONTINUE
      DO 408 JJ=K,5
      BOXX=A(K,JJ)
      A(K,JJ)=A(KKK,JJ)
  408 A(KKK,JJ)=BOXX
      DET=DET*A(K,K)
      IF(DET-.0) 413,412,413
  412 PRINT*,'DET.=.0'
      STOP
  413 K1=K+1
      DO 414 J=K1,5
      A(K,J)=A(K,J)/A(K,K)
      IF(K-N.EQ.0) GO TO 411
      DO 415 I=K1,4
  415  A(I,J)=A(I,J)-A(I,K)*A(K,J)
  414 CONTINUE
  411 CONTINUE
      XL(4)=A(4,5)
      K=4
  417 SIGNN=.0
      DO 416 J=K,4
  416 SIGNN=SIGNN+A(K-1,J)*XL(J)
      XL(K-1)=A(K-1,5)-SIGNN
      K=K-1
      IF(K.EQ.1) GO TO 418
      GO TO 417
  418 Z1=XL(1)+DDMEAN
      Z2=XL(2)
      Z3=XL(3)
      Z4=XL(4)
      DO 302 I=1,NH2
  302 D2(I)=Z1+Z2*FREQ(I)+Z3*FREQ(I)*FREQ(I)+Z4*FREQ(I)**3
C  ---D2(I) IS A BEST-FIT-CURVE OF PROPOSED DIRECTION---
      Z1=90.-Z1*DEGREE
      Z2=-Z2*DEGREE
      Z3=-Z3*DEGREE
      Z4=-Z4*DEGREE
      BB=.0
      CC=.0
      DO 305 I=L1,II
      J=I-L1+1
      D(J)=FREQ(I)*COS(D2(I))
      T33(J)=FREQ(I)*SIN(D2(I))
      CC=CC+(D1(I)-DDMEAN)**2*UP(I)
  305 BB=BB+(D1(I)-D2(I))**2*UP(I)
      BB=SQRT(BB/X12)*DEGREE
      CC=SQRT(CC/X12)*DEGREE
      XL(1)=.151
      XL(2)=.168
```

```
      YL(1)=.078
      YL(2)=.078
      CALL VECTORS
      CALL LINE(D,T33,0,J)
      CALL LINE(XL,YL,0,2)
      CALL SYMBEL(.173,.075,.0,.105,6,LX30)
      CALL NUMBER(.187,.075,.0,.08,7,Z1)
      CALL SYMBOL(.2145,.065,.0,.08,1,LX)
      IF(Z2.GT.0.) CALL SYMBOL(.17,.065,.0,.08,1,LZ10)
      CALL NUMBER(.17,.065,.0,.08,8,Z2)
      CALL SYMBOL(.2145,.055,.0,.08,1,LX)
      CALL SYMBOL(.22,.058,.0,.065,1,LZ9)
      IF(Z3.GT.0.) CALL SYMBOL(.17,.055,.0,.08,1,LZ10)
      CALL NUMBER(.17,.055,.0,.08,8,Z3)
      CALL SYMBOL(.2145,.045,.0,.08,1,LX)
      CALL SYMBOL(.22,.048,.0,.065,1,LZ8)
      IF(Z4.GT.0.) CALL SYMBOL(.17,.045,.0,.08,1,LZ10)
      CALL NUMBER(.17,.045,.0,.08,8,Z4)
      CALL SYMBEL(.173,.03,.0,.11,2,LZ5)
      CALL SYMBEL(.179,.0283,.0,.09,4,LX22)
      CALL SYMBOL(.195,.03,.0,.1,1,LX24)
      CALL SYMBOL(.229,.033,.0,.05,1,LZ2)
      CALL NUMBER(.2,.03,.0,.08,6,BB)
      CALL SYMBEL(.173,-.145,.0,.11,2,LZ5)
      CALL SYMBEL(.179,-.1467,.0,.09,4,LX22)
      CALL SYMBOL(.195,-.145,.0,.1,1,LX24)
      CALL SYMBOL(.229,-.142,.0,.05,1,LZ2)
      CALL NUMBER(.2,-.145,.0,.08,6,CC)
      END IF
      S=90.-S
      DM=90.-DMEAN
      R=100.*ABS(DM-S)/S
      L4=L1+L1/2
      DO 6068 I=L4,NM2
      II=I-L4+1
      D(II)=FREQ(I)*COS(D1(I))
 6068 T33(II)=FREQ(I)*SIN(D1(I))
      CALL BASMES
      CALL LINE(D,T33,0,II)
      INTO=1
      GO TO 7062
 6072 CALL SYMBOL(.13,.095,.0,.18,9,LY1)
      CALL SYMBEL(.15,-.0545,.0,.05,3,LY10)
      CALL SYMBOL(.17,-.055,.0,.08,10,LX7)
      CALL SYMBOL(.19,-.065,.0,.08,9,LX5)
      CALL SYMBOL(.15,-.08,.0,.09,3,LX10)
      CALL SYMBOL(.17,-.08,.0,.08,8,LX8)
      CALL SYMBOL(.19,-.09,.0,.08,9,LX5)
      CALL SYMBEL(.15,-.105,.0,.08,16,LX2)
      CALL SYMBOL(.176,-.115,.0,.08,15,R)
      CALL SYMBEL(.15,-.13,.0,.08,30,LY14)
      CALL NUMBER(.215,-.13,.0,.08,6,DM)
      IF(JUMP.EQ.1) THEN
      CALL SYMBEL(.15,-.145,.0,.08,29,LX25)
      CALL NUMBER(.215,-.145,.0,.08,6,S)
      CALL SYMBEL(.15,-.16,.0,.11,2,LZ5)
      CALL SYMBEL(.155,-.16,.0,.08,10,LX24)
      CALL NUMBER(.161,-.16,.0,.08,5,R)
      END IF
      CALL TEKPAUS
      CALL ERASE
  304 CONTINUE
C
      IF(ABS(M1-4.3).GT..5) L5=0
      DO 5043 I=1,NM1
      IF(L5.EQ.0) RECORD(I)=RECORD(I)*(COSH(UK(I)*4.333)/COSH(UK(I)*
     1M1))**2
 5043 DB(I)=RECORD(I)/FREQ(I)**2/39.47842
C  ---39.47842=CPI2**2---
C  ---DB(I) IS RAW DATA OF HORI. AMPLITUDE SPECTRUM @ 4.3' ABOVE SEA FLOOR---
C
      DO 5041 I=1,NM1
      VB(I)=DB(I)*(SINH(UK(I)*DEPTH)/COSH(UK(I)*4.333))**2
C  ---VB(I) IS RAW DATA OF WAVE ENERGY SPECTRUM AT SEA SURFACE---
      IF(VB(I).GE.2500.) GO TO 5042
 5041 CONTINUE
C
 5042 MINN=I-1
      K=MINN-1.5*L1
      IF(IDEEP.GE.MINN) IDEEP=MINN
      MAX=(IPEAK+K)/2
      IF(MAX-IPEAK.GT.L1) MAX=IPEAK+L1
      CALL SMOOTH(N,WF,VB,IDEEP,0,1)
      IIPEAK=IPEAK
```

```
      VLARGE=UP(IIPEAK)
      MAX=MAX*L1/3
      DO 5038 J=L2,MAX
      IF(UP(J).LE.VLARGE) GO TO 5038
      VLARGE=UP(J)
      IIPEAK=J
 5038 CONTINUE
      MM=K
      IF(K.GT.IIPEAK+L1*2) MM=IIPEAK+L1*2.3
      WRITE(*,5053) VLARGE,IIPEAK,UP(MM),MM,(UP(I),I=L2,MM)
 5053 FORMAT(/////////"-----CHECK 1-D. WATER SURFACE ENERGY WERE,"/"-----
     1INDEX OF PEAK ENERGY",F7.2," SHOWN WERE IS",I3,",","/"-----INDEX OF
     1UPPER BOUND",F7.2," IS",I3,",","/ "-----SMOOTHED ENERGY SERIES NEAR
     1PEAK ARE SHOWN AS FOLLOWS,"/(9F8.2))
      PRINT 7067
 7067 FORMAT(/"=====INPUT NEW INDEX FOR UPPER BOUND TO CONTINUE,"/"=====
     1OR INPUT 0 TO STOP THE PROGRAM,"/"=====OR INPUT 1 WILL RESET INDEX
     1 FOR DESIRED PEAK AND UPPER BOUND.")
      READ*,MOD
      IF(MOD.EQ.0) STOP
      IF(MOD.EQ.1) THEN
      READ*,IIPEAK,MOD
      VLARGE=UP(IIPEAK)
      END IF
      K=MOD
      XN=1.
      X2=10.
      PEAKF=FREQ(IIPEAK)
      CALL ERASE
      IF(K.LE.IIPEAK+3) PRINT*,'IIPEAK=',IIPEAK,', K=',K
      IF(K.LE.IIPEAK) STOP
C
      Y=.664187*
      LL=.62*IIPEAK
      IF(K.GT.IIPEAK+LL) K=IIPEAK+LL
C  ---LL WILL HELP AVOIDING THE OVERFLOW IN EXP---
      DO 120 I=LL,K
      C=EXP((PEAKF/FREQ(I))***1.25)*FREQ(I)**5
      TA(I)=Y/C/C
  120 TR(I)=UP(I)/C
      P(IIPEAK)=1.
      ALFA=VLARGE*PEAKF**5*3.490343/Y/GA
      MM=1
  130 MAX=1
  160 X1=.0038
      X2=4.
      IF(MAX.EQ.1) CALL LSM(FF1,X1,MAX)
      IF(MAX.EQ.1) R=FF1
      IF(MAX.EQ.2) FF1=R
  110 CALL LSM(FF2,X2,MAX)
      XN=100000.*FF1*FF2
      IF(XN.GT..0) THEN
      X2=X2+2.
      IF(X2.LE.10.) GO TO 110
      PA=.0
      PC=.0
      ALFA=.0081
      GA=1.
      DO 7055 I=IIPEAK,MM1
      TEMP=PEAKF/FREQ(I)
      V(I)=TEMP**5*EXP(1.25*(1.-TEMP**4))*VLARGE
C  ---USE P-M SPECTRUM TO EXTRAPOLATE THE TAIL PART OF RAW DATA OF WAVE ENERGY DENSITY---
 7055 UP(I)=V(I)
      DO 7056 I=1,IIPEAK
      TEMP=PEAKF/FREQ(I)
      A2=1.25*(1.-TEMP**4)
      IF(I.GE.IPEAK) V(I)=UP(I)
      IF(I.LT.IPEAK) V(I)=.0
      IF(I.LT.IPEAK.AND.A2.GT.-670.) V(I)=TEMP**5*EXP(A2)*VLARGE
 7056 CONTINUE
      GO TO 220
      END IF
      DO 140 I=1,15
      X=(X1+X2)/2.
      CALL LSM(FF,X,MAX)
      XN=100000.*FF*FF1
      IF(XN.LE..0) THEN
      X2=X
      FF2=FF
      ELSE
      X1=X
      FF1=FF
      END IF
      IF(ABS(FF)-1.E-8) 150,150,140
  140 CONTINUE
```

```
  150 IF(MAX.EQ.1) PA=X
      IF(MAX.EQ.2) PC=X
      MAX=MAX+1
      IF(MAX.LE.2) GO TO 160
      Z1=.0
      Z2=.0
      Z3=.0
      Z4=.0
      DO 170 I=LL,M
      TEMP=PC
      IF(I.LT.IIPEAK) TEMP=PA
      P(I)=(1./EXP(((FREQ(I)-PEAKF)/PEAKF/TEMP)**2/26.))**13
C  ---WHERE .3678=1/EXP---
      C=GA**P(I)
      Z1=Z1+TA(I)*C*C
      Z2=Z2+TB(I)*C
      Z3=Z3+TA(I)*P(I)*C*C/GA
  170 Z4=Z4+TB(I)*P(I)*C/GA
      Z1=Z2/Z1
      Z2=Z4/Z3
      ALFA=(Z1+Z2)/2.
      GA=VLARGE*PEAKF**5*3.490343/Y/ALFA
      IF(ABS((Z1-Z2)/Z1).LE..01) GO TO 180
      MM=MM+1
      IF(MM.LE.15) GO TO 130
  180 MAX=FLOAT(IIPEAK)*(1.+125.*PC)
      DO 190 I=LL,MM1
      IF(I.LE.K) V(I)=ALFA*Y/FREQ(I)**5/EXP((PEAKF/FREQ(I))**4*1.25)
     1*GA**P(I)
C  ---V(I) IS AN APPLIED JONSWAP SPECTRUM AT SEA SURFACE---
      IF(I.GT.K.AND.I.LE.MAX) THEN
      P(I)=(1./EXP(((FREQ(I)-PEAKF)/PEAKF/PC)**2/26.))**13
      V(I)=ALFA*Y/FREQ(I)**5/EXP((PEAKF/FREQ(I))**4*1.25)*GA**P(I)
      END IF
      IF(I.GT.MAX) V(I)=V(MAX)
  190 IF(I.GT.IDEEP) UP(I)=V(I)
C  ---USE JONSWAP TO EXTRAPULATE THE TAIL PART OF RAW DATA OF WAVE ENERGY SPECTRUM---
      VALUE=FLOAT(IIPEAK)*(1.-125.*PA)+1.
      DO 5034 I=1,LL
      A2=(PEAKF/FREQ(I))**4*1.25
      IF(A2.GT.740.) THEN
      V(I)=.0
      ELSE
      V(I)=.0
      IF(I.GT.VALUE)P(I)=(1./EXP(((FREQ(I)-PEAKF)/PEAKF/PA)**2/26.))**13
      IF(I.GT.VALUE) V(I)=ALFA*Y/FREQ(I)**5/EXP(A2)*GA**P(I)
      END IF
 5034 CONTINUE
  220 B2=.0
      B3=.0
      ESDA=.0
      DO 7063 I=1,MM1
C     IF(I.LT.IIPEAK.AND.V(I).LT.UP(I)) V(I)=UP(I)
C     IF(I.LE.IIPEAK) D2(I)=V(I)
C  ---D2(I) IS ORIGINAL FRONT PART OF JONSWAP SPECTRUM---
      ESDA=ESDA+RECORD(I)
      B2=B2+FREQ(I)*V(I)
 7063 B3=B3+V(I)/FREQ(I)
      VMS=ESDA*FREQ1
      B2=SQRT(B2/B3)
      B=.0
      DO 5065 I=L1,IDPEAK
      ESDB=ESDB+V(I)
 5065 B=B+(V(I)-UP(I))**2
      TOT=ESDB*FREQ1
      ERR1=100.*SQRT(B)/ESDB
      DO 7064 I=1,KSIMU
      IF(S1(I).GT.1000.) S1(I)=1000.
      IF(S2(I).GT.1000.) S2(I)=1000.
C  ---ASSUME THAT SPREADING PARAMTER NEVER ACCESSES 50.---
      IS=INT(S1(I))
      IF(IS.EQ.0) THEN
      T13(I)=S1(I)
      ELSE
      IF(IS.LT.100) T13(I)=FS(IS)+(S1(I)-IS)*(FS(IS+1)-FS(IS))
      IF(IS.GE.100) T13(I)=8.87335+.022*(S1(I)-100.)
      END IF
      IS=INT(S2(I))
      IF(IS.EQ.0) THEN
      T23(I)=S2(I)
      ELSE
      IF(IS.LT.100) T23(I)=FS(IS)+(S2(I)-IS)*(FS(IS+1)-FS(IS))
      IF(IS.GE.100) T23(I)=8.87335+.022*(S2(I)-100.)
      END IF
 7064 CONTINUE
```

```
C  ---T13 & T23 REPRESENT G(S)*CPI AS SHOWN IN THEORITICAL SOLUTION---
      IF(KSIMU.EQ.NN6)WRITE(8,1000) M1,DEPTH,V1,DI,PI,AA,SV,IIPEAK,(V(I)
     1,S2(I),T23(I),WK(I),I=1,NN6)
 1000 FORMAT(/7F8.3,I4/(8E15.9))
C
C ***************************************************************************
C *---PART VIII: DRAWING ONE DIMENSIONAL KINEMATIC SPECTRUM IN LOG. SCALE---   *
C ***************************************************************************
      PRINT 5032
      READ*,MODE
C  ---MODE=1 : WILL CALCULATE HORIZONTAL VELOCITY SPECTRUM AT 4.3 FT ABOVE SEA BUTTOM---
C  ---MODE=2 : WILL CALCULATE HORIZONTAL AMPLITUDE SPECTRUM AT 4.3 FT ABOVE SEA BUTTOM---
C  ---MODE=3 : WILL CALCULATE WAVE ENERGY SPECTRUM AT SEA SURFACE---
      IF(MODE.EQ.4) GO TO 7072
C
C  ---ONCE CALCULATION THROUGH THIS LINE WILL DISCONNECT WITH ABOVE PART---
C
 5048 PRINT 5035
 5035 FORMAT(/// "=====INPUT 1 TO DRAW ONE DIMENSIONAL SPECTRUM,"/"=====
     1OR INPUT 2 TO DRAW DIRECTIONAL SPECTRUM.")
      READ*,JMODE
      IF(JMODE.EQ.2) THEN
      IF(MODE.EQ.3) GO TO 5046
      GO TO 5052
      END IF
      CALL ERASE
C
      IF(MODE.NE.3) GO TO 5029
      CALL SCALE(8.3,.76,1.1,1.,.0,-2.)
      CALL AXISL(.0,.6,.0,-2.,3.,-2.,.1,1.,1,0,1,0,1.,1.,.1,0)
      CALL SYMBOL(-.1,-3.06,.0,.1,60,LY5)
      CALL NUMBER(.579,-3.08,.0,.1,7,DEPTH)
      CALL SYMBEL(-.05,3.65,.0,.18,17,LY2)
      DO 5037 J=1,MINN
      IF(VR(J).LT..01) T12(J)=-2.
 5037 IF(VR(J).GE..01) T12(J)=ALOG10(VR(J))
      CALL POINTS
      CALL LINE(FREQ,T12,19,MINN)
      CALL PLOT(.47,-.21,1,19)
 5046 DO 5036 J=1,NN1
      PR(J)=UP(J)
      IF(JMODE.EQ.1) THEN
      IF(PR(J).LT..01.AND.J.LE.IDEEP) T12(J)=-2.
      IF(PR(J).GE..01.AND.J.LE.IDEEP) T12(J)=ALOG10(PR(J))
      IF(V(J).LT..01) T33(J)=-2.
      IF(V(J).GE..01) T33(J)=ALOG10(V(J))
      END IF
 5036 P(J)=V(J)
      IF(JMODE.EQ.2) GO TO 7060
      PEAKF=FREQ(IIPEAK)
      VLARGE=V(IIPEAK)
      XL(1)=.452
      XL(2)=.482
      YL(1)=-1.
      YL(2)=-1.
      CALL VECTORS
      CALL LINE(XL,YL,0,2)
      CALL LINE(FREQ,T33,0,NN1)
      CALL DASHES
      CALL LINE(FREQ,T12,0,IDEEP)
      CALL SYMBOL(-.1,-2.,.90,.,15,24,LY8)
      CALL SYMBOL(.18,-2.68,.0,.15,15,LX)
      CALL NUMBER(-.088,2.95,.0,.1,7,1000.0)
      CALL NUMBER(-.088,1.95,.0,.1,7,100.00)
      CALL NUMBER(-.088,.95,.0,.1,7,10.000)
      CALL NUMBER(-.088,-.05,.0,.1,7,1.0000)
      CALL NUMBER(-.088,-1.05,.0,.1,7,0.1000)
      CALL NUMBER(-.088,-2.05,.0,.1,7,0.0100)
      CALL SYMBOL(.36,3.3,.0,.15,20,GE)
      CALL SYMBEL(.5,2.86,.0,.09,2,LZ5)
      CALL SYMBEL(.511,2.83,.0,.08.4,LX22)
      CALL SYMBEL(.555,2.86,.0,.09,10,LX24)
      CALL NUMBER(.57,2.86,.0,.088,5,ERR1)
      CALL SYMBEL(.46,2.5,.0,.09,29,LX20)
      CALL NUMBER(.583,2.5,.0,.09,6,TOT)
      CALL SYMBEL(.5,2.14,.0,.09,7,LX15)
      CALL NUMBER(.545,2.14,.0,.09,7,ALFA)
      CALL SYMBEL(.5,1.82,.0,.09,7,LY15)
      CALL NUMBER(.545,1.82,.0,.09,5,GA)
      CALL SYMBEL(.5,1.5,.0,.09,10,LX16)
      CALL NUMBER(.545,1.5,.0,.09,5,PA)
      CALL SYMBEL(.5,1.18,.0,.09,10,LY16)
      CALL NUMBER(.545,1.18,.0,.09,5,PC)
      CALL SYMBEL(.46,.84,.0,.09,18,LX11)
      CALL NUMBER(.615,.84,.0,.09,6,PEAKF)
      CALL SYMBEL(.46,.44,.0,.09,15,LY11)
```

```
      CALL NUMBER(.59,.44,.0,.09,7,VLARGE)
      CALL SYMBEL(.5,.14,.0,.09,27,LY20)
      CALL NUMBER(.546,.14,.0,.09,6,R2)
      CALL SYMBOL(.495,-.26,.0,.09,9,LX9)
      CALL SYMBOL(.45,-.66,.0,.09,3,LX10)
      CALL SYMBOL(.495,-.66,.0,.09,8,LX8)
      CALL SYMBOL(.605,-.66,.0,.09,8,LX6)
      CALL SYMBOL(.495,-1.06,.0,.09,10,LY9)
      CALL SYMBOL(.588,-1.06,.0,.09,8,LX6)
      CALL SYMBEL(.46,-1.46,.0,.09,14,LX2)
      CALL SYMBOL(.496,-1.71,.0,.09,15,R)
      CALL TEKPAUS
C
      IF(MODE.EQ.3) GO TO 7060
 5029 CALL SCALE(8.3,.76,1.1,1.,0.0,-4.)
      CALL AXISL(.0,.6,.0,-4.,1.,-4.,.1,1.,1,0,1,0,1.,1.,.1,0)
      IF(MODE.EQ.1) THEN
      CALL SYMBOL(-.1,-5.08,.0,.1,55,LY7)
      CALL SYMBEL(-.05,1.65,.0,.18,18,LX1)
      CALL SYMBEL(.504,.26,.0,.105,5,LX21)
      CALL SYMBEL(.55,.25,.0,.1,20,LY21)
      CALL SYMBEL(.517,.22,.0,.08,5,LX22)
      CALL NUMBER(.561,.25,.0,.088,6,VMS)
      R=100.*ABS(SV-VMS)/VMS
      CALL SYMBOL(.504,-.05,.0,.09,4,LX25)
      CALL NUMBER(.56,-.05,.0,.088,6,SV)
      CALL SYMBEL(.64,-.05,.0,.1,10,LY26)
      CALL NUMBER(.65,-.05,.0,.088,5,R)
      ELSE
      CALL SYMBOL(-.1,-5.08,.0,.1,56,LY6)
      CALL SYMBEL(-.05,1.65,.0,.18,15,LY)
      END IF
 5052 IF(MODE.EQ.1) CALL SMOOTH(N,PR,RECORD,NH1,0,1)
      IF(MODE.EQ.2) CALL SMOOTH(N,PR,DR,NH1,0,1)
      PEAKF=FREQ(IPEAK)
      VLARGE=.0
      DO 5031 I=1,NH1
      IF(MODE.EQ.1) THEN
      IF(I.LE.IPEAK)P(I)=V(I)*RECORD(I)/VR(I)
      IF(I.GT.IPEAK)P(I)=V(I)*(COSH(WK(I)*4.333)*FREQ(I)*CPI2/SINH(WK(I)
     1*DEPTH))**2
      IF(JMODE.EQ.1.AND.RECORD(I).LT.ADEP) T12(I)=-4.
      IF(JMODE.EQ.1.AND.RECORD(I).GE.ADEP)T12(I)=ALOG10(RECORD(I))-EDEP
      ELSE
      IF(I.LE.IPEAK)P(I)=V(I)*DR(I)/VR(I)
      IF(I.GT.IPEAK) P(I)=V(I)*(COSH(WK(I)*4.333)/SINH(WK(I)*DEPTH))**2
      IF(JMODE.EQ.1.AND.DR(I).LT.ADEP) T12(I)=-4.
      IF(JMODE.EQ.1.AND.DR(I).GE.ADEP)T12(I)=ALOG10(DR(I))-EDEP
      END IF
      IF(JMODE.EQ.1) THEN
      IF(P(I).LT.ADEP) P(I)=-4.
      IF(PR(I).LT.ADEP) T33(I)=-4.
      IF(P(I).GE.ADEP) P(I)=ALOG10(P(I))-EDEP
      IF(PR(I).GE.ADEP) T33(I)=ALOG10(PR(I))-EDEP
      END IF
      IF(I.LT.L1.AND.I.GT.NH5) GO TO 5031
      IF(P(I).LT.VLARGE) GO TO 5031
      VLARGE=P(I)
      II=I
 5031 CONTINUE
      PEAKF=FREQ(II)
      IF(JMODE.EQ.2) GO TO 7060
      IF(MODE.EQ.1) THEN
      R=.0
      ESDR=.0
      DO 5066 I=L1,IPEAK
      ESDR=ESDR+P(I)
 5066 R=R+(P(I)-PR(I))**2
      ERR2=100.*SQRT(R)/ESDR
      CALL SYMBEL(.504,.65,.0,.09,2,LZ5)
      CALL SYMBEL(.517,.62,.0,.08,4,LX22)
      CALL SYMBEL(.55,.65,.0,.1,10,LX24)
      CALL NUMBER(.561,.65,.0,.088,5,ERR2)
      END IF
      CALL POINTS
      CALL LINE(FREQ,T12,17,NH1)
      CALL PLOT(.47,-1.29,1,17)
      CALL DASHES
      CALL LINE(FREQ,T33,0,NH1)
      XL(1)=.452
      XL(2)=.482
      YL(1)=-2.4
      YL(2)=-2.4
      CALL VECTORS
      CALL LINE(XL,YL,0,2)
      CALL LINE(FREQ,D.0,NH1)
```

```
      CALL SYMBOL(-.08,-4.,90.,.15,24,LY8)
      CALL SYMBOL(.18,-4.68,0.0,0.15,15,LX)
      IF(EDEP.LT.1.) CALL NUMBER(-.07,-4.05,.0,.1,6,.0001)
      IF(EDEP.LT.1.) CALL NUMBER(-.07,-3.05,.0,.1,5,.001)
      IF(EDEP.LT.1.) CALL NUMBER(-.07,-2.05,.0,.1,5,.010)
      IF(EDEP.LT.1.) CALL NUMBER(-.07,-1.05,.0,.1,5,.100)
      IF(EDEP.LT.1.) CALL NUMBER(-.07,-.05,.0,.1,5,1.00)
      IF(EDEP.LT.1.) CALL NUMBER(-.07,.95,.0,.1,5,10.0)
      IF(EDEP.GE.1.) CALL NUMBER(-.07,-4.05,.0,.1,5,.010)
      IF(EDEP.GE.1.) CALL NUMBER(-.07,-3.05,.0,.1,5,.100)
      IF(EDEP.GE.1.) CALL NUMBER(-.07,-2.05,.0,.1,5,1.00)
      IF(EDEP.GE.1.) CALL NUMBER(-.07,-1.05,.0,.1,5,10.0)
      IF(EDEP.GE.1.) CALL NUMBER(-.07,-.05,.0,.1,5,100.)
      IF(EDEP.GE.1.) CALL NUMBER(-.07,.95,.0,.1,6,1000.)
      CALL SYMBOL(.36,1.3,.0,.15,20,GE)
      CALL SYMBOL(.46,-.55,.0,.09,18,LX11)
      CALL NUMBER(.615,-.55,.0,.09,6,PEAKF)
      CALL SYMBOL(.46,-.95,.0,.09,15,LY11)
      CALL NUMBER(.59,-.95,.0,.09,6,VLARGE)
      CALL SYMBOL(.495,-1.35,.0,.09,9,LX9)
      CALL SYMBOL(.45,-1.76,.0,.09,3,LX10)
      CALL SYMBOL(.495,-1.76,.0,.09,8,LX8)
      CALL SYMBOL(.54,-2.06,.0,.09,8,LX6)
      CALL SYMBOL(.495,-2.46,.0,.09,4,LY14)
      CALL SYMBOL(.553,-2.46,.0,.09,10,LY9)
      CALL SYMBOL(.54,-2.76,.0,.09,8,LX6)
      CALL SYMBOL(.46,-3.16,.0,.09,16,LX2)
      CALL SYMBOL(.496,-3.46,.0,.09,15,M)
      CALL TEKPAUS
C
C ***************************************************************************
C *---PART IX: DRAWING DIRECTIONAL SPECTRUM IN THREE DIMENSION SPACE---      *
C ***************************************************************************
C  ---THIS PART WILL BE MORE FLEXIBLE AS APPLIED TO SMOOTHED DIRECTIONAL SPECTRUM---
 7060 CONTINUE
C  ---THE FOLLOWING 137 LINE CAN BE DELETED IF IT IS NOT INTENDED TO HAVE---
C
C
      IF(MODE.EQ.2.OR.JMODE.EQ.2) GO TO 7057
      BDEP=.01
      IF(MODE.EQ.1.AND.DEPTH.LT.140.) BDEP=1.
      CALL ERASE
      IF(MODE.EQ.1) CALL SCALE(8.3,.76,1.1,1.,.0,-2.)
      DO 7058 I=1,NM2
      COSDA=COS((DDMEAN-D1(I))/2.)**2
      TEMP=ALOG10(COSDA**S1(I)
      IF(TEMP.GE.-120.) T12(I)=PB(I)*T13(I)/CPI*COSDA**S1(I)
      IF(TEMP.LT.-120.) T12(I)=PB(I)*T13(I)/CPI*1.E-120
      IF(MODE.EQ.1) T12(I)=T12(I)*100.
      IF(T12(I).LT.BDEP) THEN
      T12(I)=-2.
      ELSE
      T12(I)=ALOG10(T12(I))
      IF(BDEP.GE..5) T12(I)=T12(I)-EDEP
      END IF
 7058 CONTINUE
      XL(1)=.499
      XL(2)=.528
      YL(1)=.1
      YL(2)=.1
      IF(MODE.EQ.3) THEN
      CALL SYMBEL(-.05,3.65,.0,.18,17,LY2)
      CALL SYMBOL(.18,-2.68,.0,.15,15,LX)
      CALL NUMBER(-.088,2.95,.0,.1,7,1000.0)
      CALL NUMBER(-.088,1.95,.0,.1,7,100.00)
      CALL NUMBER(-.088,.95,.0,.1,7,10.000)
      CALL NUMBER(-.088,-.05,.0,.1,7,1.0000)
      CALL NUMBER(-.088,-1.05,.0,0.1,7,.1000)
      CALL NUMBER(-.088,-2.05,.0,.1,7,0.0100)
      ELSE
      CALL SYMBEL(-.05,3.65,.0,.18,18,LX1)
      CALL SYMBOL(.18,-2.68,.0,.15,15,LX)
      IF(BDEP.LT..5) CALL NUMBER(-.07,-2.05,.0,.1,6,.0001)
      IF(BDEP.LT..5) CALL NUMBER(-.07,-1.05,.0,.1,5,.001)
      IF(BDEP.LT..5) CALL NUMBER(-.07,-.05,.0,.1,5,.010)
      IF(BDEP.LT..5) CALL NUMBER(-.07,.95,.0,.1,5,.100)
      IF(BDEP.LT..5) CALL NUMBER(-.07,1.95,.0,.1,5,1.00)
      IF(BDEP.LT..5) CALL NUMBER(-.07,2.95,.0,.1,5,10.0)
      IF(BDEP.GE..5) CALL NUMBER(-.07,-2.05,.0,.1,5,.010)
      IF(BDEP.GE..5) CALL NUMBER(-.07,-1.05,.0,.1,5,.100)
      IF(BDEP.GE..5) CALL NUMBER(-.07,-.05,.0,.1,5,1.00)
      IF(BDEP.GE..5) CALL NUMBER(-.07,.95,.0,.1,5,10.0)
      IF(BDEP.GE..5) CALL NUMBER(-.07,1.95,.0,.1,5,100.)
      IF(BDEP.GE..5) CALL NUMBER(-.07,2.95,.0,.1,6,1000.)
      CALL SYMBOL(.504,1.67,.0,.09,12,LY23)
```

```
      CALL NUMBER(.495,1.37,.0,.085,4,4.3)
      CALL SYMBEL(.511,1.37,.0,.09,24,LY12)
      END IF
      CALL AXISL(.0,.6,.0,-2.,3.,-2.,.1,1.,1,0,1,0,1.,1.,.1,0)
      CALL LINE(FREQ,T12,0,NM2)
      CALL LINE(XL,YL,0,2)
      CALL SYMBOL(.393,2.6,.0,.15,9,LX)
      CALL SYMBOL(.594,2.6,.0,.15,8,LX6)
      CALL SYMBOL(.393,2.07,.0,.15,2,LZ2)
      CALL SYMBOL(.4515,2.07,.0,.15,14,LY14)
      CALL SYMBOL(.54,.04,.0,.09,8,LX8)
      CALL SYMBOL(.585,-.26,.0,.09,8,LX6)
      CALL SYMBEL(.504,-.66,.0,.09,16,LX2)
      CALL SYMBOL(.54,-.96,.0,.09,15,M)
      CALL SYMBEL(.504,-1.36,.0,.09,18,LY14)
      CALL NUMBER(.585,-1.66,.0,.085,6,DM)
      CALL SYMBOL(.648,-1.57,.0,.06,1,LZ4)
      CALL TEKPAUS
      CALL ERASE
C
      IF(MODE.EQ.1) IPNOW=IPEAK
      IF(MODE.EQ.3) IPNOW=IIPEAK
      DO 7059 I=1,120
      C=FLOAT(I)*3.*RW-CPI
      COSDA=COS((C-D1(IPNOW))/2.)**2
      TEMP=ALOG10(COSDA)*S1(IPNOW)
      IF(TEMP.GE.-120.) T12(I)=VLARGE*T13(IPNOW)/CPI*COSDA**S1(IPNOW)
      IF(TEMP.LT.-120.) T12(I)=VLARGE*T13(IPNOW)/CPI*1.E-120
      IF(MODE.EQ.1) T12(I)=T12(I)*100.
      T33(I)=FLOAT(I)/300.
      IF(T12(I).LT.BDEP) THEN
      T12(I)=-2.
      ELSE
      T12(I)=ALOG10(T12(I))
      IF(BDEP.GE..5) T12(I)=T12(I)-EDEP
      END IF
 7059 CONTINUE
      IF(MODE.EQ.3) THEN
      CALL SYMBEL(-.05,3.65,.0,.18,17,LY2)
      CALL NUMBER(-.088,2.95,.0,.1,7,1000.0)
      CALL NUMBER(-.088,1.95,.0,.1,7,100.00)
      CALL NUMBER(-.088,.95,.0,.1,7,10.000)
      CALL NUMBER(-.088,-.05,.0,.1,7,1.0000)
      CALL NUMBER(-.088,-1.05,.0,0.1,7,.1000)
      CALL NUMBER(-.088,-2.05,.0,.1,7,0.0100)
      ELSE
      CALL SYMBEL(-.05,3.65,.0,.18,18,LX1)
      IF(BDEP.LT..5) CALL NUMBER(-.07,-2.05,.0,.1,6,.0001)
      IF(BDEP.LT..5) CALL NUMBER(-.07,-1.05,.0,.1,5,.001)
      IF(BDEP.LT..5) CALL NUMBER(-.07,-.05,.0,.1,5,.010)
      IF(BDEP.LT..5) CALL NUMBER(-.07,.95,.0,.1,5,.100)
      IF(BDEP.LT..5) CALL NUMBER(-.07,1.95,.0,.1,5,1.00)
      IF(BDEP.LT..5) CALL NUMBER(-.07,2.95,.0,.1,5,10.)
      IF(BDEP.GE..5) CALL NUMBER(-.07,-2.05,.0,.1,5,.010)
      IF(BDEP.GE..5) CALL NUMBER(-.07,-1.05,.0,.1,5,.100)
      IF(BDEP.GE..5) CALL NUMBER(-.07,-.05,.0,.1,5,1.00)
      IF(BDEP.GE..5) CALL NUMBER(-.07,.95,.0,.1,5,10.0)
      IF(BDEP.GE..5) CALL NUMBER(-.07,1.95,.0,.1,5,100.)
      IF(BDEP.GE..5) CALL NUMBER(-.07,2.95,.0,.1,6,1000.)
      CALL SYMBOL(.504,1.67,.0,.09,12,LY23)
      CALL NUMBER(.495,1.37,.0,.085,4,4.3)
      CALL SYMBEL(.511,1.37,.0,.09,24,LY12)
      END IF
      CALL AXISL(.0,.4,.0,-2.,3.,-2.,.05,1.,1,0,0,0,1.,1.,.1,0)
      CALL LINE(T33,T12,0,120)
      CALL LINE(XL,YL,0,2)
      CALL SYMBOL(-.006,-2.26,.0,.11,1,LX4)
      CALL SYMBOL(.094,-2.26,.0,.11,1,LY4)
      CALL SYMBOL(.194,-2.26,.0,.11,1,LX3)
      CALL SYMBOL(.294,-2.26,.0,.11,1,LY3)
      CALL SYMBOL(.394,-2.26,.0,.11,1,LX4)
      CALL SYMBOL(.09,-2.72,.0,.15,9,LX5)
      CALL SYMBOL(.294,-2.72,.0,.15,8,LX23)
      CALL SYMBOL(.336,2.6,.0,.15,11,LX5)
      CALL SYMBOL(.5646,2.6,.0,.15,8,LX6)
      CALL SYMBOL(.336,2.07,.0,.15,2,LZ2)
      CALL SYMBOL(.3945,2.07,.0,.15,18,LY24)
      CALL SYMBOL(.54,.04,.0,.09,8,LX8)
      CALL SYMBOL(.585,-.26,.0,.09,8,LX6)
      CALL SYMBEL(.504,-.66,.0,.09,16,LX2)
      CALL SYMBOL(.54,-.96,.0,.09,15,M)
      CALL SYMBEL(.504,-1.36,.0,.09,22,LY24)
      CALL NUMBER(.6,-1.66,.0,.085,6,PEAKF)
      CALL SYMBOL(.678,-1.66,.0,.088,2,LZ3)
      CALL TEKPAUS
 7057 CONTINUE
```

```
C
C
      CALL ERASE
      CALL SCALE(17.4,16.,.42,.42,.0,.0)
      PRINT 7069
      READ*, JMODE
      GO TO (7068,7068,7071,7072) JMODE
 7068 PRINT 7061, MODE
 7061 FORMAT(1X/"=====INPUT CONSTANT, CMODE, FOR RANGING THE CONTOURS."/
     1"-----CMODE=1. WILL COVER 1,4,10,40,100,400,700,1000."/"-----CMODE
     1 IS THE VALUE 10**INTEGER, RANGE: (1,4,...,1000)*CMODE."/"-----FOR
     1 EXAMPLE: CMODE=.1 COVERS (.1,.4,1,4,...,100)."/"-----GUIDE: CMODE
     1=.1,1.,10. RESPECT TO MODE=1,2,3. MODE=",I1," NOW.")
      READ*,CMODE
      PRINT 800
  800 FORMAT(/"=====INPUT ANGULAR INTERVAL (DEG.) FOR ITERATIVE COMPUTAT
     1ION." /"-----GUIDE: 4 FOR ROUGH DRAW, OR LESS FOR SHARP VIEW.")
      READ*,NH3
      VLARGE=.002+.0002*NH3
      R=.0
      SUM=.0
      ALL=.0
      PRINT 7099
 7099 FORMAT(1X/"=====INPUT NUMBER OF POINT-INCREMENT IN FREQUENCY INDEX
     1."/"-----E.G. INPUT 3 WILL SKIP 2 POINTS, ETC."/"-----GUIDE: INPUT
     1 1 FOR N.LE.256, INPUT (N/256)*2 FOR N.GT.256.")
      READ*,NH4
      FREQ2=FREQ1*FLOAT(NH4)
      CALL ERASE
      CALL ORIGIN(3.03,2.83)
      DO 7070 I=2,NH2,NH4
      IF(JMODE.EQ.1) THEN
      T12(I)=T13(I)/CMODE/CPI*PB(I)
      ELSE
      T33(I)=T23(I)/CMODE/CPI*P(I)
      IF(I.GE.L1.AND.I.LE.IPEAK) T12(I)=T13(I)/CMODE/CPI*PB(I)
      END IF
 7070 CONTINUE
C  ---P(I) IS THE PROPOSED JONSWAP SPECTRUM, AND PB(I) IS THE SMOOTHED DATA---
      MIN=INT(DMEAN)-90
      MAX=2*INT(DMEAN)-MIN
C
      DO 7065 J=MIN,MAX,NH3
      C=FLOAT(J)
      BIG=C*RN
      COSJ=COS(BIG)
      SINJ=SIN(BIG)
      ESDA=1.E-7
      DO 200 JJ=1,7
  200 IXY(JJ)=0
C
      IF(JMODE.EQ.2.AND.JUMP.EQ.2) COSDA=COS((BIG-DDMEAN)/2.)**2
      DO 7066 I=2,NH2,NH4
      IF(JMODE.EQ.1.OR.JUMP.EQ.1) COSDA=COS((BIG-D1(I))/2.)**2
      IF(JMODE.EQ.2.AND.JUMP.EQ.3) COSDA=COS((BIG-D2(I))/2.)**2
      IF(JMODE.EQ.1) THEN
      TEMP=ALOG10(COSDA)*S1(I)
      IF(TEMP.GE.-120.) ESDB=T12(I)*COSDA**S1(I)
      IF(TEMP.LT.-120.) ESDB=T12(I)*1.E-120
      ELSE
      TEMP=ALOG10(COSDA)*S2(I)
      IF(TEMP.GE.-120.) ESDB=T33(I)*COSDA**S2(I)
      IF(TEMP.GE.-120..AND.I.GE.L1.AND.I.LE.IPEAK) L2=10
      IF(L2.EQ.10) BDXX=COS((BIG-D1(I))/2.)**2
      IF(L2.EQ.10) SUM=SUM+(ESDB-T12(I)*BDXX**S1(I))**2
      IF(TEMP.LT.-120.) ESDB=T33(I)*1.E-120
      END IF
      ALL=ALL+ESDB
      IF(ESDA.LT.1..AND.ESDB.LT.1.) GO TO 7066
      IF(ESDA.GT.1000..AND.ESDB.GT.1000.) GO TO 7066
      IF(I.LT.IPEAK-10.OR.I.GT.IPEAK+10) GO TO 700
      IF(C.LT.DMEAN-20..OR.C.GT.DMEAN+20.) GO TO 700
      IF(ESDB.GT.R) THEN
      R=ESDB
      L3=I
      CC=C
      END IF
C  ---WHERE ESDB IS THE DISCRETE DIRECTIONAL SPECTRUM OF INTERESTED WAVE PROPERTY---
  700 L00=INT(ESDA)
      L11=INT(ESDB)
      IF(L00.GE.1.AND.L00.LE.4) THEN
      L00=1
      ELSE IF(L00.GE.5.AND.L00.LE.9) THEN
      L00=2
      ELSE IF(L00.GE.10.AND.L00.LE.49) THEN
      L00=3
```

```
      ELSE IF(L00.GE.50.AND.L00.LE.99) THEN
      L00=4
      ELSE IF(L00.GE.100.AND.L00.LE.499) THEN
      L00=5
      ELSE IF(L00.GE.500.AND.L00.LE.999) THEN
      L00=6
      ELSE IF(L00.GE.1000) THEN
      L00=7
      END IF
      IF(L11.GE.1.AND.L11.LE.4) THEN
      L11=1
      ELSE IF(L11.GE.5.AND.L11.LE.9) THEN
      L11=2
      ELSE IF(L11.GE.10.AND.L11.LE.49) THEN
      L11=3
      ELSE IF(L11.GE.50.AND.L11.LE.99) THEN
      L11=4
      ELSE IF(L11.GE.100.AND.L11.LE.499) THEN
      L11=5
      ELSE IF(L11.GE.500.AND.L11.LE.999) THEN
      L11=6
      ELSE IF(L11.GE.1000) THEN
      L11=7
      END IF
      LLL=L11
      L2=1
      IF(L11-L00) 10,7066,20
   10 L11=L00
      L00=LLL
      L2=0
   20 L00=L00+1
      IF(L11.GT.11) L11=11
      DO 100 K=L00,L11
      IF(K.EQ.1.OR.K.EQ.3.OR.K.EQ.5.OR.K.EQ.7) KMODE=10**(K/2)
      IF(K.EQ.2.OR.K.EQ.4.OR.K.EQ.6) KMODE=5.*10**(K/2-1)
      TEMP=FREQ(I)-ABS((KMODE-ESDB)/(ESDA-ESDB))*FREQ2
      K1=IXY(K)+1
      IF(K1.GT.14) GO TO 100
      K2=1
      IF(XX(K,K1,1).NE.1.) K2=2
      XX(K,K1,K2)=TEMP*COSJ
      YY(K,K1,K2)=TEMP*SINJ
C  ---K: "MEMORY CODE" FOR TRACING THE RELATIVE CONTOURS---
C  ---K1: "ORDER CODE" FOR CONNECTING PRESENT(I) & LAST(I-1)-RUN CONTOUR LOCATION---
C  ---K2: "ITERATION CODE", K2=1 FOR LAST-RUN, K2=2 FOR PRESENT RUN---
      IXY(K)=K1
      IF(K2.NE.2) GO TO 100
   30 XL(1)=XX(K,K1,1)
      XL(2)=XX(K,K1,2)
      YL(1)=YY(K,K1,1)
      YL(2)=YY(K,K1,2)
      X12=SQRT(XL(2)*XL(2)+YL(2)*YL(2))-SQRT(XL(1)*XL(1)+YL(1)*YL(1))
      IF(ABS(X12).LT.VLARGE) GO TO 300
      IF(X12) 40,300,50
   40 DO 60 L=13,K1,-1
      XX(K,L+1,1)=XX(K,L,1)
   60 YY(K,L+1,1)=YY(K,L,1)
      XX(K,K1,1)=XX(K,K1,2)
      YY(K,K1,1)=YY(K,K1,2)
      GO TO 30
   50 MM=K1+1
      DO 70 II=MM,14
      XL(1)=XX(K,II,1)
      IF(XL(1).EQ.1.) GO TO 400
      YL(1)=YY(K,II,1)
      X12=SQRT(XL(2)*XL(2)+YL(2)*YL(2))-SQRT(XL(1)*XL(1)+YL(1)*YL(1))
      IF(ABS(X12).LT.VLARGE) THEN
      DO 80 LL=1,13
      XX(K,K1+LL,1)=XX(K,II+LL,1)
      YY(K,K1+LL,1)=YY(K,II+LL,1)
      IF(II+LL.GE.14) XX(K,14,1)=1.
   80 IF(XX(K,K1+LL,1).EQ.1.) GO TO 300
      END IF
   70 CONTINUE
      GO TO 400
  300 IF(L2.EQ.1) GO TO 90
      IF(I.LE.L1) GO TO 90
      L5=J-60
      L4=J-15
      NH5=J+25
      IF(L5.LT.NH3.AND.L5.GE.0) GO TO 91
      IF(L4.LT.NH3.AND.L4.GE.0) GO TO 91
      IF(NH5.LT.NH3.AND.NH5.GE.0) GO TO 91
      GO TO 90
   91 VALUE=FLOAT(KMODE)*CMODE
```

```
      IF(K.EQ.2.OR.K.EQ.4.OR.K.EQ.6) IPNOW=1
      IF(IPNOW.EQ.1.AND.FREQ(I).LT..12.AND.ABS(C-D1(I)*DEGREE).LT
     1.17.) GO TO 90
      X=XL(2)-.0025
      Y=YL(2)-.0015
      Y1=YL(2)-.006
      INTO=INT(VALUE)
      IF(INTO.GE.1) THEN
      IF(INTO.EQ.1) CALL SYMBOL(X,Y,.0,.06,1,LZ)
      IF(INTO.EQ.5) CALL SYMBOL(X,Y1,.0,.06,1,LZ1)
      IF(INTO.EQ.10) CALL SYMBOL(X,Y,.0,.06,2,LZ)
      IF(INTO.EQ.50) CALL SYMBOL(X,Y1,.0,.06,2,LZ1)
      IF(INTO.EQ.100) CALL SYMBOL(X,Y,.0,.06,3,LZ)
      IF(INTO.EQ.500) CALL SYMBOL(X,Y1,.0,.06,3,LZ1)
      GO TO 400
      END IF
      NUM=INT(ABS(ALOG10(VALUE*1.2)))+3
      X=X-.001
      IF(IPNOW.EQ.1) Y=Y1
      CALL NUMBER(X,Y,.0,.06,NUM,VALUE)
      GO TO 400
   90 CALL LINE(XL,YL,0,2)
  400 XX(K,K1,1)=XX(K,K1,2)
      YY(K,K1,1)=YY(K,K1,2)
  100 CONTINUE
 7066 ESDA=ESDR
      DO 500 K=1,7
      KK=IXY(K)+1
      DO 500 K1=KK,14
      XX(K,K1,1)=1.
  500 CONTINUE
 7065 CONTINUE
      DO 600 K=1,7
      KK=IXY(K)
      DO 600 K1=1,KK
      XX(K,K1,1)=1.
  600 CONTINUE
      INTO=2
      C=FREQ(L3)
      X=C*COS(CC*RN)
      Y=C*SIN(CC*RN)
      CC=90.-CC
      SUM=100.*SQRT(SUM)/ALL
      ALL=ALL*FREQ2*WN4*RN*CMODE
      B=B*CMODE
      TEMP=90.-DII
      CALL SYMBOL(X,Y,.0,.05,1,LY10)
      CALL SYMBEL(.0,-.0045,TEMP,.09,25,LY13)
      CALL SYMBOL(.138,.095,0.,.18,8,LX6)
      IF(MODE.EQ.1) THEN
      CALL SYMBEL(.158,.07,.0,.18,18,LX1)
      CALL SYMBEL(.168,-.038,.0,.105,5,LX21)
      CALL SYMBEL(.172,-.04,.0,.08,4,LX22)
      CALL SYMBEL(.186,-.038,.0,.08,20,LY21)
      CALL NUMBER(.19,-.038,.0,.08,6,ALL)
      END IF
      IF(MODE.EQ.2) CALL SYMBEL(.158,.07,.0,.18,15,LY)
      IF(MODE.EQ.3) THEN
      CALL SYMBEL(.158,.07,.0,.18,17,LY2)
      CALL SYMBEL(.168,-.038,.0,.08,15,LX20)
      CALL NUMBER(.222,-.038,.0,.08,7,ALL)
      ELSE
      CALL SYMBOL(.165,.053,.0,.08,12,LY23)
      CALL SYMBEL(.167,.041,.0,.09,25,LY12)
      CALL NUMBER(.16,.041,.0,.077,4,4.3)
      END IF
 7062 CALL AXISL(-.15,.15,0.,-.15,.15,0.,.05,.05,0,0,0,0,1.,1.,.1,0)
      CALL CIRCLE(0.,0.,0.,90.,.15,.15,.1)
      CALL CIRCLE(0.,0.,98.,180.,.15,.15,.1)
      CALL CIRCLE(0.,0.,185.,261.,.15,.15,.1)
      CALL CIRCLE(0.,0.,290.,355.,.15,.15,.1)
      CALL SYMBOL(.159,-.006,.0,.2,1,LX3)
      CALL SYMBOL(-.168,-.006,.0,.2,1,LX4)
      CALL SYMBOL(-.0038,.159,0.,.2,1,LY3)
      CALL SYMBOL(-.0038,-.171,.0,.2,1,LY4)
      CALL SYMBOL(.11,.12,0.,.18,11,LX5)
      CALL NUMBER(.131,-.01,0.,.1,4,.15)
      CALL NUMBER(-.157,-.01,0.,.1,4,.15)
      CALL NUMBER(-.022,-.01,.0,.107,4,.00)
      CALL NUMBER(-.024,.145,0.,.1,4,.15)
      CALL NUMBER(-.024,-.150,0.,.1,4,.15)
      CALL SYMBOL(.0043,-.151,0.,.1,14,LX)
      CALL SYMBOL(.08,.158,.0,.15,20,GE)
      IF(INTO.EQ.1) GO TO 6072
      IF(JMODE.EQ.1) THEN
      CALL SYMBOL(.168,-.055,.0,.08,8,LX8)
```

```
      ELSE
      CALL SYMBEL(.18,-.021,.0,.11,2,LZ5)
      CALL SYMBEL(.184,-.023,.0,.088,4,LX22)
      CALL SYMBEL(.201,-.021,.0,.09,10,LX24)
      CALL NUMBER(.205,-.021,.0,.08,5,SUM)
      CALL SYMBOL(.168,-.055,.0,.08,10,LY19)
      END IF
      CALL SYMBOL(.19,-.065,.0,.08,8,LX6)
      CALL SYMBEL(.1418,-.1058,.0,.08,25,LX12)
      CALL SYMBEL(.1789,-.1166,.0,.08,25,LY12)
      CALL NUMBER(.1645,-.1166,.0,.075,6,H1)
      CALL SYMBEL(.194,-.1276,.0,.08,19,LX13)
      CALL NUMBER(.1653,-.1276,.0,.075,6,PII)
      CALL NUMBER(.215,-.1276,.0,.075,6,DII)
      CALL SYMBOL(.154,-.1422,.0,.05,1,LY10)
      CALL SYMBEL(.168,-.1426,.0,.08,15,LY11)
      CALL NUMBER(.219,-.1426,.0,.08,7,B)
      CALL NUMBER(.1653,-.1536,.0,.075,6,C)
      CALL NUMBER(.212,-.1536,.0,.075,6,CC)
      CALL SYMBEL(.194,-.1536,.0,.08,15,LZ3)
      CALL SYMBEL(.168,-.08,.0,.08,16,LX2)
      CALL SYMBOL(.18,-.0908,.0,.08,15,H)
      CALL TEKPAUS
      CALL ERASE
      PRINT 7069
7069  FORMAT(/"=========================================="/
     1      /     /"=====INPUT 1 TO DRAW AN SMOOTHED SPECTRUM,"/"=====OR
     1 INPUT 2 TO DRAW A PROPOSED SPECTRUM,"/"=====OR INPUT 3 TO EXECUTE
     1 THE PROGRAM IN OTHER MODE."     /"=====OR INPUT 4 TO TERMINATE THE
     1 EXECUTION OF THIS PROGRAM.")
      READ*, JMODE
      GO TO (7068,7068,7071,7072) JMODE
7071  PRINT 5032
5032  FORMAT(/"=========================================="/
     1      /     /"=====INPUT MODE CODE,"/"-----MODE=1 RUN A HORIZONTAL
     1 VELOCITY SPECTRUM (4.3' ABOVE SEA FLOOR)"/"-----MODE=2 RUN A HORI
     1ZONTAL AMPLITUDE SPECTRUM (4.3' ABOVE SEA FLOOR)"/ "-----MODE=3 WI
     1LL RUN A WAVE ENERGY SPECTRUM AT SEA SURFACE,  "/"-----MODE=4 WILL
     1 TERMINATE THE PROGRAM.")
      READ*, MODE
      IF(MODE.NE.4) GO TO 5048
      STOP
7072  END
C
C ***************************************************************************
C *---PART X: COLLECTION OF SUBROUTINES AND BLOCK DATA---                     *
C ***************************************************************************
      SUBROUTINE TRANS(DEPTH,H1,MM)
      COMMON /DATA10/ FREQ(720),TA(720),TB(720),P(720),UP(720),UK(720)
     1,FREQ1,FREQ2,ALFA,GA,PEAKF,LL,IPEAK,IDPEAK,IIPEAK,K,A1,ICPEAK,L1
      FREQ3=FREQ2/6.
C  ---FREQ3(HZ) CIRCUMSCRIBES SHALLOW WATER WAVES---
      UK(MM+1)=.1
      H2=H1+3.4167
C  ---3.4167(FT) IS THE DISTANCE BETWEEN CURRENT-METER AND PRESSURE GAUGE---
      DO 130 I=MM,1,-1
      FREQ(I)=FLOAT(I)*FREQ1
      IF(FREQ(I).GT.FREQ2) THEN
      UK(I)=FREQ(I)*FREQ(I)*1.2270286
C  ---1.2270286=(CPI2)**2/32.174---
      UP(I)=.0058855*COSH(UK(I)*H2)/COSH(UK(I)*H1)/FREQ(I)
C  ---.0058855=(UNIT WEIGHT OF SEA WATER)/CPI2=(64./12**3 PSI)/CPI2---
      ELSE IF(FREQ(I).LE.FREQ3) THEN
      UK(I)=FREQ(I)*SQRT(1.2270286/DEPTH)
      UP(I)=.0058855*UK(I)*DEPTH/FREQ(I)
      ELSE
C  ---CONSIDER THE INTERMEDIATE WATER CONDITION---
      XX=UK(I+1)*DEPTH
      UH=FREQ(I)*FREQ(I)*DEPTH*1.2270286
      TANHH=TANH(XX)
      DO 170 J=1,10
      DH=(UH-XX*TANHH)/(TANHH+XX/COSH(XX)**2)
      XX=DH+XX
      TANHH=TANH(XX)
      IF(ABS(DH/XX).LT..005) GO TO 150
  170 CONTINUE
  150 UK(I)=XX/DEPTH
      UK(I)=XX/DEPTH
      UP(I)=.0058855*TANHH*COSH(UK(I)*H2)/COSH(UK(I)*H1)/FREQ(I)
      END IF
  130 CONTINUE
      RETURN
      END
C
      SUBROUTINE SMOOTH(NN,S2,S1,MM,ICPEAK,MOD)
      DIMENSION S1(MM),S2(MM)
```

```
C  ---USING BARTLETT WINDOW: 1=2M/3, BASEWIDTH=2/M (HZ)------
C     N(SEC)   M(SEC)   D.O.F.   80% C.I.
C      256      128       6       (.58)(2.6)
C      512      128      12       (.65)(1.8)
C     1024      128      24       (.72)(1.5)
      IF(NN.GE.1024) MOD=4
      S2(1)=(S1(1)+S1(2))/2.
      S2(MH)=(S1(MH-1)+S1(MH))/2.
      GO TO (5,20,40,70) MOD
    5 S2(2)=(S1(1)+S1(3))/3.25+S1(2)/2.6
      S2(3)=(S1(2)+S1(4))/3.25+S1(3)/2.6
      NS=MH-3
      IF(NN.EQ.512) THEN
      DO 10 I=4,NS
   10 S2(I)=(S1(I-3)+S1(I+3))/36.+(S1(I-2)+S1(I+2))/9.+(S1(I-1)+S1(I+1))
     1/4.5+S1(I)/3.6
      S2(NS+1)=(S1(NS)+S1(NS+2))/3.25+S1(NS+1)/2.6
      S2(MH-1)=(S1(MH-2)+S1(MH))/3.25+S1(MH-1)/2.6
      ELSE
      NS=MH-1
      DO 11 I=2,NS
   11 S2(I)=(S1(I-1)+S1(I+1))/4.5+S1(I)/1.8
      END IF
      RETURN
   20 NS=MH-1
      DO 30 I=2,NS
   30 S2(I)=S1(I-1)*.2+S1(I)*.6+S1(I+1)*.2
      RETURN
   40 NS=ICPEAK-1
      DO 50 I=2,NS
   50 S2(I)=S1(I-1)*.2+S1(I)*.6+S1(I+1)*.2
      NS=ICPEAK+1
      II=MH-1
      DO 60 I=NS,II
   60 S2(I)=S1(I-1)*.2+S1(I)*.6+S1(I+1)*.2
      S2(ICPEAK)=S1(ICPEAK)
      RETURN
   70 S2(2)=(S1(1)+S1(3))/3.05+S1(2)/2.9
      S2(3)=(S1(1)+S1(5))/5.625+(S1(2)+S1(4))/4.737+S1(3)/4.5
      S2(4)=(S1(2)+S1(6))/5.625+(S1(3)+S1(5))/4.737+S1(4)/4.5
      S2(5)=(S1(3)+S1(7))/5.625+(S1(4)+S1(6))/4.737+S1(5)/4.5
      S2(6)=(S1(4)+S1(8))/5.625+(S1(5)+S1(7))/4.737+S1(6)/4.5
      NS=MH-6
      DO 80 I=7,NS
   80 S2(I)=(S1(I-6)+S1(I+6))*.0125+(S1(I-5)+S1(I+5))*.0306+
     1(S1(I-4)+S1(I+4))*.0562+(S1(I-3)+S1(I+3))*.0853+
     1(S1(I-2)+S1(I+2))*.1123+(S1(I-1)+S1(I+1))*.1319+S1(I)*.1389
      S2(NS+1)=(S1(NS-1)+S1(NS+3))/5.625+(S1(NS)+S1(NS+2))/4.737
     1+S1(NS+1)/4.5
      S2(NS+2)=(S1(NS)+S1(NS+4))/5.625+(S1(NS+1)+S1(NS+3))/4.737
     1+S1(NS+2)/4.5
      S2(NS+3)=(S1(NS+1)+S1(NS+5))/5.625+(S1(NS+2)+S1(NS+4))/4.737
     1+S1(NS+3)/4.5
      S2(NS+4)=(S1(NS+2)+S1(MH))/5.625+(S1(NS+3)+S1(NS+5))/4.737
     1+S1(NS+4)/4.5
      S2(NS+5)=(S1(NS+4)+S1(MH))/3.05+S1(NS+5)/2.9
      RETURN
      END
C
      SUBROUTINE LSM(AIM,X,MAX)
      COMMON /DATA10/ FREQ(720),TA(720),TB(720),P(720),WP(720),WK(720)
     1,FREQ1,FREQ2,ALFA,GA,PEAKF,LL,IPEAK,IDPEAK,IIPEAK,K,A1,ICPEAK,L1
      Z1=.0
      Z2=.0
      IA=LL
      IB=K
      IF(MAX.EQ.1) IB=IIPEAK
      IF(MAX.EQ.2) IA=IIPEAK
      DO 10 I=IA,IB
      BATA=(1./EXP(((FREQ(I)-PEAKF)/PEAKF/X)**2/26.1)**13
      TEMP=GA**BATA
      C=BATA*TEMP*(FREQ(I)-PEAKF)**2
      Z1=Z1+TA(I)*C*TEMP
   10 Z2=Z2+TB(I)*C
      AIM=ALFA*Z1-Z2
      RETURN
      END
C
      SUBROUTINE LST(AIM,X,M)
      DIMENSION PB(720)
      COMMON /DATA10/ FREQ(720),TA(720),TB(720),P(720),WP(720),WK(720)
     1,FREQ1,FREQ2,ALFA,GA,PEAKF,LL,IPEAK,IDPEAK,IIPEAK,K,A1,ICPEAK,L1
      Z1=0.
      Z2=0.
      Z3=0.
```

```
      Z4=0.
      IF(IIPEAK.EQ..0) THEN
      IA=ICPEAK
      IB=IIPEAK
      ELSE
      IA=ICPEAK-L1
      IB=ICPEAK
      END IF
      DO 10 I=IA,IB
      IF(IIPEAK.EQ.0) THEN
      IF(M.EQ.1) PB(I)=P(I)
      IF(M.EQ.2) PB(I)=UP(I)
      IF(PB(I).GT.PB(ICPEAK)) PB(I)=PB(ICPEAK)
      ELSE
      PB(I)=P(I)
      END IF
      B=FREQ(I)**X
      C=B*ALOG(FREQ(I))
      Z1=Z1+PB(I)*B
      Z2=Z2+PB(I)*C
      Z3=Z3+B*B
   10 Z4=Z4+B*C
      A1=Z1/Z3
      A1M=A1-Z2/Z4
      RETURN
      END
EOI ENCOUNTERED.
/
```